UNIVERSITÉ DE
NEUCHÂTEL
Laboratoire de Microbiologie

Anaerobic iron cycling in a Neoarchean Ocean analogue

Xavier Alexis WALTER

Thesis Submitted in Partial Fulfilment of the Requirements for the Degree of Doctor of Philosophy in Microbial Ecology.

PhD. Director:
Prof. Michel ARAGNO

PhD. Supervisor:
Dr. Jakob ZOPFI

Jury committee:
Prof. Michel Aragno, University of Neuchâtel
Dr. Jakob Zopfi, University of Neuchâtel
Prof. Pilar Junier, University of Neuchâtel
Prof. Antonio Camacho, University of Valencia
Prof. Andreas Kappler, University of Tübingen

Neuchâtel, 22/09/2011

Laboratoire de microbiologie – Institut de biologie - Université de Neuchâtel

Université de Neuchâtel

FACULTE DES SCIENCES
Secrétariat-Décanat de la faculté
Rue Emile-Argand 11
CH-2000 Neuchâtel

IMPRIMATUR POUR LA THESE

Anaerobic iron cycling in a neoarchaen ocean analogue

Alexis-Xavier Walter

UNIVERSITE DE NEUCHATEL

FACULTE DES SCIENCES

La Faculté des sciences de l'Université de Neuchâtel,
sur le rapport des membres du jury

Mme P. Junier (UniNe), MM. M. Aragno (directeur de thèse, UniNe),
J. Zopfi (UniNe), A. Kappler (Uni. Tübingen D) et
A. Camacho (Uni. Valencia E)

autorise l'impression de la présente thèse.

Neuchâtel, le 22 septembre 2011

Le doyen :
P. Kropf

Acknowledgments

I would like to thank **Dr. Jakob Zopfi** for providing me with the opportunity to work on a project that allowed me to travel in time to the dawn of evolution: trying to better understand the emergence of life diversity. Thank you also for teaching me, since my master in 2005, how to integrate geochemical and biological data, in order to understand the functioning of stratified microbial ecosystems.

I would like to thank **Prof. Michel Aragno** for offering me a place in his laboratory. I would also thank him for all the time he spent assisting me to communicate my results in an understandable manner, as well as for the opportunities he has offered me to pass on his passion of microbiology to the next generation of researchers.

I would like to give a huge thank to **Antonio Picazo-Mozo** for all the help, advice, encouragementsand of course for his "way of life" in science: "don't worry" he used to say. Thank you also for the IT support and for providing me with a "bibliography". I would like to emphisise the effort Antonio put into helping me, in the field and in the lab, without taking into account the endless hours which often continued until the early hours of the morning. Most of the time I was learning from him: from methodological approaches to data interpretations (e.g. primary production incubations). I would like also to thank him for the nitrate, pigments and sulfate analysis he made for the project.

A warm thanks to **the parents** of Antonio Picazo-Mozo: they are warm earthed and kind, they always have a smile on their face and never expect anything in return. Thank you very much for opening the doors of our home to our team. I promise, next time I will put less chili in the "carry"!

Prof. Rosa Maria Miracle has to be thanked for opening her department to our team: we could access an incredible amount of material needed for our project, as well as the logistic for the field expeditions (e.g.: car, boat, seabird...), and of course for the insight to their knowledge of the numerous and well furnished studies they have carried out on Lake La Cruz. I would especially like to thank her for letting us transform her office into a bedroom as we needed to remain close by our running experiments.

I would like to thanks **Prof. Eduardo Vicente** for helping us in our field expeditions, but also for obtaining, through his network, authorizations for carrying out detail investigation of Lake La Cruz: this lake is protected and swimming in it is forbidden. Moreover, he facilitated the use of all the required instruments and infrastructure of Valencia University, by introducing us to the right individuals. In addition, thank you very much for providing us with such beautiful accommodation in the center of Valencia, as well as organizing a visit to one of the nicest places in Spain, the old city of Cuenca and its "casas colgadas".

A great thanks to **Prof. Antonio Camacho** for taking the time, in his busy schedule, to help us on the field for the different samplings and experiments. Thank you also for all the discussions we had to resolve the different scientific problematics we encountered, and therefore helping us to accomplish our objectives! I would also like to acknowledge him for the transmission of his knowledge on ^{14}C-bicarbonate incubations.

I would like to thank the members of the jury, **Prof. Michel Aragno, Dr. Jakob Zopfi, Prof. Pilar Junier, Prof. Antonio Camacho and Prof Andreas Kappler**, for the constructive advice they offered me. Indeed, the only way to move forward in science is to have knowledgeable people who point you in the right direction of the "how to" and help you learn from your mistakes.

I would like to thank **Christophe Paul** for helping me during the majority of the field experiments as well as for following and supporting me during those extremely long days, even if he needed Bob Dylan for it! Thank you also for his advise on the scientific schedule of the different experiments and for his outspokenness.

Alexandre Bagnoud was one of my colleagues from the university of Neuchâtel. I would like to thank him for the helping me during the winter expedition in Lake La Cruz: it was almost impossible to sample the freezing water all over the profile without having a second pair of hands! He was also one of the two drivers that had to bring back samples during the direct return from Valencia to Neuchâtel: we smoked so much in our rented car that one week after we returned he quit nicotine forever!

I would like to thank **Nicole Jeanneret** for helping me in the treatment of my clone library. Nicole was more than just a help: since the beginning of my studies at the University she has constantly been there to teach us the reality of working in science. Moreover, she has always been there to answer our questions with a lot of kindness. Thank you for being the person you are.

Thank to **Dr. Enrique Lara** for helping me in treating the DNA sequences from the clone library: he taught me how to clean, compare and finally build maximum likelihood phylogenetic trees.

I also want to thank **Bertrand Fournier** for leading me though the labyrinth of statistical analysis and the particular IT language of R software.

A great thanks to **Dr. Saskia Bindschedler** for introducing me to InDesign (Adobe) and for helping me use it, this allowed me to circumvent the Microsoft Office software that started to get on my nerves, and therefore to get a better layout of my manuscript.

I would like to thank the kind **Unknown Woman**, we met at the lake shore, for the umbrella she gave us which allowed us to sample Lake La Cruz without having any contamination from rain waters!

I want to give a huge thank to all the members of the Laboratory of Microbial Ecology here in Neuchâtel, for their continuous helps: **Prof. Pilar Junier, Nicole Jeanneret, Dr. Sonia Tarnawski, Gaëtan Martin, Dr. Sylvia Humbert, Martin Clerc, Dr. Saskia Bindschedler, Tina Wunderlin and Daniel Bravo**. Moreover, these individuals have always been there in the difficult moments that can be encountered during a PhD. Thank you for being there and helping me during such moments!

I would like to give a huge thank to **Sandra Walter** who helped me enormously throughout the project by putting up with me everyday. She was the one giving me energy to face the challenging project through her patience and kindness. Thank you for these morning smiles that only left me on evenings where a new one was waiting for me.

I would also like to thank **Annie Walter** for supporting me during all my studies at Neuchâtel and offering me the means to live my passion. Thank you for giving me the tools that will allow to think freely in my future working life!

Thanks to the **Swiss National Science Foundation** for financing the project (N°3103A-112563).

Contents

CHAPTER I: Introduction

CHAPTER II: Photoferrotrophy in a ferruginous Neoarchean Ocean analogue

CHAPTER I: INTRODUCTION

CHAPTER I: Introduction

1. Knowledge of Early Earth history

1.1. Early Life evolution

Understanding the mechanisms of the emergence of life and its development on Earth is one of the most difficult areas for research. The difficulty is clear: how does one study processes that happened 4 billion years ago (Ga)? In order to tackle this problem, scientists use various research approaches, from paleontological records to modern molecular biology. Since its accretion, Earth has recycled most of its mantel crust, thereby altering many traces left by life's fragile structures. Nevertheless, some biotic and abiotic reactions have left detectable signatures (e.g. lipid biomarkers; stable isotope signatures) and have, therefore, allowed us to identify some of the major processes that did take place during Earth's early history. At the same time, experimental setup and modern natural systems are studied to test and verify the biogeochemical feasibility of some key reactions (e.g. Bahamas microbial mats in stromatolites formations understanding; Vissher *et al.*, 2010). Thus, clearer interpretation of geological records and therefore a better knowledge of Early Life influences on the past biogeosphere could be achieved.

The oldest discovered earth mineral - zircons from the Jack Hills (Western Australia) - were used to date Earth crust formation around 4.5-4.4 Ga (Wilde *et al.,* 2001; Harrison *et al.,* 2008). A similar study, also based on zircon analysis, showed that water was liquid 4.3 Ga ago (Mojzsis *et al.,* 2001). Since then, the earth should have been a habitable planet with regard to the availability of liquid water. It has been demonstrated, based on the graphite carbon isotope composition analysis of ~3.80 Ga old rocks (Banded iron formation, Issua supercrustal belt, West Greenland, Moorbath *et al.,* 1986), that life had emerged and had already diversified in oceanic environment around 3.850 Ga (Mojzsis *et al.,* 1996). However, new research on other samples from the same site (Akilia, SW Greenland), showed that these rocks were unsuitable for life-traces recognition, having developed to a too high intensity of metamorphism (Nuteman & Friends, 2006; Whitehouse *et al.,* 2009). On the other hand, the same team recognized trace of life in 3.700 Ga old samples (Fedo *et al.,* 2006), but reconsidered this in the 2009 article (Whitehouse *et al.,* 2009).

An earlier emergence of life might have even been possible. Indeed, a recent study (Abramov & Mojzsis, 2009) showed that even during the height of "Late heavy bombardments" (LHB, 4.1 to 3.8 Ga; Tera *et al.,* 1974) life could have resisted ocean heating: e.g. the centre of a 200 km diameter meteoritic crater could have been re-colonized in 20'000 years. Their conclusion was that "*…there is no plausible situation in which the habitable zone was fully sterilized on Earth*". Therefore, life could have started to influence Earth's chemical reactions and to have been influenced by them earlier. This hypothesis is also supported by the works of Mojzsis (1996) and Rothschild (2009) However, life evolution from 3.8 Ga should have been based on thermophilic metabolisms (e.g. hydrothermal vents: Russell & Hall, 1997; Nisbet & Sleep, 2001). Indeed, in the case of an origin earlier than 3.8 Ga, the metabolisms-diversity evolution should have suffered a bottleneck effect due to the LHB. If it didn't sterilize Earth, it would have increased ocean temperatures and therefore limited life expansion to hydrothermal regions where Life was already adapted (Nisbet & Sleep, 2001; Abramov & Mojzsis, 2009).

Even if it is still debated, we will assume in the following work that life was already developed 3.8 Ga ago. Moreover, we will assume that all Life's evolution, from first cell to a higher degree of complexity, happened on planet Earth. We will not take into account the very interesting hypothesis of a Martian Life emergence that would have colonized Earth through meteoritic shuttles (Nisbet & Sleep, 2001; Nisbet *et al.,* 2007[1]; Rothschild, 2009). If life appeared around 3.8 Ga ago on earth, photosynthesis emergence is still unresolved. Although the evolution of photosynthesis is complex and horizontal gene transfer has played an important role, it is now generally accepted that anoxygenic phototrophic bacteria evolved before the oxygen

producing cyanobacteria, which represent the pinnacle of bacterial phototrophy regarding the complexity of their photosynthetic apparatus (Xiong *et al.,* 2000; Des Marais, 2000; Raymond *et al.,* 2003; Canfield, 2005). Some recent findings even suggest an earlier possible apparition of oxygenic photosynthesis (Buick, 2008), but it is as yet speculation. Nevertheless, it was demonstrated that photosynthetic organisms had evolved 3.416 Ga ago, in a microbial mat (Tice & Lowe, 2004), and that oxygenic photosynthesis appeared around 2.75 Ga ago (detection of 2-methylbacteriohopanepolyol derivatives such as 2α-methylhopanes, amount of mass-independent fractionation of sulphur isotopes, Mo detection, and $\partial^{15}N$ values of kerogen found in shales; Brocks *et al.*, 1999; Des Marais, 2000; Raymond *et al.,* 2003; Canfield, 2005; Kump, 2008; Schwartzman *et al.,* 2008; Buick, 2008; Godfrey & Falkowski, 2009). Reduced carbon isotopic composition even shows a typical form I Rubisco signature in 2.9 Ga old samples (Nisbet *et al.,* 2007[2]) – it is, however, probably a sample contamination (Brocks & Rasmussen, 2010). We will still consider, in this study, that anoxygenic photosynthesis appeared 3.4 Ga ago and oxygenic photosynthesis 2.75 Ga ago. It is important to note that if oxygenic populations emerged around 2.75 Ga ago, oxygen accumulation in the atmosphere, and into the ocean compartment, only started around 2.4 Ga ago (Great oxidation event, Zahnle *et al.,* 2006; Konhauser *et al.,* 2009). In this work, assumed dates for early-Life development are exposed in Figure 1.

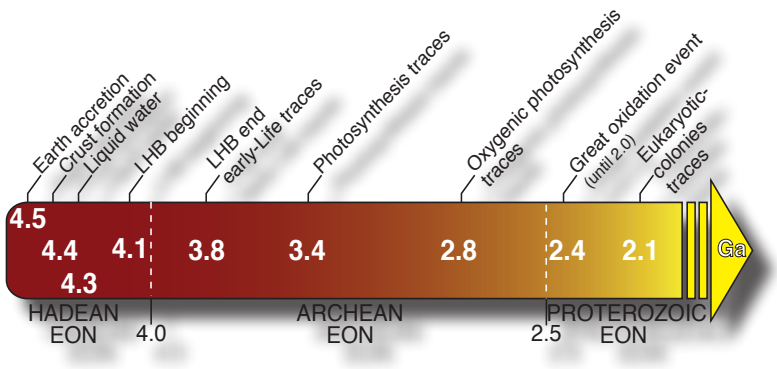

Figure 1: Timeline of the major developments in the evolution of Early Earth. The diagram only covers the beginning of Earth history, from the Hadean eon to the Paleoproterozoic. Ga stands for billion years before present.

1.2. Banded Iron Formation: a ferrous iron-oxidation product

Since the availability of liquid water, Earth's ocean-chemistry evolution has been mainly marked by the redox state of three elements: iron dominated the Archean chemistry, sulfur was the major element during the Proterozoic and oxygen became the most important component of modern ocean chemistry (Fig. 2.A/B).

Stratified water bodies with sulfidic bottom waters, resembling middle to late Proterozoic ocean, have received considerable attention (e.g. Black Sea, Cariaco Trench, Framvaren Fjord, meromictic lakes) and the chemical and microbiological processes in chemocline, water column and sediments are relatively well known (in e.g., Garcia-Gil *et al.,* 1988; Hanselmann & Hutter, 1998; Zopfi *et al.,* 2001; Rozan *et al.,* 2002; Manske *et al.,* 2005; Grote *et al.,* 2008). Results from such studies have been indispensable for the interpretation of the geological record and for the evaluation of biological implications (in e.g., Canfield, 1998; Habicht *et al.,* 2002; Shen *et al.,* 2003, Canfield, 2004; Arnold *et al.,* 2004; Anbar *et al.,* 2005; Lyons *et al.,* 2009[1]) (Fig. 2.A/B). For example, Arnold *et al*. (2004) used molybdenum isotope data from ancient and modern euxinic sediments (Cariaco Trench, Black Sea) to determine the redox conditions in the mid-Proterozoic ocean.

An early Earth characteristic sedimentary feature, called Banded iron formation (BIF), extends in geological records from 3.8 Ga to 0.6 Ga (Fig. 2.C). These typical Archean and Paleoproterozoic records are one of the most important sources of samples for our understanding of the ocean chemistry of that period. However, if the Proterozoic ocean chemistry is quite well understood, by a combination of

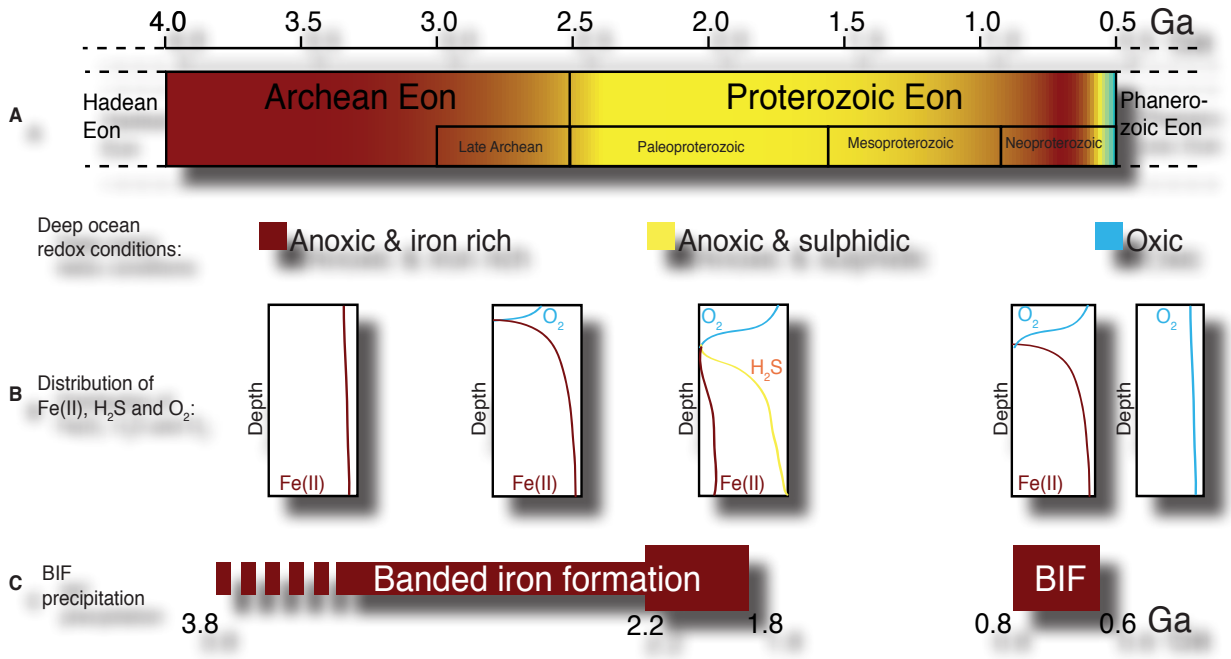

Figure 2: Geochemical change in the late Archean and Proterozoic ocean. **A |** Time before present in Giga years (Ga), where colour gradients denote postulated changes in deep-sea redox conditions. **B |** Schematic distribution of reduced iron (Fe(II)), sulfides (H_2S) and oxygen in the water column of the ocean. **C |** Periods of banded iron formation (BIF) deposition. The bar-thickness is an indication of BIF precipitation amounts. Diagram compiled and modified from Anbar & Knoll (2002), Knoll (2003) and Canfield *et al.* (2008).

geological-records studies and modern analogues investigations, the processes of BIFs settlement and the implication of an early biosphere is still very much under debate. BIFs are laminated iron-rich sedimentary rocks and are the most abundant type of sediment deposited from the late Archean to early Proterozoic period. They are essentially composed of rocks characterized by alternating layers rich in silica, and layers rich in iron minerals such as hematite (Fe_2O_3), magnetite (Fe_3O_4), iron-silicates (e.g. chamosite, greenalite) and iron carbonates such as siderite ($FeCO_3$) or ankerite ($CaFe[CO_3]_2$) (Fig. 3.A). Ferric iron (Fe(III)) dominates over ferrous iron (Fe(II)) in the Fe-rich layers (Ehrlich & Newman, 2009). This type of sedimentary deposit can be of a hundred meters thickness and contain $>10^{13}$ t of iron (Hamersley Group, Western Australia; Fig. 3.B) (Trendall & Blockley, 2002; Klein, 2005). Ancient BIF deposits, are found on all continents (Klein, 2005), may cover vast areas, and make up more than 90% of the world's commercial iron supply (Lunine, 1999; Fig. 3.C).

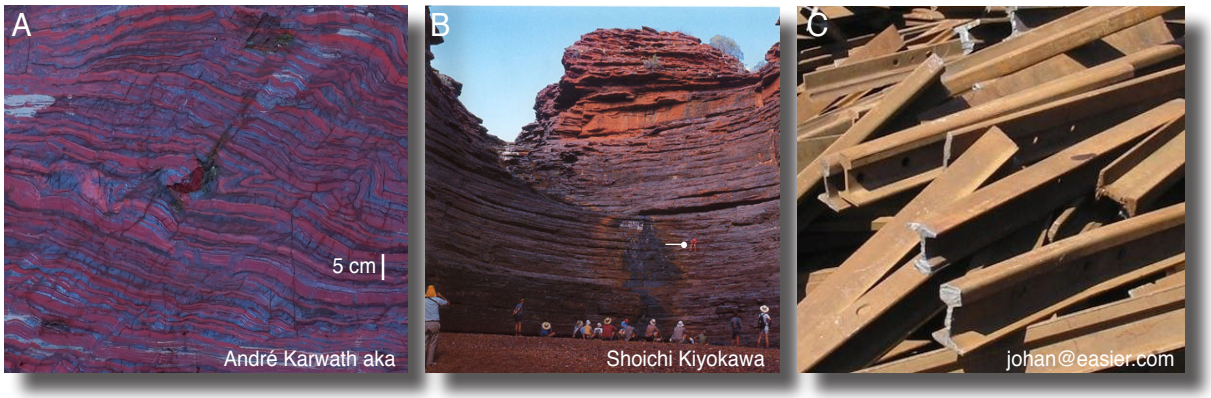

Figure 3: Banded iron formation photographs**. A |** Close-up on the fine stratification between iron-rich layers (red) and silica-rich layers (light grey). **B |** Banded iron formation from Hamersley Group. The tiny red point is a seated human being. **C |** The Fe(III) contained in BIFs is the major iron source for industries. These pictures have been "*googled*".

The late-Archean to early-Proterozoic ocean, from where most of the BIFs originate (2.2-1.8 Ga = billion years before present; Kasting, 2001; Klein, 2005; Holland, 2006), was anoxic, sulfate-poor and

ferrous iron-rich, at least at depth (Holland, 1984; Canfield, 1998; Canfield and Raiswell, 1999; Habicht *et al.*, 2002; Shen *et al.*, 2003; Canfield *et al.*, 20085; Canfield *et al.*, 2008; Fig. 2-4). It has been proposed that this ferrous iron was fuelled to the ocean by hydrothermal activity at mid-ocean ridges. Fe(II) was transported onto continental shelf by upwelling, where it was oxidized (Holland, 1973; Bau & Möller, 1993). However, the upwelling flux needed to be 1 order of magnitude higher to account for BIF sedimentation rates (Konhauser *et al.*, 2007[1]). Another view suggests that large tectono-magmatic events brought Fe(II) up to the continental shelf through volcanic plumes reaching photic layers (Barley *et al.*, 1997 / 2005; Canfield, 1998; Kump & Seyfried, 2005; Canfield *et al.*, 2006). The mid-ocean-ridge, in deep Archean ocean, could easily have transported reduced compounds (e.g. Fe(II)) to the photic compartment, mainly due to high magmatic activity. Moreover, sedimentological and petrographic studies showed a correlation between the maximum of BIF precipitation (2.2-1.8 Ga) and the past tectonic activity (Barley *et al.*, 1997 / 2005; Konhauser *et al.*, 2007[1] Fig. 4): the Fe(II) that formed the Hamersley BIF's could have come from the remobilization of pelagic mud that was lying on the flanks of submarine volcanoes (Pickard *et al.*, 2004 ; Fig. 4). According to Severmann *et al.* (2008), part of the Fe(III) sedimenting from the euphotic chemocline was reduced, by dissimilatory iron reduction, back into dissolved Fe(II). This Fe(II) was then transported to deep ocean, where it was quantitatively sequestered through reaction with sulfide, thus producing pyrite (Fig. 4).

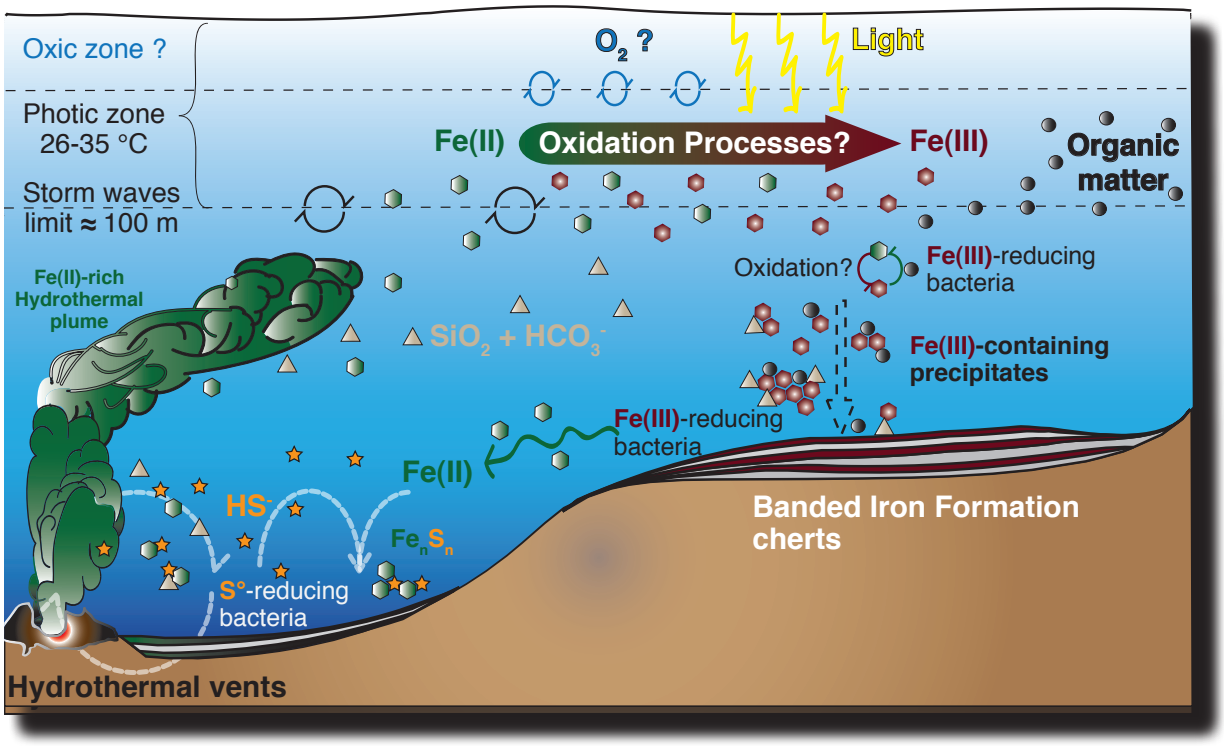

Figure 4: Possible model for BIF formation on the continental shelf. Deep anoxic water, rich in dissolved Fe(II) of hydrothermal origin, is transported onto the continental shelf, where iron gets oxidized. The produced oxides will precipitate from solution on the seafloor, in association with diverse components such as silica, carbonates or organic matter. However, the oxidation mechanisms are still unknown. It may be a chemical reaction with dissolved O_2, a UV light mediated photo-oxidation, or a biological iron-oxidation by anoxygenic photosynthesis using Fe(II) as an electron donor. Illustration compiled from Konhauser *et al.* (2002), Kappler *et al.* (2005[1]), Canfield *et al.* (2006), Konhauser *et al.* (2007[1]), Severmann *et al.* (2008), Blake *et al.* (2010), Tangalos *et al.* (2010).

If the transport of Fe(II) to a distant oxidation zone is more or less understood, the processes that drove this oxidation are still under discussion.

2. Project context: the biotic origin for BIFs

2.1. Abiotic Fe(II)-oxidations

It is generally believed that BIFs were formed by the oxidation of hydrothermal iron (e.g. Hamade *et al.,* 2003; Fig. 4). However, despite more than a century of research, the mechanisms of BIF deposition are still unresolved (Konhauser *et al.,* 2002) and the reason why BIF formation ceased after 1.8 Ga are disputed (Fig. 2C). Even the BIF's origin from 0.8-0.6 Ga, which was always understood to be the product of the abiotic reaction between Fe(II) and oxygen after the extensive Neoproterozoic glaciations was up for debate. It has been shown that the deep Neoproterozoic ocean was anoxic and ferruginous (Canfield *et al.,* 2008), and have thus raised the implication of the sulfur cycle in BIFs deposition. It seems that the ocean conditions were a zonal patchwork of oxygenated, sulfidic and ferruginous deep oceans, with a dominance of Fe(II) anoxia (Canfield *et al.,* 2008).

According to the traditional view, BIF formation ceased at 1.8 Ga when the bottom waters became oxic due to increasing atmospheric oxygen concentrations (Cloud, 1968[1-2]; Lunine, 1999). Oxygen produced by cyanobacteria would have then combined with dissolved ferrous iron of the water column and have formed insoluble ferric iron oxides, which would have precipitated and built out massive iron oxides deposits (Holland, 1984; Fig. 5).

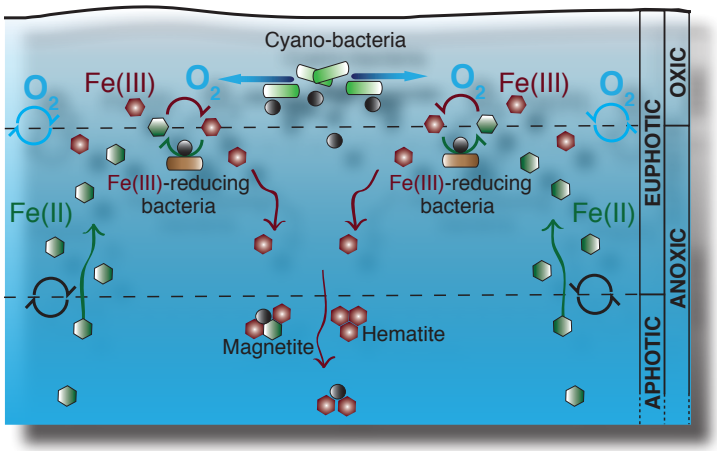

Figure 5: Oxygenic model for BIF settlement. Deep Fe(II)-rich water is transported into the cyanobacterial-layer. The cyano-bacteria release oxygen and organic matter in the water. The produced oxides will then precipitate on the seafloor. There is a possible recycling of Fe(II) through ferrireduction in the water column (Konhauser *et al.*, 2005).

UV radiation during the Archean was higher than nowadays. It was thus postulated that Fe(II) could also have been oxidized by a photo-oxidative process (Cairns-Smith, 1978; Braterman *et al.,* 1983; Francois, 1986). Indeed, ferrous iron could have adsorbed light of 200-400 nm wavelength and been oxidized to ferric iron. However, it has been shown experimentally that the amount of Fe(II) potentially oxidized by a light-catalyzed reaction is insignificant compared to the amount of Fe(III) present in BIFs (Konhauser *et al.,* 2007[1]).

Another view suggests that sulfide, not oxygen, was responsible for removing ferrous iron from solution, and thus terminating BIF formation (Canfield, 1998, Poulton *et al.,* 2004). According to this model, atmospheric oxygen concentrations were still too low to render oxic the deep-ocean waters, but they were sufficient to increase the weathering rate of continental metal sulfides. As a consequence, riverine input of sulfate increased the oceanic concentrations and stimulated bacterial sulfate reduction in anoxic waters and sediments. The produced sulfide would then react with ferrous iron and form insoluble iron sulfides that dramatically reduced the amount of dissolved iron in the water column. The iron-rich but sulfate-poor late Archaean to early-Proterozoic ocean was thus replaced in the mid-Proterozoic Ocean by an anoxic, sulfidic ocean, resembling modern euxinic basins such as the Black Sea. It was not until 1.0-0.5 Ga that a further increase in atmospheric oxygen finally gave rise to oxic deep-ocean waters (Des Marais *et al.,* 1992; Logan *et al.,* 1995; Canfield, 1998; Knoll, 2003; Kump, 2008; Fig. 2).

2.2. Biotic Fe(II)-oxidation hypothesis

An alternative hypothesis for the BIF deposition suggest that anoxygenic iron-oxidizing phototrophs (IOP) were responsible for Fe(II)-oxidation. A study using oxygen and hydrogen isotope signature from

black-and-white banded cherts suggest that Archean ocean temperatures did not exceed 40°C (Hren *et al.*, 2009). This results were confirmed by Blake (2010) who showed, using oxygen isotopes of phosphates, that the average temperature in the 3.2-3.5 Ga old ocean was between 26 and 35°C (Fig. 4). These temperatures were sufficiently cool to allow the existence and functioning of photosynthetic apparatus (Blake *et al.*, 2010). The isolation of anoxygenic phototrophic Fe(II)-oxidizing bacteria (Widdel *et al.*, 1993; Heising *et al.*, 1999) was crucial and allowed to test factors influencing iron oxidation rates (light, pH and temperatures; Hegler *et al.*, 2008). In addition, the new discovery of a colonial-microorganisms fossil from Gabon (black shales of the Paleoproterozoic Francevillian B Formation; El Albani *et al.*, 2010), prove the existence of an eukaryotic pluricellular life at 2.1 Ga (Fig. 1). It has been demonstrated that these fossils have grown in shallow waters under an oxygenated water column. Therefore, the velocity of life expansion and diversification was higher than primarily thought: until this major discovery it was accepted that multicellular eukaryotes organisms emerged on Earth only around 0.6 Ga. This discovery is thus in accordance with the Neoproterozoic ocean chemistry patchwork (Canfield, 2008). This breakthrough confirmed phototrophic Fe(II) oxidation as a likely process for BIF precipitation in absence of oxygen in the Archean ocean. Indeed, one of the main arguments limiting this hypothesis was that if BIFs are the product of photoferrotrophy, then anoxygenic photosynthesis should have already been evolved to form the oldest BIF at 3.8 Ga. This point of view was relevant since photosynthesis is a metabolism with a complex apparatus and therefore needed time to evolve, with respect to time between dated biological breakthrough. However, having the development of oxygenic prokaryotes at 2.75 Ga and the development of eukaryotic life at 2.1 Ga illustrates how Life forms can evolve quickly to higher complexity levels. Therefore the presence of an anoxygenic photosynthetic apparatus around 3.8 Ga is plausible, even if the earliest phototrophic presence is attested at 3.4 Ga (Fig. 1; Olson, 2006).

The composition of the BIFs (Dales Gorge Member, Hamersley group, DDH 44, Western Australia) in trace element and phosphate, showed that the availability of nutrients was sufficient to sustain the growth of such organisms (Konhauser *et al.*, 2007[2]). It has also been shown that the BIFs from the Roper Group (west of Gulf of Carpenteria, Northern territory, Australia) were formed under anoxic conditions (Shen *et al.*, 2003). Those results have been confirmed by studying the stratigraphy of Buck Reef Chert (Australia; Kappler *et al.*, 2005[1]) showing the offshore formation of iron-rich chert under anoxic conditions at the base of storm waves. Furthermore, the study of Kappler *et al.* (2005[1]) suggests that the cultivated iron-oxidizing anoxygenic phototrophs have the physiological potential to oxidize all of the reduced iron from hydrothermal vents, before it reaches a possible upper oxic water layer, and form iron oxides precipitates (Fig. 6). More precisely, they have shown that the light intensity, reaching the depth where anoxygenic phototrophs could have developed, was sufficient to sustain their growth in a layer up to 17,5 m thick with 10^6 cells ml^{-1}. Overmann

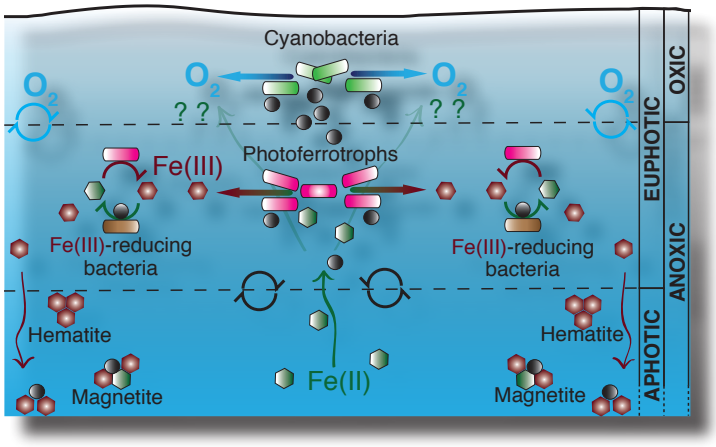

Figure 6: Photoferrotrophic BIF precipitation. The Fe(II) is used as an electron donor for photosynthesis, before it reaches the oxic cyanobacterial-layer. The produced oxides will then precipitate on the seafloor. Recycling of Fe(II) through ferrireduction within the water column is possible.

showed (1992) for the Black Sea that anoxygenic phototrophs can indeed grow at 60 m to 110 m depth with as little light as 0.0005 % of the surface intensity.

Moreover, a recent study has linked the layering succession of iron and silica in BIFs to temperature fluctuations (Posth *et al.,* 2008). They have shown experimentally that the temperature influenced the iron-oxidation rates of IOP and therefore the amount of Fe(III) precipitates (Fig. 7). In concomitance with a silica precipitation at cool temperature (5°C) they have obtained a layering of Fe(III) and silica reassembling BIFs stratification (Fig. 3.A; Fig. 7). Those results, however, are based on Fe(II)-oxidation rates determined with pure cultures that are isolated from sediments and grew in optimized mineral media.

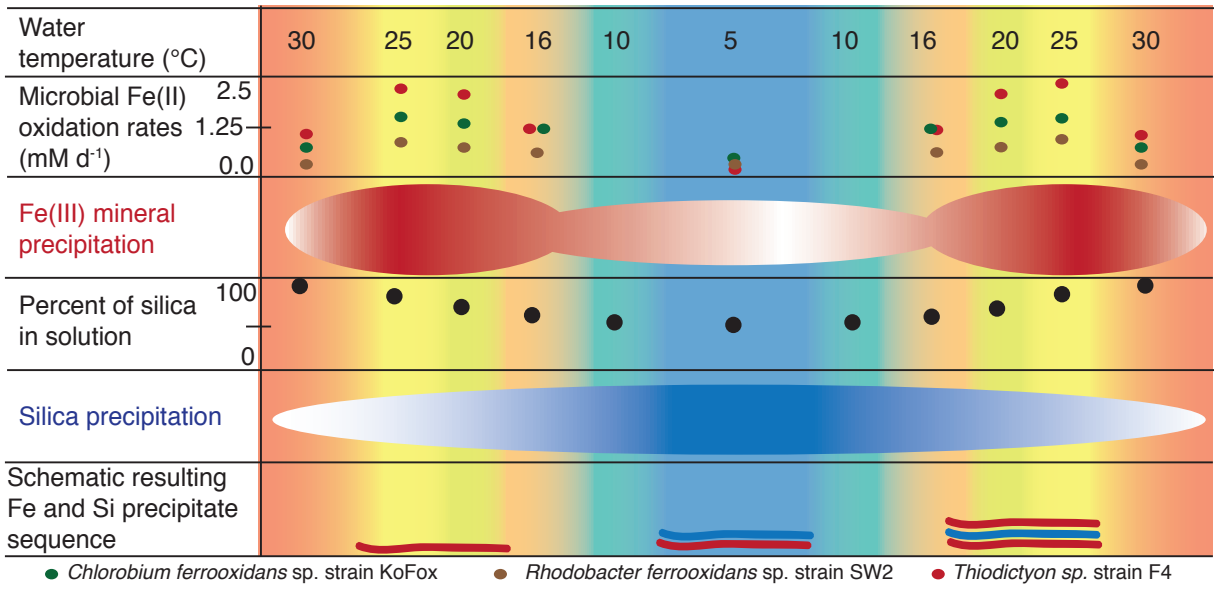

Figure 7: Temperature-dependant Fe(II) and silica alternation in a phototrophic BIFs model. Experimentally determined microbial Fe(II) oxidation rates at fluctuating temperature and the resulting Fe(III) mineral precipitation. The effect of temperature fluctuations, between 5 and 30 °C, on abiotic silica precipitation. The coloured gradient (red and blue) indicates the intensity of precipitation: intense colour for high intensity, and white for trace precipitation. This experiment was performed with three strains of IOP. Figure and legend slightly modified from Posth *et al.,* 2008.

An experimental work aimed at illustrating the role of phototrophic Fe(II)-oxidation in BIF formation under the environmental conditions as they may have existed during the Archean is still strongly needed (Konhauser *et al.,* 2005; Johnston *et al.,* 2009; Severmann *et al.,* 2009; Tangalos *et al.,* 2010). Indeed, a recent model for an Archean Ocean would help research in the Early Earth field (Caiazza *et al.*, 2007), just as Proterozoic analogues (e.g. Black Sea) did with the sulfur cycle (Thamdrup, 2000; Algeo & Lyons, 2006; Meyer & Kump, 2008; Lyons *et al.*, 2009[2]; Montoya-Pino *et al.*, 2010). In a recent study, Crowe *et al.* (2008[1]) reported the presence of anoxygenic phototrophic green sulfur bacteria in the chemocline of an Archean Ocean analogue (Lake Matano, Indonesia; Crowe *et al.,* 2008[2]), although both sulfate-reduction rates and sulfate concentrations were insufficient to maintain an estimated population density of 10^9 cell ml^{-1} (Crowe *et al.* 2008[1]). Since this lake is Fe(II) rich, they suggested that a photoferrotrophic metabolism was implied to sustain their growth. However, direct evidence for a ferrotrophic activity could not be provided. Alternatively these green anoxygenic phototrophs could have grown photoheterotrophically or with H_2 as an electron donor. Therefore, the potential for a modern Archean model exists, although it is still needed to identify a photoferrotrophic activity in it. Archean iron-oxidation processes are still to be determined, as well as their possible interaction with an earlier oxygen production (Fig. 6: question marks). Furthermore, while calculation shows the possibility for Fe(II) to be oxidized before reaching oxic layer (Kappler *et al.,*

2005[1]), we do not have any experimental data, or natural model, demonstrating a cohabitation between photoferrotrophs and oxygenic bacteria. We therefore looked for a modern water column, approaching Archean ocean chemistry (Crowe *et al.*, 2008[2]), to verify how the ecosystem is structured with regard to the main phototrophic guilds and to the microbial iron cycle.

3. Microbial iron cycle

This section is mainly based on the reviews of Thamdrup (2000), Roden (2004[1-2]) and Weber (2006[1]). The general microbial iron cycling according to Roden (2004[2]) is summarized in Figure 8.

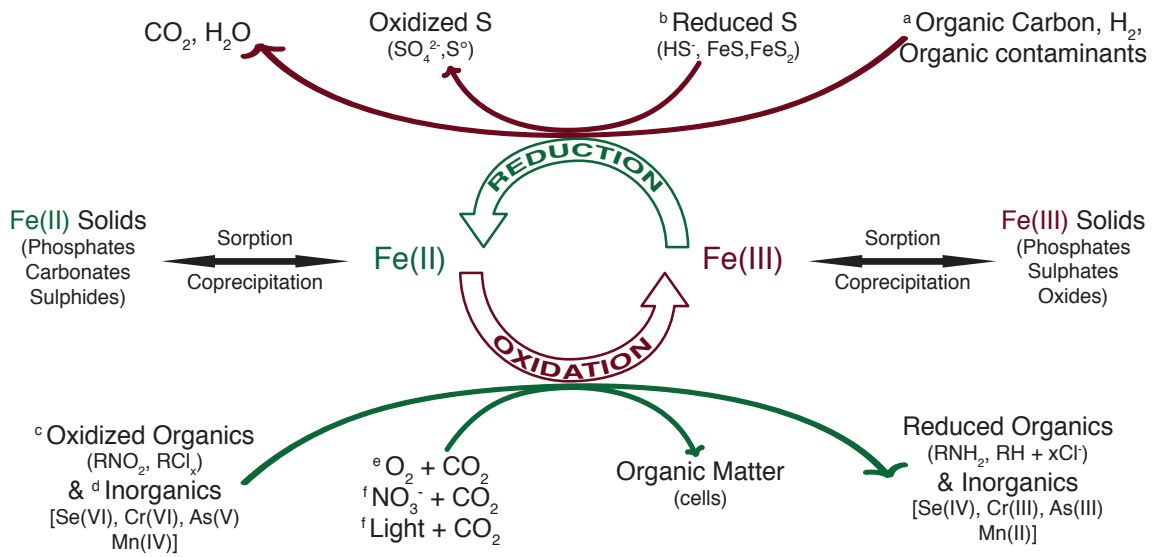

Figure 8: Summary of the known microbial iron transformation. a | circumneutral pH: Lovley (2000), Thamdrup (2000[2]); acidic pH: Johnson (1998), Blake & Johnson (2000), see also Küsel(1999) and Peine *et al.*, (2000) **b |** circumneutral pH: direct enzymatic catalysis doubtful; see Thamdrup (1993), Lovley (1994), and Schippers & Jørgensen (2002); acidic pH: Blake & Johnson (2000), Pronk & Johnson (1992). **c |** and **d |** involvement of enzymatic catalysis not yet known. **e |** circumneutral pH: Emerson (2000); acidic pH: Johnson (1998), Blake & Johnson (2000); see also Edwards *et al.*, (2000). **f |** Straub *et al.*, (2001). Figure and legend modified from Roden *et al.*, (2004[2]).

3.1. Fe(III)-reduction: An ancient respiration

Iron respiration was proposed as one of the first microbial metabolisms to have evolved, before the sulfate/sulfur, nitrate and oxygen respiration (Vargas *et al.*, 1998), thus questioning on the availability of Fe(III) at that time. Fe(III)-respiration has been observed in a wide range of microorganisms, including those most closely related to the last universal common ancestor (Weber *et al.*, 2006[1]). The electron transfer to extracellular Fe(III) has been conserved in *Archaea* (Vargas *et al.*, 1998; ; Kashefi & Lovley, 2000) and in *Eubacteria* (Lovley, 2004).

It is now established that microbial reduction of Fe(III) oxides by ferrireducing bacteria (FRB) controls the Fe(III) reductive processes and the degradation of organic matter (up to 90%) in non-sulfidogenic sedimentary environment (Canfield *et al.*, 1993). Organic matter is not the only source of electrons as also H_2 can be used as substrate (Lovley *et al.*, 2004).

The model established by Konhauser *et al.* (2005), to understand the fate of the of organic matter (as an electron donor) when temporally attached to Fe(III), implies an excess of Fe(III) in the sediments. The first of the four ways proposed by this team is that there were more ferric (hydr)oxides produced relative

to carbon fixation. A second view is that there was a non-quantitative association of cells with the ferric (hydr)oxide due to segregation between dense Fe(III) particles and dissolved organic carbon (DOC): i.e. part of planktonic dead cells remains in suspension and is mineralized in the same or upper layer (Kappler *et al.*, 2005[1]). The two other hypotheses focus on the sediment itself. The first is that part of the fermentation products could have diffused away from Fe(III) particles. It would therefore not have been available for ferrireduction and would have left the iron in its oxidized state. The final theory is that another anaerobic respiration, such as methanogenesis, would have competed with FRB for fermentation products (Rothman *et al.*, 2003). An alternative possibility for FRB "inhibition" is that there was a reduced surface-site availability for Fe(III) reduction. This could have been either due to a faster rate of Fe(III) sedimentation which would thus separated organic matter from ferric (hydr)oxide (Kappler *et al.*, 2005[1]), or to the covering of organic matter by ferrireduction end products (Stolz *et al.*, 1990; Davis *et al.*, 2002). Furthermore, the adsorbtion/ precipitation of Fe(II) on Fe(III) oxide surface, as for example the formation of goethite by adsorption of Fe(II) on Fe(III) (Roden & Urrutia, 2002), could have limited Fe(III)-respiration.

3.2. Photoferrotrophic Fe(II)-oxidation

Photoferrotrophic bacteria (IOP: Iron Oxidizing Phototrophs) as anaerobic photolithoautotrophs, use light as energy and reduced iron as electron donor for CO_2 fixation and biomass formation (equation 1; Widdel *et al.,* 1993):

$$4\ Fe(II) + HCO_3^- + 10\ H_2O + \textit{Light} \longrightarrow 4\ Fe(OH)_3 + \{CH_2O\} + 7\ H^+ \quad (1)$$

So far no archeal IOP has been identified, but seven eubacterial pure cultures have been characterized (eg. Jiao *et al.*, 2005; Straub *et al.*, 1999; Tab. 1). They have been isolated from freshwater environments. They are phylogenetically related to purple sulfur phototrophs (*Thiodictyon sp., Rhodovulum iodosum* and *Rhodovulum robiginosum*), purple non-sulfur phototrophs (*Rhodobacter ferrooxidans, Rhodopseudomonas palustris* and *Rhodomicrobium vannielii*) and green sulfur phototrophs (*Chlorobium ferrooxidans*) (tab. 1). As other anoxygenic photosynthetic organisms, photoferrotrophs only use photosystem I.

Table 1 : Samples sources of all known and isolated photoferrotrophs.

Strain	Samples sources	References
	Freshwater environment	
Rhodobacter ferrooxidans	Iron rich ditches (Schaumburg Forest, Germany)	Ehrenreich, 1994
Rhodomicrobium vannielii	Ditches (Tübingen-Bebenhausen, Germany)	Heising, 1998
Chlorobium ferrooxidans	Freshwater creeks / ditches (Constance, Germany)	Heising, 1999
Thiodictyon sp.	Marsh (Woods Hole, USA)	Croal, 2004
Rhodopseudomonas palustris	Iron-rich mats (School Street Marsh, USA)	Jiao, 2005
	Marine environment	
Rhodovulum iodosum *Rhodovulum robiginosum*	Mud flat (North Sea, Germany)	Straub, 1999

At pH=0 the redox potential of Fe^{3+}/Fe^{2+} is of +770 mV (E_0), at neutral pH this potential (E_0') is much lower: +220 mV. The reaction centre of green sulfur phototrophs being higher than purple sulfur phototrophs, -300mV (Heising *et al.*, 1999) instead of -450 mV (Widdel *et al.*, 1993), the energy gain from the electron transfer between Fe(II) and the reaction centre may be insufficient for autotrophy (Heising *et al.*, 1999). In addition, most of the IOP are considered as photoferroautotrophs. Caiazza, however, has shown that the strain *R. capsulatus* SB1003 is only capable of photoferroheterotrophy (Caiazza *et al.*, 2007). This strain could not grow lithoautotrophically on soluble Fe(II) but was able to grow when iron was associated with citrate. The explanation given by Caiazza is that these microorganisms used Fe(II) as an electron donor for a

heterotrophic growth with citrate as a carbon source: the formed Fe(III)-citrate undergoes a photochemical reaction resulting in Fe(II) and acetoacetic acid that can be assimilated as a carbon source (Fig. 9). His results suggest that "... *Fe(II) oxidation may be a general mechanism whereby some Fe(II)-oxidizing bacteria mine otherwise inaccessible organic carbon sources*" (Caiazza *et al.*, 2007).

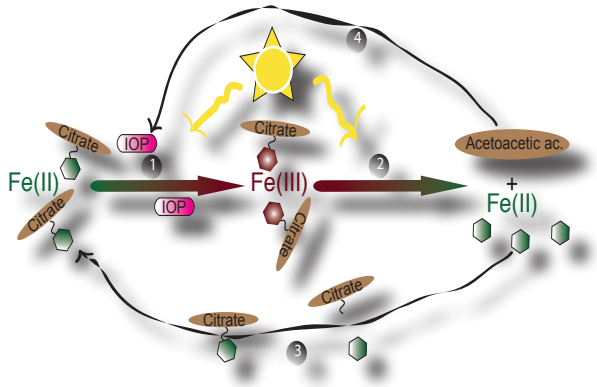

Figure 9: Model of Fe(II)-oxidation leading to carbon acquisition. In presence of Fe(II)-citrate, *Rhodobacter capsulatus* SB1003 oxidizes Fe(II) to Fe(III)-citrate (1). In the presence of light, Fe(III)-citrate undergoes a photochemical reaction yielding Fe(II) and 3-oxoglutarate, the latter of which spontaneously decarboxylates and becomes acetoacetic acid (2). As a result of the photochemical reaction, the resulting Fe(II) can become bound by citrate (3) and microbially reoxidized. The acetoacetic acid is used as a carbon source for growth (4). Legend and figure modified from Caiazza *et al.* (2007).

Photoferrotrophy is considered to be the earliest type of photosynthetic process undergone by life (Xiong *et al.*, 2000; Des Marais, 2000; Raymond *et al.*, 2003). Even if purple sulfur bacteria are found to oxidize reduced iron (*Thiodictyon* sp.), purple non-sulfur bacteria (*Rhodobacter ferrooxidans*) oxidize iron more efficiently in the same cultural setup (Kappler *et al.*, 2005[1]). As studies indicate that photoferrotrophs are unable to promote Fe(II) mineral dissolution and are limited by the mineral solubility (Kappler & Newman, 2004), therefore, the impact of those microorganisms on iron cycling in soils should be of minor importance on a global scale (Weber *et al.*, 2006).

3.3. Microaerophilic Fe(II)-oxidation

Some microaerophilic chemolithoautotrophic microorganisms can also grow by the oxidation of reduced iron accordingly to:

$$4\ Fe(II) + 2\ O_2 + 8\ H_2O \longrightarrow 4\ Fe(OH)_3 + 4\ H^+ \quad (2)$$

In the present work they will be abbreviated as IOOR, which stands for iron oxidizing oxygen reducing bacteria. Cultural studies with opposing gradients of Fe(II)-O_2 (Kucera and Wolfe, 1967; Jones, 1983) have extended the range of bacteria known to oxidize Fe(II) with O_2 from the well known *Gallionella sp.* and bacteria from the *Sphaerotilus-Leptotrix* group to the γ-*Proteobacteria* (Emerson & Moyer, 1997; Emerson, 2000). Roden *et al.*, (2004[1]) have shown through cultural experiments that IOOR were able to outperform the natural chemical oxidation of Fe(II) with O_2 in environments where they are both present.

3.4. Nitrate dependent Fe(II)-oxidation

The third known metabolic pathway is the anaerobic nitrate-dependent iron-oxidation (NDIO):

$$10\ Fe(II) + 2\ NO_3^- + 24\ H_2O \longrightarrow 10\ Fe(OH)_3 + N_2 + 18\ H^+ \quad (3)$$
$$2\ Fe(II) + NO_3^- + 5\ H_2O \longrightarrow 2\ Fe(OH)_3 + NO_2^- + 4\ H^+ \quad (4)$$

NDIO metabolisms have been identified in organisms from various fresh water and saline sediments (Straub *et al.*, 1996; Benz *et al.*, 1998; Edwards *et al.*, 2003; Weber *et al.*, 2006[2-3]). Only one strain was shown to be an obligate lithoautotroph (Edwards *et al.*, 2003), while all others needed a second electron donor and/or an organic co-substrate such as acetate for Fe(II)-oxidation (Straub *et al.*, 1996; Chaudhuri *et al.*, 2001; Hauck *et al.*, 2001; Lack *et al.*, 2002). Most of NDIOs are heterotrophs (Straub *et al.*, 2004; Hauck *et al.*, 2001; Weber *et al.*, 2001/2006[2]) and facultative anaerobes (Benz *et al.*, 1998; Hauck *et al.*, 2001; Lack *et al.*, 2002; Edwards *et al.*, 2003).

Although N_2 is the main product of nitrate reduction (Straub, 1996; Nielsen, 1998; Chaudhuri, 2001; Weber *et al.,* 2001/2006[2]), intermediary products such as NO, NO_2^- or N_2O may also be produced (Hafenbradl *et al.,* 1996; Straub *et al.,* 1996; Weber, 2001/2006[2-3]; Finneran *et al.,* 2002). The end product of nitrate oxidation can vary depending on the growth state of the same culture (weber, 2006[3]).

It is interesting to note that some NDIOs can use different electron acceptors for iron oxidation, such as chlorates and perchlorates (Finneran *et al.,* 2002; Weber, 2006[1]). They can also use alternative electron donors and even perform a dissimilatory iron reduction with organic matter as an electron source (Finneran *et al.,* 2002; Shelobolina *et al.,* 2003; Weber, 2006[3]). In addition to this metabolic versatility, it has been shown that some NDIOs are able to oxidize, in addition to soluble Fe(II) also Fe(II) in neosilicates, phylosilicates or even FeAsS (Weber *et al.,* 2001; Shelobolina *et al.,* 2003). Weber (2006[1]) suggested that the metabolic ubiquity of NDIO may influence modern anoxic iron oxidation on a global scale. With regard to to their implication in BIF settlement, NDIO may have played a role because of the possible production of nitrogen oxides independently from the presence of oxygen: "*... light-independent Fe(II) oxidation coupled to nitrate reduction has received much less attention as a model; however, it does provide an additional mechanism leading to BIF formation in the Precambrian and, in contrast to known phototrophic FOM* (ferro-oxidizing microorganisms)*, extant nitrate-dependent FOM have been shown to produce significant quantities of extracellular magnetite and hematite. Lightning discharge contributed to the fixation of nitrogen (N_2) into nitric oxide (NO, ~10^{12} g per yr) further forming nitrous oxide (N_2O), the nitrite ion (NO_2^-) and the nitrate ion (NO_3^-) through abiotic disproportion reactions. Such oxidized nitrogen species could have functioned as an electron acceptor for early FOM, leading to BIFs in anoxic environments*" (Weber, 2006[1]).

3.5. Fe(III)-solubility

Nitrate dependent Fe(II)-oxidizers seem to oxidize Fe(II) on cell surface (Benz *et al.,* 1998; Chaudhuri *et al.,* 2001; Edwards *et al.,* 2003), photoferrotrophs oxidize Fe(II), presumably by a periplasmic c-type cytochrome (Croal *et al.,* 2007; Jiao & Newman, 2007). Once oxidized, Fe(III) seems to be released as a colloidal Fe(III) (hydr) oxide that will form Fe(III) aggregates. One major problem for ferrooxidizing microorganisms is that the end product of Fe(II)-oxidation is highly insoluble at neutral pH.

Mechanisms for Fe(III) excretion and other strategies to prevent cell incrustation are required. Although Fe(III) (hydr)oxides remain attached to the cell wall of photoferrotrophs they never get completely encrusted (Straub *et al.,* 2001; Kapller *et al.,* 2004/2008). Kappler (2004) proposed that Fe(III) (hydr)oxides only aggregate when a critical size is reached. Another study suggested that acidification in the immediate proximity of photoferrotrophic cells influences Fe(III) solubility and/or aggregate size, thereby preventing cell incrustation (Jiao *et al.,* 2005). Even if it has not been shown that photoferrotrophs excrete organic chelating agents, the presence of organic matter in natural ecosystem does alter the availability of Fe(II) and Fe(III) and could therefore be a means of exporting Fe(III) away from the cells (Caiazza *et al.,* 2007). Sobolev and Roden (2002) showed that a strain of NDIO had an area of iron-oxide precipitation larger than the biological development area, suggesting precipitation of iron oxide up to a depth of two centimeters into the anoxic zone. This suggests the excretion of low molecular weight compounds that would be complexed with the ferric iron, and therefore prevent cell incrustation. Roden (2004[1-2]) proposed that when the chelates move towards the cell by diffusion they become unstable and then precipitate. This mechanism produces reactive iron oxides that could readily be used by FRB which would create an interaction with a total cycling of iron between those two types of microorganisms (Roden *et al.,* 2004[1-2]; Weber *et al.,* 2006[1]).

On the reductive side of the Fe-cycle, iron oxides particles cannot pass the cell wall to be reduced (Weber *et al.*, 2006[1]). Three mechanisms have been proposed to overcome this limitation: direct contact (*Geobacter* spp., Nevin & Lovley, 2000[1]), exogenous and endogenously produced external electron shuttles, or through the use of a chelating ligand (Nevin & Lovley, 2000[2]; Nevin & Lovley, 2002). These mechanisms are

summarized in figure 10.

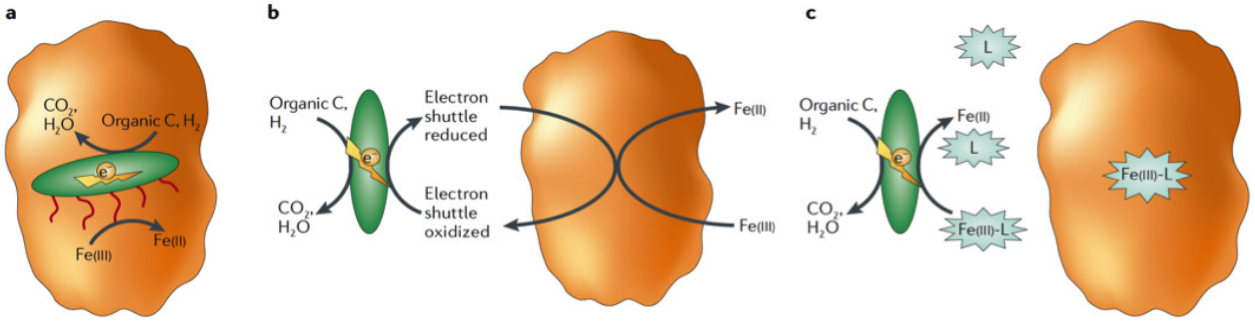

Figure 10: Microbial strategies mediating electron transfer to insoluble Fe(III) oxides. Three primary strategies have been proposed to facilitate the electron transfer between microorganisms and solid Fe(III) oxide surfaces. **a** | In Geobacter spp. direct contact with the oxide surface is required. The production of 'nanowires', conductive extracellular appendages, facilitates electron transfer by functioning as an electrical conduit to the Fe(III) oxide surface. **b** | An endogenously or exogenously produced electron shuttle mediates electron transfer to solid-phase Fe(III) oxides. **c** | The production of complexing ligands as in the case of Geothrix sp. aids in the dissolution of the solid-phase Fe(III) oxide providing a soluble Fe(III) form more readily available to the microorganism. Although these strategies have only been demonstrated for Fe(III)-reducing microorganisms, similar strategies might be used by Fe(II)-oxidizing microorganisms that are utilizing solid-phase Fe(II) electron donors. e^-, electrons; L, ligand. Figure and legend from weber (2006[1]).

4. Study site

4.1. Iron meromictic lakes

Meromictic lakes in general are lakes with chemically enhanced density stratification whose bottom water (monimolimnion) never mix with the overlaying waters (Fig. 11). Factors supporting a permanent stagnation of the water column include: lake morphometry, wind-sheltered situation, climate, and low rate of water inflow. Furthermore, the deepest water usually contains a relatively high concentration of dissolved salts, which renders them dense and increases the stratification by the establishment of a density gradient (e.g. Wetzel, 2001; Ehrlich *et al.*, 2009).

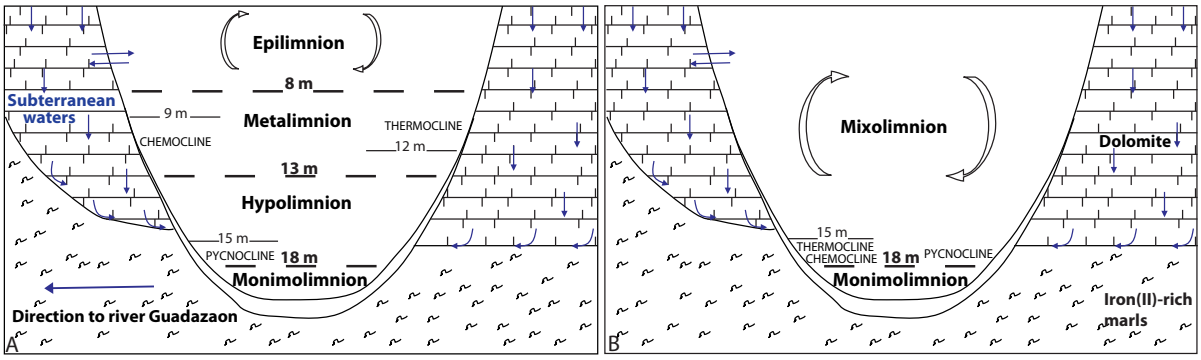

Figure 11: Stratification patterns of the meromictic Lake La Cruz. **A |** Summer stratification **B |** Winter stratification with an upper mixed layer (mixolimnion) and a permanently anoxic bottom water (monimolimnion). Modified from Rodrigo *et al.*, (2001).

Organic matter of autochthonous (produced in the lake) or allochthonous (e.g. riverine input) origin fuels the reduction of ferric oxides in the sediment. The liberated ferrous iron and bicarbonate diffuse into the water column, where they accumulate and greatly contribute to the stability of the water column. Kjensmo (1967) showed that the hypolimnic iron accumulation can reach such levels (>250 mg l^{-1}) that the

corresponding density gradient renders a lake permanently meromictic. The term "iron-meromixis" was then used by this author to describe such a state. However, lake stability due to accumulation of ferrous bicarbonate is very labile, i.e. such stability is easily broken or reduced by the introduction of oxygen or sulfide. Both compounds react with ferrous iron to produce insoluble products (FeOOH, FeS), thus relieving the water column from its iron burden (Kjensmo, 1967). It should be mentioned that in the scientific literature the term "iron meromixis" is applied in a less strict sense than used by Kjensmo. It is generally used for iron-rich permanently stratified lakes even when iron is not responsible for the density stratification (e.g. Lake La Cruz, Spain). However, we prefer to use in this work "iron-rich meromictic lake", instead of "iron -meromictic lake".

The majority of meromictic lakes, however, possess sulfidic hypolimnic waters due to the activity of sulfate reducing bacteria: e.g. Lago di Cadagno in Switzerland (Orem *et al.,* 1991; Overmann *et al.,* 1996; Rodrigo *et al.,* 1999; Wetzel, 2001; Canfield *et al.,* 2010). Iron-rich meromictic lakes are conversely rare and unusual ecosystems and only a handful have been discovered worldwide: Store Aakalungen (Kjensmo, 1967), Lake Nordbytjernet and some other small lakes in southeast Norway (Hongve, 1999/2003), Lake of the Clouds (Anthony, 1977), Lake Hall (Balistrieri *et al.,* 1994), Lake Paul (Taillefert & Gaillard, 2002), Lake Matano (Crowe *et al.,* 2008[2]), Lake La Cruz (Rodrigo *et al.,* 2001) and the volcanic Lake Pavin in France (Martin, 1985; Aeschbach *et al.*, 2002).

4.2. Lake La Cruz

Lake La Cruz is a small mesotrophic doline lake in the Dolomites of the Central Iberian Ranges, located at 1000m near Cuenca (Spain). The small surface/depth ratio and its location inside a dissolution basin with steep vertical walls rising 20-30 m above the water surface reduces the forces of wind-driven currents in the lake and limits vertical mixing. The lake is meromictic but differs from other karstic lakes in Spain (e.g. Lake Vilar, Lake Banyoles, Lake Cisó) because of its low sulfate concentrations, which are due to the absence of gypsum in the surrounding rock substrate (Vicente and Miracle, 1988; Miracle *et al.,* 1992). High concentrations of dissolved bicarbonate, calcium, ammonium, and magnesium in the hypolimnion contribute to the stability of the water column (Rodrigo *et al.,* 2001). Iron is much more abundant than sulfur and Fe(II) reaches concentrations as high as 250 µM at the sediment water interface. The chemocline of Lake La Cruz is situated in the euphotic zone at a depth of about 10-13 m, depending on the climatic conditions and the season (Julia *et al.*, 1998; Rodrigo *et al.,* 2001; Fig. 11)

A very intriguing feature of Lake La Cruz that purple and green anoxygenic phototrophic bacteria are found in the sulfide-poor but ferrous iron-rich water column (Vicente and Miracle, 1988; Rodrigo *et al*, 2000/2001; Romero *et al.,* 2006; Romero-Viana *et al.*, 2010). At the O_2/H_2S interface sulfide never exceeds 3 µM and barely reaches 20 µM at the sediment water interface. Since it has been shown in pure cultures that some species of both groups are able to perform anoxygenic photosynthesis with Fe(II) as electron donor (Ehrenreich and Widdel, 1994; Heising *et al.,* 1999) they may well be involved in the anoxic oxidation of ferrous iron in Lake La Cruz. Three anoxygenic phototrophic sulfur bacteria were isolated with sulfide as electron donor by Rodrigo *et al*. (2000) and described as *Amoebobacter sp.* (purple), *Chlorobium clathratiforme* (green), and *Chlorobium phaeobacterioides* (brown-green). Whether the isolates grow with Fe(II) was unfortunately not tested. The green isolates, however, were able to grow on solid FeS while *Amoebobacter sp*. was not (Rodrigo *et al.,* 2000). The abundance and distribution of *Amoebobacter sp*. and *Chl. clathratiforme* was studied during two annual cycles by direct counts and pigment analysis and it was found that light was probably the major limiting factor for their development (Rodrigo *et al.*, 2000). The role of the electron donor (H_2S, Fe(II)) in limiting photosynthesis, however, was not explored. There is thus a clear gap of knowledge as to whether the anoxygenic photosynthetic bacteria present in this lake participate actively in Fe(II)-oxidation.

Julia *et al.,* (1998) published the only study dealing with sediments of Lake La Cruz. Pollen, diatom, chydorid, ostracod, charcoal as well as data on authigenic mineral composition were used to date the onset of meromixis and to determine the trophic evolution since the Middle ages. The onset of meromixis at about 1700 AD coincides with the Maunder minimum in the Little Ice Age as well as with the period of increasing human population, woodland clearance and agricultural expansion.

Further studies on Lake La Cruz were mostly concerned with the biology and population dynamics of phyto- and zooplankton (Dasí and Miracle, 1991; Armengol and Miracle, 2000) and the description of a short-term calcite precipitation event (Rodrigo *et al.,* 1993).

Romero *et al.* (2006) investigated the sedimentation patterns of anoxygenic photosynthetic bacteria pigments over a three-year period. They concluded that an important population of anoxygenic photosynthetic bacteria were developed at the chemocline of lake La Cruz. Casamayor *et al.,* (2001) studied the composition of planktonic *Archaea* in several (mostly Spanish) sulfidic lakes using PCR-denaturing gradient gel electrophoresis (DGGE) and sequencing targeting the 16S rRNA gene. The focus of their study was on Lake Cisó and Lake Vilar but a sample from Lake La Cruz from 12.25 m depth was also included. It was found that the archaeal community consisted of some 40% *Thermoplasmales* and 35% methanogens, with the rest of the sequences remaining unidentified.

However, the microbiology and biogeochemistry of iron oxidation and reduction has not been studied at all. Although some values of dissolved and particulate iron are reported (Vicente and Miracle 1988; Rodrigo *et al.,* 2001) a detailed chemical speciation of iron in the water column and the sediment is lacking.

5. Project objectives

Konhauser (2002) and Kappler (2005) have demonstrated the potential for BIF to be the oxidization product of photoferrotrophy in the Archean Ocean euphotic zone. Crowe (2008[1,2]) have described the biogeochemical conditions that characterize an ecosystem as a potential Archean Ocean analogue: a Fe(II)-rich and sulfate-poor water column with the presence of anoxygenic phototrophs at the chemocline. Studies have reported and described Lake La Cruz water column as ferruginous, sulfate-poor (Rodrigo *et al.*, 2001) and presenting dense population of anoxygenic phototrophs (Romero *et al.*, 2006). However, to date no natural system characterized by Archean environmental conditions and hosting actives anaerobic Fe(II)-oxidizers have been described.

The first aim of this thesis was to characterize, in collaboration with the Department of Microbiology and Ecology in Valencia (Spain), the physical and chemical structure of Lake La Cruz with a particular focus on iron cycling. As the Archean Ocean was an anoxic environment, the second aim was to investigate the microbiological anaerobic Fe-cycling in Lake La Cruz chemocline, with a particular interest on Fe(II)-oxidation. The objectives were i) to prove any *in situ* anaerobic Fe(II)-oxidation and to determine whether it was light- or nitrate-dependent, ii) to measure potential Fe(II)-oxidation rates for a comparison with estimated values for the Archean (Konhauser *et al.*, 2002; Kappler *et al.*, 2005) and iii) to enrich and to identify the organisms responsible for anaerobic Fe(II)-oxidation.

A third goal was to create a conceptual model of the biogeochemical interactions in the cycling of iron, sulfur, and oxygen in Lake La Cruz. This may allow to compare this natural Archean Ocean analogue with existing theoretical models. Such an approach may lead to an improvement of the tools used in paleoecology and to the understanding of Archean Ocean stratification.

If Lake La Cruz water column represents an Archean Ocean analogue, we should be able to detect an anaerobic Fe(II)-oxidation at the chemocline. Then, the fate of the potentially formed Fe(III) will be determined.

CHAPTER II: Photoferrotrophy in a ferruginous Neoarchean Ocean analogue

X. Alexis Walter, Antonio Picazo-Mozo, Maria R. Miracle, Eduardo Vicente, Antonio Camacho, Michel Aragno, Jakob Zopfi

1. Article

1.1. Abstract

The deposition of Banded Iron Formation (BIF) during the Archean and Paleoproterozoic is conventionally attributed to the precipitation of iron-oxides resulting from the abiotic reaction of ferrous iron (Fe(II)) with oxygen (Cloud, 1968). Oxygenic photosynthesis, however, appeared only around 2.7 Ga (Des Marais, 2000; Kump, 2008; Godfrey & Falkowski, 2009), thus raising questions as to what may have caused BIF precipitation before that time. The discovery of anoxygenic phototrophs thriving through the oxidation of Fe(II) (Widdel *et al.*, 1993; Heising*et al.*, 1999) has provided support for a bacterial origin for early BIFs (Konhauser*et al.*, 2002; Kappler *et al.*, 2005[1]). Despite reports of anoxygenic phototrophs that may oxidise Fe(II) in the environment (Crowe *et al.*, 2008), a model ecosystem where photoferrotrophs are demonstrably active is still lacking (Svermann & Anbar, 2009; Johnston *et al.*, 2009). Here, we show direct evidences of a photoferrotrophic activity in the ferruginous meromictic lake La Cruz (Spain) that sustains dense populations of purple and green anoxygenic phototrophic bacteria despite low sulphate and sulphide concentrations. We observed *in situ* photoferrotrophic activity through stimulation of phototrophic carbon uptake in the presence of Fe(II), and quantified light-dependent Fe(II)-oxidation by the natural chemocline microbiota to assess their potential quantitative contribution to ancient BIF formation. In addition, a green photoferrotrophic bacterial consortium was enriched for the first time from a ferruginous water column. This new model ecosystem will allow testing current concepts on ancient primary productivity and its interactions with the iron- and sulphur cycles and may help to refine paleoenvironmental proxies.

1.2. Introduction

The anoxic Archean ocean chemistry was characterized by a low sulphate content and high concentrations of ferrous iron (Fe(II)) of probable hydrothermal origin (Holland, 19973; Anbar & Knoll, 2002; Canfield, 2005). From this water column, alternating sedimentary deposits of iron oxide minerals and silica precipitated between 3.8 and 1.8 Ga ago (Anbar & Knoll, 2002) and became preserved in the geological record as Banded Iron Formations (BIF). Mechanisms of Fe(II) oxidation are still debated and include, besides the widely accepted abiotic reaction with photosynthetically produced oxygen (Cloud, 1968), photocatalytic oxidation by UV radiation (Braterman *et al.*, 1983), and direct oxidation by anoxygenic photosynthesis (Konhauser *et al.*, 2002; Kappler *et al.*, 2005[1]). Such photoferrotrophic bacteria use light as energy and reduced iron as an electron source for CO_2 fixation and biomass formation, according to equation (1) (Widdel *et al.*, 1993; Heising *et al.*, 1999):

$$4\ Fe(II) + HCO_3^- + 10\ H_2O + Light \rightarrow 4\ Fe(OH)_3 + \{CH_2O\} + 7\ H^+ \quad (1)$$

While recent experimental work is not in favour of a significant contribution of photochemical processes to BIF formation (Konhauser *et al.*, 2007), microbial Fe(II) oxidation remains an appealing possibility (Konhauser *et al.*, 2002; Posth *et al.*, 2008). Although the evolution of photosynthesis is complex and horizontal gene transfer has played an important role, it is now generally accepted that anoxygenic phototrophic bacteria evolved before oxygen-producing cyanobacteria, which represent the pinnacle of bacterial phototrophy regarding the complexity of their photosynthetic apparatus (Xiong *et al.*, 2000; Raymond *et al.*, 2003). The isolation of phototrophic Fe(II)-oxidizing bacteria (Widdel *et al.*, 1993; Heising *et al.*, 1999) has allowed the influence of light intensity on iron oxidation and the role of temperature on the alternating precipitation of iron oxides and silica to be tested experimentally (Posth *et al.*, 2008). Those estimates, however, were based on Fe(II)-oxidation rates determined in optimized mineral media with bacterial cultures isolated from sediments. Therefore, experimental work aimed at elucidating the role of phototrophic Fe(II)-oxidation under environmental conditions as they may have existed during the Archean is strongly needed (Svermann & Anbar, 2009; Johnston *et al.,* 2009). In a recent study, the presence of green anoxygenic phototrophic bacteria in the water column of an Archean Ocean analogue (Lake Matano, Indonesia) has been reported, and it has was suggested that they may be involved in Fe(II)-oxidation (Crowe *et al.,* 2008). Nevertheless, direct evidence for photoferrotrophic activity in a recent water column and quantitative data on their contribution to Fe(II)-oxidation are still lacking. To address this, we have investigated the iron-rich, sulphate-poor meromictic lake La Cruz (Spain; Rodrigo *et al.,* 2001). Our results provide evidences for anaerobic phototrophic Fe(II)-oxidation in a ferruginous water column. Oxidation rates determined with natural microbial communities from the chemocline agreed well with previous estimates (Kappler *et al.,* 2005[1]; Lyons *et al.,* 2009).

1.3. Results and discussions

Lake La Cruz is a oligo-mesotrophic lake in the dolomites of the Central Iberian Ranges with an oxygenic primary production of 146 g C m^{-2} $year^{-1}$. Meromictic since the Maunder Minimum, it possesses a permanently stratified anoxic water column exhibiting pronounced seasonal dynamics (Rodrigo *et al.,* 2001). Most meromictic lakes and other permanently stratified water bodies are euxinic, i.e. anoxic and sulphidic below the chemocline (Lyons *et al.,* 2009). Lake La Cruz is a rare exception as its anoxic bottom water layers contain little sulphide but are rich in Fe(II) (Fig. 12A).

Sulphate concentrations are low (<35 µM; Fig. 12A) due to the virtual absence of sulphur containing minerals in the surrounding dolomite rocks and marlstones (Rodrigo *et al.,* 2001). The parallel decrease

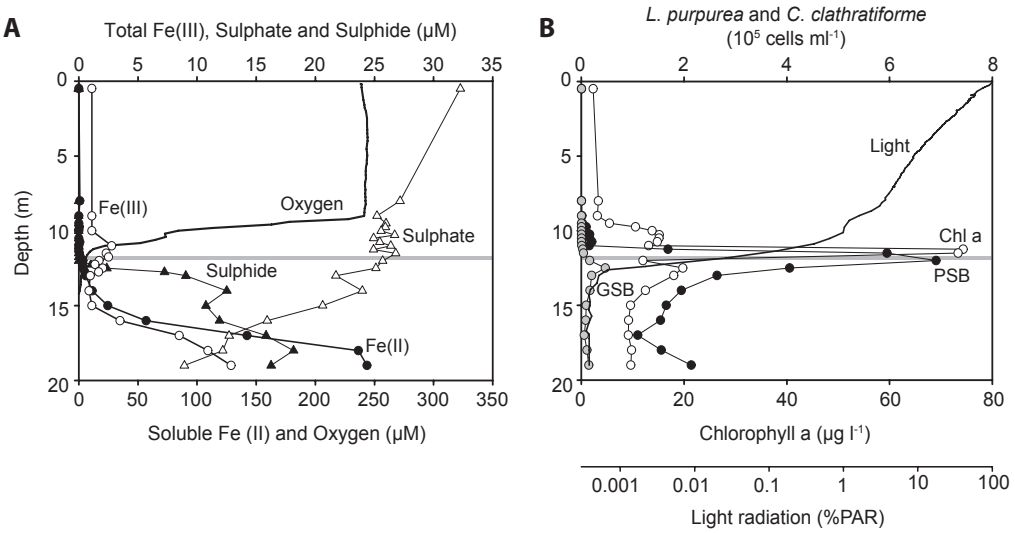

Figure 12: Summer stratification water column data of Lake La Cruz. **A |** Chemical stratification at the time when incubation experiments were performed (13/10/2008). **B |** Vertical distribution of oxygenic (chlorophyll a concentration, open circles) and anoxygenic phototrophs. Black symbols stand for microscopic cell counts of the dominant purple sulphur bacterium (PSB) *Lamprocystis purpurea*) and gray symbols for the dominant green sulphur bacterium (GSB) *Chlorobium clathratiforme*. The horizontal line at 11.8 m indicates the sampling depth for the in situ radiocarbon-incubations and ex situ iron-oxidation experiments.

sulphate concentrations with depth and 16S rRNA gene sequences of sulphate-reducing bacteria (*Desulfomonile sp.*) in a clone library from the anoxic part of the chemocline (supplemental material: 2.3) suggest that they may contribute to sulphide production as well. Sulphide was determined with the photometric Cline assay, which overestimates free sulphide concentrations as it detects also colloidal, amorphous forms of FeS (Bura-Nakic *et al.,* 2009). In the hypolimnion of the ferruginous Lake Pavin (Supplementary material: 2.2, Tab. 3) 80% of the methylene-blue reactive sulphides were identified as amorphous FeS, produced by the reaction of free sulphide and Fe(II) (Bura-Nakic *et al.,* 2009). Most of the iron in the anoxic water column, however, was present as dissolved Fe(II) and derived from the Fe(II)-rich marlstone (Rodrigo *et al.,* 2001). The flux of dissolved Fe(II) towards the oxic/anoxic interface estimated from the concentration profiles ranged between 0.031-0.244 µmol cm^2 d^{-1} (Supplementary material: 2.2, Tab. 2).

Fe(II) was oxidized in the chemocline as indicated by two separate Fe(III) peaks (Fig. 12A). An upper broad peak of about 2.8 µM Fe(III) was located between 10 m and 11.75 m, where picocyanobacteria were most abundant and Fe(III) was presumably formed by direct chemical reaction with O_2 or by microaerophilic chemotrophs (e.g. *Gallionela sp.*; Lehours *et al.,* 2007). As nitrate was also present at that depth (2.0 µM), chemotrophic nitrate-dependent iron-oxidation cannot be excluded but should be of minor importance due to the limited supply of this oxidant as well as competition for nitrate with denitrifying bacteria and nitrate-assimilating phototrophs. A second peak of Fe(III) (~2.0 µM, 12.0-13 m) was typically observed in the anoxic part of the chemocline and coincided with the biomass maxima of the anoxygenic phototrophs *Chlorobium clathratiforme* and *Lamprocystis purpurea*, (Fig. 12B). Prevailing light intensities of 0.02-0.002 % PAR (Supplementary material: Fig. 1) and a continuous supply of Fe(II) from the hypolimnion constitute environmental conditions suitable for the development of photoferrotrophs (Supplementary material: 2.4.1, -2, -3).

Photoferrotrophy is an autotrophic metabolism and *in situ* ^{14}C-incubation experiments were conducted to test this hypothesis by detecting Fe(II)-dependent stimulation of carbon uptake in the light. Incubations were performed with water samples from the anoxic part of the chemocline (CAP) at 11.8 m, where

sulphide and Fe(II) concentrations were minimal. The incubations were spiked with various electron donors and acceptors, which may fuel autotrophic metabolism, including Fe(II), sulphide, and nitrate. Since both oxygenic and anoxygenic phototrophs were present at this depth (Fig. 12B), incubations were also made with addition of DCMU (3-[3,4-dichlorophenyl]-1,1-dimethylurea) in order to suppress oxygen production by photosystem II (PSII). In absence of DCMU, none of the additions had a significant influence on carbon uptake (Fig. 13). The inorganic carbon-uptake rates decreased by about 35-40% in presence of DCMU as compared to the untreated controls, with the exception of the Fe(II) treatment where a significant increase of 40% was observed ($P<0.05$; Fig. 13).

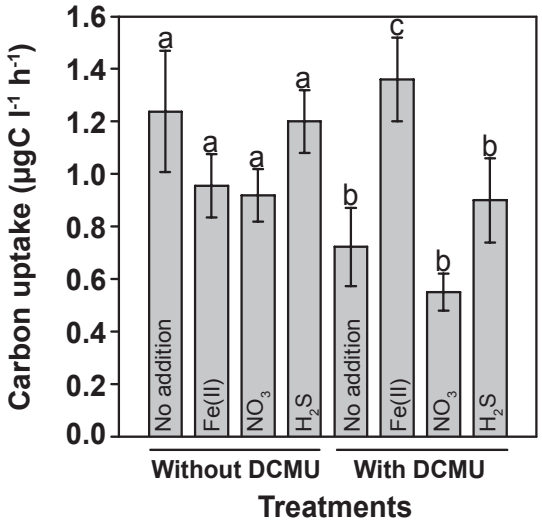

Figure 13: Light-dependent inorganic carbon uptake in presence of potential substrates for lithoautotrophic iron- and sulphur-transforming microorganisms. *In situ* net photosynthetic carbon fixation experiments showing a stimulation upon Fe(II) addition in presence of DCMU (-c-, $p<0.05$). The net photosynthetic carbon uptake was obtained by subtracting the dark incubation values from the carbon uptake in the light. Letters represent the statistical groups using generalized linear models (see Supplementary information). Average values and standard deviations are presented.

This result suggests that i) there was a Fe(II)light-dependent inorganic carbon uptake in the anoxic part of the chemocline, and ii) oxygenic photosynthesis needed to be inhibited to detect photoferrotrophic autotrophy. It has been proposed that ancestral cyanobacteria could photosynthesize with PS I alone and probably used H_2, H_2S or Fe(II) to reduce CO_2 to organic matter (Pierson, 1994). Also some modern cyanobacteria show considerable versatility and may switch in response to the environmental conditions, from oxygenic to anoxygenic photosynthesis with H_2S (Cohen *et al.,* 1986). A contribution of cyanobacteria to the observed stimulation in the presence of DCMU cannot be entirely excluded, although it has never shown for picocyanobacteria (Pierson *et al.,* 1999). Similar incubations done during winter stratification, when the different phototrophic populations were less compact and better separated in the water column, revealed that the fuelling of ^{14}C-uptake by Fe(II) was most pronounced in water layers where anoxygenic phototrophs were present. Conversely, only a weak stimulation was observed in samples from the upper cyanobacterial layer or the aphotic hypolimnion, respectively (Supplementary material: 2.5).

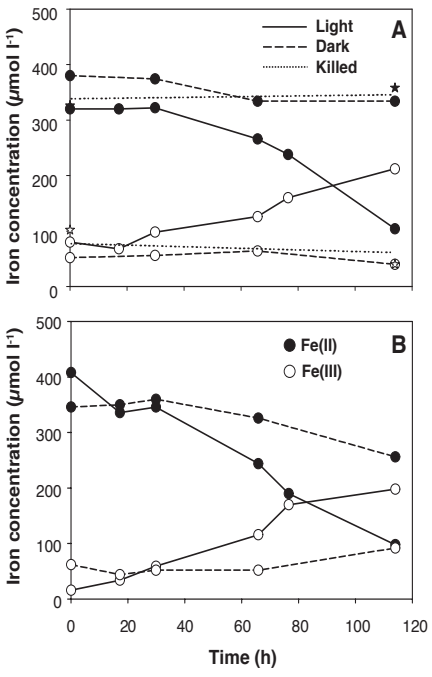

Figure 14: Light-dependent iron-oxidation by the natural microbiota from the anoxic part of the Lake La Cruz chemocline at 11.8 m depth. Anoxic laboratory (ex situ) incubation experiment **A |** without DCMU addition, where oxygenic photosynthesis is active and abiotic Fe(II) oxidation with O_2 may occur; and **B |** Fe(II) evolution under anoxic conditions in absence of oxygenic photosynthesis (with DCMU addition). Light conditions involved consecutive periods of 12 h illumination at 61 µE m^{-2} s^{-1} and 12 h darkness. Solid symbols stand for Fe(II) and open symbols for Fe(III) concentrations. The dotted lines represent means of killed controls (stars).

No data on rates of anoxygenic phototrophic Fe(II)-oxidation in a natural ecosystem exist so far. Anaerobic light dependent oxidation of iron was quantified using *ex situ* incubations with Fe(II)-spiked water from the same depth as used for the ^{14}C-incubations (Fig. 14; Supplementary material: 2.1, 2.6). The oxidation of Fe(II) to Fe(III) was light dependent. Fe(II) oxidation

by the natural chemocline microbiota proceeded at a rate of 2.65 µmol l^{-1} h^{-1} (Supplementary material: Tab. 3) and was similar for incubations with and without DCMU, alluding that oxygenic phototrophs (e.g. picocyanobacteria) from this depth were not very active under the experimental conditions. Nevertheless, this estimate shows that under optimal conditions the Fe(II) oxidation rate of the chemocline-microbiota would have been sufficient to account for all of the Fe(III) formed in BIFs (Kappler *et al.,* 2005[1]) (with estimated precipitation rates of 14.0 µmol l^{-1} d^{-1}; Supplementary material: Tab. 3). However, alternative Fe(II) oxidation rate estimates based on equation (1) and the amount $^{14}CO_2$ incorporated in situ under Fe(II) stimulation conditions amounted only to 0.213 µmol Fe(II) l^{-1} h^{-1} (Supplementary material: Tab. 3), which was likely due to the lower light intensities prevailing in the lake. Alternatively, it also may indicate that photoferrotrophs in Lake La Cruz are not strict autotrophic organisms as suggested in equation (1) and assimilate additional organic compounds for biomass formation (Heising *et al.,* 1999).

Attempts to grow phototrophic Fe(II)-oxidizing organisms from CAP water samples resulted in a co-culture consisting of *Chlorobium sp.* (Fig. 15, 80%) and uncultivated *Acidobacteria* (20%)(Supplementary material: 2.7).The new *Chlorobium* strain was closely related to *Chlorobium ferroxidans*, the only green photoferrotrophic culture known so far, and to *Chlorobium clathratiforme*, the dominant green phototrophic sulphur bacterium in La Cruz (Rodrigo *et al.,* 2001; Romero-Viana *et al.,* 2010). The enrichment culture contained both photoferrotrophic and Fe(III)-reducing bacteria (Supplementary material: 2.2, Fig. 17) suggesting that Fe(II)-oxidizing and reducing processes in the chemocline of Lake Cruz are tightly coupled. The observed Fe(II) oxidation rate of 2.6 µmol l^{-1} h^{-1} (Supplementary material: 2.2, Fig. 17) may represents a net rate depending on the relative kinetics of the processes, yet it is consistent with previous measurements in pure cultures of Fe(II)-oxidizing phototrophs. No photoferrotrophic enrichment cultures with cyanobacteria or purple sulphur bacteria were obtained (Supplementary material: 2.6).

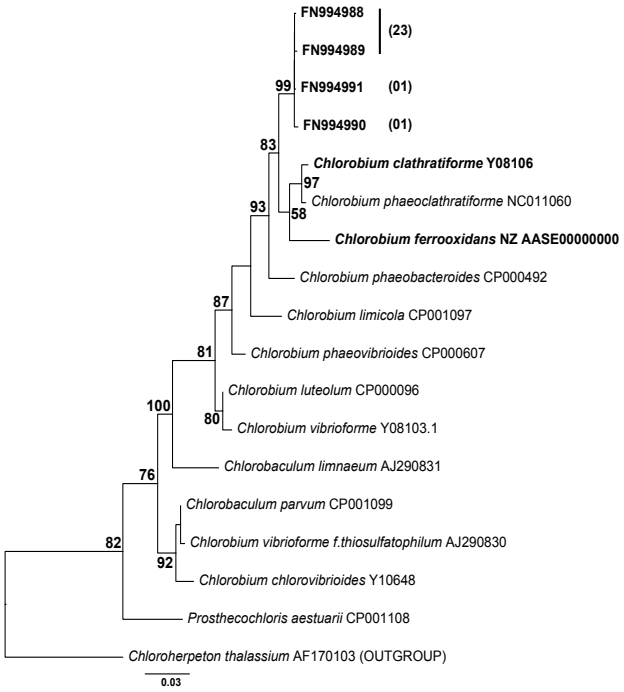

Figure 15: Phylogeny of the photoferrotrophic enrichment culture based on nearly complete 16S rRNA gene sequences and maximum likelihood analysis. Among the retrieved sequences 80% fell into a well-defined cluster within the *Chlorobia* (25/31 clones); the rest of the sequences were most closely related to uncultivated *Acidobacteria* (5/31 clones). Numbers in brackets signify the number of clones possessing the same sequence. Bootstrap values >50% for 1000 replications are shown.

Despite a continuous flux of sedimenting Fe(III) toward the bottom of the lake (Fig. 12A), there was no accumulation of iron oxide minerals in the sediments. Only 3 µmol Fe(III) g^{-1} was detected at the sediment surface. Below 0.5 cm depth, HCl extractable iron was reduced and bound to sulphur as combined iron and sulphur measurements suggested. Average contents of acid volatile sulphur (mostly FeS) and chromium reducible sulphur (i.e. FeS_2, Fe_3S_4 and S^0) were 23±5 µmol S g^{-1} and 10±2 µmol S g^{-1}, respectively. Iron

sulphides are continuously produced just below the chemocline and settles down the water column (Ma *et al.,* 2006), however, in contrast to Fe(III)-oxides, which can be reduced again to Fe(II), FeS is stable and will accumulate in sediments. Iron sulphide minerals may also be produced at the sediment surface from Fe(III)-oxides reacting with sulphide liberated through organic matter degradation and dissimilatory sulphate reduction. An accumulation of Fe(III) in the sediment can only be explained by strongly reduced primary productivity and significant degradation of organic matter by methanogenesis during sedimentation. The fraction of degraded organic matter released as methane into the atmosphere, representing a loss of reducing power, consequently, will determine the amount of iron accumulating in the sediment in its oxidized state.

1.4. Conclusions

In summary, chemical profiles of iron with a recurrent secondary peak of Fe(III) in the anoxic, euphotic part of the chemocline, the increased inorganic carbon-uptake in presence of Fe(II), and the light-dependent Fe(II) oxidation provide consistent evidence for photoferrotrophic activity in the La Cruz chemocline. Our study demonstrates, for the first time, the coexistence of iron- and sulphur-driven anoxygenic photosynthesis and oxygenic photosynthesis in the same environment. However, we also note that photoferrotrophy under the prevailing environmental conditions is a slow process and that most of the Fe(II) at the chemocline is likely oxidized by oxygen.

Lake La Cruz represents an excellent model system for studying microbial iron cycling and the geochemistry of redox sensitive elements under anoxic but non-sulphidic conditions. This will help to develop, test, and refine proxies for paleo-oceanic redox conditions (Ohmoto *et al.,* 2008; Severmann & Anbar, 2009; Lyons *et al.,* 2009). For example, the description of a ferruginous water column over an euxinic sediments (anoxic and iron-sulphide rich) and harbouring dense populations of anoxygenic phototrophic bacteria may require a re-evaluation of markers for photic zone euxinia (Meyer & Kump, 2008).

Methods and associated references as well as additional Results are available as Online Supplementary Information.

Acknowledgments

This work was supported by the Swiss National Science Foundation (No. 3103A – 112563). We thank A. Bagnoud and C. Paul for their assistance in the field. E. Lara and N. Jeanneret are acknowledged for advise and technical help with the phylogenetic characterisation of the enrichment culture. B. Fournier is thanked for advise on statistical analyses. We thank S. Poulton and D. Canfield for commenting on an earlier version of the manuscript.

Author Contributions

X.A.W., A.P., A.C., M.R.M., E.V., J.Z. participated in the fieldwork, planned and performed field experiments, and contributed to data interpretation. Additional laboratory experiments and molecular analyses were performed by X.A.W.. J.Z. established the project design and wrote the paper together with X.A.W. All authors discussed the results and commented on the manuscript.

2. Supplemental Material

2.1. Material and methods

Physico-chemical profiling. Water column profiles of temperature, conductivity, pH, redox potential, dissolved oxygen, and chlorophyll *a* were recorded using a Sea-Bird CTD multiprofiler. Light intensity was measured as photosynthetically active radiation (PAR) scalar irradiance with a flat Li-Cor Quantum Sensor (Li 192 SA), which was vertically mounted on a lowering frame and connected to a Li-Cor data logger (L-1000). Water samples were collected using a battery-driven peristaltic pump from a boat fixed in the centre of the lake. Samples for Fe were preserved with HCl (0.5 M final concentration), and samples for sulphide with zinc acetate 5% (w/v). Concentrations of iron and sulphide were determined by the ferrozine (Viollier *et al.,* 2000; *Annex II.4*) and Cline (Cline, 1969) assays, respectively, as described in detail elsewhere(Zopfi *et al.,* 200).

Water samples. During summer stratification (13-17 October 08) samples for both *in situ* and *ex situ* incubation experiments were collected at 11.8 m depth, the euphotic and anoxic part of the chemocline (CAP), where both purple and green anoxygenic sulphur bacteria were present (Fig. 12). At that time the CAP extended from 11.5 m to 12.5 m depth (Fig. 16). At the sampling depth 1.8 µM O_2, 1.4 µM Fe(II), 2.5 µM Fe(III), no HS^- and a pH of 8.32 were measured. In winter (7-12 February 08) the CAP was between 14.5 m and 15.5 m depth, whereby samples for the incubation experiments were collected from 15 m. The water at this depth was characterized by the absence of oxygen, 5 µM Fe(II), 1.8 µM Fe(III), 1.3 µM HS^- and a pH of 8.21.

Flux calculations. The vertical flux (F_z) of Fe(II) towards the oxic/anoxic interface was calculated according to $F_z = -K_z * (\Delta C/\Delta z)$, using the linear concentration gradient between 15 m and 18 m. As values for vertical eddy diffusivities (K_z) we used 5.0×10^{-4} and 4.0×10^{-3} cm^{-2} s^{-1}, which represent the reported minimum values for the iron-rich 95 m deep meromictic crater Lake Pavin, and the euxinic 20 m deep meromictic Lake Cadagno, both resembling most Lake La Cruz (Bura-Nakic *et al.,* 2009; Dahl *et al.,* 2010). An upward flux of 0.031-0.244 µmol cm^2 d^{-1} of Fe(II) towards the oxic/anoxic interface was calculated (Supplementary Tab. 2). In the Supplementary Table 3, La Cruz water column data are compared with conditions proposed for an Archean Ocean and with potential modern analogues like Lake Mantano and Lake Pavin.

***In situ* bicarbonate-uptake experiments.** Modified *in situ* ^{14}C-bicarbonate incubations were used to assess the influence of different substrates potentially involved in microbial iron and sulphur cycling. For this, water was sampled during summer stratification (CAP: 11.8 m). Incubations were done in 10 ml N_2-preflushed Vacutainer tubes (Becton Dickinson) with the following additions from anoxic stock solutions (final concentrations): i) untreated control, ii) $FeCl_2$ (100 µM), iii) $NaNO_3$ (50 µM), iiii) sulfide (100 µM). All of the treatments were done in duplicates, with and without DCMU, as well as in the light as in the dark. For the incubations with DCMU, the water sample was treated with the inhibitor 30 minutes prior the start of the experiment assuring its effect on PSII. The tubes were spiked with 5 µCi of anoxic ^{14}C-bicarbonate (DHI, Hørsholm, Denmark) and immediately incubated for 4 h at 10 m depth (2% PAR, 12.6°C), corresponding to the upper boundary of the Chl *a* peak, in order to avoid shading of the different phototrophic guilds. After incubation, samples were killed with formalin (2% final concentration) and filtered (GF/F Whatman). Filters were rinsed twice with 0.05 M HCl and finally with milliQ water. After a drying period of 36 h under a fume-hood, filters counted in 10 ml of Ultima Gold aqueous scintillation liquid on a Wallac 1409 liquid scintillation analyzer. Rates were calculated according to: Uptake rate = ^{14}C-fixed x $[\Sigma CO_2]$ x 1.06 / $\Sigma^{14}CO_2$ x *t*, where ^{14}C-fixed is the radioactivity counts per filter minus control, $[\Sigma CO_2]$ is the total DIC concentration in the water at the sampling depth, 1.06 is the correction factor for isotopic fractionation between ^{12}C

and ^{14}C, $\Sigma^{14}CO_2$ is the total DIC radioactivity per vial, and *t* is the incubation time. The net photosynthetic carbon uptake was obtained by subtracting the dark incubation values from the carbon uptake in the light. Chemoautotrophy can be higher in samples incubated in the dark than in the ones incubated in light, due to competition for nutrients with phototrophs in illuminated bottles. Therefore, we consider the presented phototrophic carbon uptake value as the minimum for photoautotrophy. Uptake rates were used to build two generalized linear models (-C- uptake ~ Fe + NO_3^- + H_2S; Mac Cullagh & Nelder, 1989) with a binomial distribution, once with DCMU additions and once without. The influence of the treatments on carbon uptake was tested using ANOVA. All analyses were performed using the statistical software "R" (R development core tean, 2009).

***Ex situ* Fe(II) oxidation experiments.** N_2-flushed 500 ml bottles were filled with water from 11.8 m depth and closed anoxically with thick butyl rubber stoppers. The samples were directly transported to the laboratory at the University of Valencia under dark and cool conditions. After addition of $FeCl_2$ (≈ 500 µM final concentration), bottles were incubated with and without DCMU at 14 ºC for 120 hours. Half of them were incubated under a 12 h light-dark regime with a direct light intensity of 61 µE m^{-2} s^{-1}; the rest was kept under continuous dark conditions. For the bottles with DCMU, 10 ml of an anoxic, saturated aqueous solution of DCMU were added one hour before the $FeCl_2$ addition to inhibit PSII of oxygenic phototrophs. A killed control was incubated under continuous light to maximize any potential photo-oxidative effects on iron speciation. The evolution of ferric and ferrous iron was followed by the ferrozine assay (Viollier *et al.,* 2000). The oxidation of Fe(II) in the dark incubation (Fig. 14b) towards the end of the experiment may be explained by O_2 contamination upon sampling.

Enrichment and molecular identification of photoferrotrophs. Enrichments were established with CAP water collected at 15 m during winter stratification (see water sampling). A sample of 200 ml was anoxically transferred to a sterile, N_2-flushed serum bottle and amended with about 200 µM $FeCl_2$ and DCMU. The bottle was incubated at room temperature under a 12h light-dark regime for one month. A sub-sample was afterwards transferred into bicarbonate-buffered (pH 6.8) freshwater mineral medium (Heising *et al.*, 1999) that contained 10 mM $FeCO_3$, trace elements, and vitamins including vitamin $B_{12.}$ After an initial serial dilution to extinction, the tubes were exposed to 61 µE m^{-2} s^{-1} direct light (12 h L/D). For the phylogenetic characterisation of the photoferrotrophic culture a clone library targeting the 16S rRNA gene was established after the 5th enrichment transfer. Thirty-one clones were sequenced after a prior restriction fragment analysis using *Hae*III and *Taq*I. The nearly complete 16S rRNA sequences were aligned in ClustalW and manually refined (1344 positions). The phylogenetic tree is based on the results of a maximum likelihood analysis of sequences from the *Chlorobiaceae* family, including *C. clathratiforme* the presumably dominant green sulphur bacterium in this lake (Julia *et al.*, 1998; Rodrigo *et al.*, 2001; Ronero-Viana *et al.*, 2010). The phylogenetic tree was created by using GTR (General Time Reversible) model + Γ + invariant and 4 substitution rate categories (1000 bootstrap) using Treefinder (Jobb *et al.*, 2004).

Fe(II)-oxidation by the photoferrotrophic enrichment culture. Hungate tubes (10 ml) containing the same medium as above were inoculated with the enrichment culture, that had been subcultured for 9 months (corresponding to 5 enrichment transfers) before using it for the experiment. The inoculated tubes were incubated in triplicates at 20°C under continuous dark and continuous light conditions (70 µE m^{-2} s^{-1}). The photometric ferrozine assay[1] was used to follow the evolution of Fe(II)/Fe(III) in the tubes. Average Fe(II) oxidation rates were calculated from the Fe(II) concentration changes between day 7, corresponding to the end of Fe(III) reduction phase, and day 60.

2.2. Figures and tables

Table 2: Flux calculation of ferrous iron towards the oxic/anoxic interface in Lake La Cruz during summer stratification (October 2008).

Fe(II) gradient	**K_z**	**Fe(II) flux**	**Fe(II) oxidation***
µmol cm^{-4}	cm^2 s^{-1}	µmol cm^{-2} d^{-1}	µmol l^{-1} d^{-1}
7.07 $x10^{-04}$	0.0005	0.031	0.174
	0.0040	0.244	1.396

* Fe(II) oxidation rate calculated for a 1.75 m thick iron-oxidizing zone in the water column and 24 h day. The upper boundary of this zone was defined by the complete disappearance of Fe(II) (11.25 m) and the lower boundary by the limit of the secondary Fe(III) peak at 13 m depth.

Table 3: Comparison of water chemistry, iron fluxes towards the oxic/anoxic interface, and Fe(II)-oxidation rates of different modern Archean Ocean analogues.

	Lake La Cruz		**Lake Matano[1]**	**Lake Pavin[2]**	**Archean Ocean**
	Mixed layer	Anoxic layer	Anoxic layer	Anoxic layer	Anoxic layer
Fe(II) (µM)	-	230	140	1000	40 - 120 (1)
SO_4^{2-} (µM)	< 33	< 25	< 0.1	< 5.0	< 200 (3)
O_2 (µM)	238	0	0	0	< 0.03 (1)
PO_4^{3-} (µM)	< 0.26	< 1.6	9	-	0.03 - 0.29 (1)
pH	8.60	7.00	7.00	6.08	> 6.5 (1)
T° (°C)	16	6	25 - 28	4	≈ 36 (1)
Fe(II) flux (µmol cm^2 d^{-1})	0.031 - 0.244		0.034 - 0.27	-	12.3 a)
Estimated *In-situ* Fe(II) oxidation rate (µmol l^{-1} d^{-1})	0.174 - 1.396 b)		0.034 - 0.27	-	14 (4)
Fe(II) oxidation rate ("^{14}C") (µmol l^{-1} d^{-1})	2.56 c)				
Fe(II) oxidation rate ("ex-situ") (µmol l^{-1} d^{-1})	31.8 d)		-	-	
Number of cells (cell ml^{-1})	0.5 x 10^5, 7.0 x 10^5 e)		0.3-16 x 10^9	-	10^6 (4)

a) Calculation based on the surface of Hamersley Basin (10^{11} m^2) and a maximum Fe(III) precipitation rate of 4.5 $x10^{12}$ mol Fe(III) y^{-1} required to form the Hamersley Basin BIFs ((4) Kappler *et al.*, 2005[1]).

b) Calculation see Supplementary Table 2.

c) Calculation based on the amount of ^{14}C-bicarbonate fixed in "Fe(II) + DCMU" treatments (1.36 µg C l^{-1} h^{-1}, Fig. 13) minus the "No addition + DCMU" treatment and assuming a ratio of 4 Fe(II) oxidized per CO_2 assimilated as shown in equation (1). Calculated for 12 h illumination.

d) Calculation based on the average iron-oxidation rate of 2.65 µmol l^{-1} h^{-1} determined in the *ex situ* light incubation with 12 h of illumination per day (Fig. 14) and assuming that all Fe(II) was oxidized through photoferrotrophy.

e) Maxima of GSB and PSB microscopic cell counts, respectively, at 11.8 m during summer stratification.

(1) Crowe *et al.*, 2008 (2) Bura-Nakic *et al.*, 2009 (3) Canfield, 2005

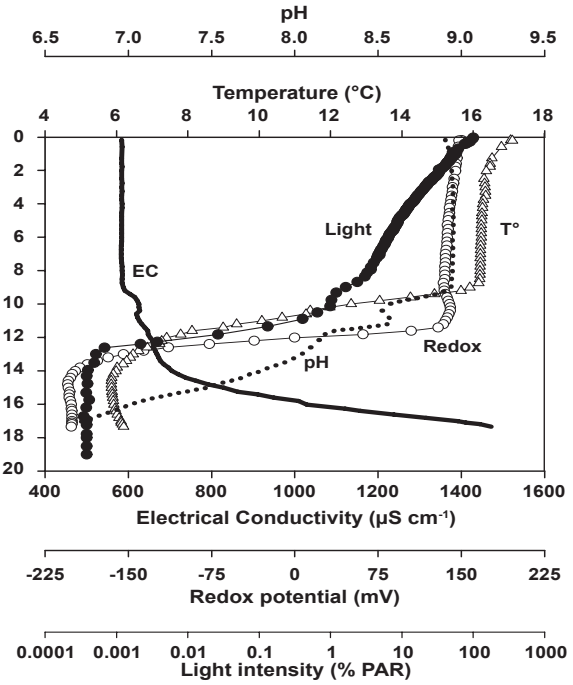

Figure 16: Depth profiles of physico-chemical parameters in the water column of the meromictic Lake La Cruz during summer stratification conditions (October 2008).

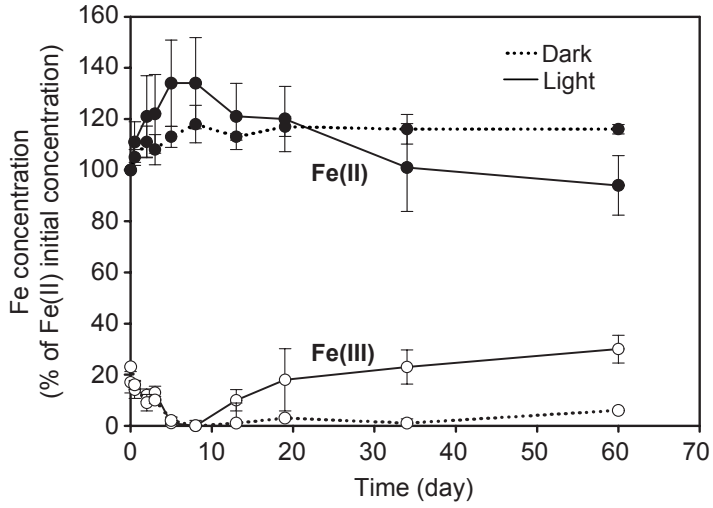

Figure 17: Net Fe(II)-oxidation by the photoferrotrophic enrichment culture. Results display the dependence of Fe(II)-oxidation on light. Furthermore, Fe(III) added with the inoculum at the beginning of the experiment was reduced during the first 8 h, presumably mediated by Acidobacteria, the second most abundant bacterial group in the enrichment culture. Data are average values of three independent experiments with error bars representing standard deviation (n=3).

2.3. 16S rRNA gene clone libraries

Molecular analyses were performed on water samples collected during winter stratification (2008, 15.5 m and 17.0 m). Samples were filtrated on polycarbonate membranes (50 ml, 0.2 µm ⦸; Whatman), and were conserved at -80 °C until DNA extraction using the FastDNA Kit for soil (Q-BIOgene). The nearly complete eubacterial 16S rRNA gene was amplified by PCR, using primers GM3f and GM4r (AGA GTT TGA TC(AC) TGG C and TAC CTT GTT ACG ACT T, respectively) (Muyzer *et al.*, 1995; Pronk *et al.*, 2009).Two clone libraries were established consisting of 102 (15.5 m) and 58 (17.0 m) clones, respectively. After a RFLP analysis using *Taq*I and *Hae*III 75 and 49 clones were sequenced in both direction at Eurofins MWG GmbH. Were retained 69 and 42 sequences (15.5 m and 17.0 m, respectively), after elimination of chimera and quality checks, for phylogenetic analysis (CLC Main Workbench software, CLCbio, Denmark). A template database consisting of 16S rRNA gene sequences from isolated and characterized strains was built up. We included representative samples from all different Eubacterial phyla. The tree obtained allowed us to position our samples into the Eubacterial Domain, and thus to restrain the numbers of sequences, used

as template, for the building of smaller trees. Afterwards, the number of clones with the same restriction profiles as sequenced ones was reported (Fig. 18).

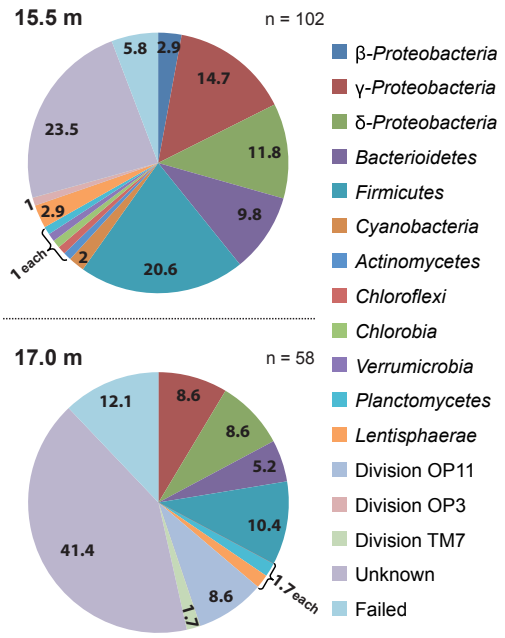

Figure 18: Phylum level diversity based on retrieved 16S rRNA sequences from two depths in the water column of La Cruz: 15.5 m depth, in the anoxic part of the chemocline, and 17 m at the top of the monimolimnion. The indicated numbers are the percentage of each phylogenetic groups.

Regarding the distribution of *Bacterioidetes* and *Firmicutes*, they were more abundant at 15.5 m depth than at 17.0 m (Figs. 18-19). About 42 % of the sequences retrieved from 17.0 m depth were unclassified or unknown while 12 % of the sequences failed to be sequenced (Fig. 18). The results from this depth are of particular interest as the microbial community shows an unusual composition. Only 18% of the retrieved 16S rRNA sequences fell into the *Proteobacteria*, a phylum that accounts often for about 40% of the sequences in clone libraries from various environment, including the Fe(II)-rich water column of Lake Pavin (Lehours *et al.*, 2007). Conversely, clone sequences belonging to unusual and little studied groups such as *Verrucomicrobia*, *Lentisphaera* as well as candidate divisions OP11 and TM7 were found (Fig. 18). Interestingly, 8.6 % of the retrieved sequences were closely related to candidate divisions OP11 (Figs. 18-20).

About 50 % of the *Proteobacteria* sequences from 15.5 m depth were γ-*Proteobacteria* and belonged either to *Methylococcocales,* to *pseudomonadales* or to *Chromatiales*. One other half of these retrieved sequences were closely related to organism of the *Methylococcaceae* family, from which most of the organisms are aerobic methanotrophs (*Methylobacter tundripaludum*; Fig. 21). The other half γ-*Proteobacteria* sequences fell into the *Chromatiales*, a cluster that groups most anoxygenic purple phototrophs which are usually able to use sulfur as an electron donor. This results is supported by microscopic observations of Lake La Cruz samples. The majority of the remaining *Proteobacteria* sequences (n=15) were affiliated to the *δ-Proteobacteria* (n=12), and were members of the *Synthrophobacterales* (Fig. 21). Some organisms of this order have a sulfate-reducing respiration pathway (e.g. *Syntrophobacter wolinii*), but are also often obligate synthrophs of methanogens (e.g. *Smithella propionica;* Fig. 21). The N-serve effects observed on chemoautotrophy (*Chap III: 6.2; Fig. 45*) suggest that acetoclastic methanogenes should be the main methanogenic metabolism. However, the detection of obligate syntrophs (*Syntrophaceae*, Fig. 21) indicate that the inferred methanogenic population should thrive on CO_2 and H_2. It is thus difficult to identify which methanogenic metabolism dominate the system, especially that the domains Archaea was not investigated. In any environment, methanogens and sulfate reducers are competing for fermentation products (e.g. H_2 or acetate; Lovley & Phillips, 1984). In most cases, it is the availability of sulfate that favor sulfate-reducers because they have a wider substrate spectrum than methanogens which depend mainly on H_2 and acetate (Wetzel, 2001). In Lake La Cruz sulfate is scarce (Fig. 12A , Fig. 28), therefore, limiting sulfate reducing respiration. However, sequences of dissimilatory sulfate reducing bacteria (DSR) have been retrieved (e.g. *Desulfomonile Limimaris,* Fig. 21). This result suggests that the few sulfides measured in Lake La Cruz, which were previously attributed to biomass decaying, were in fact essentially due to DSR (Romero-Viana *et al.,* 2010).

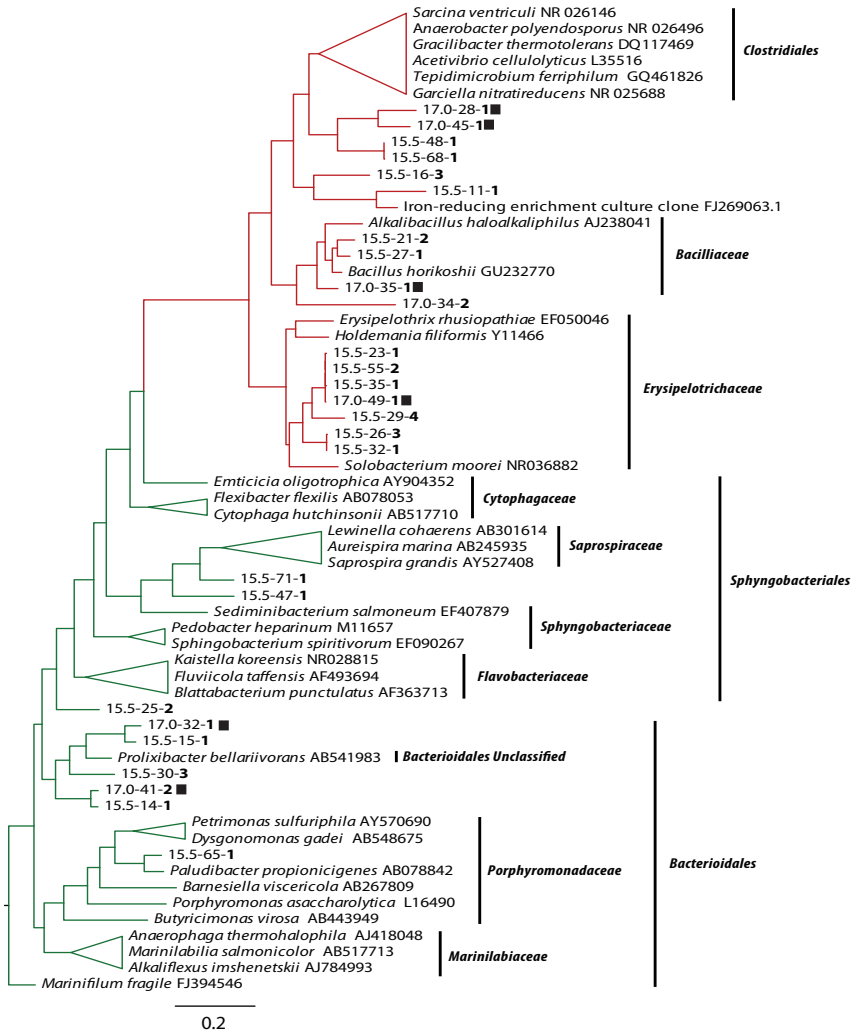

Figure 19: Maximum likelihood phylogenetic tree of the 16S rRNA gene sequences retrieved (15.5 m and 17.0m depth) and the closest related cultivated species of the *Bacterioidetes* and *Firmicutes* (UPGMA tree, GTR substitution model). Red lines stand for *Firmicutes* and green ones for *Bacterioidetes*. Clone numbers indicate the depth (15.5 or 17.0 m), the identification number and the number of clones having the same sequence (bold). Black squares stand for 17.0 m depth samples.

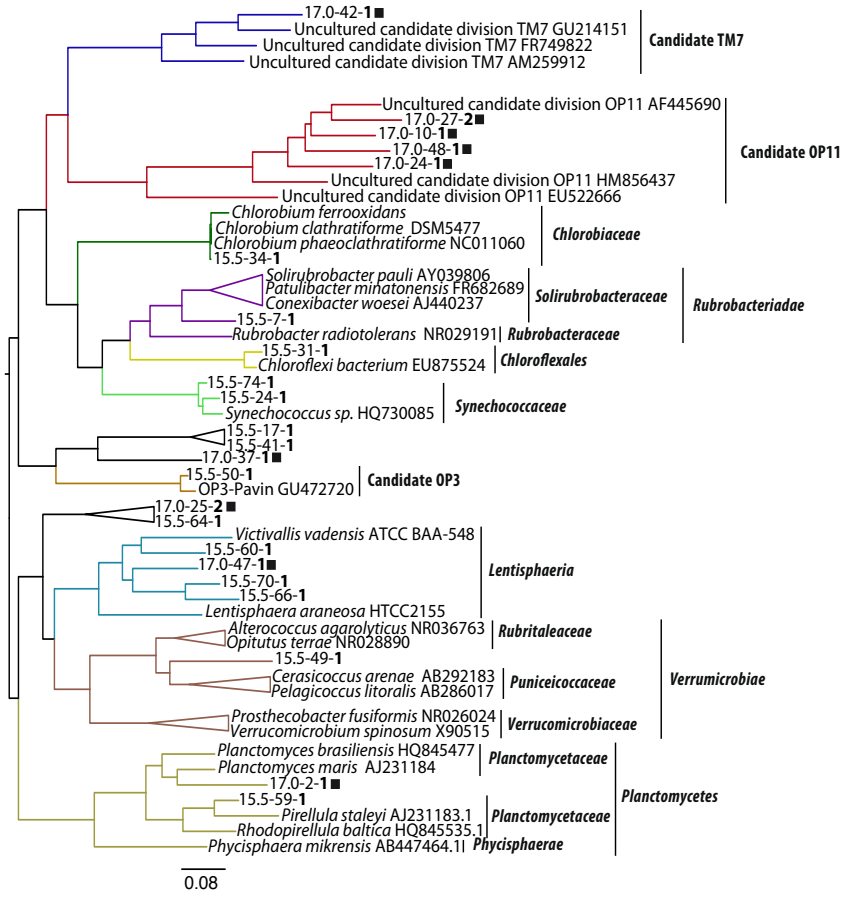

Figure 20: Maximum likelihood phylogenetic tree of the 16S rRNA gene of the less abundant retrieved sequences (15.5 m and 17.0m depth) and the closest related cultivated species (UPGMA tree, GTR substitution model). Each colored line stands for the phylum. When the line is black, it means that the phylum was not identified with certainty. Clone numbers indicate the depth (15.5 or 17.0 m), the identification number, and the number of clones having the same sequence (bold). Black squares stand for 17.0 m depth samples.

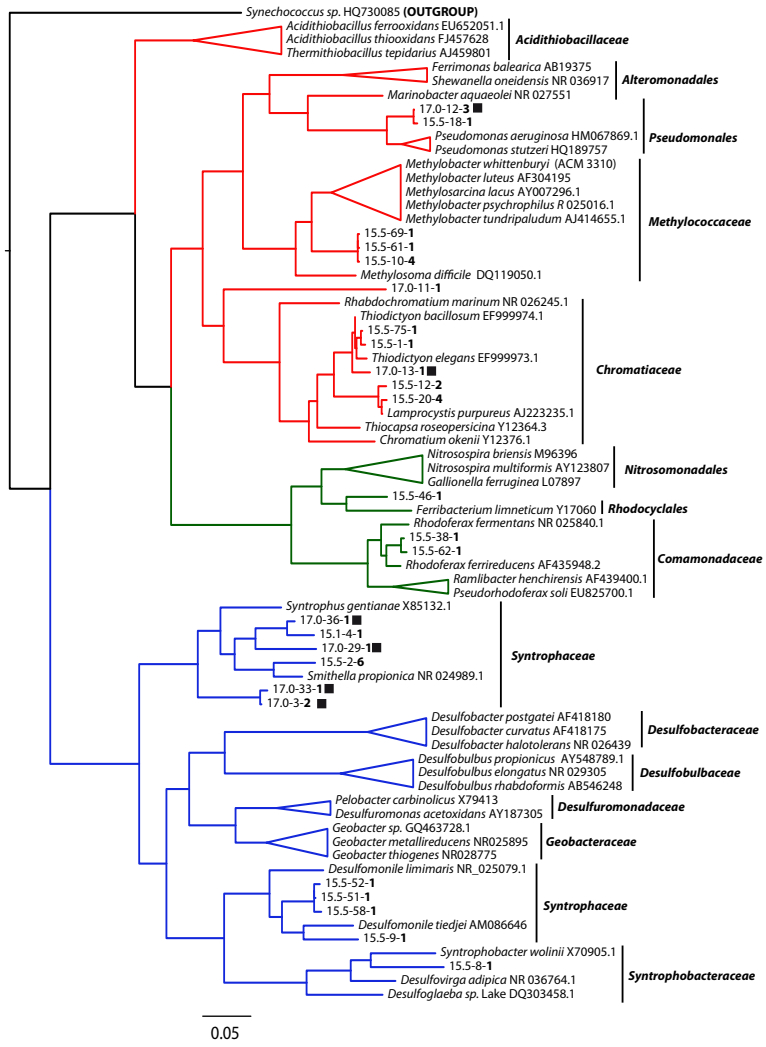

Figure 21: Maximum likelihood phylogenetic tree of the 16S rRNA gene sequences retrieved from 15.5 m depth and the closest related cultivated species of the *Proteobacteria* (UPGMA tree, GTR substitution model). Red lines stand for γ-*Proteobacteria*, green for *β*-***Proteobacteria***, and blue for *δ*-*Proteobacteria*. Clone numbers indicate the depth (15.5 or 17.0 m), the identification number and the number of clones having the same sequence (bold). Black squares stand for 17.0 m depth samples.

All the major phototrophic pathways previously described were found at 15.5 m depth (Rodrigo *et al.*, 2000; Romero-Viana *et al.*, 2010): oxygenic phototrophs (*Synechococcus*, Fig. 20), phototrophic anoxygenic purple sulfur bacteria (*Chromatiaceae*, Fig. 21), and anoxygenic green sulfur bacteria (*Chlorobiaceae*; Fig. 20). Conversely at 17.0 m depth, only sequences of anoxygenic purple sulfur bacteria were retrieved (*Chromatiaceae*, Fig. 21). Organisms depending on oxygen, CH_4 and Fe(II) respiration were also absent (Fig. 21): methanotrophs from the *Metylococcales* and Fe(II)-oxidizing bacteria from the *Comamonadaceae*. However, *Syntrophobacterales* sequences were also present at that depth, but no *Syntrophobacteraceae* sequence have been retrieved (Fig. 20): this suggest a lower potential sulfatoreduction at 17.0 m than at chemocline depth. Presence of *Syntrophaceae*, together with the measure of cDOM concentrations decreases (Fig. 24D), suggesting that, in layers bellow the chemocline, hydrogenotrophic methanogenesis should be the major respiration process.

As in the ferruginous Lake Pavin, sequences from Candidate division OP11 and TM7 were retrieved from 17.0 m depth (96-98 % similarity depending on the clone; Lehours *et al.*, 2007; Lehours *et al.*, 2009). However, much less *Proteobacteria* were detected and no *Gallionellaceae* were found (*Nitrosomonadales*, Fig. 21). Normally, even if they are not well developed at such depth (17.0 m), we should have retrieved some sequences from precipitating dead cells (e.g. oxygenic phototrophs and anoxygenic green sulfur phototrophs). Therefore, regarding the number of clone from that depth (42 16S rRNA gene sequences longer than 1300 bp), the lower diversity and abundance as well as the proportionally fewer known sequences found could be caused by an insufficiently sampled clone library (Haler *et al.*, 2011). On the other hand, this water layer is located between the chemocline and the sediments, two different types of trophic compartment. The

sediment is rich in accumulating organic matter as the above water layer never get mixed. It's a very reduced environment with no electron acceptor other that bicarbonate and potentially S° inside sedimented purple sulfur bacteria. Conversely, the chemocline is a rich environment of mixed electrons donor and acceptor. The organisms present in those water layers are thinly stratified along the redoxcline (14.5 m to15.5 m depth). For those reasons, from the lower part of the redoxcline to the sediment itself, the environment is not favorable for a dense microbial colonization: the temperature is to low for a slow organic matter degradation (sedimentation), and there is no sufficient electron acceptors, that pass trough the chemocline "biological pump", to allow more energetic pathways. In such a scenario, the resulting environment is poorly diversified and little colonized. Thus, the small number of retrieved sequences could still be representative of the local "nutrients desert" that extends along the pycnocline.

This molecular approach allowed to complete the list of the different metabolic pathways occurring in Lake La Cruz anoxic waters: detection of *Syntrophobacteriales* in both samples indirectly support the presence of hydrogenotrophic methanogenesis; sequences of sulfate- Fe(III)- reducing bacteria, Fe(II)-oxidizing bacteria, oxygenic phototrophs, anoxygenic green sulfur phototrophs and methanotrophs have only been retrieved from the chemocline sample. Interestingly, the Fe(III)-reducing bacteria were not from *Geobacteraceae* or *Shewanellaceae* family (*δ-Proteobacteria*, Fig. 21; Loveley *et al.*, 1993) but from the *Rhodocyclaceae* and the *Comamonadaceae* (*β-Proteobacteria,* Fig 21; Cummings *et al.*, 1999; Finneran *et al.*, 2003). Moreover, instead of Fe(II)-oxidizing bacteria from the *Gallionellaceae* family (*β-Proteobacteria*; Hallbeck *et al.*, 1993), the one present in the chemocline were from the *Pseudomonadaceae* or from the *Alteromonadales* (Fig. 21: γ-*Proteobacteria*, e.g. *Pseudomonas stutzeri* or *Marinobacter aquaeolei* respectivelly; Weber *et al.*, 2006[1]). Thus, the recovered Eubacterial sequences were closely linked to organisms having metabolisms putatively present in the Neoarchean Ocean. This, together with a resembling water chemistry, make of Lake La Cruz a potential Neoarchean Ocean analogue.

2.4. Lake La Cruz stratification patterns

In this part, an overall description of Lake La Cruz will be made. The presented results are discussed in order to better explain/understand the interpretations made during this work. Five aspects characterizing Lake La Cruz stratifications will be treated in this part. In the first place, focus will be given to the physical structures of the stratifications and its evolution during a seasonal cycle. In a second step, the variations of the main phototrophic communities stratifications will be discussed. The third part will comment the different iron analysis in order to detect layers of Fe(II)-oxidation. The two last parts will focus on the sulfide and methane productions, respectively, in order to understand the physical/biological context in which ferrotrophy occurs in Lake La Cruz. It is on the basis of those results that the experimental incubations/ experiments have been conducted.

2.4.1. Physical stratifications

The physical parameters we choose for describing the water column were: electroconductivity to detect the pycnocline, the temperature to find the thermocline, the redoxcline to define the chemocline, and the pH to visualize the impact of biological processes. The cited parameters were measured with a CTD multiprofiler (Sea-Bird Electronics, Inc.) provided by the laboratory of *Biodiversitat i Biologia Evolutiva* (Valencia, Spain). The water column stratifications have been investigated three times in summer, and only once in winter. Each characterization has been carried out when the water body was stratified. This lake being meromictic, the bottom water layer never get mixed with the rest of the water column. This monimolimnion extends from 18 m down to the bottom of the lake at 19.9 m (Fig. 22).

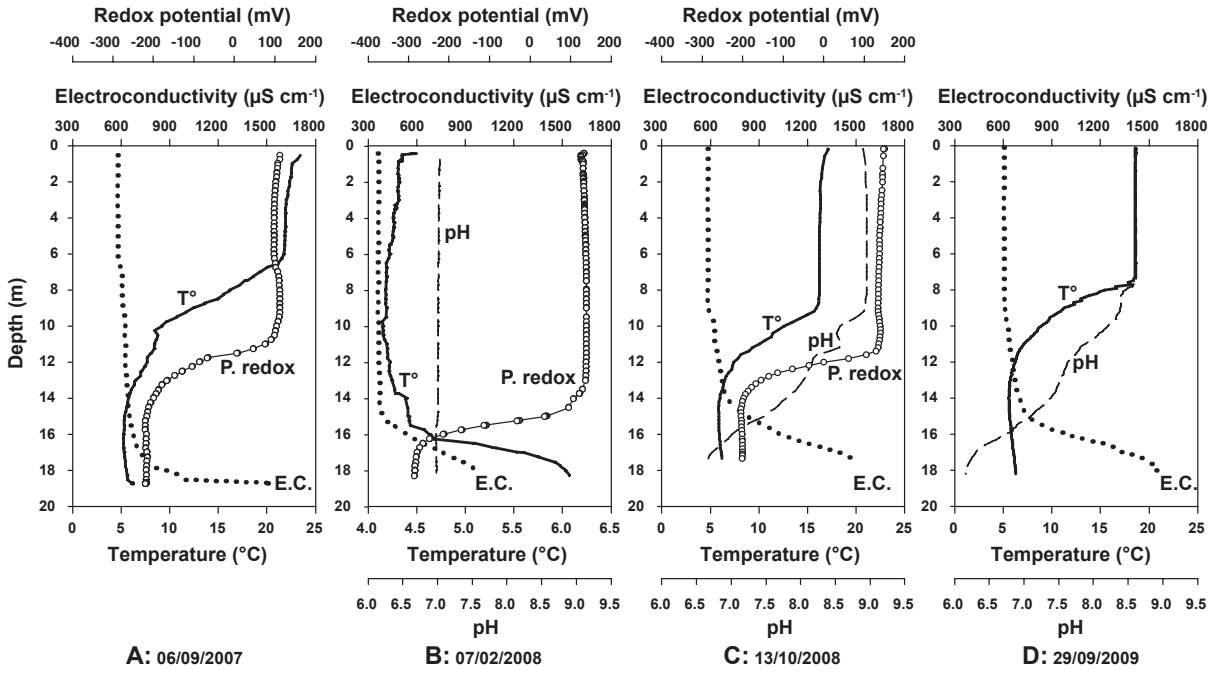

Figure 22: Depth profiles of physical parameters in the water column of Lake La Cruz. Temperatures from winter profile (**B**) have a smaller scale. Those profiles show the evolution of the different "clines" position over the different seasonal periods.

The first characterization (September 2007) was performed about 1 week after the maximum of the summer whiting event where a massive formation of calcite occurred due to a phytoplanktonic bloom (Miracle *et al.*, 2001). In 2007 this whiting event started around the 26th of August and peaked the 30th (Spanish ranger, personal communications; Fig. 23A). However, even if light penetration was shallower, the stratification was not affected by this whiting event: the layer of phototrophic organisms were still at the same depth as in early August (Antonio Picazo-Mozo, personal communications).

Figure 23: Lake La Cruz evolution after summer 2007 whiting event. **A |** maximum of the whiting event (30/08/2007; Spanish ranger) B | one week after the whiting event (08/09/2007) **C |** normal lake situation (28/09/2009).

During both summer stratifications (Fig. 22C-D) pH profiles were similar and varied between 8.7 in the epilimnion, and 6.3 in the monimolimnion upper boundary. The clearer variations of pH were observed in October 2008 stratification (Fig. 22C). A pH peak around 11 m depth, indicating a local alkalinization due to oxygenic photosynthesis (OH^- release, Dupraz *et al.*, 2009), matched the chlorophyll a peak (Fig. 22B), thus confirming the activity of those phototrophic organisms. Just below this pH peak, a slight decrease of pH was visible (11.7 m). This decrease matched the turbidity peak (Fig. 22C), potentially signaling a slight activity of anoxygenic sulfur oxidizing bacteria (SO_4^{2-} release, Dupraz *et al.*, 2009). Below this depth, the pH decreased progressively up to 18 m depth. Overall, the summer "pH-cline" started at the same depth as the thermocline and ended at the upper boundary of the monimolimnion. Conversely, winter pH profile (Fig. 22B) had a very homogeneous distribution over the whole water column: between 7.03 at the lake

surface and 6.99 at 18.4 m. We could interpret this absence of variation as the result of the interaction between a very low biological activity and the mixing of the water column.

Winter thermocline and pycnocline indicated that the mixolimnion (winter mixed water layer) ranged from 0 to 14.0 m depth (Fig. 22B). Summer stratification profiles displayed different positions of the thermocline and pycnocline. Shallower ones were observed in September 2008 (Fig. 22A), while the deepest ones were observed in October 2008 (Fig. 22C). In addition to a deepening of the two clines, a thinning was also observed. Those variations, in depth and thickness, illustrate the slow stratification erosion towards the end of the summer. When upper layers reach 4°C, the autumnal mixing occurs. Although a survey over a complete seasonal cycle has not been done, we may consider those profiles as the different sequences occurring along a single seasonal variation (Rodrigo *et al.*, 2001, Camacho *et al.*, 2003). The period of time represented would extend from early September (Fig. 22A) to early February (Fig. 22B). We therefore have a chronosequence from the different phase occurring between the last whiting event of the year until the stabilization of a stratification in winter (Fig 22: A > D > C > B).

2.4.2. Distribution of the photosynthetic communities

The easiest organisms that can be detected with a CTD multiprofiler are the phototrophic ones: oxygenic phototrophs through spectrophotometric measures of chlorophyll a (Fig. 24B), and anoxygenic purple sulfur bacteria, mainly *Lamprocystis purpurea* (Rodrigo *et al.*, 2001; Camacho *et al.*, 2003; Romero *et al.*, 2006), through turbidity measures (Nephelometric method, Antonio Picazo-Mozo personal communication; Fig. 24C). The main observation is the classical stratification of the phototrophs depending on the light quality needed for the functioning of their photosynthetic antenna: first an upper layer of oxygenic phototrophs (chlorophyll a), and secondly a deeper layer of anoxygenic purple sulfur phototrophs (Bacteriochlorophyll a).

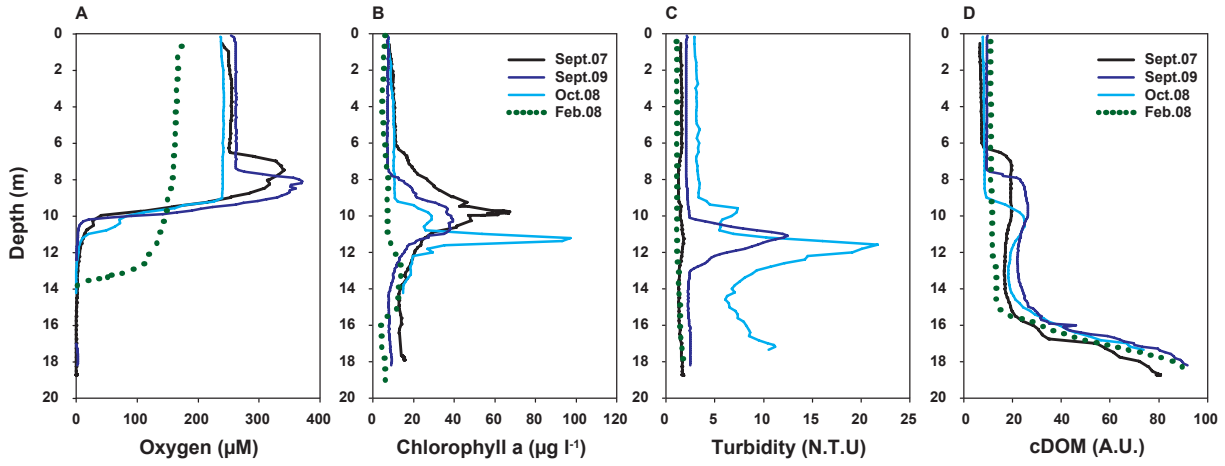

Figure 24: Profiles of four biological parameters using CTD multiprofiler: **A |** Oxygen concentrations, **B |** Chlorophyll a concentrations, **C |** Turbidity measurements to track anoxygenic purple sulfur phototrophs (NTU stands for nephelometric turbidity units), and **D |** the water charge in colored dissolved organic matter (A.U. stands for absorbance unite).

In winter, all four descriptors (O_2, Chl a, Turbidity and cDOM) displayed the lowest measured values (Fig. 24). This stratification period was characterized by the deepest oxygen penetration (14 m, Fig. 24A), the lowest density of oxygenic and anoxygenic phototrophs (Fig. 24B-C), and by the lowest amount of cDOM (Fig. 24D). The oxycline position confirmed physical data: the mixolimnion ended at 14 m (Fig. 22B/24A). Altogether, those descriptors indicated a situation with clear water and thus, a greater light penetration depth (*Chap. IV.4.2, Fig. 57*). There was a slight augmentation of cDOM concentration at 13 m depth, after which the concentration was homogeneous up to 15 m and then, progressively increased towards the

monimolimnion. The first cDOM increase coincided with the augmentation in chlorophyll a (Chl a) and turbidity values, indicating the implication of oxygenic photosynthesis as the main primary producers in Lake La Cruz.

Oxygen and organic matter are produced by the activity of oxygenic photosynthesis. The produced organic carbon is then mineralized by heterotrophic and fermentative metabolisms. At the end of this degradation, only humic compounds are left: they are the detected cDOM (chromophoric/colored dissolved organic matter). The oxygen and cDOM profiles can thus be seen as the product of primary production and its mineralization (Fig. 24A-D). Moreover, it has been shown that part of the cDOM can be consumed by microbes (Nelson *et al.*, 2004). However, not all the cDOM can be degraded and part of it stays as recalcitrant components, depending on the initial carbon source (complex organic compounds or simple organic molecules; Nelson *et al.*, 2004).

Such a correspondence between cDOM, Chl a and turbidity was also observed in summer profiles (Fig. 24). Focusing on October 2008 profile we see that the maximum peak of Chl a is indeed more or less matching the cDOM increase. However, the turbidity peak was just below the inflection of the cDOM curve, thus indicating either that anoxygenic purple sulfur bacteria could potentially be responsible for this cDOM diminution (Fig. 24C-D) or that organic matter mineralization mainly occurs in the oxic part of the chemocline. If those anoxygenic phototrophs were indeed participating to the decrease, we could postulate that part of their population was functioning on photoheterotrophy. When considering the oxygenic and anoxygenic phototrophs functioning over the 3 summer snapshots, two major equilibria seem to occur: one at the "beginning" of the summer (September 2007) and another one at the summer's end (October 2008). The "early" summer stratification (September 2007) was characterized by an abundant presence of active oxygenic phototrophs (Fig. 24A-B), as well as by a high amount of cDOM (Fig. 24D). This stratification was also characterized by a very small population of anoxygenic purple sulfur oxidizing phototrophs (Fig. 24C). Conversely, the end of summer stratification (October 2008) was characterized by the smallest population of oxygenic phototrophs (within summer profiles, Fig. 24B) and, the smallest oxygen/cDOM production (Fig. 24A-D), but presented the highest number of purple sulfur oxidizing phototrophs (Fig. 24C).

As for the physical characterization, those profiles (Fig. 24) can be seen as snapshots of the different stratification periods that occur over a year: winter stratification with a deep chemocline, and three successive moments of the summer stratification period, between the last whiting event and the autumnal mixing (September 2007, September 2009 and October 2008). Thus winter profiles could be seen as the beginning of a seasonal cycle.

2.4.3. Iron profiling: detection of Fe(II)-oxidation layers

The iron content of Lake La Cruz has been investigated four times over a period of 3 years. Summer stratification have been characterized three times (September 2007, October 2008 and September 2009), while winter stratification was considered only once, in February 2008. Iron occurs in nature either as a divalent species (Fe(II)) or as a trivalent species (Fe(III)). Fe(II) is soluble at neutral pH whereas Fe(III) is only soluble at pH<2 (Weber *et al.*, 2001). As Lake La Cruz water column has a neutral pH, the Fe(III) detected should be found as Fe(III)-oxides particles. Therefore, we analyzed the soluble fraction of Fe(II) (filtration), while Fe(III) analysis focused on three types of samples: the colloidal fraction which was the Fe(III) passing through GF/F filters (pore size of ≈ 0.70 µm), the total Fe(III) corresponded to a direct fixation of the sample into hydrochloric acid, and the particulate Fe(III) was the fraction retained on the GF/F filters. All three fractions of Fe(III) were only investigated in October 2008 stratification (Fig. 25). For this reason we used those profiling to interpret the representativeness of each analyzed fraction.

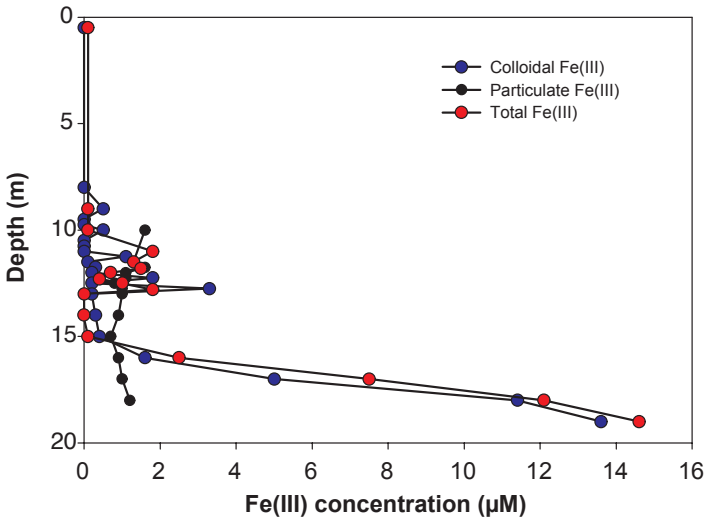

Figure 25: Lake La Cruz Fe(III) profiles measured during summer stratification (13/10/2008).

The particulate Fe(III) fraction was more or less constant along the water column and did not carry much information, specially with so low concentrations. This could be due to the sample treatments or analysis. Conversely, the two other fractions showed clear variations: peaks around the chemocline, no signal in the hypolimnion upper part, and an augmentation towards the bottom of the lake. For those reasons we will not take in account particulate Fe(III) measurements. Comparison between the colloidal fraction and the total fraction indicated that much of the Fe(III) was in colloidal form (Fig. 25), and that colloidal fraction can be over estimated if the filter was not correctly purged by anoxic miliQ water. The total Fe(III) profile shows a more homogeneous concentration distribution throughout depth and thicker peaks than the colloidal Fe(III) one (Fig. 25). Thus, total Fe(III) measurements appear to be more adequate to detect layers of formation (Fe(II)-oxidation). Still, in absence of total Fe(III) data, colloidal Fe(III) can be considered to verify any Fe(III) accumulated toward sediments (Fig. 25).

When comparing iron profiles of the four periods, only the ones from late summer stratifications show an accumulation of iron oxides towards sediments (Fig. 26C-D). As indicated by the absence of Fe(III) accumulation (Fig. 26B), its production/consumption equilibrium suggest a higher ferrireduction in winter than in summer. In opposition, higher Fe(III) concentration in lower layers (Fig. 26C) suggest a higher Fe(II)-oxidation in late summer (October 2008), or a lower ferrireduction. While ferrireduction is a biological process, Fe(II)-oxidation can be a biotic and/or an abiotic reaction. In addition, Fe(III) summer profiles show

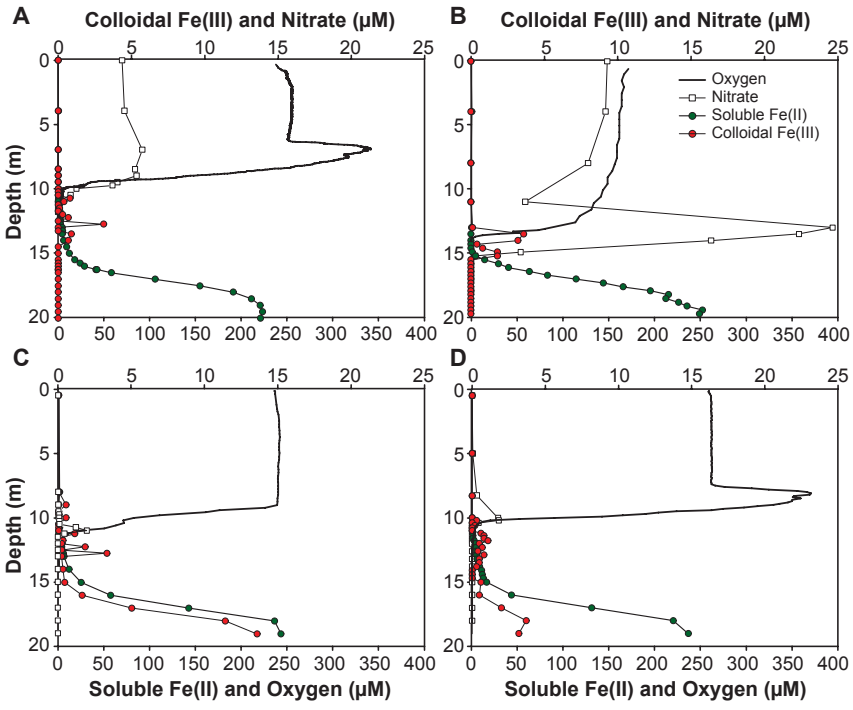

Figure 26: Profiles of the four parameters used to detect layers of iron oxidation: **A |** beginning of the late summer period: after the whiting event (06/09/2007), **B |** the sole characterized winter stratification (07/02/2008), **C |** end of the late summer period, just before the winter mixing (13/10/2008), **D |** it represents an intermediate situation of the late summer stratification evolution (29/09/2009).

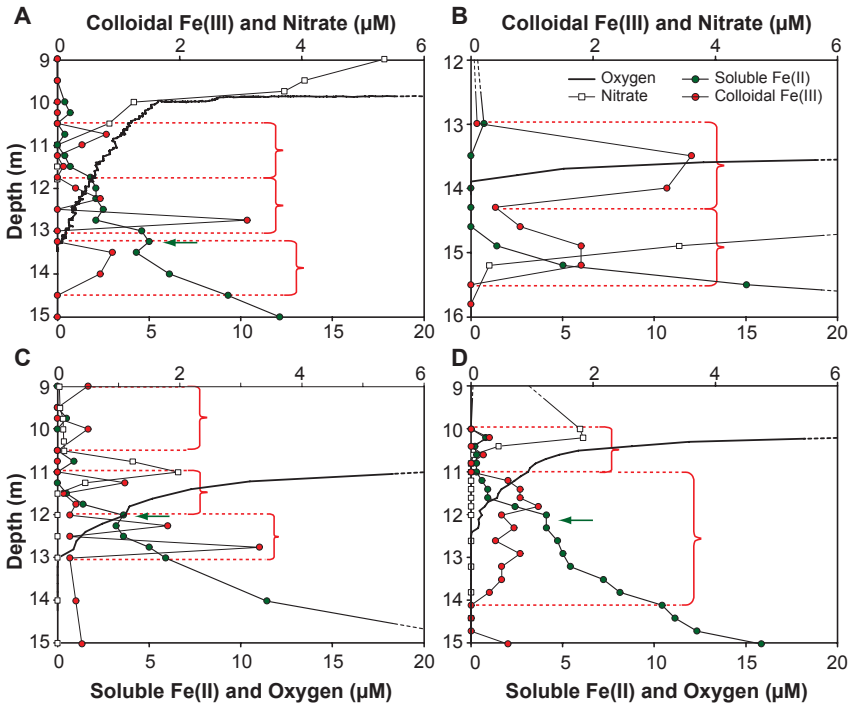

Figure 27: Close up of the same profiles shown in Fig. 28: from 9 m to 15 m depth. **A |** 06/09/2007. **B |** 07/02/2008 **C |** 13/10/2008 **D |** 29/09/2009. The depths enclosed in brackets represent potential layer of Fe(II)-oxidation: a local accumulation of Fe(III) was measured. Arrows indicate depth of Fe(III) respiration: a local Fe(II) vertical gradient or accumulation is observed. Winter chemocline being thicker and deeper, profile **C** has another depth scale: from 12 m to 16 m depth.

three oxidation layers while winter profile only show two (Fig. 27). Differentiation between both biotic and abiotic Fe(II)-oxidations can be deduced on the basis of depths where Fe(III) peaks are detected, and on their relative position regarding the "nitrate-" and the oxycline. Lake La Cruz iron profiling shows two different types of situation: on the one hand Fe(III) peaks are all located within and below the micro-oxic part of the chemocline (O_2 < 10 µM; Fig. 27A-D), while on the other hand the upper peaks are situated in more oxygenated layers (up to 50 µM of O_2; Fig. 27B-C). We could then postulate that Fe(III) detected in oxygenated layer is due to an abiotic Fe(II)-oxidation with oxygen (equation 5).

$$4\,Fe^{2+} + 3\,O_2 + 6\,H_2O \longrightarrow 4\,Fe^{3+}(OH)_3 \qquad (\mathbf{5})$$

As nitrate detection limit is usually below depth of oxygen extinction, Fe(III) peaks just below the oxycline could be the results of nitrate dependent iron oxidizers activity (*see Chap. I.4.4*). Indeed, a close up on the Fe(III) profiles between 9 to 15 m shows the correspondence of Fe(III) and nitrate in the same layers (Fig. 27B-C-D). However, nitrate detection has a lower precision than oxygen detection and thus, the correspondence of the nitrate and Fe(III) is not always matching (Fig. 27A). Concerning the deepest Fe(III) peaks, as there is little to no oxygen or nitrate, they can be considered as the product of the second anaerobic Fe(II)-oxidation process known: anaerobic phototrophic Fe(II)-oxidation (Fig. 27A-C-D).

Regarding oxygen and nitrate profiles, we could consider, if we assume that all three years had a same seasonal evolution, that we have a picture of the physical and chemical variation over a season. Based on this assumption, we can say that Fe(III) does accumulate from middle September to late October (Fig. 40). Therefore, the highest Fe(II)-oxidation occurs at the end of summer. Usually, between the end of August and early September a second whiting event removes an important proportion of oxygenic phytoplankton (Rodrigo *et al.*, 1993; Miracle *et al.*, 2000; Fig. 23A): the summer oxygenic phototrophs bloom results in the precipitation of mostly aragonite and some calcite on organic templates such as living cells, which then sink towards sediments (Miracle *et al.*, 2000). In addition, the oxygenic phytoplankton declines at the end of summer, due to nutrient exhaustion (Romero *et al.*, 2006). This could be an explanation for the Fe(III) accumulation toward sediments at the end of summer: there is less organic matter produced by the less abundant oxygenic phototrophs, thus, less ferrireduction within the water column, which

resulted in a balance in favor of a Fe(III) excess. Another possibility would be the removal of Fe(III)-reducing bacteria by the whiting event. However, Rodrigo (2000) indicated that the whiting event did extract part of the photosynthetic biomass, but there was a differential precipitation: the organic matter sank very slowly, compared to aragonite, but still enriching anoxic waters in electron donors for heterotrophic respiration. Therefore, ferrireduction should not have been limited and Fe(III) should not have accumulated towards bottom water layers. Nonetheless, as methanogenesis is the major pathway for organic matter mineralization in this lake and as Fe(III) settles faster than biomass, ferrireduction should have been limited.

2.4.4. A shadowed sulfur cycling

Sulfur exists in many different redox states, but only sulfate and methylene-blue-reactive sulfide concentrations were investigated. The first observation is that Lake La Cruz is indeed a sulfate-poor water column (max. 46 µM of sulfate; Fig. 28B) and may, as such, be considered as an analogue for an Archean Ocean.

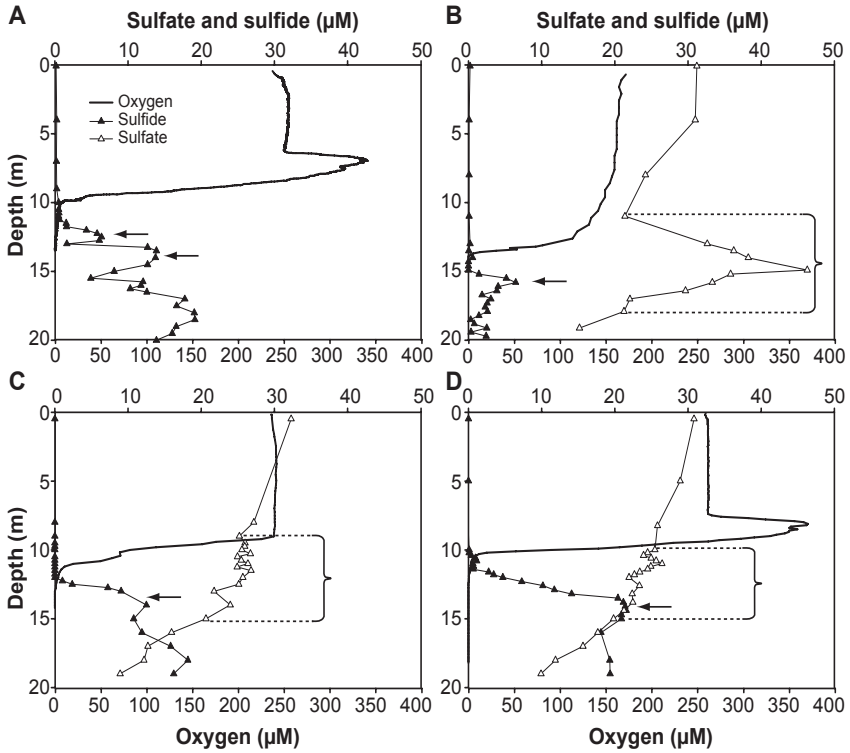

Figure 28: Sulfur and sulfate concentration profiles at the same date as in Fig. 28: **A |** 06/09/2007. **B |** 07/02/2008 **C|** 13/10/2008 **D|** 29/09/2009. Brackets indicate zones of sulfur-compounds oxidation and arrows layers of sulfide production. They were determined on the basis of either local sulfate vertical gradient or local increase of sulfide concentrations. Winter profiles show a sulfate concentration peak where anoxygenic purple phototrophs were present.

As shown by its profile, sulfate is partly consumed within the water column. As previously explained (*Chap. II.1*), the sulfur measured in the water column is essentially as FeS. Indeed, Fe(II) and sulfur react chemically to form FeS particles (< 45 µm; filters pores). Overall, sulfide concentrations are very low (max. 22 µM) compared to other lakes that present euxinic bottom layers (***Chap. III.4.1*, Fig. 19**). All summer sulfide profiles showed an accumulation toward sediments (Fig. 28A-C-D). Conversely, sulfide concentrations in winter (Fig. 28B) did not show such an accumulation. It was during winter stratifications that *Chlorobium clathratiforme*, the dominant green phototrophic sulfur bacteria, had its maximum abundance (Fig. 29). Moreover, it had been shown that the *Chlorobium clathratiforme* were the only anoxygenic phototrophs, isolated from La Cruz, able to grow on FeS (Rodrigo *et al.*, 2000). Therefore, we could postulate that they were responsible for the absence of sulfide accumulation in winter 2008. Alternatively, the lower winter sulfide concentrations (max. 6.4 µM), could be due to a reduced primary production and the subsequent lower organic matter mineralization.

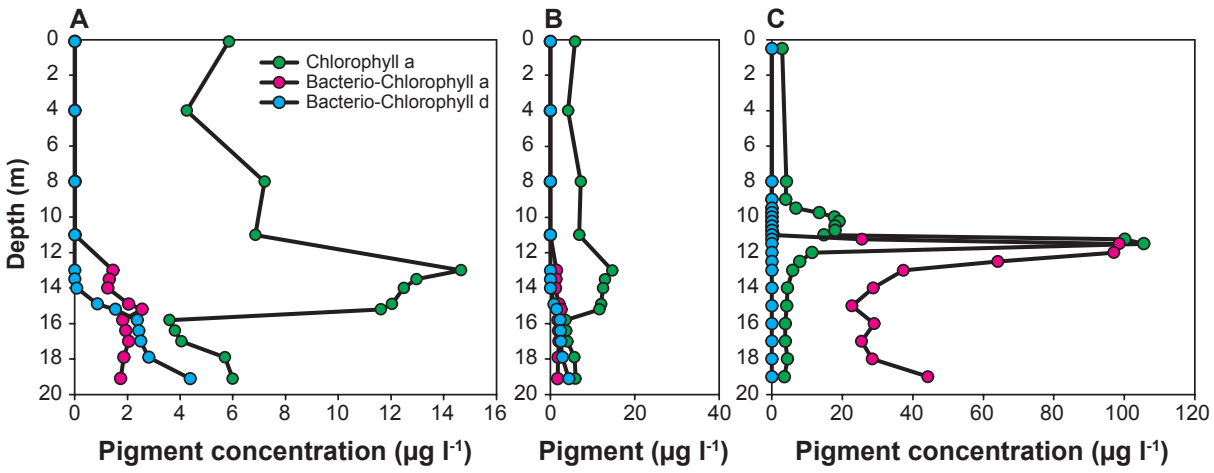

Figure 29: Pigment concentration profiles of the dominant phototrophic populations: chlorophyll a illustrates the distribution of oxygenic organisms, bacteriochlorophyll a stands for the distribution of anoxygenic purple sulfur bacteria and bacteriochlorophyll d report the presence of anoxygenic green sulfur bacteria. **A |** winter stratification marked by the highest density of anoxygenic green sulfur bacteria (07/02/2008). **B |** A profile with the same scale as the summer profile C for comparison. **C|** summer pigments concentration profiles showing the thin layering of the phototrophic populations (13/10/2008).

Differences between winter and summer sulfur cycles were also marked by sulfate profiles. In summer, the layer where anoxygenic phototrophs were most abundant (10-15 m, Fig. 29) exhibited homogenous concentrations (Fig. 28C-D). In contrast, winter sulfate profile showed a local concentration peak (Fig. 28B), indicating an intense sulfate release. In summer, anoxygenic purple sulfur phototrophs (*Lamprocystis purpurea*) are light-limited due to the development of dense populations of oxygenic phototrophs above them. Thus, they have a slow growth (doubling time of 76 days; Rodrigo *et al.*, 2000). It has been proposed that during period of unfavorable light conditions *Lamprocystis purpurea* have alternative mechanisms to maintain cellular viability (Rodrigo *et al.*, 2000). For example they may stock chemolithotrophicaly energy from summer sulfide production as intracellular sulfur inclusions (Visscher *et al.*, 1992). When light conditions get more favorable in winter, but less sulfide is present, they could use the sulfur phototrophically, thus releasing relatively high amount of sulfate (Fig. 28B). In addition, the autumnal mixing transfers part of the anoxygenic phototrophic biomass to the sediment, thereby bringing sulfur and organic matter. This contribution of electron donor and electron acceptor can consequently enable a sulfatoreduction, which could be seen in the summer increase of sulfide concentrations (Fig. 28).

2.4.5. A methanogenic water column

Methane concentrations were determined once only, in September 2007. Water samples were collected in 116 ml glass bottles, using a battery-driven peristaltic pump. The bottles contained 4 NaOH pellets (~ 10 mM final concentration) and were filled to the top. We filled the bottle directly with the pump's exhaust and let 300 ml pass, through and out, the sampling bottle before keeping 100 ml sample. The bottles were then immediately sealed with 1 cm thick rubber septum. Once back into the laboratory, 30 ml of sample were replaced by 30 ml of argon gaz. After an equilibrating period of 30 minutes, 250 µl of sample were injected in a gas chromatograph equipped with a Flame Ionizing Detector (FID; Carlos Erba Fractovap 4130 GC, HP3395 integrator). Methane appeared 6.60 minutes after injection (column: Porapak®N, 3 mm ⦸ and 1.8 m long). The calibration curve was obtained using 1, 100, 1'000 and 10'000 ppm CH_4 standards (Carbagas).

The most noticeable information obtained is that not all of the methane produced in the lake was oxidized within the water column and part of it escaped Lake La Cruz system (Fig. 30). Three types of consumption/production equilibriums can be distinguished based on the shape of the methane profile.

When there is a line (gray layers, Fig. 30), we can consider that methane diffuses, from a zone of high concentration (production) towards a low concentration zone (consumption). In addition, it also means that the production and consumption of methane along the gradient are equivalent. It is important to note that when production equals consumption, it does not imply that there is no methane. Therefore, a peak in concentration denotes a higher production than consumption (blue layers, Fig. 30), while a higher consumption results in a local concentration decrease (red layers, Fig. 30).

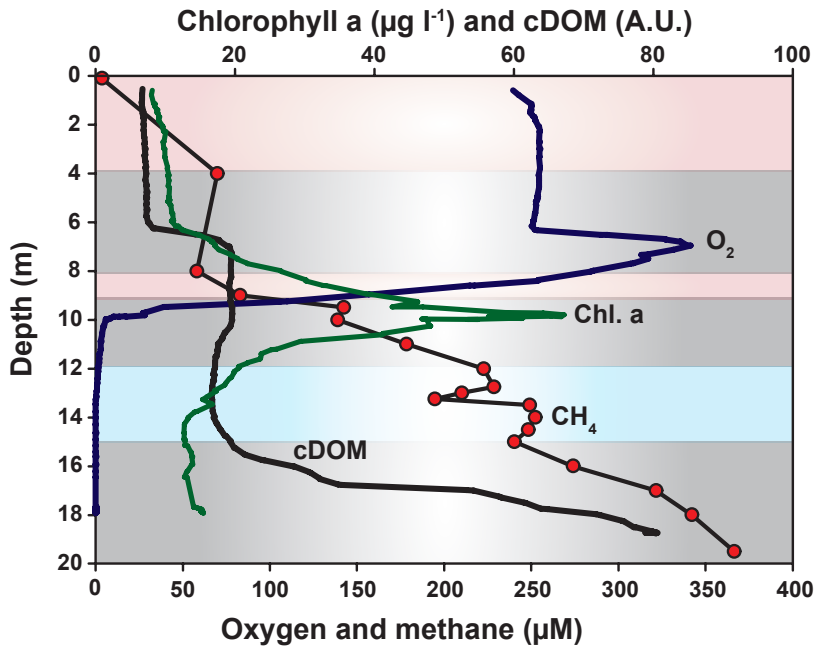

Figure 30: concentration profiles illustrating the context of Lake La Cruz methane cycle (13/10/2008). Layers of methane oxidation are represented in red, layer of local accumulation are in blue, and layers of diffusion are in gray. Part of the methane escapes the system by passing trough the epilimnion. Chlorophyll a serves to locate layers of high primary production.

Higher methane concentrations were measured at the top of the monimolimnion than in the epilimnion (Fig. 30). This points the sediments as the major source of methane and therefore as the main compartment for organic matter mineralization. However, methane concentration profile shows a production within the water column, between 12 and 15 m depth. This layer matches the depths where the cDOM profile indicates a concentration decrease (Blue layer, Fig. 30). We may hypothesise that acetoclastic methanogens could be responsible for the CH_4 production by consuming part of the DOM. The methane seems to be mostly oxidized by O_2 respiration, between 8 and 9.3 m depth (red layer, Fig. 30). In addition, the nitrate gradient starts just below 9 m depth thus excluding a possible anaerobic methane oxidation by nitrate reducers (Raghoebarsing *et al.*, 2006). Because the epilimnion still has high methane concentrations (69.7 uM at 4 m depth, Fig. 30), we consider this upper part (from 0.1 to 4.0 m) as the interface lake/atmosphere from which methane quits Lake La Cruz system. It has to be noted that this layer corresponds to mixed waters.

2.4.6. Conclusions

The four profiled stratifications represent snapshots of an annual chronosequence. It starts with the winter stratification illustrating the steady-state before the progressive evolution to the summer stratification, and it finishes after the late summer (Early September to late October after the last whiting event) by the autumnal mixing. Because anoxygenic phototrophic populations were the most developed, oxygenic one were the smallest (Fig. 22C/24A-B-C), and because accumulation of iron hydroxides was the highest(Fig. 26C), October 2008 summer profile represent our reference for the summer stratification. Moreover, the oxygen concentration profile did not show any oxygen supersaturation peaks at the thermocline (Fig. 24A).

The detection of Fe(III) was a good parameter to determine potential layers of Fe(II)-oxidation: if Fe(III) and nitrate are found in the same water layer, this layer may host nitrate dependent Fe(II)-oxidation; if Fe(III) concentration peaks match a plate of anoxygenic phototrophs, this layer may host an Fe(II)-dependent photosynthesis. The detected anoxygenic purple sulfur phototrophs seem to have a chemotrophic / photoheterotrophic metabolism in summer, while it appears that they have a phototrophic activity during winter stratification. This implies that they stock energy as elemental sulfur during summer periods and oxidize-it during winter periods, when there is more light but only little sulfide (Fig. 29).

Not all of the methane produced in Lake La Cruz was oxidized in the water column (Fig. 30). Therefore, Lake La Cruz represents a methane source for the atmosphere. In addition to the sediments, the methane profile suggests a production zone within the water column, where cDOM seems to be depleted.

2.5. Fe(II)-dependent photoautotrophy

To demonstrate the activity of photoferrotrophs in Lake La Cruz, 3 series of *in situ* experiments with ^{14}C-bicarbonate were performed. The first one was conducted during the winter stratification (11/02/2008) and the two others were carried out during summer stratifications (14/10/2008 and 02/10/2009).

In winter 2008, we started the radiocarbon experiment by evaluating the primary production at different depths (Fig. 31A). The results indicated that oxygenic photosynthesis dominated the microaerophilic layer at 13.5 m, but decreased rapidly with depth and disappeared around 14.6 m. In order to differentiate oxygenic from anoxygenic photosynthesis, we added 3-(3,4-dichlorophenyl)-1,1-dimethylurea (DCMU: 250 µl of a saturated aqueous solution in 10 ml of sample) to inhibit photosystem II (PSII). Anoxygenic photosynthesis only appeared at 14.0 m, peaked at 15.2 m and decreased with depth (Fig. 31A).

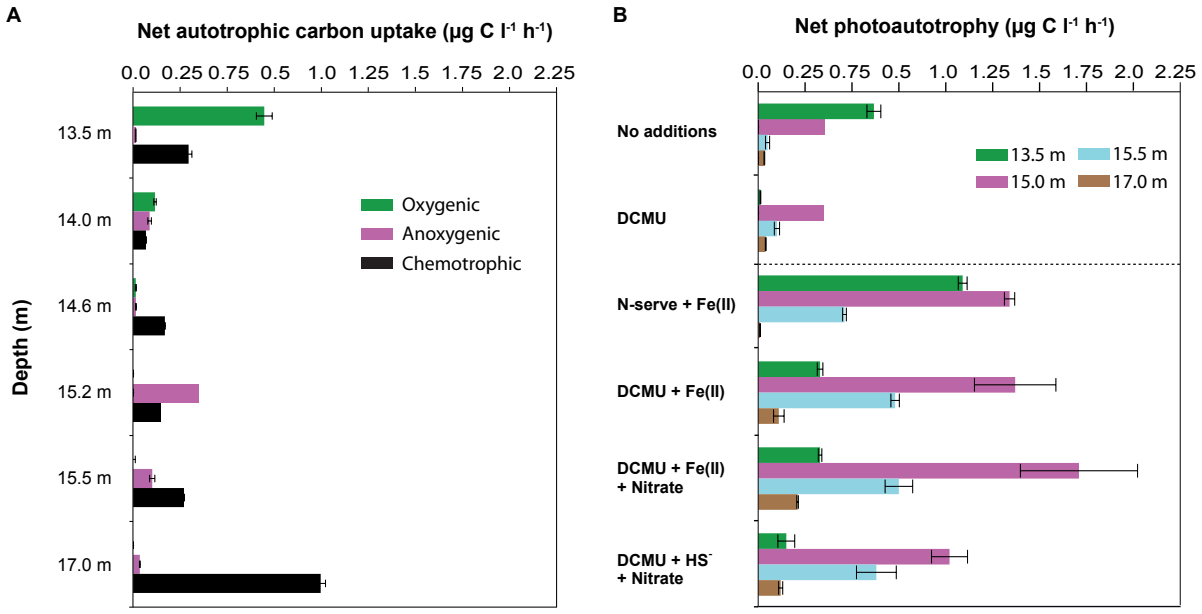

Figure 31: Inorganic carbon uptakes along depth and in presence of potential substrates for lithoautotrophic iron- and sulfur-transforming microorganisms. **A |** *in situ* net autotrophic carbon uptake profiling: net oxygenic photosynthetic carbon uptake was obtained by subtracting the dark incubation values from the carbon uptake in the light. The anoxygenic phototrophic bicarbonate fixation was obtained by subtracting value of DCMU treated light samples from oxygenic photosynthetic ones. **B |** *in situ* net photosynthetic carbon fixation experiments showing a stimulation upon Fe(II) additions. Average values and standard deviations are presented (n = 2).

It has to be noted that net photosynthesis was obtained by subtracting values from dark treatment incubations to the corresponding light treatment. Therefore, as chemoautotrophy was elevated at 17.0

m, the minor variation in the measures between light and dark treatments at those depths suggests a slight photosynthetic carbon uptake (Fig. 31A). However, photosynthesis at this depth is typically an error and should not be considered. The chemotrophic carbon assimilation was mostly present in anoxic layers, below 14.0 m, and increases from 15.2 m depth to reach a maximum at 17 m (Fig. 31A).

The photoferrotrophic metabolism was detected by the effect of Fe(II)-addition on inorganic carbon uptake (*Chap. II.1*). Additionally to Fe(II) (100 µM final concentration) and DCMU, we added 2-chloro-6-trichloromethyl pyridine (N-serve or nitrapyrin) in order to inhibit nitrification (15 µM final concentration). In samples from 13,5 m, a small stimulation of the carbon-uptake was observed (Fig. 31B) compared to the control: 0.18 µg C l^{-1} h^{-1} increase in the "Fe+Nserve". Nevertheless, when the PSII was inhibited and Fe(III) present ("Fe+DCMU" tubes at 13.5 m), an autotrophic activity was still detected. It thus indicates that the 13.5 m samples contained anoxygenic phototrophs. Even if all water layers around the chemocline can be identified by a dominating phototrophic metabolism, they are always composed of a mixture of the different possible metabolisms found in Lake La Cruz. At 15.0 m the stimulation of autotrophy was higher than in samples from 13.5 m (Fig. 31B), especially in the "Fe+DCMU" treatments. Those results indicate that the layer where anoxygenic phototrophs dominate (Fig. 45A, 15.2 m) were more responsive to Fe(II)-additions. Indeed, 15.5 m samples had a less important stimulation. In addition, the carbon incorporation was higher in those samples when treated with DCMU (with or without Fe(II), Fig. 31B: "DCMU+HS^-+Nitrate"). Therefore it illustrates the competition between organisms for nutrients, even when oxygenic phototrophs are in minority.

The controls ("no addition" and "DCMU", Fig. 31B) shown, are values obtained during the primary production profiling (Fig. 31A): they have been incubated at the depth where they were sampled. Conversely, the experimental samples were incubated at 8 m, above the layer of oxygenic phototrophs, in order to stimulate phototrophic metabolisms. Therefore, the detected inorganic carbon-uptake stimulation could be attributed either to a photoferrotrophic activity or to a higher light availability.

In order to assess the effect of light on oxygenic and anoxygenic photosynthesis, we conducted an experiment where samples were incubated at depth of sampling (Fig. 32, "*In situ*") as well as at 10 m above the cyanobacterial plate (Fig. 32, "Potential"). We observed a light stimulation of most samples incubated at shallow depth: e.g. 10.4 m samples had a ~185 % higher carbon uptake (Fig. 32). The only incubation that did not show such a stimulation was the 10.4 m sample treated with DCMU. Since this bicarbonate uptake was due to anoxygenic phototrophs we could postulate that they were not sensible to light availability. This holds true for the 11,0 m depth samples, where purple anoxygenic phototrophs were most abundant (Fig.33).

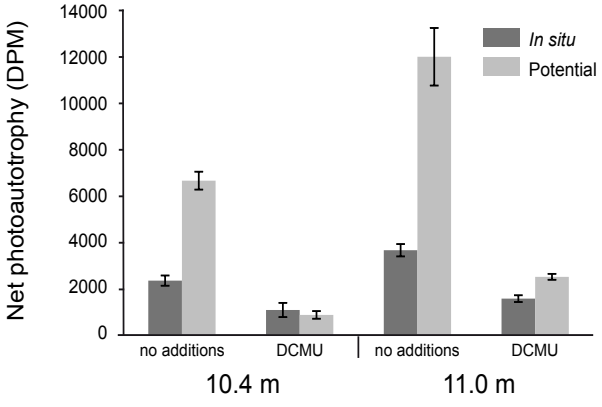

Figure 32: Summer 2009 experiment aimed at evaluating the influence of light upon photosynthetic ^{14}C-bicarbonate. The two depth categories stand for the sampling depth. Half of the tubes were incubated at sampling depth ("*in situ*") while other half were incubated shallower for a light stimulation ("potential"). DCMU was added in order to measure anoxygenic photosynthetic carbon uptake. This experiment shows that anoxygenic phototrophs were poorly stimulated, either at 10.4 m or 11.0 m depth. Average values and standard deviations are presented (n = 2).

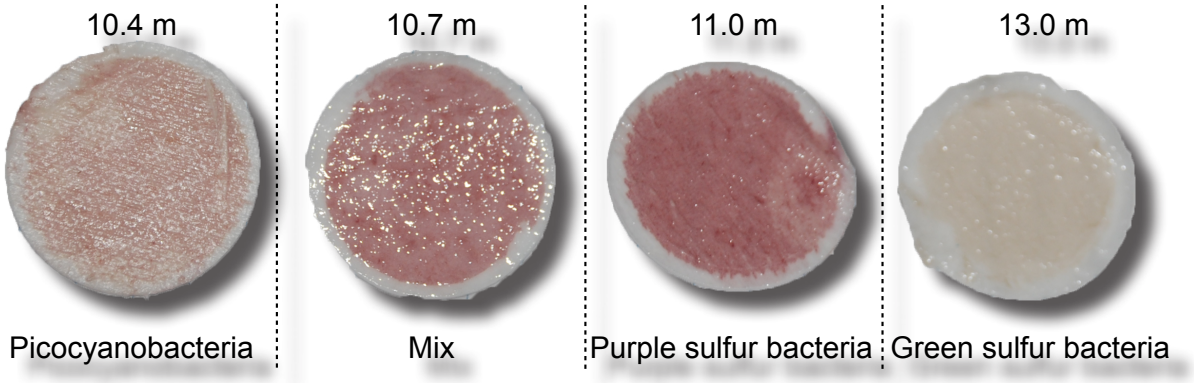

Figure 33: Illustration of the thin stratification occurring during summer stratification (29/09/2009.). Pictures of GF/F filters (Whatman) after filtrating 50 ml of sample. It was a visual control of sampling depth before launching incubations. Dominating population written below pictures, were determined using the CTD probes: phycoerythrine, phyconcyannine, chlorophyll a and turbidity for the anoxygenic purple sulfur bacteria. The depth of 13 m was established, on field, as being the layer where anoxygenic green sulfur bacteria were the more abundant (knowledge of previous surveys: A. Picazo, M. R. Miracle, E. Vicente and A. Camacho personal communications).

The observed difference between the 11.0 m *in situ* incubations (Fig. 32, with DCMU and without) indicates that oxygenic phototrophs participate at that depth to about half of the phototrophic primary production. When the same sample was incubated at shallower depth (Fig. 32, "potential"), it showed a high response to light stimulation. However, even if the autotrophy had a high response (~230 %), the DCMU treatment indicated that much of this carbon uptake stimulation was due to oxygenic phototrophs. The light stimulation on anoxygenic phototrophs did exist, but it was comparatively weak: ~60 % more carbon fixed. Therefore, we can confirm that the high stimulation of photoautotrophy in winter 2008 (Fig. 31B), although partly due to light, was essentially due to Fe(II). Consequently, we can consider that winter incubations did also demonstrate *in situ* activity of photoferrotrophs. Moreover, the strong light response of oxygenic phototrophs, present at depth of low light, confirms the need for DCMU additions: the activity of oxygenic phototrophs overprints the activity of anoxygenic ones.

The need for DCMU in radiocarbon incubations can be explained by the competition that occurs between oxygenic and anoxygenic phototrophs. As shown by the photoferrotrophic enrichment, it seems that the photoferrotrophic activity detected in Lake La Cruz was due to green anoxygenic phototrophs. The Fe(II) time course incubations performed with this enrichment indicated that those organisms had a slow growth (Fig. 17). Additionally, it has been shown that green sulfur phototrophs of Lake La Cruz have a long doubling time (*Chlorobium clathratiforme*: 159 days; Rodrigo *et al.*, 2000), and that they do not fixe more bicarbonate when more light is available (Rodrigo *et al.*, 2000). Therefore, on short term incubations and without any light limitation, the competition is in favor of oxygenic phototrophs. This is why they need to be inhibited by DCMU additions, in order to see an eventual Fe(II) stimulation on anoxygenic photoautotrophs.

2.6. Light dependent Fe(II)-oxidation

A pre-experiment was performed in winter 2008 to verify whether any Fe(II)-oxidation activity of the natural microbiota of Lake La Cruz could be detected. In a general manner we wanted to determine how would react the different samples to Fe(II) additions. We spiked water samples from 13.5 m, 14.0 m and 15 m depth with Fe(II) (~50 µM final concentration) and DCMU. The 200 ml serum bottles were then incubated at the depth of sampling for 130 h. Iron concentrations have been measured at four different time points (Fig. 34).

The first main information was that the initial Fe(II) concentration was much lower than calculated (50 µM). This could be due to the reaction with oxygen: especially in the 13.5 m samples (Fig. 34). The second

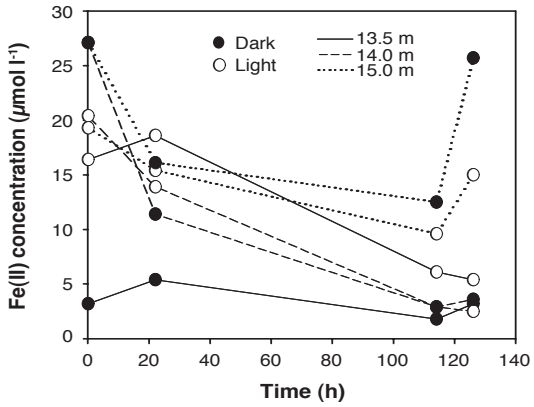

Figure 34: Pre-experiment incubations to see whether or not we could measure any Fe(II)-oxidation. Glass bottles were incubated at the depth of sampling (07/02/2008).

information was that some curves had higher Fe(II) concentration at 130 h than at 118 h. We interpreted this decrease as the change of microbial community resulting in a more reduced environment. Therefore, 500 µM of Fe(II) was added to the *ex situ* incubation performed in October 2008. We also decided to keep the experiment incubation shorter than 120 h.

October 2008 experiment clearly showed a light dependent Fe(II)-oxidation, in presence or absence of DCMU (Fig. 14). At the beginning and the end of the incubations, samples were fixed and treated by the DGGE analysis of the V3 region of the 16S rRNA gene. The profiles showed a high resemblance between the non-incubated sample and the sample incubated under 12 h light/dark regime (*Chap. III.4.2, Fig. 41*, "incubated control 1"). This resemblance indicates that the sample community stayed more or less the same, and thus that the light treatment did not affect the biological structure of the samples. In conclusion, the natural anoxygenic phototrophic guilds of Lake La Cruz oxidized Fe(II) in a light dependent manner, when sufficient light was provided.

In parallel to Fe(II) amended incubations, as the dominant anoxygenic phototrophs in lake La Cruz are sulfide oxidizers, a series of bottles have been spiked with sulfide (~200 µM final concentration) and DCMU. Afterwards, sulfide concentration have been followed in samples under different enlightenment conditions: continuous light (61 µE m^{-2} s^{-1}), continuous dark, and a 12 h L/D shifts (Fig. 35).

Light and 12 h L/D incubations showed that the samples from 11.8 m depth oxidized sulfur anaerobically.

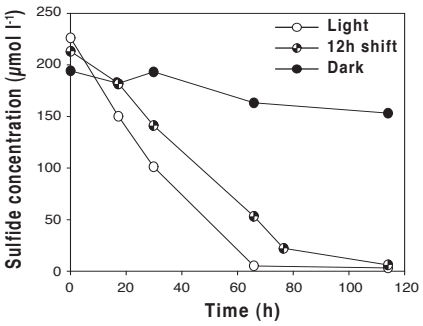

Figure 35: Summer 2008 *ex-situ* sulfide incubations: water was sampled at 11.8 m depth. This was a control treatment for the anoxygenic purple sulfur bacteria. They clearly show the capacity to oxidize sulfur.

Conversely under dark conditions, only little sulfide was oxidized, thus confirming the phototrophic sulfide oxidation by the microbiota from 11.8 m depth. The quick drop in sulfide concentrations indicated that the anoxygenic phototrophs have their enzymatic machinery ready for sulfide oxidation, thus suggesting, depending on light limitation, that they were functioning with this metabolism *in situ*. However, ^{14}C-bicarbonate incubations amended with sulfide (~200 µM final concentration, Fig. 31B) did not show such stimulation as the Fe(II) amended samples (Fig. 13; Fig. 31B). This tend to indicate that anoxygenic

phototrophs were oxidizing sulfur during this long time incubations because there was no light limitation. We could consider that those observations confirmed the theory of Rodrigo *et al.* (2000) stating that during summer stratification the dominant anoxygenic phototrophs (*Lamprocystis purpurea*) oxidize the little sulfide available to constitute energy reserves as intracellular sulfur inclusion, and function on other metabolisms for maintaining cellular viability.

2.7. Enrichment cultures for anaerobic photoferrotrophs

The media used for MPN was the bicarbonate-buffered (pH 6.8) freshwater mineral medium containing 10 mM $FeCO_3$ (Heising *et al.*, 1999; Supplementary material: 2.2). In September 2007 and February 2008 stratifications, waters from different depths were sampled in 500 ml sterile bottles. 1 ml of sub sample was retrieved in injected in the first Hungate tube of a 7 dilutions series. Each depth was investigated in triplicate for the MPN counts. Afterwards, the tubes were incubated at room temperature under a 12 hours light/dark regime. Light was provided by two 10 W tungsten-bulbs, placed at 20 cm from the tubes.

Positives growth were observed only in the winter stratification investigation. As the media was the same as in September 2007, we considered that there were no photoferrotrophs in summer 2007. The winter MPN showed a positive growth after 3 weeks of incubation: little purple aggregates (< 1mm) were visible (Fig. 36).

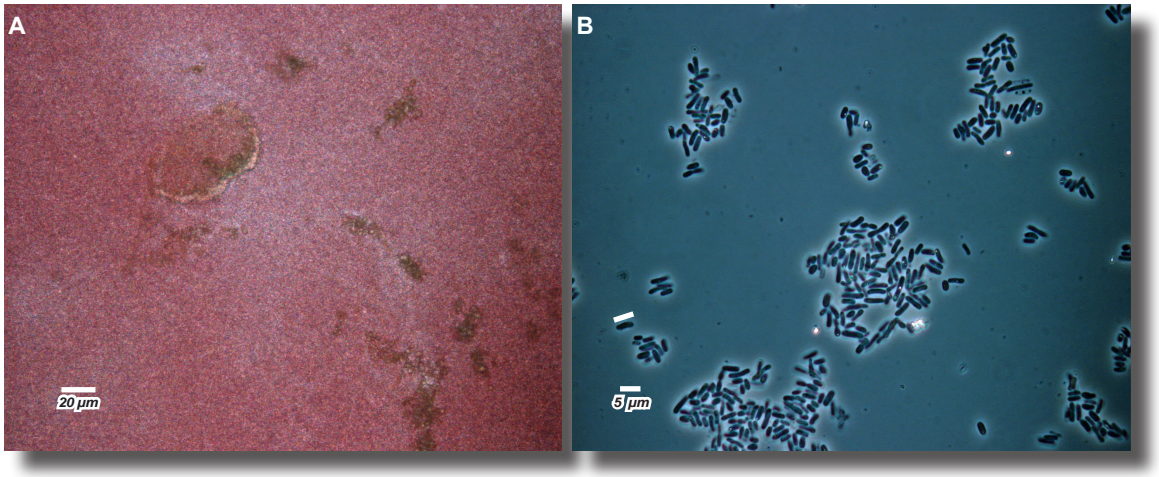

Figure 36: Images of the anoxygenic purple phototrophs that developed in our enrichment. The sequencing indicates that they were *Thiodictyon bacillosum* (99 % similarity, *Chromatiaceae*) growing on photoheterotrophy. Some few cells have 1 or 2 granular inclusions that might be elemental sulfur.

After a period of 2 months, the tubes presenting positive growth were counted and the number obtained was then compared to Mc Crady Tables (Mc Crady, 1915), thus giving us the most probable number of cells in the water sample (Tab. 4).

Table 4: MPN counts for anoxygenic phototrophs growing in the media aimed at photoferrotrophs

Depth	13.5 m	14.5 m	15 m	15.5 m	16.0 m
Cells number (ml^{-1})	$1.5\ 10^2$	$4.5\ 10^3$	$4.5\ 10^3$	$2.5\ 10^4$	$1.1\ 10^2$

However, although growth of purple anoxygenic phototrophs occurred in our tubes, no Fe(II) was oxidized. As the enrichment media contained 1 mM acetate, we concluded that it has been used as the electron donor for photosynthesis: the enriched populations were growing on photoheterotrophy and consequently were not photoferrotrophs. In agreements with this hypothesis most cells did not contain any sulfur inclusion. The 16S rRNA gene sequences of those purple

phototrophs felt into the *Chromatiaceae* family (*γ-Proteobacteria* class) and were most closely related to *Thiodictyon bacillosum* (99 % similarity). Interestingly, those phototrophs are not the dominant anoxygenic purples sulfur bacteria (*Lamprocystis pururea*; Rodrigo *et al.*, 2000; Romero-Viana *et al.*, 2010) that thrive in Lake La Cruz anoxic waters.

The media not being selective for photoferrotrophs, we decided not to use anymore the MPN approach for their enrichment. In fact, for our enrichment, we went the other way round: we took 200 ml of water sample and added 200 µM Fe(II) (final concentration). We also added DCMU to prevent oxygenic photosynthesis. We incubated those samples (different depth sampled) during one month under a 12 hours light/dark regime. Afterwards, 1 ml of each bottle was injected in Hungate tubes containing the media prepared for the MPN. Growth of green phototrophs was observed after 2 months (Fig. 37A) only in tubes inoculated with water from 16.1 m depth. In addition, a brownish precipitate was observed on tube walls (Fig. 37B).

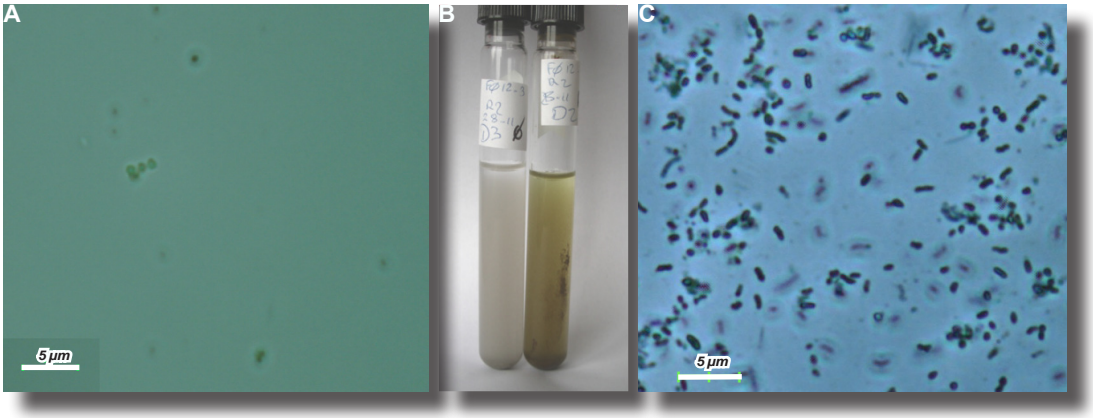

Figure 37: Images of the anoxygenic green photoferrotrophs from our 2nd enrichment approach. **A |** image of the first positive enrichment of photoferrotrophs. **B |** left tube none inoculated control. Right tube: positive growth with brownish precipitates of Fe(III) on the glass-wall. **C |** cells used for the measurement of the Fe(II)-oxidation rates of the enrichment culture.

After the 5th transfer, we took one tube of enrichment culture for a 16S rRNA gene sequencing, and a second one to inoculate a time course incubation centered on Fe(II)-oxidation (Fig. 37C). 80 % of the sequences felt into the Chlorobiaceae family and were closely related to *Chlorobium clathratiforme*, the anoxygenic green sulfur phototrophs already described in La Cruz water column, and to *Chlorobium ferrooxidans* (Heising *et al.*, 1999), the only known green photoferrotroph (Fig. 15). The 20 % remaining sequences of our co-culture were strongly related to an uncultivated *Acidobacteria sp.* (98 %), to which we may attribute the ferrireduction observed during the 5 first days of incubation (Fig. 17). This closest sequence of *Acidobacteria* was retrieved in samples from Lower Kane Cave (Wyoming, USA), an aphotic sulfide-rich environment. The iron-amended time course incubation showed that the enrichment had a light-dependent Fe(II)-oxidation activity which confirms its photoferrotrophic metabolism (Fig. 17). Even if the oxidation rate was low (2.6 µM Fe(II) h^{-1}) it would have been sufficient to account for the totality of Fe(III) found in BIFs ,which needed an oxidation rate of 14 µM d^{-1} to be formed (Table 3). However, if we consider *Acidobacteria* as a ferrireducer, we could consider 2.6 µM Fe(II) d^{-1} oxidation rate as the result of the balance between a continuous Fe(II)-oxidation and a continuous Fe(III)-reduction. Therefore, we could hypothesize, if photoferrotrophs were thriving during the Archean, that Fe(III)-reduction did occur at the chemocline, but the reduction rate was not sufficient to reduce the totality of the produced iron oxides, which thus formed the BIFs.

CHAPTER III: Nitrate-dependant Fe(II)-oxidation in the meromictic Lake La Cruz

X. Alexis Walter, Antonio Picazo-Mozo, Christophe Paul, Maria R. Miracle, Eduardo Vicente, Antonio Camacho, Michel Aragno, Jakob Zopfi

1. Abstract

The discovery of autotrophic bacteria that oxidize reduced iron with nitrate as electron acceptor at neutral pH goes back to 1996. Since then, several chemoautotrophic iron-oxidizing nitrate-reducing bacteria have been described in diverse ecosystems such as freshwater and marine sediments, soils or rice fields. It has also been hypothesized that this metabolism might have contributed to banded iron deposition (BIFs) in an early ocean when nitrate became available on Earth during the Neoarchean. To date, however, nitrate-dependent iron-oxidizing bacteria have not been investigated in any water columns. Therefore, we explored an iron-rich meromictic lake (La Cruz, Spain) to detect and characterize nitrate-dependant iron-oxidation. Physicochemical profiling and in situ ^{14}C-bicarbonate incubation experiments were employed to verify the operation of this process. The abundance of nitrate-dependent iron-oxidizers was estimated by MPN cultivation. Several enrichments were characterized by cloning/sequencing of the nearly complete 16S rDNA gene. Our results indicate, for the first time, that nitrate-dependent chemoautotrophic iron-oxidation occurred within Lake La Cruz chemocline. The organisms responsible for this Fe(II)-oxidation demonstrated, in optimized conditions, that their Fe(II)-oxidation rate was sufficiant to oxidize the totality of the dissolved Fe(II) arriving in the chemocline compartment (21.6 - 38.4 µmol Fe(II) l^{-1} d^{-1} and 0.174 - 1.393 µmol Fe(II) l^{-1} d^{-1} respectively). MPN counts for anaerobic nitrate-dependent iron-oxidizers in other stratified water columns suggest that this metabolism is more widespread than previously thought. In addition, those results support a possible participation of such metabolism to BIFs formation during the Neoarchean, once nitrates were made available after the apparition of oxygenic photosynthesis.

2. Introduction

Iron redox cycling mediated by microbial organisms is of great interest since iron is one of the main redox element in living systems. Iron occurs in nature either as a divalent species (Fe(II)) or as a trivalent species (Fe(III)). The transformation from one species to the other can be mediated by microbial processes. Until recently, only acidophilic (Küsel *et al.,* 1999) or microaerophilic-neutrophilic iron oxidizers (Emerson & Moyer, 1997; Emerson, 2000) and iron reducers were known (Lovley, 2004). The discovery of anaerobic iron oxidation has extended the research field of microbial iron-cycling. Reduced iron (Fe(II)) could be oxidized anaerobically either by photosynthesis (Widdel *et al*., 1993) or by nitrate respiration (Straub *et al*., 1996). Because of light limitation in many iron containing environments (e.g. soil), most studies have focused on the ecology of the chemotrophic anaerobic nitrate-dependent iron-oxidizers (Straub *et al*., 1998, 2004) where they would use soluble or complexed form of Fe(II). Furthermore, the capacity of using Fe(II) present in minerals such as chromite ($FeCr_2O_4$), arsenopyrite (FeAsS), almandine, staurolite (néosilicates) (Chaudhuri *et al*., 2001), or even magnetite (Weber *et al*., 2001) have also been reported.

As shown in former field studies (Hauck *et al*., 2001; Straub & Buchholz-Cleven, 1998; Benz *et al*., 1998; Straub *et al*., 2004; Muehe *et al*., 2009), in most environments Fe(II)-oxidizing nitrate-reducers are less abundant than heterotrophic denitrifiers. It also appears that mixotrophic Fe(II) oxidation with organic co-substrates is the preferred process for nitrate-dependent Fe(II)-oxidation (Chaudhuri *et al*., 2001; Edwards *et al*., 2003; Shelobolina *et al*., 2003; Straub *et al*., 2004; Weber *et al*., 2006[2], 2006[3]). Most described microorganisms seem to be essentially mixotrophs depending on an organic co-substrate such as acetate (Straub *et al*., 1996; Benz *et al*., 1998; Kappler *et al*., 2005[2]). However some enrichments appear to grow lithoautotrophically with energy gain by electron transfer between Fe(II) and nitrate (Straub *et al*., 1996; Weber *et al*., 2001; Edwards *et al*., 2003). Even if it does not dominate heterotrophic denitrification, this metabolism could contribute significantly to Fe(II)-oxidation within the oxic/anoxic boundary in sediments (Straub *et al*., 2004; Muehe *et al*., 2009).

Up to now, such activity has always been investigated in sediments (Straub *et al*., 1996, 1998; Kluber & Conrad, 1998; Nielsen & Myers, 1998; Chaudhuri *et al*., 2001; Hauck *et al*., 2001; Ratering & Schnell, 2001; Finneran *et al*., 2002; Shelobolina *et al*., 2003; Weber *et al*., 2006[2], 2006[3]) and the ecology of related organisms in aquatic environments is, to date, virtually unknown. We therefore addressed the question of the potential activity of such metabolism in a iron-rich water column. If nitrate-dependent iron-oxidation (chemoferrotrophy) thrives in a water column, we should be able to observe the simultaneous presence of nitrate, Fe(II) and also Fe(III). Such physico-chemical conditions were met in Lake La Cruz chemocline. We hypothesized that nitrate-dependent iron oxidizers (NDIO) were present in Lake La Cruz and contribute to Fe(II)-oxidation where NO_3^- and Fe(III) concentrations peaks overlapped. Fe(II)-oxidation by the natural microbial community in the chemocline and Fe(II) stimulation of chemoautotrophy were tested using *in situ* and *ex situ* experiments. MPN counts were used to estimate NDIOs abundance (Straub & Buchholz-Cleven, 1998). For comparison to Lake La Cruz, MPN counts of NDIOs were determined in two other lakes with permanent (Lake Cadagno, Switzerland) and transient (Lake Loclat, Switzerland) chemoclines.

3. Material and methods

3.1. Sites and sampling

Lake La Cruz (UTM 30SWK962272) is situated in the Central Iberian Ranges (Spain) near Cañada del Hoyo. This 122 m diameter lake is a 20 m deep karstic sinkhole laying on Fe(II)-rich marls. It started to be

meromictic at the end of the 17th beginning of the 18th century (Maunder minimum; Julia *et al*., 1998). In this lake, reduced iron originates from the underlying marls (Julia *et al*., 1998; *Chap I: 4.1,Fig. 11*). The rainwater that passes through the dolomite dissolves carbonates. After hitting the marls, rainwater dissolves marls Fe(II) which should be oxidized in Fe(III) while removing dissolved oxygen, then the anoxic fluids containing the remaining Fe(II) arrives in La Cruz sinkhole bottom (Rodrigo *et al*., 2001; *Chap. I.4*). High concentrations of dissolved bicarbonate, calcium, magnesium and ammonium, are found in the hypolimnion bottom and contribute to the physical stability of this water layer (Rodrigo *et al*., 2001). As a result, a monimolimnion layer is established. The bottom waters never mix with the overlaying hypolimnion. This meromictic lake differs from other meromictic karstic lakes in Spain (e.g. Lake Vilar, Lake Banyoles, Lake Cisó) by its low sulfate concentration due to the absence of gypsum in the surrounding rock substrate (Vicente & Miracle, 1988; Miracle *et al*., 1992). As a consequences, total sulfide/sulfate are much less abundant than dissolved Fe(II).

Lake Cadagno is a 21 m deep permanently stratified (meromictic) lake, created by glacial erosion, situated at an altitude of 1921 m in Piora Valley (Swiss Alps). The density stratification is due to dense sulfate-enriched waters that had passed a gypsum-containing dolomite vein before entering the lake through subaquatic springs (Tonolla *et al*., 1998), reaching 1.1 mM at the chemocline (~11 m depth) and 2 mM near the bottom of the lake (Canfield *et al*., 2010). As a result of sulfate reduction in the water column and sediments, sulfide concentrations of up to ~300 µM are measured in the hypolimnion sustaining dense populations of anoxygenic phototrophic sulfur bacteria (both green and purple) at the chemocline (Schanz *et al*., 1998; Tonolla *et al*., 1999). This lake represents a mesotrophic meromictic iron-poor and sulfate-rich water column.

Lake Loclat is a small holomictic eutrophic lake (Schweizer & Aragno, 1975) situated Northeast of Lake Neuchatel (Switzerland) at an altitude of 432 m, with a surface area of ca. 4.5 ha and a maximum depth of 9.7 m (Conrad *et al*., 1983[1-2]). During summer stratification Lake Loclat possesses an oxic epilimnion and an anoxic sulfidic hypolimnion. A transient chemocline at ~5.5 m depth provides favorable conditions for anoxygenic purple sulfur phototrophic bacteria.

Water samples were collected using a battery-driven peristaltic pump from a boat in the center of the lake. We used plastic syringes to keep anoxia during samples handling. Samples where immediately filtered through GF/F filters (pores of 0.7 µm; Whatman) when needed for the analysis (Fe(II), Fe(III), H_2S, NH_4^+, NO_3^-, NO_2^-, anions and cations). Each of those filters was previously flushed with 10 ml anoxic miliQ water before sample filtration (on board). Then, the 10 first ml of sample were discarded in order to eliminate any dilution effects due to the miliQ water remaining in the swinnex filter holders (Millipore).

3.2. Physical and chemical profiling

Water column profiles of temperature, conductivity, pH, redox potential, dissolved oxygen, and chlorophyll a were recorded using a Sea-Bird CTD multiprofiler. For dissolved iron analysis 9 ml of water samples were filtrated and immediately fixed in 1 ml HCl 5 M. Dissolved Fe(II) and Fe(III) concentrations were determined using Ferrozine (Viollier *et al*., 2000; *Annex I.4*). For sulfide measurements, 8 ml of filtrated samples were immediately fixed in 2 ml of zinc acetate 5% (w/v). Sulfide concentration was determined by the Cline assay (Cline, 1969). Samples were directly fixed on board. For total Fe(III) and H_2S concentrations, samples were fixed without filtration. The methodology used for SO_4^{2-}, NH_4^+, NO_3^- and NO_2^- concentration measurements have been described previously (Haller *et al*., 2011; Zopfi *et al*., 2001).

3.3. In situ radiocarbon incubations

Experiments were carried out during the summer stratification (13-17 Octobe 2008) with Lake La Cruz water samples from 11.8 m depth. Incubations were performed in 10 ml N_2-preflushed vacutainer tubes with the following additions from anoxic stock solutions (final concentrations): i) untreated control, ii) $FeCl_2$ (100 µM), iii) $NaNO_3$ (50 µM), iiii) Na_2S (100 µM). All of the treatments were set up in duplicates in the dark.

Tubes were spiked with 5 µCi of anoxic ^{14}C-bicarbonate (DHI, 2970 Hørsholm) and immediately incubated for 3 to 4 h at 10 m depth (12.6°C). After incubation the sample were immediately killed with formalin (2% final concentration), and filtered (polycarbonate membrane filters, Whatman). Filters were rinsed twice with 0.5 M HCl and finally with milliQ water. After a drying period of 36 h under a fume-hood, filters were counted in 10 ml of Sigma-Fluor LSC cocktail scintillation liquid, for non-aqueous samples, on a Wallac 1409 liquid scintillation analyzer. Rates were calculated according to: Uptake rate = ^{14}C-fixed x $[\Sigma CO_2]$ x 1.06 / $\Sigma^{14}CO_2$ x t , where ^{14}C-fixed is the radioactivity counts per filter minus control, $[\Sigma CO_2]$ is the total DIC concentration in the water at the sampling depth, 1.06 is the correction factor for isotopic fractionation between ^{12}C and ^{14}C, $\Sigma^{14}CO_2$ is the total DIC radioactivity per vial, and t is the incubation time (*Annex I.5*). Uptake rates were used to build a generalized linear model (-C- uptake ~ Fe + NO_3^- + H_2S) with a binomial distribution (MacCullagh & Nelder, 1989). The influences of the treatments on carbon uptake were tested using ANOVA. All analysis were performed using the statistical software "R" (R Development Core Team, 2009).

3.4. Ex situ dark Fe(II)-oxidation

N_2-flushed bottles (500 ml) were filled with Lake La Cruz water, also from 11.8 m depth, and closed with thick butyl rubber stoppers. The samples were directly transported to the laboratory of the university of Valencia, under dark and cool conditions. Bottles were then placed in a dark cold room (4°C). Incubations experiments were performed at 14 °C and started 36 hours after sampling by the addition of the following compounds from anoxic stock solutions (final concentrations): i) $FeCl_2$ (≈ 400 µM), ii) $FeCl_2$ + $NaNO_3$ (≈ 50 µM) and iii) $FeCl_2$ + $NaNO_3$ + N-serve (22 µM). As N-serve (nitrification inhibitor) (Knowles, 1982; Hadas *et al*., 2001) is not water-soluble, 28.01 mg were dissolved in 200 µl absolute ethanol and then added to 100 ml anoxic sterile miliQ water corresponding to a 1.2 mM stock solution. Control (Fe(II) + NO_3 + N-serve) was killed by the addition of an anoxic formalin solution (2 % final concentration). The evolution of Fe(II) and Fe(III) were followed by the Ferrozine assay (Viollier *et al*., 2000) on 1 ml sub-samples.

3.5. Cultivation media for nitrate-dependant Fe(II)-oxidizers

The medium, used for MPN counts and enrichment cultures, was a composite (*Annex I.2*) of the multipurpose medium for anaerobic respirations (Widdel & Bak, 1992) and the freshwater medium for anaerobic ferrous iron-oxidizing nitrate-reducing bacteria (Straub & Buchholz-Cleven, 1998). The basal media contained (per liter of distilled water) 0.4 g of NH_4Cl, 0.9 g of $MgCl_2$.6 H2O, 0.4 g of KH_2PO_4, 0.3 g of $CaCl_2$.2 H_2O, and 0.25 g of NaCl. After autoclaving and cooling 970 ml basal medium under an atmosphere of N_2/CO_2 (90:10), 30 ml of 1 M $NaHCO_3$ (autoclaved under CO_2), 1 ml of sodium acetate (1mM final concentration),1 ml of vitamins mix solution, 1 ml of thiamine solution, 1 ml of trace elements solution and 1 ml of selenite-tungstate solutions were added. The electron donor was added as ferrous carbonate (10 mmol l^{-1} final concentration). The medium was then distributed in 10 ml Hungate tubes. The electron acceptor was added as nitrate (1 mM final concentration) prior to pH adjustment at 7.1. $FeCO_3$ was prepared, under a continuous flow of N_2/CO_2, by combining 28 g of $FeSO_4$.7 H_2O to an anoxic solution containing 10.6 g of Na_2CO_3. The $FeCO_3$, formed as a grayish precipitate, was rinsed with boiled distilled water cooling under CO_2 flux. The Fe(II) concentration was determined using the Ferrozine assay (Viollier *et al*., 2000). A volume

of 4 ml sodium nitrate solution (1 M; electron acceptor) were also added prior to the pH adjustment at 7.1.

The abundance of NDIO was estimated using most probable number approach (MPN dilution series) using the Mc Crady tables (Straub & Buchholz-Cleven, 1998; Weber *et al*., 2006[2]). Triplicate, of 7 dilutions per sample were incubated at room temperature in the dark for 2 months. It has been shown that a positive growth of NDIOs in such media can be visually controlled by the presence on glass walls of green rust. In some cases red rust was formed, but it was occasional (Paul, 2011). We therefore used the presence of compact green rust as the signal identifying a positive growth. We investigated Lake La Cruz water column using MPN approach during two stratification periods: once in summer equilibrium (September 2007) and once during winter stratification (February 2008). Lake Loclat and Lake Cadagno were considered for MPN approach during their summer stratification. Lake La Cruz was sampled at 10.8 m, 11.5 m, 12.3 m and 13.5 m depth for MPN counts and for enrichments. Lake Cadagno was sampled for MPN counts in the lowest part of the epilimnion (5.5 m), in the anoxic part of the chemocline (12 m) and in hypolimnion (17 m) . In Lake Loclat, the MPN counts were focused more into the chemocline, by a sampling at 5.25 m, 5.75 m and 6 m depth.

3.6. Fe(II)-oxidation of enrichment cultures

We inoculated 2 ml of the NDIO pre-culture, the last positive tube of the 5th dilution to extinction series, into tubes containing 9 ml of media (*Annex I.2*). Incubations were carried out in duplicate under continuous light and continuous dark conditions at 22°C. Light incubations were performed to check for any photooxidatives effects. Controls were killed by addition of anoxic formalin (2% final concentration). One duplicate of the controls was incubated in continuous light and the second one in the dark. The Fe(II)/Fe(III) evolution was then followed, using Ferrozine assay (Viollier *et al*., 2000). Because initial concentrations varied from tube to tube, concentrations were expressed as percentage of the initial Fe(II) concentration.

3.7. Molecular analysis

One goal was to describe how the *ex situ* treatments impacted on the microbial community composition at 11.8 m depth. At the end of the experiment we extracted DNA from 50 ml filtered sample of the following incubation conditions: "Fe(II) + NO_3 + light", "Fe(II) + NO_3 + dark", "NO_3 + dark" , a non-amended incubated sample (incubated control 1) and a non-incubated sample ("control 1").

A second 50 ml filtered sample of the anoxic euphotic part of summer 2007 chemocline (10.8 m), was treated. In addition, its enrichment culture ("Sample 2 enrichment") and the three-isolated clone from it (clone 1, 2 and 3) were also processed through DGGE profiling. Protocoles for PCR amplification and DGGE have been described previously (Pronk *et al*., 2009; *Annex I.6*).

4. Results and discussion

4.1. Physical and chemical stratification of Lake La Cruz

September 2007 stratification was characterized by i) a chemocline in the metalimnion between 9.0 m and 12.8 m depth (from +110 mV to -215 mV), and ii) a pycnocline between 15 m and 18 m depth (700 µS cm^{-1} to 1450 µS cm^{-1} respectively), delimiting the monimolimnion (18-20 m). In comparison, in October 2008 the chemocline was deeper and 80 cm thinner (11.2-14.2 m; +133 mV and -200 mV, respectively; *Annex II.3*). In October 2007, sulfate concentrations ranged from ≈ 25 µM in the metalimnion to 8.9 µM at 19.0 m depth (*Annex II.2*). At the same time sulfide concentrations rose from 1.0 µM at 12.25 m depth to 18.1 µM at 18 m depth. In October 2008, a sulfide concentrations increase was measured between 13.0 m

and 15.0 m depth (maximum of 12.5 µM, Fig.38). A similar increase of sulfide concentrations was also detected, during September 2007 stratification, between 13.25 m and 14.5 m depth (maximum of 13.8 µM, Fig.38). These results suggest that part of the sulfide arriving at the chemocline was produced within the water column. The 16S rRNA gene of sulfate reducers retrieved from the chemocline also supports this hypothesis (*chap II: 2.3*). In overall, the inter-annual variations are within the range of previously reported values (Rodrigo *et al*., 2001, Camacho *et al*., 2003).

Lake la Cruz vertical mixing is limited because of its location inside a dissolution basin with steep vertical walls rising 20-30 m above the water surface. The Fe(II)-rich Lake Pavin (Massif Central, France) and the sulfide rich Lake Cadagno (Alpine valley, Switzerland) are both meromictic (Bura-Nakic *et al*., 2009; Dahl *et al*., 2010), either due to a small surface/depth ratio (Lake Pavin) or to a wind-sheltered position (Lake Cadagno). For these reasons, we chose their eddy diffusivity values (K_z) to estimate the minimum Fe(II) vertical flux (*Fz*) according to $F_z = -K_z * (\Delta C/\Delta Z)$. The two vertical eddy diffusivity (K_z) values chosen ranges from $5.0x10^{-4}$ cm^{-2} s^{-1} (Lake Pavin) to $4.0x10^{-3}$ cm^{-2} s^{-1} (Lake Cadagno). A minimum upward flux of 0.031-0.244 µmol Fe(II) cm^{-2} d^{-1} towards the oxic/anoxic interface was calculated. We postulated that the water layer, where iron-oxidation could occur, was situated between the upper limit of Fe(II) (11.25 m) and the lower limit of the Fe(III) peak (13.00 m, Fig. 38). The Fe(II) arriving at the oxycline (0.031-0.244 µmol Fe(II) cm^{-2} d^{-1}) is thus completely oxidized within a 1.75 m thick water layer. Without taking into account recycling by Fe(III)-reduction, the calculated minimum oxidation rates within the 1.75 m water layer were ranging between 0.174 and 1.393 µmol Fe(II) l^{-1} d^{-1}.

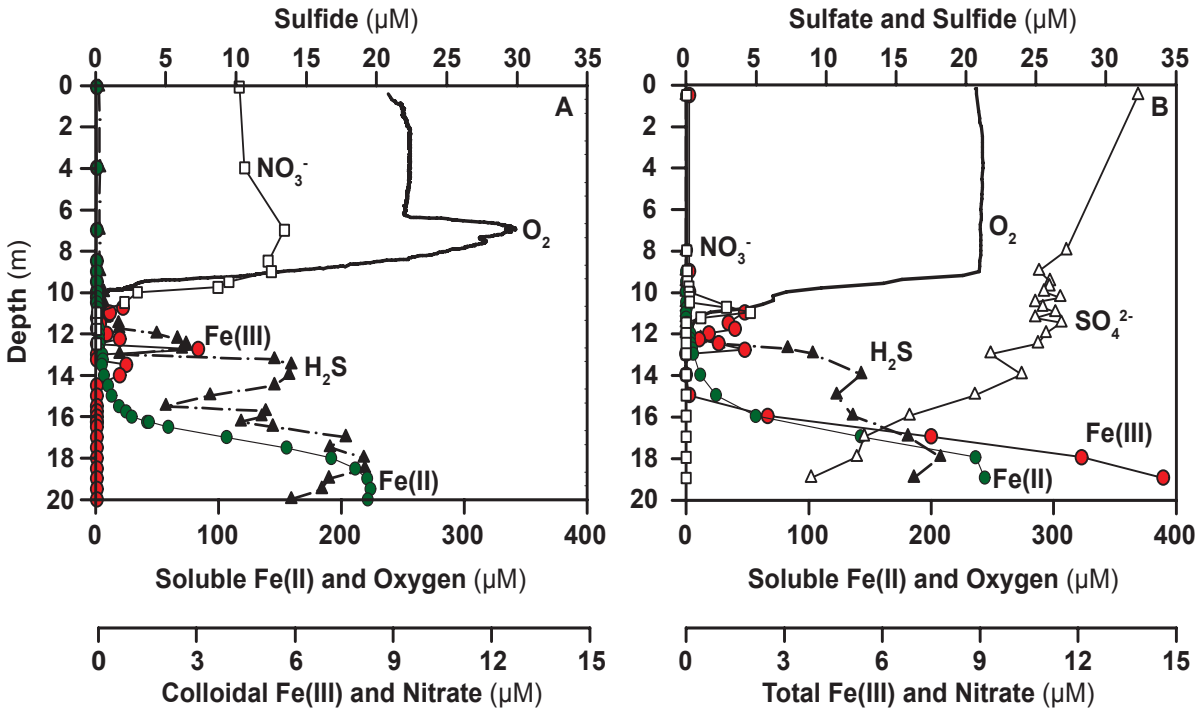

Figure 38: Chemical stratification of the Iron-rich and sulfate-poor Lake La Cruz: **A |** 06/09/2007 **B |** the 13/10/2008. Fe(III) measured in summer 2007 was the colloidal fraction (pass GF/F filters), while the summer 2008 profile consist of total Fe(III) (no filtration). As shown by the O_2 profile, the October oxycline was 1 m lower than in September 2007. Whatever the chemocline depth was, both Fe(III) and NO_3 were detected in the micro-oxic layer during summer stratification.

The comparison between summer 2007 colloidal Fe(III) profile (Fig. 18A) and the summer 2008 one (Fig. 38B), indicates that the accumulation toward the monimolimnion only occurs in October 2008 (14.6 µM Fe(III) at 19.0 m; *Chap. II: 2.4.3*). It could be due to the filtration step performed in September 2007, which removed Fe(III) particles larger than ≈ 0.7 µm diameter (GF/F pore size). However, the colloidal Fe(III)

analysis performed in October 2008 also indicated an accumulation of Fe(III) toward the sediment (13.6 µM Fe(III) at 19.0 m).

The signal given by the detection of colloidal Fe(III) was constituted of thinner peaks emerging from the background noise (Fig. 38A). Therefore, total Fe(III) measurements (without filtration step) seems to be more adequate for detection of a potential Fe(II) oxidation zone. During both stratifications, NO_3^- and Fe(III) were present at the same depth (Tab. 5). At this depth, Fe(II) residual concentration was bellow detection limit, but we assumed that this layer was a potential zone for NDIOs development. However nitrite, as potential intermediary product of such activity, was not detectable because of the high nutrients dynamic in summer stratification (Picazo *et al*., 2011).

Table 5: Nitrate and Fe(III) concentrations in Lake La Cruz chemocline.

09/09/2007				13/10/2008			
Depth (m)	**NO_3^- (µM)**	**Depth (m)**	**Fe(III) (µM)**	**Depth (m)**	**NO_3^- (µM)**	**Depth (m)**	**Fe(III) (µM)**
10.00	1.25	10.50	0	11.00	1.98	10.00	0.1
10.50	0.85	10.75	0.8	11.25	0.45	11.00	1.8
11.00	0.00	11.00	0.4	11.50	0.00	11.50	1.3

4.2. Chemoferrotrophy in Lake La Cruz water column

Our hypothesis was that NDIOs are present where NO_3^- and Fe(III) concentration peaks overlap (*Chap II: 2.4.3*). Therefore, we sampled Lake La Cruz chemocline, in summer and in winter (06/09/2007 and in 07/02/2008, respectively), using MPN approach for nitrate-dependent iron-oxidizers (Straub & Buchholz-Cleven, 1998). Only the summer MPN counts showed a significant presence of NDIOs at the chemocline (Tab. 6). Results showed a presence maxima at the depth where NO_3^- and Fe(III) were both detected (summer profile): 10.8 m and 11.5 m (Tab. 5). Bellow the summer NO_3^- extinction depth, MPN counts indicated a weak presence of NDIOs (12.3 m and 13.5 m, Tab. 6), thus suggesting that the counted NDIOs were obligate nitrate-dependent Fe(II)-oxidizers. Conversely, even if NO_3^- and Fe(III) were both measured in the same layer during winter stratification, MPN counts indicated that they were nearly absent from the water column (Tab. 6).

Table 6: MPN counts for NDIOs in Lake La Cruz, Lake Cadagno and Lake Loclat water columns. Those counts were made the 06/09/2007 and the 07/02/20008 in Lake La Cruz, the 28/07/2009 in Lake Cadagno, and the 25/09/2008 in Lake Loclat. All the MPN were performed using the same media. The sample depth are centered around the oxycline. * data obtained by Christophe Paul for his Master thesis.

Lake La Cruz				Lake Cadagno *		Lake Loclat *	
Summer 2007		Winter 2008		Summer 2008		Summer 2009	
Sampling depth	**Cell counts (cells ml^{-1})**	**Sampling depth**	**Cell counts (cells ml^{-1})**	**Sampling depth**	**Cell counts (cells ml^{-1})**	**Sampling depth**	**Cell counts (cells ml^{-1})**
10.8 m	$1.15\ 10^4$	13.5 m	$4.0\ 10^1$	5.5 m	$2.5\ 10^1$	5.25 m	$1.5\ 10^5$
11.5 m	$2.5\ 10^4$	15.0 m	$9.0\ 10^1$	12.0 m	$4.5\ 10^5$	5.75 m	$1.4\ 10^5$
12.3 m	$9.5\ 10^1$	15.5 m	$9.0\ 10^1$	17.0 m	$1.1\ 10^6$	6.00 m	$4.5\ 10^5$
13.5 m	$9.5\ 10^1$	16.0 m	$9.0\ 10^1$	-	-	-	-

However, the MPN counts performed in Lake Cadagno and Lake Loclat show first that the number of NDIOs were higher than in Lake La Cruz, and secondly that they were found in all the sampling depth, independently from the presence of Fe(III) (Tab. 6). As those lakes are iron-poor (Supplemental material: Fig. 43), the natural development of obligate NDIOs should have been limited. Therefore, those high positive

counts suggest that nitrate dependent iron oxidation is a facultative metabolic pathway. In addition, it suggests that NDIOs are more abundant in water columns than in sediments: NDIOs generally represent 0.004-0.04 % of the total sediment bacterial community, with maximum of 3 % ($2.4x10^3$ et $5.0x10^8$ cell g^{-1}; Straub & Buchholz-Cleven, 1998; Weber *et al*., 2006[2]), while in Lake Cadagno and Lake Loclat show that they may constitute theoritically 1-10 % of the whole bacterial population (average of 10^6-10^7 cell ml^{-1} in lakes; Chrost *et al*., 2009 ; Lehours *et al*., 2005). Furthermore, their detection in different lakes, from iron-rich to iron-poor and from oligotrophic to eutrophic water columns, indicates that this pathway could be widespread among denitrifiers (Paul, 2011).

As MPN counts showed the presence, in Lake La Cruz, of NDIOs at the layer where both Fe(III) and NO_3^- were detected, the next objective was to detect a stimulation of dark autotrophy by Fe(II), NO_3^- and H_2S additions. We therefore performed *in-situ* ^{14}C-bicarbonate assimilation experiments (October 2008) with water from 11.8 m depth. As these were short-time *in-situ* incubations (maximum of 4 hours), we assumed that only active autotrophs in sufficient numbers would give a measurable signal. With regard to the carbon-uptake amount in controls ("No addition"), the sole addition of nitrate or sulfides did not affect rates of CO_2 uptake (Fig. 39). Conversely, Fe(II) addition stimulated dark fixation by about ≈ 400 % (p = 0.011). The addition of nitrate together with Fe(II) further increased chemoautotrophy by 15 % but this was not statistically significant (Fig. 39).

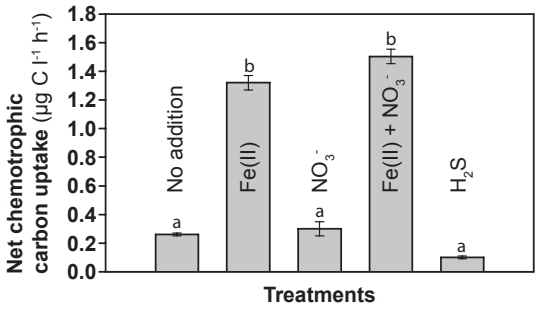

Figure 39: Dark bicarbonate uptake in presence of potential substrates for chemolithoautotrophic iron- and sulfur-oxidizing microorganisms**.** *In-situ* net chemotrophic carbon uptake experiments show a stimulation under Fe(II) addition ($p<0.05$). Note that neither nitrate nor sulfide addition does stimulate carbon uptake. Letters represent statistical group.

If summer 2008 clearly showed the presence of actives Fe(II)-dependent chemoautotrophs, the same radiocarbon incubations performed earlier, in winter 2008 stratification, didn't show such a stimulation (Supplemental material: 6.2). *In-situ* ^{14}C-bicarbonate assimilation experiments, thus, confirm the MPN counts results: NDIOs in Lake La Cruz are more active/present during summer stratification.

To complement those results, we verified if the same guilds (October 2008, 11.8 m) could actually oxidize Fe(II) in a nitrate-dependent manner. A long-term *ex-situ* incubations (120 hours) was therefore performed with the same samples as the one used for the radiocarbon incubations. Results showed that a clear Fe(II)-oxidation only occurred when both $FeCl_2$ and $NaNO_3$ were present (Fig. 40). Indeed, no clear Fe(II)-oxidation was observed when only $FeCl_2$ was added (Fig. 40).

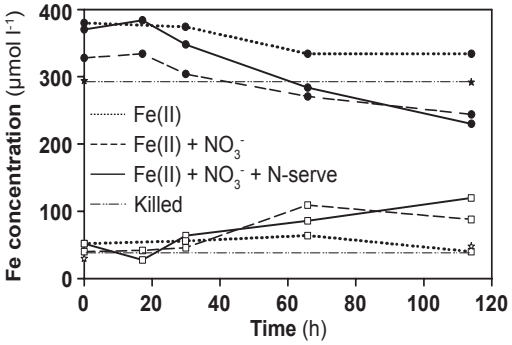

Figure 40: Nitrate-dependent iron-oxidation experiments with water samples from 11.8 m depth (15/10/2008). All incubations were performed in the dark. Fe(II) (solid circles) and Fe(III) (open squares) concentrations evolution in Fe(II) amended 11.8 m deep samples. We see that most of the Fe(II) is oxidized in Fe(III). Four treatments are illustrated: "no addition" treatment, "Fe(II)" amended treatments, "Fe(II) + NO_3^-" treatments. "Fe(II) + NO_3^-+ Nserve" addition and "Fe(II) + NO_3^-" killed control. Note that, the Fe(III) measurements may underestimate the real concentration because of Fe(III) adsorption on the glass bottles walls.

Moreover, the addition of N-serve, an inhibitor of nitrification, did not decrease but even increased the iron oxidation rate to 1.6 µmol Fe l^{-1} h^{-1}, instead of 0.9 µmol Fe l^{-1} h^{-1} (Fig. 40). Thus, we could postulate that nitrification did not influence nitrate dependent Fe(II)-oxidation. However, as those incubations were carried out in simplicates, we can only conclude that the 11.8 m guilds oxidize Fe(II) in the dark and that they need nitrate to perform it (Supplemental material: 6.3).

In order to visualize if the impact of the treatments applied to the *ex situ* incubations, DGGE profiling was performed. Indeed, such a finger printing of the microbiota could indicate if the population responsible for the measured Fe(II)-oxidation are abundant, or not, in the untreated sample. Moreover, we would be able to verify that the enriched NDIOs were, or not, the one responsible for the detected nitrate-dependent Fe(II)-oxidation in Lake La Cruz chemocline. The DGGE fingerprints of the 16S rRNA V3 gene (Fig. 41) reveal that there were no impact on the samples diversity during the incubation: no difference were observed between incubated and non incubated controls ("Control 1" and "Control 1 incubated").

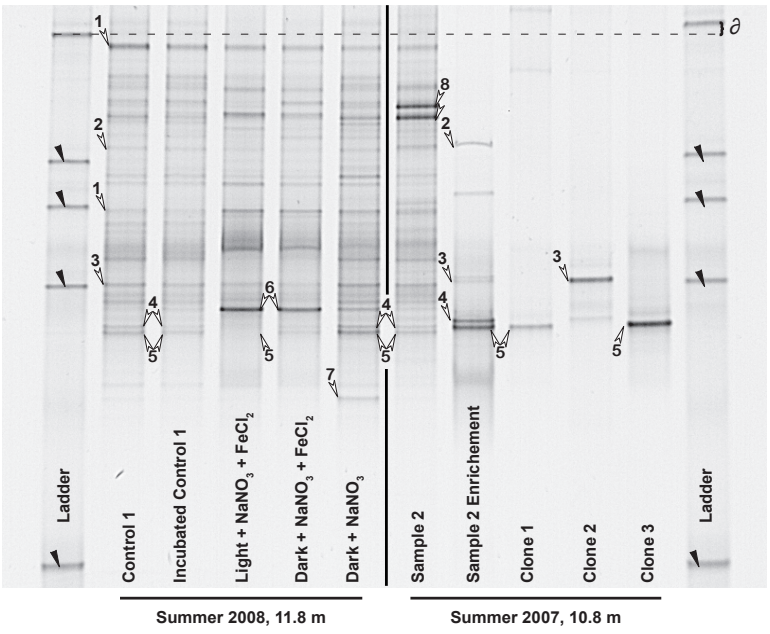

Figure 41: DGGE profiles of La Cruz microbial community, before and after *ex situ* incubations (left). Control 1 is the sample (11.8 m) on which *ex-situ* experiment have been conducted. Sample 2 was used to inoculate MPN and enrichment cultures (September 2007). Both control 1 and sample 2 correspond to the anoxic part of the chemocline of the summer stratification. The dashed line shows the migration-distance difference between the two ladders. White arrows indicate characteristic bands. "1" are the conserved bands of the different profiles. If bands "2" are the ones also present in the enrichment (10.8 m), the bands "3" are the ones that are not affected by "Fe(II) + NO_3" treatments and that have been sequenced from the enrichments. Bands "4" and "5" are conserved bands affected by the "Fe(II) + NO_3" additions. Bands "5" are also the sequenced bands from the enrichment.

Compared to controls, nitrate additions ("Dark + NO_3") did only marginally affect the community structures: a band appears down the migration profile (Fig. 41: arrow 7). However, different diversity patterns, compared to controls, occured in "Fe(II) + NO_3" treatments (light/dark: Fig. 41): a group of bands is absent (Fig. 41: arrows 4 and 5), whereas a band is over expressed (Fig. 41: arrows 6). The same band was observed in profiles of "Fe only" treatment (data not shown) but is much less intense than in "Fe(II) + NO_3". Band 6 is hence characteristic for "Fe(II)" treatment. The control 2 shows the same pattern of diversity as control 1. However the intensity of some bands (Fig. 41: arrow 8) suggested the dominance of certain populations in summer 2007 that seems to be less present in summer 2008 stratification (late summer, *Chap II.2.4.1*).

To characterize the nitrate-reducing Fe(II)-oxidizing metabolism of our enrichments, the concentration of Fe(II)/Fe(III) was followed over time (Fig. 42). Results confirmed the chemoferrotrophic activity under both light and dark conditions of the enrichment cultures (Fig. 42). Because there were no significant differences between the two killed duplicates (light and dark), their values have been averaged together. Killed treatments indicate no significant Fe(II) oxidation by any physico-chemical process as oxygen contamination during manipulation, or Fe(II)-photooxidation. This time-course incubation confirmed the

Fe(II)-oxidation activity of the enrichment culture (80 µM Fe(II) h^{-1}), as well as its non inhibition by light.

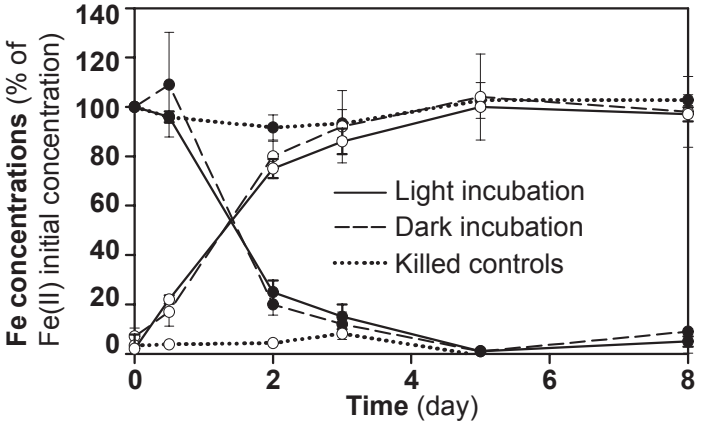

Figure 42: Fe(II)-oxidation of a NDIO enrichment culture from Lake La Cruz. (2007, 10.8 m). Fe(II) (solid circles) and Fe(III) (open circles) concentrations are expressed as percentage of each tube initial Fe(II) concentration. Fe(II) oxidation occurs either in light treatments and dark treatments, but was not measured in killed controls. Error bars show the variation between duplicates at each time point.

When comparing the DGGE profiles of the enrichment culture and its inoculate, we see that the enriched populations were present in all the compared profiles (Fig. 41: arrows 2, 3, 4 and 5). However, not all of the populations in the enrichment were identified (Fig. 41: arrow 2). One sequences of our enrichments' clones was closely related to a clone from an anoxic arsenite-oxidizing denitrifying enrichment culture (Fig. 41, clone 1 and 3: EU708506; 99% similarity), while another one was closely related to *Bradyrhizobium sp.* (strain RS-46) from the *α-Proteobacterium* class (Fig. 41, clone 2: FM998034.1; 98% similarity). Normally, member of the *Bradyrhizobiaceae* are known to be N_2-fixing in symbiosis with plants roots. Moreover, some members of this family have also a photosynthetic capability {http://www.cns.fr/spip/Bradyrhizobium-symbiote-des.html}. In our case, we can exclude a photosynthetic activity of our enrichment (dark incubations), but we cannot determine what were their metabolic activities in Lake La Cruz water column. Indeed, as shown by DGGE profile (Fig. 41: arrow 4, 5), the enriched NDIOs are not the same as the ones potentially oxidizing iron in the "Fe(II)+NO_3" *ex-situ* treatment (Fig. 41: arrow 6). However, the enriched and cloned organisms are present in both summer samples controls (Fig. 41: arrow 3, 4 and 5), thus, supporting the presence of active chemoferrotrophs in Lake La Cruz chemocline.

5. Conclusion

Nitrate-dependent Fe(II)-oxidation was detected for the first time in a water column. More precisely, we showed that i) the microbial community from a layer where both Fe(III) and nitrate were measured exhibited a nitrate-dependent Fe(II)-oxidation activity, ii) the microorganisms from the same sample demonstrated a stimulation of bicarbonate uptake by Fe(II) addition, and iii) a subset of enriched anaerobic bacteria from the same zone were able to oxidize Fe(II) anaerobically with nitrate as oxidant. Therefore the presence and activity of NDIOs in the chemocline of lake La Cruz, where both Fe(III) and nitrate were measured, has been proved. Because the *ex situ* time-course experiments showed that nitrate was needed for Fe(II)-oxidation but the *in situ* radiocarbon incubations did not, we postulate that the organisms showing Fe(II)-stimulated autotrophy may have intracellular nitrate reserves. Moreover, the higher MPN counts of NDIOs in the iron-poor water columns of lakes Cadagno and Lake Loclat suggest that anaerobic nitrate-dependant Fe(II)-oxidation is a widespread and facultative metabolism. However, the detection of active NDIOs in chemically different water columns rise the question of the relevance of NDIOs in the global denitrification process occurring in modern and ancient environments.

The presence of NDIOs in a ferruginous water column supports the hypothesis of their possible implication in BIF settling (Weber *et al*., 2006[1]). This hypothesis was supported by the possible production

of nitrite and nitrate independently from the presence of oxygen by lightning discharge through abiotic disproportion reactions (NO, ~10^{12} g per yr; Yung & Mcelroy, 1979; Moncinelli & McKay, 1988). This nitrate production may not have been sufficient to be used by early-life metabolisms (Navarro-Gonzales *et al*., 2001; Garvin *et al*., 2009). Consequently also NDIOs would have also been limited by the low nitrate availability. Recent researche, however, have proposed another microbiologically mediated mechanism by which NO_x could be produced anaerobically: the oxidation of NH_4^+ to NO_2^- using Fe(III) as an electron acceptor (Clement *et al*., 2005; Park *et al*., 2009; Shrestha *et al*., 2009). Such mechanism would have permitted the formation of NO_2^- in the Late Archean Ocean and its subsequent use for nitrate-dependent iron-oxidation since Fe(III) was present in large quantity. However, this hypothesis needs to be supported by enrichment or pure cultures to demonstrate the feasibility of this mechanism. In addition, it has to be shown that this metabolic process does not leave any detectable isotopic fractionation signals in order to be consistent with the Archean stable N-isotope records (Garvin *et al.*, 2009).

6. Supplemental material

6.1. Lake Cadagno and Lake Loclat chemical stratifications

Lake Cadagno presented an oxycline between 9.5 m and 11.25 m depth (July 2009, Fig. 19A), and a thick pycnocline between 5.5 m and 12.0 m. As sulfidic waters ranged from 12 m depth up to lake bottom, we considered the chemocline being between 9.5 m and 12.0 m. Because iron concentrations were quite low in Lake Cadagno (< 1 µM, Fig. 43A), it was difficult to clearly determine where both Fe(III) and nitrate were present. On the contrary, the holomictic Lake Loclat had an overlapping zone, between 5 m and 6 m depth, where NDIOs could be active (detection of Fe(II) and NO_3^-, Fig. 43B). The iron measured at 9 m depth was not representative of the water content because sediments particles could have been sampled. However, even with sulfidic conditions dominating the anoxic part of the water column, Fe(II) concentrations reached ~10 µM (September 2008, 8 m, Fig. 43B).

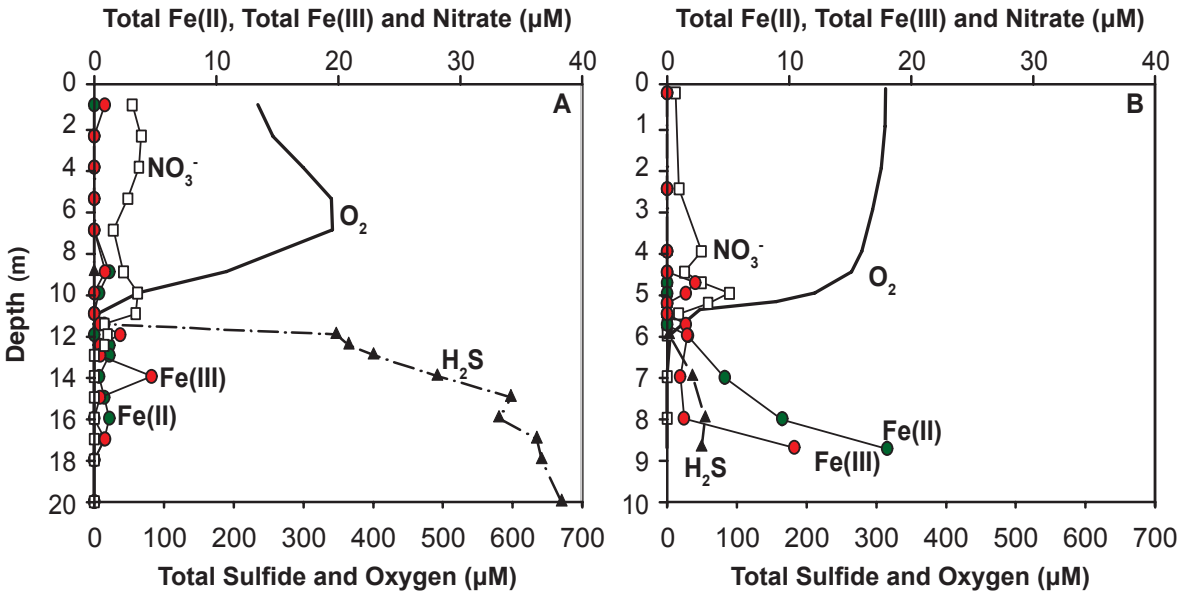

Figure 43: Chemical stratification of **A |** the meromictic Lake Cadagno (28/07/2009) and **B |** the eutrophic Lake Loclat (25/09/2008).

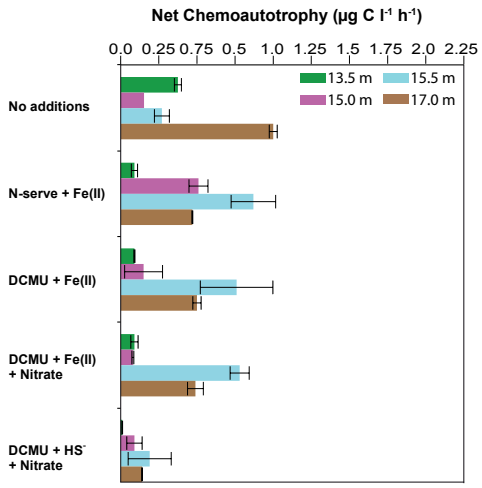

Figure 44: Bicarbonate uptake experiments designed to measure a chemoautotrophic stimulation by the addition of potential substrates iron- and sulfur-transforming microorganisms.

6.2. Fe(II)-dependent chemoautotrophy

As we were focusing on anaerobic ferrotrophy, we decided to set-up experiments to detected *in situ* NDIOs activity: ^{14}C-bicarbonate incubations. As chemoferrotrophs use nitrate as an electron acceptor (*Chap. I.4.4*), 40 µM of nitrate (final concentration) was spiked in addition to Fe(II) additions.

In winter 2008, temperatures were homogeneous over the water column (~4.2 °C between 0.1 m to 15.0 m) and the bottles were incubated under dark conditions. Therefore, we can consider the "no addition" tubes that were incubated at the sampling depth as valid control for the incubations carried out at 8.0 m (Fig. 44). However, samples retrieved from 17.0 m were not incubated under the same conditions as bottom water temperatures were higher (5.7 °C at 17.0 m). As a result we assumed that chemoautotrophy would be somewhat higher in controls than in the treated samples. This postulation was indeed supported by the results (Fig. 44). It was consequently difficult to see whether Fe(II) addition stimulated chemoautotrophy or not. We may only conclude that the absence of sulfide stimulation (compared to Fe(II) treatments) indicates an absence of anaerobic sulfide oxidizing chemotrophs at 17.0 m. This observation was verified for all the sampled layers (Fig. 44). In 13.5 m samples, the addition of Fe(II) seems to inhibit chemoautotrophy. We could postulate that as this layer was dominated by oxygenic phototrophs, the injected Fe(II) reacted with the oxygen surrounding cells and encrusted them. However, in 15.0 m samples Fe(II) seems to have no effect on chemoautotrophy. This sample showed a stimulation when treated with Fe(II) and N-serve, whereas "DCMU+ Fe(II)" treatments did not show any stimulation (Fig. 44). N-serve was injected in order to inhibit nitrification (15 µM final concentration; Knowles, 1982; Hadas *et al.*, 2001). We could thus postulate that nitrifying bacteria were not active at 15 m. Surprisingly, MPN counts did not indicate a significant presence of NDIOs in Lake La Cruz (Tab. 6), but the ^{14}C-incubations at 15.5 m clearly showed the stimulation of chemoautotrophy when Fe(II) was added (~255-295 %, Fig. 44). Moreover, no difference were visible when nitrate was spiked in addition to Fe(II), thus rising the question of the electron acceptor used. For those reasons we consider that the detection of active chemoferrotrophs should include at least two approaches: on the one hand, a stimulation of chemoautotrophy by Fe(II) additions, and on the other hand either positives MPN counts and/or a Fe(II) time course incubation with natural samples amended with Fe(II).

In summer 2008 only samples from 11.8 m depth have been incubated, for dark carbon uptake measurements, with a more detailed treatment plan aimed at assessing the effects of Fe(II), nitrate and inhibitors. Every added compound was tested individually and in combination (Fig. 45). Beside Fe(II), no added compounds stimulated autotrophy. Concerning the implication of Fe(II) in the detected chemoautotrophy (Fig. 45, "No addition" treatment), we wanted to evaluate the amount of Fe(II) necessary if NDIOs were the only chemotrophs responsible for the measured primary fixation. We had a dark fixation of 0.26 µg C l^{-1} h^{-1} over the 3.5 hours of incubation. Thus, we have fixed 0.91 µg C l^{-1} which is equal to 0.076 µmol C l^{-1}. A study showed that Fe(II)-oxidizing pure cultures (Neubauer *et al.*, 2002; Weber *et al.*, 2006[2]) oxidized 1 µmol of Fe(II) in order to fix 0.25-0.28 µmol of carbon as biomass. Therefore, 0.27-0.30 µmol of Fe(II) per liter were required to fix the totality of the measured primary production (0.076 µmol C l^{-1}). This calculation shows

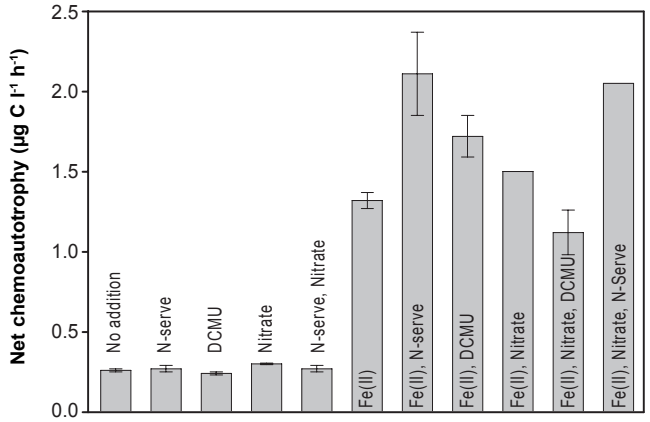

Figure 45: *In situ* dark bicarbonate uptake in presence of Fe(II) as a potential substrate for autotrophic Fe(II)-oxidizing microorganisms (13/10/2008). These experiments show a clear stimulation of chemoautotrophy by Fe(II) addition. As for winter incubations, nitrate did not stimulate carbon fixation. An N-serve effect is only observed in tubes amended with Fe(II). n=2

that there was 5 time more reduced iron available than needed to explain the observed carbon fixation. We could conclude that iron is not limiting. However, a great stimulation of chemoautotrophy occurred each time Fe(II) was added (Fig. 45): from a 425 % increase (Fig. 45, "Fe(II) + nitrate + DCMU")to 805 % increase (Fig. 45, "Fe(II) + N-serve"). We considered that, in incubations without Fe(II) additions, all nutrients were in sufficient quantity to allow a dark fixation as high as in Fe(II) treatments. This suggests that Fe(II) was a limiting factor for dark autotrophy in 11.8 m depth samples.

There are two possibilities that may explain the limited carbon fixation, with respect to the available Fe(II) . One could be that only a small fraction of the measured Fe(II) (1.4 µM) is bioavailable for ferrotrophy. Alternatively, it could be due to the competition of NDIOs with other organisms. Such organisms did not compete with NDIOs in absence of Fe(II) additions, but was inhibited by N-serve addition when Fe(II) was present. N-serve is known for inhibiting nitrification, but it does also inhibit methanogenesis and methanotrophy (Donlon *et al.*, 1995; Mc Carty, 1999; Sahrawat, 2004). Those results lead to the suggestion that acetoclastic methanogenesis may have been the competing metabolism, as it did not contribute to the autotrophic signal but was inhibited by N-serve additions.

Regarding the electron acceptor, results showed that nitrate additions did not increase carbon fixation, neither in control tubes nor in Fe(II)-amended tubes. Some nitrate-reducing sulfur-oxidizing anaerobes possess nitrate reserves (*Thioploca sp.*; Zopfi *et al.*, 2001; Burgin and Hamilton, 2007; De Gusseme *et al.*, 2009), and some other can even use Fe(II) as an electron donor (*Thiobacillus denitrificans*, Beller *et al.*, 2006). One might speculate that the detected autotrophic NDIOs were able to concentrate nitrate as intracellular reserves.

6.3. Nitrate-dependent Fe(II)-oxidation

The same *ex situ* incubations approach as the one used to measure light-dependent Fe(II)-oxidation was applied to detect nitrate-dependent Fe(II)-oxidation: samples for the Fe(II) amended incubations were retrieved from the same layer as sampled for the ^{14}C-bicarbonate experiment (11.8 m). Samples were amended with Fe(II), nitrate and N-serve. They were incubated under continuous dark (Dark), continuous light (Light) and under 12 h L/D. As photoferrotrophs were present in the same water sample, only "Dark" samples were considered for Fe(II)-oxidation detection (40). Fe(II) and Fe(III) concentrations were then followed using the ferrrozine assay (Viollier *et al.*, 2000). The "Killed" simplicate assays contained 500 µM $FeCl_2$, 50 µM $NaNO_3$, 22 µM N-serve. Results demonstrated that the microbiota from the sampled depth showed a Fe(II)-oxidation potential which was dependent on nitrate (Fig. 40). A higher Fe(II)-oxidation was observed in samples amended with N-serve, but as this treatment was applied only to one sample it is not possible to attribute this Fe(II)-oxidation enhancement specifically to N-serve addition. The small Fe(II) concentration decrease in the *ex situ* Fe(II)-experiments (Fig. 40, "Fe(II)" treatments) suggest that if NDIOs had nitrate storage it was not sufficient to oxidize a measurable amount of Fe(II).

In addition to Fe(II) analysis, nitrate concentrations were measured during the time course incubation. 5 ml of sample was filtrated trough a polycarbonate membrane (0.2 µm pore size; Whatman) prior to analysis. When sample was amended with Fe(II), 50 µl of EDTA 2 % was added (0.02 % final concentration, w/v) in order to avoid the formation of iron oxides. The latter might have interfere with the photometric nitrate measurement. Nitrate has an absorption maximum at 224 nm. Thus, we scan samples between 190 and 250 nm and the 2nd derivative of the slope at 224 nm was used to determine nitrate concentrations (Antonio Picazo-Mozo personal communications, Ferre & Shannon, 2001). The results are grouped by light treatment conditions: dark (Fig. 46A), light (Fig. 46.B) and $12^{L}/_{D}$ (Fig. 46C).

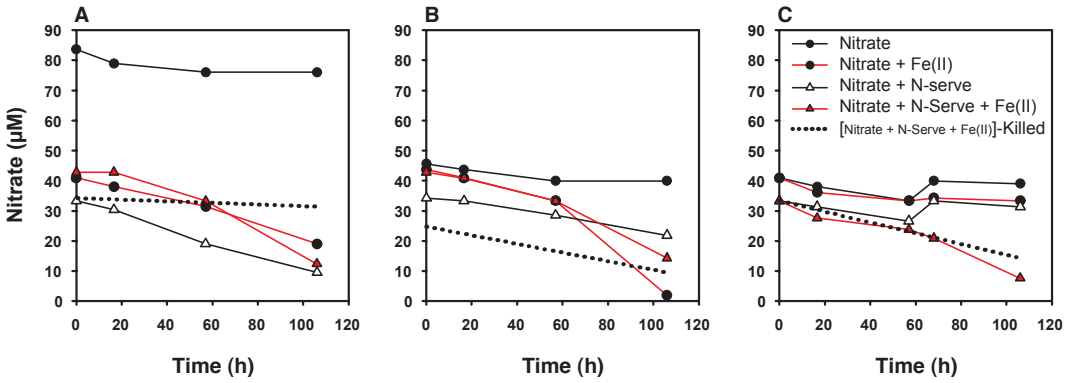

Figure 46: Nitrate concentrations of the Fe(II) time course incubations using 11.8 m depth samples (13/10/2008). **A |** continuous dark conditions, **B |** incubations under continuous illumination, **C |** 12 hours light/dark shift. One dark treatment (**A**) was spiked twice by error.

Globally, when nitrate and reduced iron were both present, a nitrate concentration decrease was observed (red lines, Fig. 46). For example, when Fe(II) was oxidized in "Dark" treatments (Fig. 40), the amount of nitrate consumed (Fig. 46) was equivalent to the stoichiometrical Fe(II) according to equations (3), (4) and (5) (from 2Fe : $1NO_3^-$ to 5Fe : $1NO_3^-$; *Chap. I.4.4*): 42 µmol of Fe(II) for 11 µmol nitrate and 76 µmol of Fe(II) for 15.2 µmol nitrate, in "Fe(II) + NO_3^-" and "Fe(II) + NO_3^- + N-serve" treatments respectively. Those results suggest that the measured decrease in nitrate concentrations was linked to the oxidation of Fe(II).

Samples amended solely with NO_3^- showed a slight decrease in concentration under "Dark", "Light" and "$12^{L}/_{D}$ " conditions (Fig. 46). The small nitrate consumption observed in " NO_3^-" series suggest that its use is limited, either as a nutrient or as an electron acceptor (Fig. 46). However, when N-serve and NO_3^- were added without any electron donors, a diminution of nitrate concentration was measured in both "Dark" and "Light" conditions (Fig. 46A-B). This decrease suggests an implication of N-serve in the observed nitrate concentration drop. As no electron donor was present in samples, nitrate consumption may have been used as a nutrient rather than as an electron donor. Based on the results of the "Killed-Dark", where no nitrate decrease was observed (Fig. 46A), chemical reaction between N-serve and NO_3^- can be excluded. On the other hand, "Killed" controls incubated under light and 12 h L/D, showed a nitrate concentration decrease (Fig. 46B-C). We could thus postulate a photochemical reaction with nitrate when Fe(II), N-serve and paraformaldehyde were present.

When nitrate and reduced iron were both present, there was a nitrate concentration decrease (red lines, Fig. 46A-B). However, this was not the case in the sample under 12 h L/D treatment (Fig. 46C). Because such sample experienced a "day and night" regime, it could have hosted a recycling of nitrate (e.g. nitrification) that would have been sustained by oxygenic photosynthesis. Therefore, it is difficult to have clear answers that are verified in all implicated treatments: e.g. "Killed-12 h L/D" and " NO_3^-/N-serve-12 h L/D" had nitrate concentration diminutions, whereas "NO_3^-/Fe(II)- 12 h L/D" did not (Fig. 46C). Consequently, we needed to

analyze the variation of nitrate concentrations with a statistical tool in order to overcome the ambiguous results. In order to identify the factors that explain best the nitrate decrease in the differet incubations, a generalized linear model was built (GLM, NO_3^- concentrations ~ Light + Dark + Fe + N-serve; Tab. 7) with a binomial distribution (MacCullagh & Nelder, 1989).

Table 7: Matrix of the differences between initial and final nitrate concentrations. The results of the GLM analysis (*Pr* value) are indicated in the last row. It represents the impact of the tested elements on nitrate diminution: the more nitrate decreases, the more the value is elevated.

	Treatments			
∂NO_3^- (µM)	**Light**	**dark**	**Fe**	**Nserve**
1.9	1	1	0	0
7.6	1	1	1	0
1.9	1	1	0	1
25.65	1	1	1	1
5.7	1	0	0	0
41.8	1	0	1	0
12.35	1	0	0	1
28.5	1	0	1	1
7.6	0	1	0	0
21.85	0	1	1	0
23.75	0	1	0	1
30.4	0	1	1	1
Pr(>F)	0.329	0.061	**0.008**	0.241

The influences of the treatments on nitrate consumption were tested using ANOVA. All analysis were performed using the statistical software "R" (R Development Core Team, 2009). As all tested elements were present and as another product (paraformaldehyde) was present, without any crossed incubations to verify it, the 3 "killed" controls were not included in the matrix used for the GLM (Tab. 7). This model demonstrated that nitrate decrease (high difference between initial and final nitrate concentrations) were highly correlated to the presence of Fe(II) ($P_r < 0.01$, Tab. 7).

CHAPTER IV: Lake La Cruz: a Neoarchean Ecotone Ocean Analogue

1. Abstract

Recent research on the biogeochemistry of the Late Archean Ocean (2.7-2.5 Ga) showed that there was a spatial patchwork of physical-chemical conditions. A simplified model of an Archean Ocean would thus consist of two distinct compartments with different dominating biogeochemical processes: I) a shallow Ocean Margin compartment with oxygenic photosynthesis in the upper water column, and euxinic conditions (anoxic and sulfidic) below the chemocline and in the sediments; II) an anoxic Fe(II)-rich Open Ocean compartment with a primary production dominated by anoxygenic photoferrotrophy and methanogenesis prevailing organic matter degradation.

While analogues of an ocean with an established sulfur cycle, corresponding to compartment I, have been described and well studied (e.g. Black Sea or Lake Cadagno), modern analogues of the ferruginous open water compartment were lacking. Therefore, the study of the microbial iron cycling, in the ferruginous water column of Lake La Cruz (Spain), allowed to understand the integration of this cycle with the sulfur and oxygen microbial cycles.

Indeed, an anaerobic Fe(II)-oxidizing activity was detected, in Lake La Cruz chemocline, and it was demonstrated that these autotrophic microbes thrive by photo-ferrotrophy (anoxygenic photosynthesis) or by chemoferrotrophy (nitrate-dependent respiration). Moreover, oxygenic photosynthetic bacteria, anoxygenic purple and green phototrophic sulfide oxidizers, sulfate and iron-reducers, as well as methanogens and methanotrophs were also active. Therefore, the results from this study combined with those of previous studies allowed us to establish a biogeochemical model, including all the metabolisms thought to have existed in the Late Archean Ocean. Thus, Lake La Cruz illustrates how those microorganisms could have driven and shaped biogeochemical cycles during this period.

Accordingly, the water column of Lake La Cruz may represent an ecotone between the two main Neoarchean Ocean compartments and, consequently, be a good model system, or samples source, for studying metabolic activity interactions in experimental conditions that reflect theoretical models of the Archean Ocean.

2. The Neoarchean Ocean

2.1. A spatial patchwork of chemical conditions

Recent studies on the biogeochemistry of the Late Archean Ocean (2.7-2.5 Ga: Neoarchean) showed that there was a spatial patchwork of physical and chemical conditions (Kaufman *et al.*, 2007; Sleep and Bird, 2008; Reinhard *et al.*, 2009; Voegelin *et al.*, 2010; Farquhar *et al.*, 2010; Czaja *et al.*, 2010; Kendall *et al.*, 2010). The Late Archean marine topography has then to be considered to understand how dissolved chemical compounds were distributed and how they influenced early life. A simplified model of the Neoarchean ocean would be composed of at least two main compartments: I) shallow waters on the ocean margins, and II) the deep waters of the open ocean (Fig. 47), rich in reduced iron fueled by hydrothermal vents.

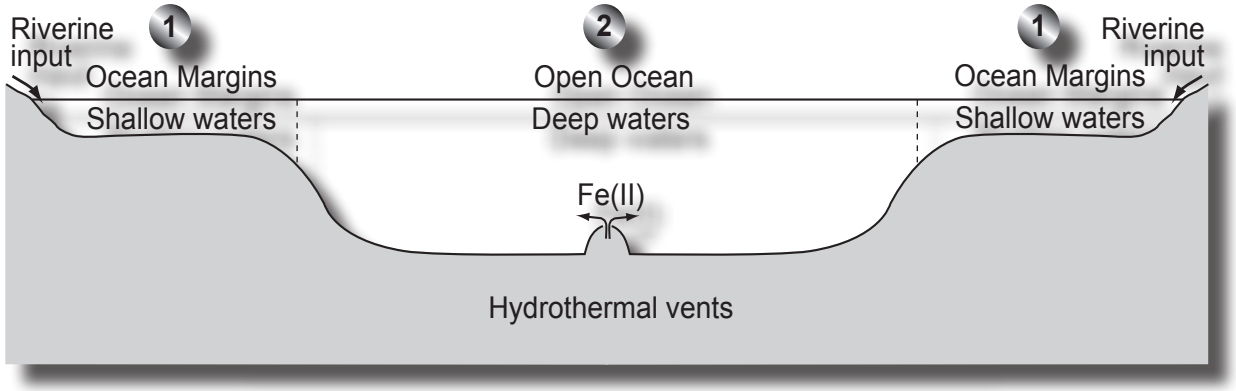

Figure 47: Schematic topography illustrating a simplified model of an Archean Ocean composed of two main compartments: 1) shallow waters under the influence of both riverine and marine inputs; 2) deep waters under the influence of hydrothermal inputs (Fe(II), H_2S, FeS, H_2, CH_4).

During the Neoarchean reduced iron (Fe(II)) and oxygen were the two major chemical components because of their influence on other elements cycles. The Fe(II) was the most abundant reductant due to large fuelling from mid-ocean ridges (*Chapter I*; Holland, 1984; Canfield *et al.,* 2005), and oxygen enhanced the sulfur cycle. Indeed, it allowed the release of sulfate into oceans, thus, enabling its use by dissimilatory sulfate reduction. Oxygen, linked to the apparition of oxygenic photosynthesis (2.75 Ga; Des Marais, 2000), only started to significantly accumulate around 2.45 Ga (Zahnle *et al.,* 2006; Konhauser *et al.,* 2009) and triggered the sulfur cycle that dominated the Proterozoïc Ocean (Canfield & Raiswell, 1999). This is why it is important to understand how the early-produced oxygen (2.75-2.45 Ga) did interact with the Neoarchean Oceans chemistry.

Kendall *et al.* (2010) is the most recent and it is summarizing arguments of previously cited studies (Kaufman *et al.*, 2007; Sleep and Bird, 2008; Reinhard *et al.*, 2009; Voegelin *et al.*, 2010), thus, the following paragraph is mainly based on it.

When balanced by the Fe_{HR}/Fe_T ratio (Fe_{HR} stands for **H**ighly **R**eactive iron, and Fe_T for the **T**otal iron), the rhenium (Re) and molybdenum (Mo) abundance in sediment reflects the redox state of a water column (Voegelin *et al.*, 2010; Kendall *et al.*, 2010). Re and Mo are mobilized by oxidative weathering and transported by the rivers to oceans as unreactive ReO_4^- and MoO_4^-. They will then be removed from solution and accumulate in sediment through their reactions with organic matter or sulfides. On one hand Re accumulation is independent from sulfide concentrations (Sundby *et al.*, 2004; Yamashita *et al.*, 2007), while on the other hand Mo will react with sulfide and therefore be removed from solution (Erickson and Helz, 2000; Alego and Lyons, 2006). For example, in modern oxygenated water column with low content of sulfate, Re will accumulate when Mo sequestration will be limited (Crusius *et al.*, 1996; Morford & Emerson,

1999; Morford *et al.*, 2005). For a detailed explanation of the different reactions of Re and Mo as well as the limits for their interpretation for the evaluation of a water column redox state, see cited reference. Kendall *et al.* (2010) found in 2.6-2.5 Ga old black shales, from the Campbellrand-Malmani carbonate platform (South Africa), high Fe_{HR}/Fe_T ratio, a high abundance of Re and a low abundance of Mo. Based on these results, they suggested that while the Open Ocean was anoxic and ferruginous (compartment 2, Fig. 47), the ocean margins were the site of substantial O_2 production/accumulation (in the water column). In addition, the water column Re/Mo inventories were larger in shallow water in comparison to deeper water. Together with a smaller Mo/TOC ratios (**T**otal **O**rganic **C**arbon) than the Proterozoic euxinic shales (sulfidic and anoxic), it suggested that Mo and Re entered the ocean through riverine input (compartment 1, Fig. 47; Kendall *et al.*, 2010). Thus, indicating an oxidative weathering. Even low concentration of oxygen (<0.001 % P.A.L.) were sufficient for an oxidative weathering of MoS_2 and ReS_2 (Anbar *et al.*, 2007; Reinhard *et al.*, 2009). Such a model suggest that this oxidative weathering occurred near regions of photosynthetic oxygen production in the adjacent shallow ocean (Cloud, 1973; Bekker *et al.*, 2010). Thus, O_2 accumulation in the atmosphere did not happen before 2.45 Ga: the rate of oxygenic photosynthesis was not sufficient to overcome oxygen consumption by oxidative crust weathering and the reaction with ocean's Fe(II) and/or sulfides (Kendall *et al.*, 2010). However, the presence of oxygen, triggering sulfate release in the ocean by oxidative weathering, allowed the development of euxinic bottom waters in ocean margins (Fig. 48).

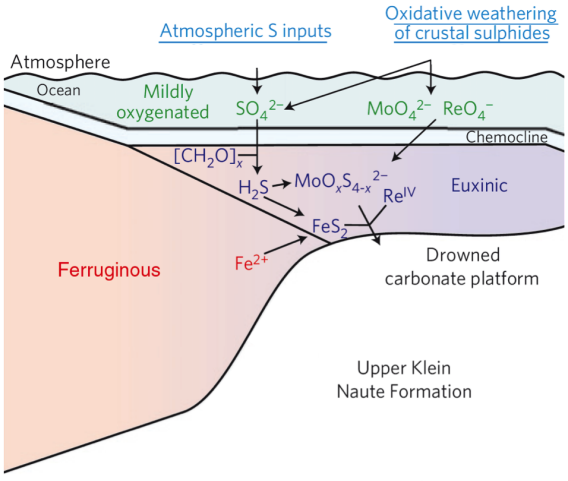

Figure 48: Ocean redox conditions on the platform and slope. O_2 accumulation was confined to the shallow waters (up to several hundred meters) along the ocean margin where rates of photosynthetic O_2 production were high. At mid-water depths, locally high organic carbon and sulfate fluxes promoted extensive microbial H_2S production, leading to euxinic conditions. Otherwise, the deep (and open) ocean was anoxic and ferruginous. Figure and legend from Kendall *et al.*, 2010.

From a microbial metabolic point of view, compartment 1 (Fig. 47) was a good environment for the development of oxygenic photosynthesis: ocean margins are the most distant zones from the hydrothermal Fe(II) and lower concentrations would have allow O_2 to be produced without causing an immediate incrustation of the photosynthetic cells by iron hydroxides (Cloud, 1973; Bekker *et al.*, 2010). It is consequently in ocean margins that oxygen started to influence microbial life as well as water geochemistry.

2.2. Possible microbial-pathways and their interactions

The oxygen presence in ocean margins (Kaufman *et al.*, 2007; Sleep & Bird, 2008; Reinhard *et al.*, 2009; Voegelin *et al.*, 2010; Farquhar *et al.*, 2010; Kendall *et al.*, 2010) is also supported by studies suggesting the establishment of an early aerobic nitrogen cycle between 2.67 and 2.50 Ga (Fig. 49; Garvin *et al.*, 2009; Godfrey & Falkowski, 2009), most probably in compartment 1. As lighting was not sufficient to produce a significant amount, NO_2^- could not be present in sufficient quantity to be used by early-life metabolisms before the apparition of oxygenic photosynthesis (Navarro-Gonzales *et al.*, 2001; Garvin *et al.*, 2009). Therefore the nitrogen cycle was quite simple: N_2 would have been biologically reduced to NH_4^+, with a part being recycled and the other part buried into sediments (Garvin *et al.*, 2009; Fig. 49). It should be noted that

recent studies have indicated two new metabolic pathways that could have completed this nitrogen cycle: i) the anaerobic oxidation of ammonium using Fe(III) as an electron acceptor (ferric "de-ammonification"; Clement *et al.*, 2005; Park *et al.*, 2009; Shrestha *et al.*, 2009) producing NO_3^-, and ii) anaerobic methane oxidation coupled to the reduction of NO_2^- to N_2 (Ettwig *et al.*, 2010). Still, these hypothesis needs enrichment and pure cultures, respectively, to study the environmental conditions on which those mechanisms depend. In addition, to be in accordance with the $\partial^{15}N$ found in kerogenous shales of the Neoarchean (Garvin *et al.*, 2009) it has to be shown that those two metabolic processes do not increase the $\partial^{15}N$ in buried organic matter. However, the ferric de-ammonification could explain why the Fe(III) precipitation was lower before the Neoarchean: part of it would have been reduced back to Fe(II).

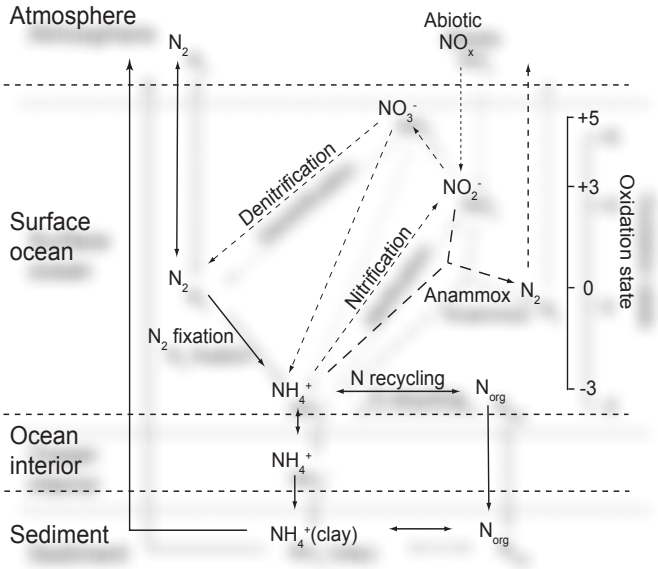

Figure 49: Upwelling of ocean interior NH_4^+, N fixation and efficient N recycling support surface productivity. In a totally anoxic ocean (solid arrows) the only sink of ocean N is burial in sediments. Once oxygenic photosynthesis starts, N can exist in higher oxidation states (fluxes indicated by short-dashed arrows). Coupled nitrification–denitrification allows N to escape from the ocean as N_2, increasing the remaining $\delta^{15}N$ fixed as well as a decreasing the ocean N inventory. If rates of oxygen production are sufficiently high, nitrification rates exceed those of denitrification and nitrite, then nitrate, can start to accumulate. The fluxes associated with anammox (long-dashed arrows) are included and abiotic source of nitrite shown by the dotted arrow. Isotope signature of surface ocean processes is carried by organic matter sinking to the sediments. Figure and legend from Godfrey & Falkowski, 2009

Without considering those two possible metabolisms, we assumed that during the Neoarchean the macroevolution of all the known microbial metabolic pathways, from the bacteria and/or the archaea domains, was mostly completed (Garvin *et al.*, 2009; Godfrey & Falkowski, 2009; David & Alm, 2011) and present in shallow waters (Fig. 47, compartment 1; Czaja *et al.*, 2010). Therefore, at the end of the Archean eon, oxygenic phototrophs (Des Marais, 2000; Waldbauer *et al.*, 2009), anaerobic heterotrophs, including dissimilatory sulfate- and iron-reducers (Vargas *et al.*, 1998; Canfield & Raiswell, 1999; Shen *et al.*, 2001; Lovley, 2004), methanogenic chemotrophs (Schidlowski *et al.*, 1983; Eigenbrode *et al.*, 2008), aerobic methanotrophs (Eigenbrode *et al.*, 2008; Czaja *et al.*, 2010), anaerobic methanotrophs, coupled to iron reduction and/or to sulfate reduction (AOM-IR / AOM-SR; Boetius *et al.*, 2000; Beal *et al.*, 2009; Czaja *et al.*, 2010), were active in Ocean Margins. Anoxygenic phototrophs, sulfide oxidizing and Fe(II)-oxidizing bacteria (Widdel *et al.*, 1993; Kappler *et al.*, 2005; Kendall *et al.*, 2010) were also present.

Assuming an oxygen production in ocean margins, as well as the potential metabolic pathways that could have developed in relation to it, we will try to model the biogeochemical cycles occurring in both compartment of the Neoarchean Ocean.

As explained previously, oxygenic photosynthesis developed in shallow waters close to continental coast. The products of such primary producers are O_2 and organic matter (C_{org}). The C_{org} will sink towards the sediment while part of O_2 will be released in the lower layer of the atmosphere bringing SO_4^{2-} to the ocean through riverine input after an oxidative weathering of continental metal sulfides (Canfield, 1998, Poulton *et al.*, 2004; Czaja *et al.*, 2010). In such an environment, the two potential metabolic pathways involved in the organic matter mineralization should have been the **d**issimilatory **s**ulfate **r**eduction (DSR) and the

anaerobic **m**ethano**g**enesis (AMG). Nonetheless, those metabolisms can not directly use "fresh" organic matter and can only use, as electron donors, secondary fermentation products, such as butyrate, lactate, propionate, acetate or hydrogen. Consequently, for the release of H_2S and CH_4 in the water column, DSR and AMG directly depend on the activity of fermentative organisms. Before 2.7 Ga sulfate concentrations were low (Habicht *et al.*, 2002; Canfield, 2005; bekker *et al.*, 2010), and as a resutl also the biological sulfide production. Thus, the apparition of oxygenic photosynthesis corresponded to a slow sulfate-enrichment of the oceanic system, thus generating an increasing importance of DSR over AMG. Moreover, kerogen $\delta^{13}C$ signatures indicate an aerobic oxidation of methane (AOM) in addition to the activity of **a**erobic **n**itrification (AN) (Godfrey & Falkowski, 2009; Czaja *et al.*, 2010), thus, limiting oxygen release from Ocean Margin into the atmosphere. Beside, as indicated by $\delta^{56}Fe$, there was no biological iron cycle, either by **i**ron **o**xidizing **p**hototrophs (IOP) nor **d**issimilatory **i**ron **r**educers (DIR), in compartment 1 (Fig. 47; Czaja *et al.*, 2010; Bekker *et al.*, 2010). **S**ulfide **o**xidizing **p**hototrophs (SOP) could have developed, below the **o**xygenic **p**hototrophs (OP), thus, consuming part of the sulfide, and increasing C_{org} pool and the subsequent CH_4 production, again limiting oxygen release in the atmosphere by its consumption by AOM and AN. However, based on the accumulation of Re concomitantly with the low sequestration of Mo in sedimentary records of Neaoarchean rocks, we could consider that the Ocean Margins were yet limited in sulfate (Morford *et al.*, 2005; Kendall *et al.*, 2010).

In addition, a H_2S gradient should have been established between compartment 1 and compartment 2 (Fig. 47). Part of the produced H_2S , from the ocean margins, would have reacted with Fe(II), from the open ocean, acting as a sink in an ecotone zone where it would have precipitated as pyrite. As postulated by Bekker *et al.* (2010), the precipitation of iron oxides could not occur in such an environment and would have been limited to the Open Ocean compartment. The little Fe(III) produced, by an abiotic reaction with O_2 (no isotopic fractionation), would have reacted with sulfide and form pyrite (equation 5, 6 and 7; Bura-Nakic *et al.*, 2009; Fig. 50).

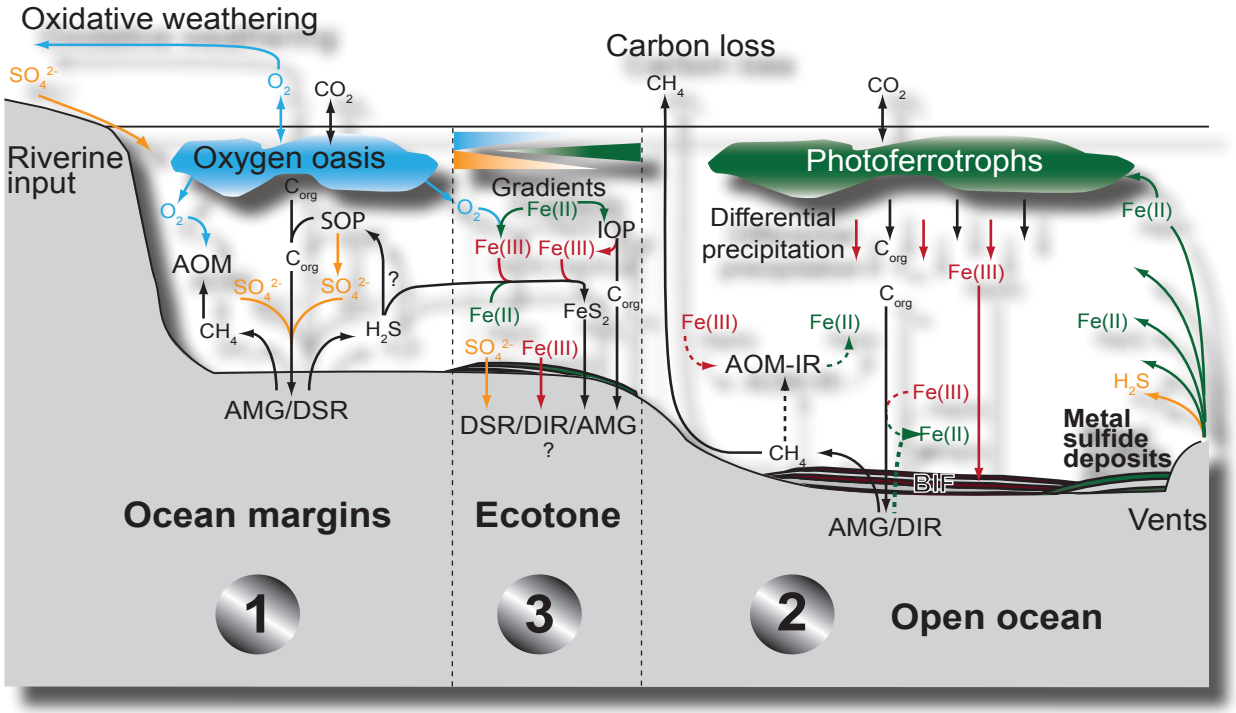

Figure 50: Schematic diagram illustrating the intra/interplay of biogeochemical processes between the oxic Ocean Margins and the ferruginous Open Ocean. The third compartment is inferred as an ecotone zone were the organisms of both compartment could be found. However, we assume that this ecotone was mainly under the influence of the Open Ocean, because of its volume, with some intrusion of chemicals from Ocean Margins. "AOM-IR" stand for an anaerobic oxidation of methane combined to an iron reduction (Beal *et al.*, 2009). However, this metabolism is limited by the Fe(III) availability. "Vents" stands for hydrothermal vents. Dashed bar indicates minor flux (assumptions).

$$Fe^{2+} + H_2S \longrightarrow FeS + H^+ \quad (5)$$

$$2\,Fe^{3+} + H_2S \longrightarrow 2\,Fe^{2+} + S^\circ + H^+ \quad (6)$$

$$FeS + S^\circ \longrightarrow FeS_2 \quad (7)$$

In the open ocean (compartment 2; Fig. 50), microorganisms implied in the iron cycle were the dominant life form. We will assume that primary producers were the iron oxidizing phototrophs which use the abundant Fe(II) fuelled by hydrothermal vents (*Chapter II* confirm such possibility). Consequently, there was a production of both C_{org} and Fe(III) that precipitated towards the oceanic floor. If Fe(III) would have sunken at the same speed as the C_{org}, we would have concluded that the main degradation pathway would have been dissimilatory iron reduction. However, two main biomineralization patterns exist: on one hand, Fe(III) precipitate away from the photosynthetic cells (Johnson *et al.*, 2007; Schadler *et al.*, 2009), while on the other hand Fe(III) precipitate on cell walls (Miot *et al.*, 2009). Even if our knowledge of biomineralization is restricted (Schadler *et al.*, 2009), we can describe the consequences of those two scenarios. If cells were not incrusted by Fe(III), a differential precipitation would occur: because of its weight, Fe(III) would have drown faster than the C_{org}. Therefore, the activity of DIR should have been limited as they need a physical contact with their electron acceptor (Lovley, 2004). This implies the presence in the cell surroundings of both electron donor (C_{org}) and acceptor (Fe(III)). In addition, we can assume that the oceanic currents would have enhanced this differential sedimentation between Fe(III) and C_{org}. Cell incrustation by Fe(III) offer an alternative to the presence of both Fe(III) and C_{org} (Miot *et al.*, 2009; Schadler *et al.*, 2009). If the cell was completely covered with iron oxides, DIR would not access the C_{org}, and therefore the reduction of Fe(III) back in Fe(II) would not occur. However, slightly negative $\delta^{56}Fe$ values from Archean BIFs tend to indicate an activity of DIR (Severmann *et al.*, 2008). This shift being little and since there was a Fe(III) accumulation we may assume that their activity was limited. In addition to DIR activity, the little $\delta^{34}S$ variation measured suggest that DSR activity was as well limited (Czaja *et al.*, 2010). As a result, organic matter degradation should have been dominated by anaerobic methanogenesis. As methanogenesis retrieved the majority of C_{org}, Fe(III) could then accumulate in the Open Ocean and form BIFs, even with the little presence of actives DIRs and DSRs (Fig. 50).

The ecology of compartment 1 and 2 of the Neoarchean Ocean are more or less understood and established. However, the functioning of compartment 3 is difficult to model because of its ecotone characteristics which makes it site-specific: the Ecotone Ocean being a mixture of Open Oceans and Ocean Margins conditions, its biogeochemistry depends on the development level of oxygenic photosynthesis and the amount of Fe(II) fuelled by mid ocean ridges. Neoarchean Ecotone Oceans should have been all different in topography, chemical composition and biological structure. Therefore, ferruginous water columns where photoferrotrophs thrives (Lake La Cruz, Lake Matano) could be seen as potential Neoarchean Ecotone Ocean analogue (NEO). In the Fe(II) rich Lake La Cruz all the organisms that would have potentially existed during the Neoarchean period are present. This lake is thus a good modern system for studying it as a potential NEO analogue.

3. Summer stratification: a model for the Neoarchean Ecotone Ocean (NEO)

3.1. Absence of Fe(III) accumulation in Lake La Cruz sediments

The increase of sulfide and the decrease of sulfate with depth indicate that sulfide production in Lake La Cruz is mainly in the water column (*Chapter II*). Retrieved 16S rRNA sequences of sulfate-reducing bacteria (*Desulfomonile sp. Chap II: 2.3*) were detected repeatedly in a clone library from the anoxic part of the chemocline,

therefore confirming that the sulfur produced in the water column mainly originated from microbial sulfato-reduction rather than from organic matter decomposition (Romero-Viana *et al.*, 2010). As previously explained (*Chapter II*), the sulfur measured in the water column is essentially as FeS. Indeed, Fe(II) and sulfur chemically react to form FeS particles (< 45 µm; equation 5).

There was therefore a FeS flux toward the sediments due to low amounts of sulfides. It was produced continuously just below the chemocline and then settled down the water column, thus, accumulating progressively in sediments. In addition, there was a Fe(III) flux toward the sediment (*Chap II: 2.4.3, Fig. 26*). However, only 3 µmol g^{-1} were detected at the surface of sediment cores (0-0.5 cm). Below the surface layer and down to 17 cm, iron was essentially linked to sulfur: 23±5 µmol S g^{-1} acid volatile sulfur (mostly FeS) and 10±2 µmol S g^{-1} chromium reducible sulfur, i.e. FeS_2, Fe_3S_4 and S^0, were measured (Fig. 51). Those measurements indicate that Fe(III) (hydro)oxides are reacting with sulfur to form S° and Fe(II) (equation 6, Bura-Nakic *et al.*, 2009).

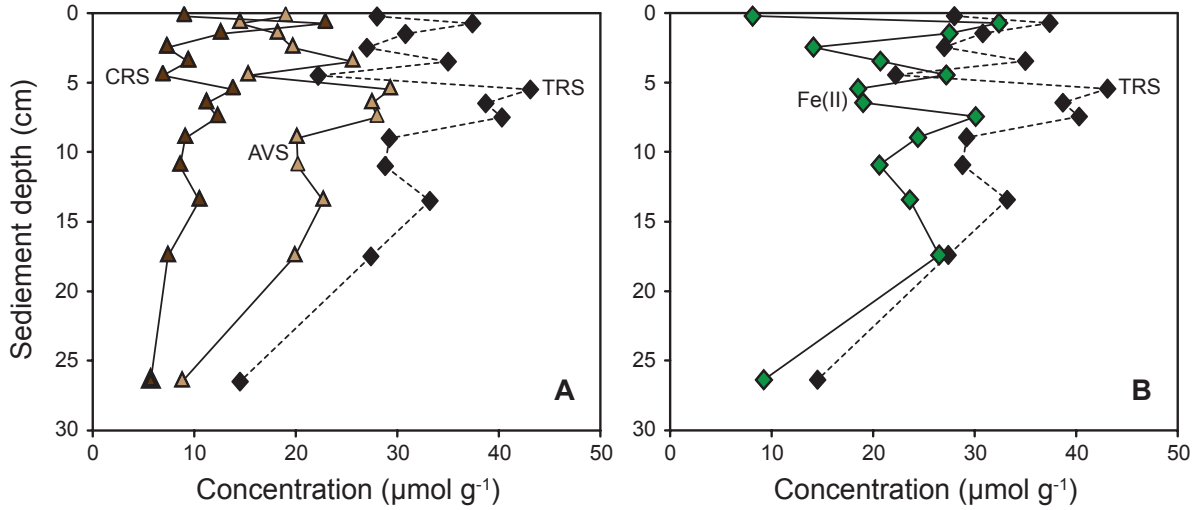

Figure 51: A | Sulfide concentration profile of La Cruz sediment. TRS is total reactive sulfide, composed of both AVS (acid volatile sulfide) and CRS (chromium reactive sulfide). **B |** Correlation between TRS and Fe(II), contained in Lake La Cruz sediment. The point at 26 cm corresponds to the sediment of La Cruz when it was not yet meromictic: it is a detritical layer.

In the organic-rich sediment anaerobic mineralization is mainly dominated by methanogenesis. Sulfato/sulfo reducing bacteria and ferrireducing bacteria found in Lake La Cruz sediment (Enrichment of DIRs), should be responsible for the respectively indirect or direct reduction of the Fe(III). The fate of Fe(III) arriving toward sediment, is therefore to be completely reduced back into Fe(II), either by the chemical reaction with sulfide (equation 6) or by microbial ferric respiration. Since there is a sulfur cycle in Lake La Cruz sediment, it is impossible for Fe(III) to accumulate. This means that Fe(III) fate in Lake La Cruz is directly linked to the degradation of organic matters, either by anaerobic sulfate/sulfur respiration in the sediment or HS^- released from decaying. When comparing putative sulfate concentrations for the Neoarchean Ocean to Lake La Cruz concentrations, we realize that the Archean sulfate concentrations were 10 times higher (*Chapter II.2.2*, *Tab. 3*). Therefore, Fe(III) accumulation in Archean sediments tends to indicate that the biological sulfur cycle should have been of minor importance. Thus, methanogenesis should have been the major process for organic matters mineralization.

3.2. The formation of FeS in a ferruginous water column

The detection of photoferrotrophs and nitrate dependent chemoferrotrophs complete the metabolic frame of the microbial guilds thriving in Lake La Cruz chemocline (*Chapter II-III*). Oxygenic phototrophs (algae and cyanobacteria) and anoxygenic phototrophs (green and purple sulfur oxidizers) are found in abundance

in this lake (*Chap II: 2.4.4*, *Fig. 29*). The 6 key metabolisms having a direct or indirect impact, , on the biological iron cycle are: oxygenic phototrophs (OP), sulfide-oxidizing phototrophs (SOP), iron-oxidizing phototrophs (IOP), iron-oxidizing nitrate-reducing chemotrophs (IOND), carbon-reducing chemotrophs (methanogens), and sulfate/sulfur reducing chemotrophs (DSR) (we consider that fermentative metabolisms are always present as indispensable intermediate in organic matter mineralization). Winter 2008 chemocline samples, incubated during 2 months under a 12 hours light shift, gave an enrichment of ferrireducing bacteria that reduced iron (hydro) oxide into magnetite (Fig. 52). Dissimilatory iron reduction (DIR) is therefore consider as the seventh key metabolism. The presence in the chemocline of DIR was also confirmed by the diversity 16S rRNA sequencing we have made at 15.5 m depth during winter 2008 stratification (*β-proteobacteria*, genus *Rhodoferax*; *Chap II: 2.3*).

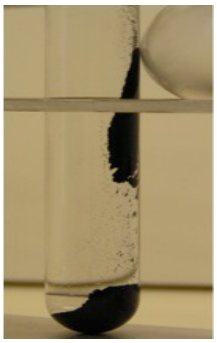

Figure 52: picture of the magnetite formed in FRB enrichment cultures (White object = magnet).

As DIR and IOP were present in the same water layer, a recycling of the Fe(III) back into reduced Fe(II) occurred. In addition to biological reduction, the chemical reaction of Fe(III) with sulfide (Eq. 2) also cause a removal of iron (hydro)oxides. However, a flux of Fe(III) toward the sediment occurs meaning that the oxidation of Fe(III) is more important than its reduction back into Fe(II). Overall, iron enter the chemocline compartment (compartment 1, Fig. 54) as Fe(II), leave it as Fe(III) and amorphous FeS towards sediment compartment (compartment 2, Fig. 54).

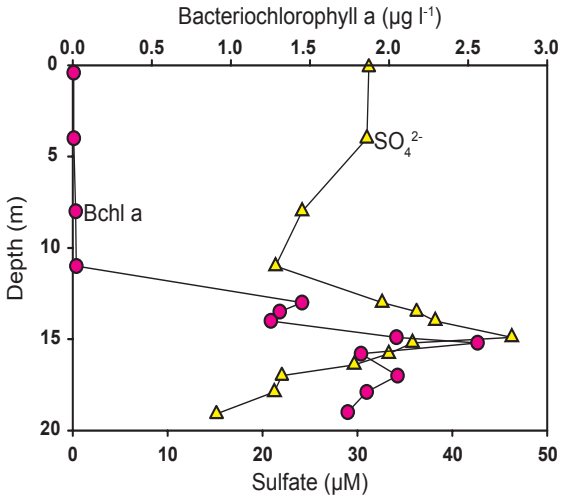

Figure 53: Bacteriochlorophyll a and sulfate concentration profiles during winter 2008 stratification (February). The correlation of those two curves shows the implication of *Lamprocystis purpurea* in sulfide oxidation. However, this sulfate pick is not seen in summer, suggesting that *Lamprocystis purpurea* are mixotrophs.

The major phototrophic sulfide oxidizers are the *Lamprocystis purpurea* which keep elemental sulfur as intracellular energy storage (Fig. 53). Because of their number (Chap II: *Fig. 29B*), the stored sulfur represent an important quantity. The elemental sulfur (S°) always seen in *Lamprocystis purpurea*, will arrive to the sediment after lake-mixing, and is therefore, with FeS, the main sulfur-output of the chemocline compartment. Organic matter from dead cells, which represent an electron donor for anaerobic respiration, also sedimentate toward compartment 2 (Fig. 54). S° and Fe(III) arriving at the bottom of the lake, thus, represent electron acceptors for organotrophic respiration. While Fe(III) will rapidly be reduced either by a chemical or a biological process (no accumulation), the S° will either be biologically reduced into sulfide that will chemically react with Fe(II) (Eq. 5) and form amorphous FeS, or chemically react with FeS to form FeS_2 (equation 7). Due to the lateral ferruginous sources, inputs of Fe(II) in this system are constant. The produced sulfide is then always trapped as FeS, due to its reaction with Fe(II). Therefore FeS_{am}, formed in the chemocline or in the sediments, will accumulate over time and be immobilized in La Cruz records (Fig. 54).

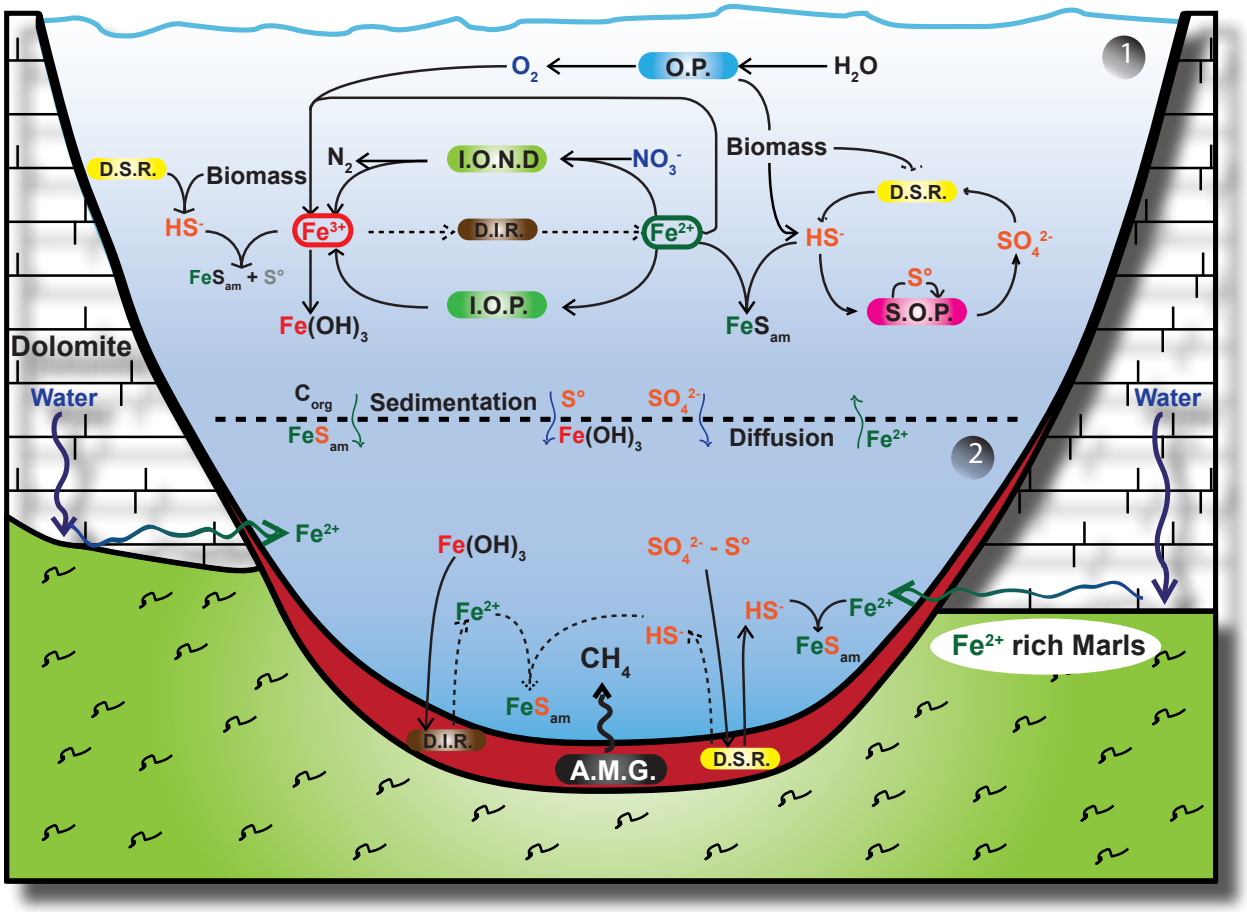

Figure 54: Model of the iron cycle in La Cruz water column. This model is an integration of the iron biogeochemical cycle to the oxygenic and sulfur one. While the chemocline compartment (**1**) could be analogue to a Neoarchean Open Ocean, the sediment compartment (**2**) does not demonstrate any Fe(III) accumulation. Plain arrows represent major flux, while dashed arrows stand for minor flux. Sediment compartment accumulate sulfur compounds as FeS_{am}. All processes from compartment 1 are established along the chemocline. The limit between compartment 1 and 2 is conceptual and would be situated few centimeters above the sediment. As such, this model gives an image of what could have been a Neoarchean Ecotone Ocean.

This study allowed us to establish an integration of the iron and sulfur biogeochemical cycles in an iron-rich sulfate-poor lake. One of our main observation is that in a ferruginous water column, the presence of sulfides reacting with iron (hydro)oxides will not let any Fe(III) accumulation in sediments: our model shows that in a sulfate-poor and iron-rich system we have no accumulation of Fe(III), but an accumulation of FeS_{am} that act as a sulfur sink. Geological records of FeS-rich sediment are actually attributed to either past euxinic conditions (anoxic and sulfidic; Meyer & Kump, 2008) or eutrophic conditions (Spadini *et al.*, 2003). But, as illustrated by this natural model, such a straightforward interpretation should not be done since FeS is the main sedimentary records of a ferruginous oligo-mesotrophic lake. In addition, the presence of maker pigments for phototrophic sulfur bacteria (e.g. bacteriochlorophyll a derivatives, okenone or chlorobactene) should not be directly interpreted as indicator of an euxinic water column since they can thrive in an iron-rich environment.

As to the microbial metabolic-web of Lake La Cruz, we can say that all metabolisms that would have been present in the Neoarchean Ocean are present in this water column. Therefore, this lake is confirmed as a model of the NEO, at the time of the early development of the oxygenic photosynthesis in the ocean margins.

4. Lake La Cruz in winter: another NEO analogue

4.1. Winter stratification

Lake La Cruz possess two stratification periods corresponding to two dynamic-equilibrium states: the summer stratification and the winter stratification. While summer stratification is characterized by the presence of an epilimnion, a metalimnion and a hypolimnion over the monimolimnion (*Chapter I*, *Fig. 11A*), the winter stratification is characterized by a single mixolimnic layer over the monimolimnic bottom layer (*Chapter I, Fig. 11B*). Therefore, the physical, chemical and biological water-column structure fluctuates from one equilibrium state to the other. The data presented here are well into the range of previously described seasonal structure dynamics (Rodrigo *et al*., 2001, Camacho *et al*., 2003). In summer (October 2008), the thermocline, the redoxicline and picnocline were established respectively between 8.75-13.90 m, 9.40-14.45 m and 13.80-17.40 m (Fig. 55). Conversely, in winter period all the three gradients were ranging between 14.50-18.00 m (February 2008; Fig. 55). Another characteristic is that in winter stratified water column, from mid-December to mid-February, gradients are thicker than in summer ones (Fig. 55).

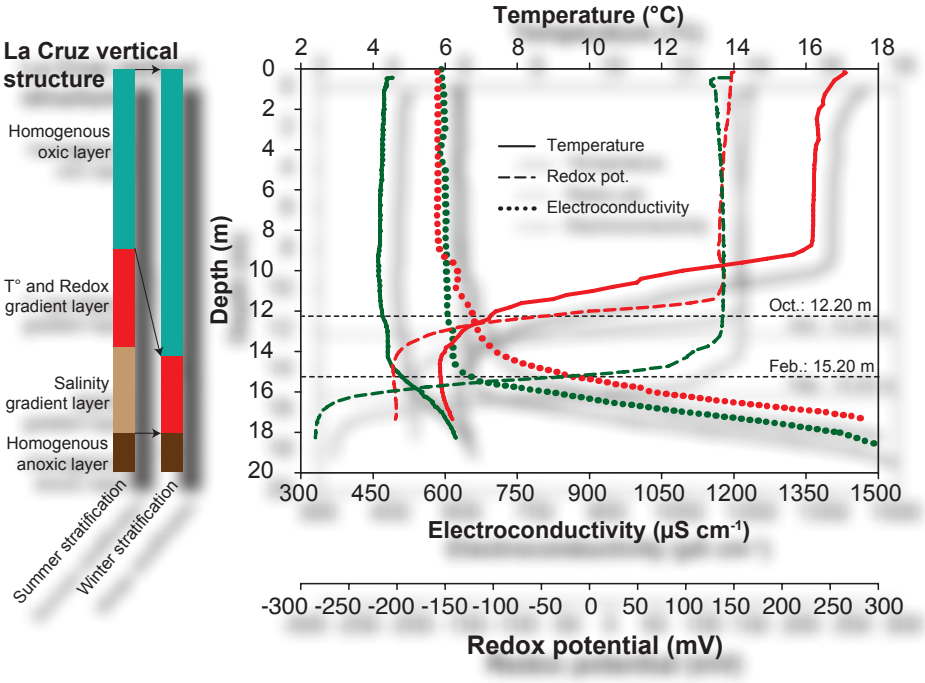

Figure 55: October 2008 (red) and February 2008 (green) stratifications. In summer, the redoxcline and thermocline, situated in the metalimnion, were separated from the picnocline, situated in the hypolimnion. On the contrary, in winter all the physical gradients were situated in the same water layer: from 14.50 m to 18.0 m depth. The dashed lines indicates depths at which oxygen was not anymore measured. The diagram on the left illustrate Lake la Cruz vertical layering during both stratification.

Like the physical and chemical parameters, the biological structure of the different phototrophic guilds also fluctuate between those two distinct equilibrium states. In summer, phototrophic guilds present a stratification of thin and dense layers, depending on the wavelength used for light harvesting: first the algae, then the oxygenic prokaryotes followed by the purple sulfur bacteria and finally the green sulfur bacteria (*Chap. II: 2.4.4, Fig. 29C*). In comparison, winter phototrophic guilds developed thicker and less dense picks (*Chap. II: 2.4.4, Fig. 29B*). Even if pigments are not a direct measure of abundance, there was clearly an augmentation of phototrophic populations between winter and summer 2008 (*Chap. II: 2.4.4, Fig. 29B-C*). This augmentation is confirmed by the biomass measurements performed by Antonio Picazo-Mozo: Lake La Cruz total biomass increase from 1.52 g C m^{-2} in January to 5.39 g C m^{-2} in October (Fig. 56, Picazo *et al.*, 2011).

The winter biomass-drop reflects the autumnal-mixing effects on La Cruz populations. This seasonal water mixing erode the summer stratification and brings an important proportion of organic matter toward the sediments: 3.86 g C m^{-2} difference between October 2006 and January 2007. The water column is therefore

less densely colonized by microorganisms. In addition to the winter biomass-drop, the relative abundance of the phototrophic guilds changes. Algal population declined from 79.8 % of the biomass (October 2006) to 25.3 % (February 2006). Conversely, it is during summer that anoxygenic photosynthesizers (PSB plus GSB) had smaller relative biomass (0.77 % in October 2006), while it is in winter that they were relatively more abundant (1.25 % in february 2006; Fig. 33; Picazo *et al.*, 2011). However, they had a similar total-biomass over the year: ± 42 mg C m^{-2} in October 2006; ± 37mg C m^{-2} in February 2006 (Fig. 56). Therefore, it is in winter that anoxygenic photosynthesizers should influence most Lake La Cruz biological cycles.

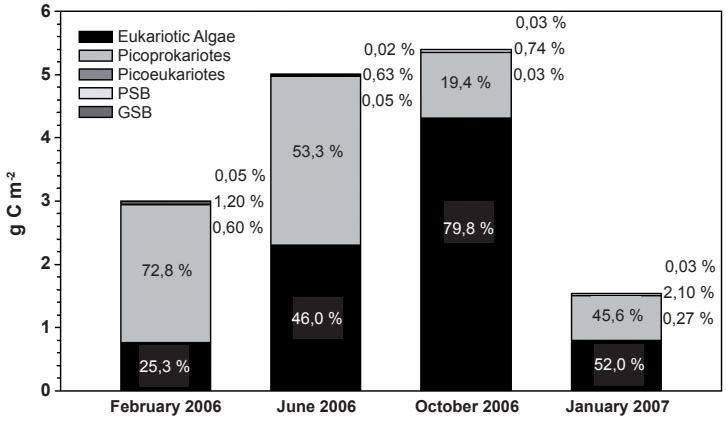

Figure 56: Lake La Cruz biomass over a year. Picoprokaryotes include mainly picocyanobacteria and chemotrophs. PSB and GSB stand respectively for purple and green sulfur bacteria. Figure from Picaso *et al*., 2011).

Concerning phototrophic carbon assimilation, it is in summer that anoxygenic phototrophs fixed more carbon. Even if in summer the competition for light is more intense, it is in summer that they have a higher participation to total primary production: in October 2006 they fixed 7.3 % of the phototrophically assimilated carbon, while they participated to 3.5 % of the phototrophic primary production in February 2006 (Tab. 8). However, regarding layers where anoxygenic phototrophs dominate (the monimolimnion in February 2006 and the hypolimnion in October 2006), it is in winter that they fixed a higher proportion of carbon: 90.6 % in February and 87.5 % in October.

Table 8: Phototrophic carbon assimilation in Lake La Cruz. Those data have been obtained by Antonio Picazo-Mozo (Picazo *et al*., 2011).

	All layers	***mg C m^{-2} day^{-1}***	***(%)***	**Hypolimnion**	***mg C m^{-2} day^{-1}***	***(%)***
October 2006	Oxygenic	553.2	92.7	Oxygenic	5.3	12.5
	Anoxygenic	43.4	7.3	Anoxygenic	36.7	87.5
	Total	596.6	100.0	Total	41.9	100.0
	All layers	***mg C m^{-2} day^{-1}***	***(%)***	**Monimolimnion**	***mg C m^{-2} day^{-1}***	***(%)***
February 2006	Oxygenic	214.9	96.5	Oxygenic	0.6	9.4
	Anoxygenic	7.9	3.5	Anoxygenic	6.2	90.6
	Total	222.7	100.0	Total	6.8	100.0

To summarize, Lake La Cruz winter stratification is characterized by cooler temperatures and a deeper chemocline. Thicker winter gradients together with a less densely colonized water column allowed light to penetrate in anoxic water layers, thus, supporting anoxygenic photosynthesis activity (Fig. 57). In addition to winter lower carbon assimilation, anoxygenic photosynthesizers participate in a higher proportion to the photosynthetically fixed carbon. We thus postulate that in winter periods the detection of anoxygenic phototrophs activity is less shadowed by oxygenic phototrophs. Moreover, it is in winter that the green sulfur bacteria, as potential photoferrotrophs, are the most developed (*Chap. II: 2.4.4, Fig. 29*).

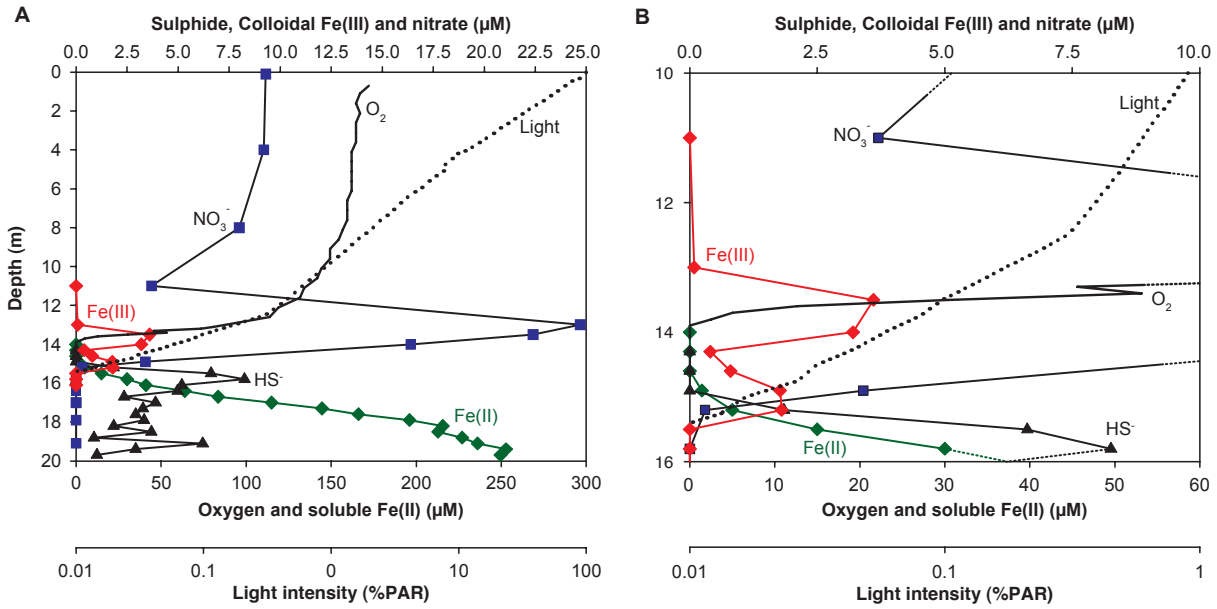

Figure 57: Winter stratification situation in Lake La Cruz. **A |** October 2008. Oxygen extinction depth was at 14.00 m, while light reaches 16.25 m. During winter nitrate get to its highest concentrations: 24.7 µM at 13.00 m. Based on the represented chemical gradients, we define the chemocline being between 11.5 m and 16.7 m. **B |** close-up, from 10 to 16 m depth.

4.2. Winter ferrotrophy and the photoferrotrophs

As explained previously (less oxygenic photosynthesis, clearer water, little sulfur cycle), winter stratification seems to be more favorable for the development of anoxygenic phototrophs. Therefore, the same approach as used in October 2008 (*Chap II*) was applied for photoferrotrophy detection. First, the depth of iron oxidation was determined through Fe(III), oxygen, nitrate, Fe(II) and sulfide profiling (Fig. 57). Thereafter, the positioning of the different phototrophic guilds was established, using pigments analysis (*Chap. II: 2.4.4, Fig. 29A*). Once the potential layer for photoferrotrophs determined on the basis of Fe(III) concentrations, ^{14}C-bicarbonate incubations were performed in order to detect any stimulation of autotrophy under Fe(II) treatments.

During winter stratifications, the picnocline begins at 15.0 m with electroconductivity values ranging from 580 µS cm^{-1}, in the chemocline, to 1550 µS cm^{-1} at 18.0 m (Fig. 55). Anoxygenic phototrophic populations are dominated by purple *Lamprocystis purpurea* and the green *Chlorobium clathratiforme* (*Chap. II: 2.4.4, Fig. 29A*). In the anoxic part of the chemocline (APC: 14 and 16 m), the presence of light (15.8 m: 0.03-0.025 % PAR) and an electron donor, 30 µM Fe(II) at 15.8 m, settle conditions in which photoferrotrophs could developed (Fig. 34). The colloidal Fe(III) concentration profile indicates 2 peaks (Fig. 57). The upper one, 3.6 µM of Fe(III) at 13.5m, is found in the oxic part of the chemocline (OPC), where the oxygenic phototrophs were more abundant and green sulfur bacteria absents (Fig. 57; *Chap. II: 2.4.4, Fig. 29A*). The second lower peak, 1.8 µM of Fe(III) at 15-15.5 m, matches abundant populations of anoxygenic phototrophs (Fig. 57; *Chap. II: 2.4.4, Fig. 29A*). The upper peak could be the result of the Fe(III) reaction with oxygen through a microaerophilic chemotrophic oxidation (ex: *Ferribacterium limneticum*; *Chap II: 2.3*), and/or an abiotic oxidation. Conversely, the lower peak could be the result of an anaerobic Fe(II) oxidation, either phototrophic or chemotrophic.

Winter ^{14}C-bicarbonate incubations confirmed the presence of a light dependent Fe(II) oxidation activity and, in a less important measure, of a nitrate dependent Fe(II) oxidation activity (*Chap. II: 2.5*; *Chap. III: 6.2*). However, MPN counts of chemoferrotrophs indicated a very weak presence of NDIOs in all sampled depths (*Chap. III.4.2*, *Tab. 6*), thus confirming the low winter activity of NDIOs. The layer where was detected

the highest stimulation of phototrophs was situated at 15.0 m depth, at the picnocline's beginning. It was also at that depth that anoxygenic phototrophs maxima were measured: both purple and green sulfur oxidizing bacteria (*Chap. II: 2.4.4, Fig. 29*). Interestingly, the only significant proof of NDIOs activity was the stimulated dark autotrophy at 15.5 m depth (*Chap. II: 2.5, Fig. 31B*): no nitrate were measured at this depth (NO_3^- extinction at 15.2 m), and NDIOs were thus situated below photoferrotrophs.

Lake La Cruz winter situation is a stratification period with clearer waters and few NDIOs. Even if the temperatures were cooler than in summer, under a Fe(II) stimulated environment the phototrophic guilds fixed as much carbon than in summer. In addition, we have shown that Fe(II) stimulated anoxygenic photoautotrophs were not very sensitive to light stimulation (*Chap. II: 2.5, Fig. 32*). Those observations might imply that photoferrotrophs were more abundant in winter. The cDOM and sulfur profiles (*Chap. II: 2.4.2* and *24.4, Fig. 24D* and *Fig. 28B*, respectively) illustrate the low winter primary production (Tab. 8; max of 245.3 mg C m^{-2} d^{-1}; Picazo *et al.*, 2011). Even if anoxygenic sulfur oxidizing bacteria had a higher activity than in summer (Fig. 56), the lower primary productivity and the subsequent lower sulfatoreduction tend to support a less present sulfur cycle. This, together with a lower oxygenic phototrophic activity and presence, suggest winter stratification to be more favorable for photoferrotrophy. This hypothesis is supported by the fact that it was in winter that Fe(III) concentrations were the highest (*Chap. II: 2.4.3, Fig. 26B* and *Fig. 27B*). However, as one could not determine the part of Fe(II) oxidized chemically from the part oxidized biologically, the higher Fe(III) production may be of a chemical origin. The whole of these factors characterize winter stratification as a NEO analogue. This winter analogue, contrarily to the summer one, would represent a NEO which would be more under the influence of the open ocean: a lower sulfur cycle and a higher iron one. Therefore, winter stratification would be more favorable than the summer one for the study of the Neoarchean Open Ocean processes.

5. Conclusion

During this project, new studies revealed that between 3.0 Ga and 2.5 Ga, at the end of the Archean (Neoarchean), oxygen was already present in the water column of Ocean Margins (Kaufman *et al.*, 2007; Sleep & Bird, 2008; Reinhard *et al.*, 2009; Voegelin *et al.*, 2010; Farquhar *et al.*, 2010; Czaja *et al.*, 2010; Kendall *et al.*, 2010). It was also during the Neoarchean that the maximum precipitation of Fe(III) occurred (Fig. 58).

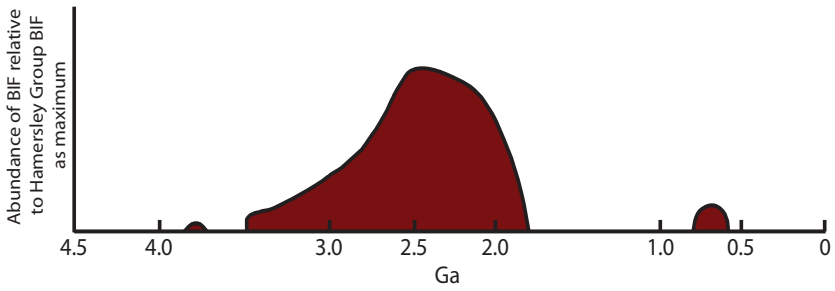

Figure 58: Schematic timeline of the amount of BIFs formed during Earth history. Figure from Klein (2005).

Those studies showed that oxygen was present due to the activity of oxygenic photosynthesis, and that most of the aerobic metabolisms were already present. Moreover, the oxygen in the atmosphere enhanced the sulfur cycle by the release of sulfate in Ocean Margins due to the oxidative weathering of continental sulfide minerals. During the maximum of BIF precipitation, the Neoarchean Ocean seemed to consist of at least two different compartments: i) the Open Ocean characterized by the absence of oxygen and the presence of intense Fe(II)-oxidation, and ii) the Ocean Margins characterized by oxic upper water layers and euxinic bottom water layers.

In the light of those new informations, we may consider Lake La Cruz as a natural analogue of what may have been the ecotone zone between the Open Ocean and the Ocean Margins: oxic upper layers due to oxygenic photosynthesis, ferruginous bottom layers, minor biological sulfur cycle, presence of photoferrotrophs, and euxinic sediments.

Lake La Cruz winter stratification seems to be closer to Open Ocean compartment than the summer one. Indeed, a higher proportion of anoxygenic phototrophs (both purple and green sulfur one) and a deeper depth of light penetration were observed. In addition, this situation was marked by a carbon uptake equivalent to the summer one, when Fe(II) was added (≈ 1.25 µg C l^{-1} h^{-1}), even tough the temperature was cooler and the primary fixation lower. However, no Fe(III) accumulation toward the sediment was observed. Conversely, during summer stratification, an accumulation of Fe(III) towards the bottom of the water column was observed, suggesting that hydrogen sulfides were not present in sufficient quantity to react with all the Fe(III) (equation 6). However, no Fe(III) accumulation occurred in Lake La Cruz sediments. We therefore postulate that the Fe(III) arriving at the sediment surface was reduced back into Fe(II) either by ferrireduction, or by a chemical reaction (equation 5, 6 and 7) with the free sulfide produced by dissimilatory sulfur or sulfate reduction. Thus, we may postulate that in the Neoarchean Ocean Fe(III) could have only accumulated if sulfate- and ferri-reducing bacteria were not/little active. Therefore, we may consider that Fe(III) could only have accumulated in the Open Ocean compartment where anaerobic methanogenesis was the dominant mineralization pathway, faraway from the euxinic waters of the Ocean Margin (Fig. 50).

It has been shown, either from pure culture experiments (Kappler *et al.*, 2005; Hegler *et al.*, 2008) or from Lake La Cruz chemocline microbiota, that Fe(II)-oxidation rates of modern photoferrotrophs were sufficient to oxidize the totality of the estimated Fe(II) flux from hydrothermal vents in the Archean Ocean. Moreover, photoinhibition of oxygenic phototrophs occurs at higher light intensity (520 µE m^{-1} s^{-1}; Pringault & Garcia-Pichel, 2000) than anoxygenic photoferrotrophs which have a light-saturation at lower intensity (1.8 to 28.8 µE m^{-1} s^{-1}; Hegler *et al.*, 2008). We may, therefore, assume that photoferrotrophs did not grow up to the top of the Neoarchean Open Ocean (NOO) water column. Thus, the upper layer of this ocean should have been free of photoferrotrophs, because of light inhibition, and of Fe(II) as it was oxidized before reaching shallow depths. In addition, we may suggest that a water column containing high concentration of Fe(II) would be inappropriate for its colonization by oxygenic phototrophs. Indeed, Fe(II) would have to react immediately with the produced oxygen and precipitate as Fe(III) on the cell walls. As a result, we may postulate that anoxygenic photoferrotrophy indirectly provided a free niche for oxygenic photosynthesis (euphotic and Fe(II)-free) in the NOO upper layer, therefor, enhancing its colonization (by oxygenic photosynthesis).

CHAPTER V: Conclusion and Perspectives

1. Conclusion

At the beginning of this project, the objective was to find a modern analogue to the theoretical model of an Archean Ocean. In this model, the Fe(III) found in BIFs were the product of biotic oxidation mediated by photoferrotrophs (Kappler *et al.*, 2005). We searched, therefore, for an accessible, ferruginous water column that had low sulfate concentrations and hosted dense populations of anoxygenic phototrophs. Lake La Cruz water column was the site that has been chosen. The goal was to provide direct evidence for anaerobic Fe(II)-oxidation by photoferrotrophs. Afterwards, the aim was to integrate those results to what is known of the Archean Ocean, and to constrain the conceptual model of the biotic origin of BIFs.

Results of the *in situ* ^{14}C-bicarbonate incubations, of the *ex situ* Fe(II)-oxidation experiments, and of the enrichment cultures indicated that anaerobic ferrotrophs were present and active in the anoxic part of Lake La Cruz chemocline. It is the first time that the presence and activity of both photoferrotrophs and nitrate-dependent chemoferrotrophs were demonstrated thriving in a water column. Moreover, as we proved that photoferrotrophs thrived within a water column, one can now assume that it was also the case in the Archean chemocline. Thus, our results support the implication of photoferrotrophs in the formation of BIFs. It even lead us to postulate that the activity of photoferrotrophs indirectly allowed the colonization of the Neoarchean Ocean upper layer by the oxygenic phototrophs. Moreover, the MPN counts of NDIOs suggest that nitrate-dependent Fe(II)-oxidation is a widespread facultative metabolism that can be found in many different types of environment.

Together with the physical and chemical characterizations, our results allowed to consider Lake La Cruz as an Neoarchean Ecotone Ocean analogue: a ferruginous water column hosting oxygenic photosynthesis, anoxygenic sulfur photosynthesis, anoxygenic photoferrotrophy and euxinic sediments where methanogenesis is the main organic mineralization pathway. Furthermore, this natural example of a ferruginous water column presenting sedimentary features typical for euxinic water column illustrates the need to refine proxies for paleo-oceanic redox conditions (Ohmoto et al., 2008; Severmann & Anbar, 2009; Lyons et al., 2009): the detection of FeS/FeS_2 in rocks, as well as pigment-biomarkers of anoxygenic purple/green sulfur bacteria does not unambiguously prove that the sediments were deposited under a sulfidic water column.

2. Outlooks

Our study allowed to characterize Lake La Cruz as a Neoarchean Ecotone Ocean (NEO) analogue from its chemistry and from the organisms detected in it: oxygenic phototrophs, anoxygenic photoferrotrophs, anoxygenic sulfide-oxidizing phototrophs, Fe(III)-reducing heterotrophs, sulfate-reducing heterotrophs, and acetoclastic/autotrophic methanogens. However, how would such a situation be recognized when analyzing the rocks records? Maybe, the measured of the δ^{56}Fe and the δ^{34}S values of Lake La Cruz sediment would allow to restrain the isotope values used for the interpretation of Archean rock records. In addition, a precise geochemical characterization of the different fluxes (Fe(II)/Fe(III), SO_4^{2-}/H_2S, CO_2/CH_4) between the chemocline and the sediment should be performed to determine the geochemical backbone of the site.

Concerning the methane cycle, the implication of the acetoclastic and the hydrogenotrophic methanogenesis should be determined. Indeed, acetoclastic methanogenesis could occur either in the chemocline or in the sediment, depending on acetate availability, and could be a possible metabolism for limiting the activity of sulfate-reducing microorganism in a Neoarchean Ocean, thus allowing the accumulation of Fe(III). In addition, one should determine which one of the two types of methanogenesis

dominates in the water column: it could help understanding the N-serve effect observed in the ^{14}C-bicarbonate incubations. Therefore, samples from Lake La Cruz chemocline/sediment could be spiked, prior to incubation, with ^{14}C-bicarbonate, [1-^{14}C]acetate or [2-^{14}C]acetate (Conrad & Klose, 1999). Then, the analysis of the isotopic composition of the produced methane and CO_2 would allow to determine which metabolism is the most active as well as quantifying each methanogenesis rates. In parallel, a molecular characterization of the community of Archaea composition/distribution by cloning-sequencing, centered on methanogenic populations should be carried out. Then, a CARD-FISH (CAtalyzed Reporter Deposition Fluorescence In Situ Hybridization) approach could undertaken to evaluate the proportion of cells responsible for each type of methanogenesis, thus obtaining the cell specific rates.

Results have shown the absence of Fe(III) accumulation because of the activity of sulfate-reducing heterotrophs (SRB) that occur either in the chemocline or the sediment. To confirm this assumption sulfate reduction rates need to be determined as it was done in previous studies (Zopfi *et al.*, 2001; Crowe *et al.*, 2008). Here again, the involved organisms need to be identified by cloning-sequencing. A CARD-FISH analysis would be more accurate than the MPN counts to enumerate SRBs. In parallel the implication of *in situ* sulfide oxidation by the anoxygenic phototrophs need to be determined. Indeed, their capacity of oxidizing both Fe(II) and sulfide has been shown, but we do not have a clear idea of the processes/metabolisms involved in their growth: what is the *in situ* proportion between photoheterotrophy, photoferrotrophy and sulfide-dependent phototrophy?

The above problematic lead us to the quantification of the detected *in situ* photoferrotrophy and to the identification of the organism(s) responsible of it. The answer could be obtained through a HISH-SIMS (Halogen In Situ Hybridization-Secondary Ion Mass Spectroscopy) approach. This approach will allow to quantify the autotrophic activity and to identify the organisms, by a molecular micro-probing, on the same sample. By incubating samples in parallel with ^{56}Fe(II), sulfide, acetate, and ^{13}C-bicarbonate it should be possible to quantify the *in situ* participation of each of the identified organisms. Thus, we could evaluate the implication of photoferrotrophs in the iron cycle of the geochemically characterized NEO (Lake La Cruz). Furthermore, the identified photoferrotroph(s) should be isolated, and its(their) 16S rRNA gene sequence(s) compared to the ones retrieved from our enrichment culture of green photoferrotrophs. Moreover, the Fe(II)-oxidation rates measured in *ex situ* Fe(II)-incubation experiments could be repeated with water samples from different depths. Then a comparison could be made between those Fe(II)-oxidation rates, the one from the enrichment culture, and the one measured with the HISH-SIMS approach.

In conclusion, Lake La Cruz is a perfect model-system to conduct research on the Neoarchean biogeocycles, to deepen our knowledge on paleo-oceanic proxies (e.g. which proxies/values could be used to differentiate an euxinic paleo-water column from a ferruginous one?), or for testing new hypothesis on the implication of biological processes, such as photoferrotrophy, in the formation of BIFs.

References

A

Abramov O & Mojzsis SJ (**2009**) Microbial habitability of the Hadean Earth during the late heavy bombardment. Nature **459**: 419-422.

Aeschbach-Hertig W, Hofer M, Schmid M, Kipfer R & Imboden DM (**2002**) The physical structure and dynamics of a deep, meromictic crater lake (Lac Pavin, France). Hydrobiologia **487**: 111-136.

Alego TJ & Lyons TW (**2006**) Mo-total organic carbon covariation in modern anoxic environments: implication for analysis of paleoredox and paleohydrographic conditions. Paleoceanography **21**: PA1016.

Anbar AD & Knoll AH (**2002**) Proterozoic ocean chemistry and evolution: A bioinorganic bridge? Science **297**: 1137-1142.

Anbar AD, Arnold GL, Lyons TW & Barling J (**2005**) Response to comment on "Molybdenum isotope evidence for widespread anoxia in mid-proterozoic oceans". Science **309**.

Anbar AD, Duan Y, Lyons TW, et al. (**2007**) A whiff of oxygen before the Great Oxidation Event? Science **317**: 1903-1906.

Anthony RS (**1977**) Iron-rich rhythmically laminated sediments in Lake of the Clouds, northeastern Minnesota. Limnology and Oceanography. **22**: 45-54.

Armengol X & Miracle MR (**2000**) Diel vertical movements of zooplankton in lake La Cruz (Cuenca, Spain). Journal of Plankton Research **22**: 1683-1703.

Arnold GL, Anbar AD, Barling J & Lyons TW (**2004**) Molybdenum isotope evidence for widespread anoxia in mid-proterozoic oceans. Science **304**: 87-90.

B

Balistrieri LS, Murray JW & Paul B (**1994**) The geochemical cycling of trace elements in a biogenic meromictic lake. Geochimica et Cosmochimica Acta **58**: 3993-4008.

Barley ME, Pickard AL & Sylvester PJ (**1997**) Emplacement of a large igneous province as a possible cause of banded iron formation 2.45 billion years ago. Nature **385**: 55-58.

Barley ME, Bekker A & Krapez B (**2005**) Late Archean to Early Paleoproterozoic global tectonics, environmental change and the rise of atmospheric oxygen. Earth and Planetary Science Letters **238**: 156-171.

Bau M & Moller P (**1993**) Rare-Earth elements systematics of the chemically precipitated component in early Precambrian iron formation and the evolution of the terrestrial atmosphere-hydrosphere-lithosphere system. Geochimica et Cosmochimica Acta **57**: 2239-2249.

Beal EJ, House CH & Orphan VJ (**2009**) Manganese- and iron-dependent marine methane oxidation. Science **325**: 184-187.

Bekker A, Slack JF, Planavsky N, Krapez B, Hofman A, Konhauser KO & Rouxel O (**2010**) Iron formation: the sedimentary product of a complex interplay among mantle, tectonic, oceanic, and biospheric processes. Economic Geology **105**: 467-508.

Beller HR, Chain PSG, Letain TE, et al. (**2006**) The genome sequence of the obligately chemolithoautotrophic, facultatively anaerobic bacterium *Thiobacillus denitrificans*. Journal of Bacteriology **188**: 1473-1488.

Benz M, Brune A & Schink B (**1998**) Anaerobic and aerobic oxidation of ferrous iron at neutral pH by chemoheterotrophic nitrate-reducing bacteria. Archives of Microbiology **169**: 159-165.

Blake R & Johnson DB (**2000**) Phylogenetic and biochemical diversity among acidophilic bacteria that respire on iron. Environmental metal-microbe interactions,(Lovley, ed.), p. 58-78. ASM press, Washington DC.

Blake RE, Chang SJ & Lepland A (**2010**) Phosphate oxygen isotopic evidence for a temperate and biologically active Archaean ocean. Nature **464**: 1029-1033.

Boetius A, Ravenschlag K, Schubert CJ, et al. (**2000**) A marine microbial consortium apparently mediating anaerobic oxidation of methane. Nature **407**: 623-627.

Braterman PS, Cairnssmith AG & Sloper RW (**1983**) Photooxidation of Hydrated Fe^{2+} - Significance for Banded Iron Formations. Nature **303**: 163-164.

Brocks JJ, Logan GA, Buick R & Summons RE (**1999**) Archean molecular fossils and the early rise of eukaryotes. Science **285**: 1033-1036.

Brocks, J. and B. Rasmussen (**2010**) Molecular Fossils and the late rise of Eukaryotes and oxygenic photosynthesis. ISME 13 symposium, abstract IS32.001.

Burgin AJ & Hamilton SK (**2007**) Have we overemphasized the role of denitrification in aquatic ecosystems? A review of nitrate removal pathways. Frontiers in Ecology and the Environment **5**: 89-96.

Buick R (**2008**) When did oxygenic photosynthesis evolve? Philosophical Transactions of the Royal Society B-Biological Sciences **363**: 2731-2743.

Bura-Nakic E, Viollier E, Jezequel D, Thiam A & Ciglenecki I (**2009**) Reduced sulfur and iron species in anoxic water column of meromictic crater Lake Pavin (Massif Central, France). Chemical Geology **266**: 320-326.

C

Caiazza NC, Lies DP & Newman DK (**2007**) Phototrophic fe(II) oxidation promotes organic carbon acquisition by *Rhodobacter capsulatus* SB1003. Applied and Environmental Microbiology **73**: 6150-6158.

Cairns Smith AG (**1978**) Precambrian solution photochemistry, inverse segregation, and Banded iron formations. Nature **276**: 807-808.

Camacho A, Picazo A, Miracle MR & Vicente E (**2003**) Spatial distribution and temporal dynamics of picocyanobacteria in a meromictic karstic lake. Algological Studies **109**: 171-184.

Canfield DE, Thamdrup B & Hansen JW (**1993**) The anaerobic degradation of organique-matter in danish coastal sediments - Iron reduction, manganese reduction, and sulfate reduction. Geochimica et Cosmochimica Acta **57**: 3867-3883.

Canfield DE (**1998**) A new model for Proterozoic ocean chemistry. Nature **396**: 450-453.

Canfield DE & Raiswell R (**1999**) The evolution of the sulfur cycle. American Journal of Science **299**: 697-723.

Canfield DE (**2004**) The evolution of the Earth surface sulfur reservoir. American Journal of Science **304**: 839-861.

Canfield DE (**2005**) The early history of atmospheric oxygen: Homage to Robert A. Garrels. Annual Review of Earth and Planetary Sciences **33**: 1-36.

Canfield DE, Rosing MT & Bjerrum C (**2006**) Early anaerobic metabolisms. Philosophical Transactions of the Royal Society B-Biological Sciences **361**: 1819-1834.

Canfield DE, Poulton SW, Knoll AH, Narbonne GM, Ross G, Goldberg T & Strauss H (**2008**) Ferruginous conditions dominated later neoproterozoic deep-water chemistry. Science **321**: 949-952.

Canfield DE, Farquhar J & Zerkle AL (**2010**) High isotope fractionations during sulfate reduction in a low-sulfate euxinic ocean analog. Geology **38**: 415-418.

Casamayor EO, Muyzer G & Pedros-Alio C (**2001**) Composition and temporal dynamics of planktonic archaeal assemblages from anaerobic sulfurous environments studied by 16S rDNA denaturing gradient gel electrophoresis and sequencing. Aquatic Microbial Ecology **25**: 237-246.

Chaudhuri SK, Lack JG & Coates JD (**2001**) Biogenic magnetite formation through anaerobic biooxidation of Fe(II). Applied and Environmental Microbiology **67**: 2844-2848.

Chrost RJ, Tomasz A, Kalinowska K & Skowronska A (**2009**) Abundance and structure of microbial loop components (bacteria and protists) in lakes of different trophic Status. Journal of Microbiology and Biotechnology **19**: 858-868.

Clement JC, Shrestha J, Ehrenfeld JG & Jaffe PR (**2005**) Ammonium oxidation coupled to dissimilatory reduction of iron under anaerobic conditions in wetland soils. Soil Biology & Biochemistry **37**: 2323-2328.

Cline JD (**1969**) Spectrophotometric Determination of Hydrogen Sulfide in Natural Waters. Limnology and Oceanography **14**: 454-458.

Cloud PE & Licari GR (**1968**[1]) Microbiotas of the Banded Iron Formations. Proceedings of the National Academy of Sciences U S A **61**: 779-786.

Cloud PE (**1968**[2]) Atmospheric and Hydrospheric Evolution on Primitive Earth. Science **160**: 729-736.

Cloud P (**1973**) Paleoecological significance of banded iron-formation. Economic Geology **68**: 1135-1143.

Cohen Y, Jorgensen BB, Revsbech NP & Poplawski R (**1986**) Adaptation to hydrogen-sulfide of oxygenic and anoxygenic photosynthesis among cyanobacteria. Applied and Environmental Microbiology **51**: 398-407.

Conrad R, Aragno M & Seder W (**1983**[1]) Production and consumption of carbon monoxide in a eutrophic lake. Limnology and Oceanography **28**: 42-49.

Conrad R, Aragno M & Seiler W (**1983**[2]) Production and consumption of hydrogen in a eutrophic lake. Applied and Environmental Microbiology **45**: 502-510.

Conrad R & Klose M (**1999**) Anaerobic conversion of carbon dioxide to methane, acetate and propionate on washed rice roots. Fems Microbiology Ecology **30**: 147-155.

Croal LR, Johnson CM, Beard BL & Newman DK (**2004**) Iron isotope fractionation by Fe(II)-oxidizing photoautotrophic bacteria. Geochimica et Cosmochimica Acta **68**: 1227-1242.

Croal LR, Jiao YQ & Newman DK (**2007**) The fox operon from *Rhodobacter* strain SW2 promotes phototrophic fe(II) oxidation in *Rhodobacter capsulatus* SB1003. Journal of Bacteriology **189**: 1774-1782.

Crowe SA, Jones C, Katsev S, et al. (**2008**[1]) Photoferrotrophs thrive in an Archean Ocean analogue. Proceedings of the National Academy of Sciences of the United States of America **105**: 15938-15943.

Crowe SA, O'Neill AH, Katsev S, et al. (**2008**[2]) The biogeochemistry of tropical lakes: A case study from Lake Matano, Indonesia. Limnology and Oceanography **53**: 319-331.

Crusius J, Calvert S, Pedersen T & Sage D (**1996**) Rhenium and molybdenum enrichments in sediments as indicators of oxic, suboxic and sulfidic conditions of deposition. Earth and Planetary Science Letters **145**: 65-78.

Cummings DE, Caccavo F, Spring S & Rosenzweig RF (**1999**) *Ferribacterium limneticum*, gen. nov., sp. nov., an Fe(III)-reducing microorganism isolated from mining-impacted freshwater lake sediments. Archives of Microbiology **171**: 183-188.

Czaja AD, Johnson CM, Beard BL, Eigenbrode JL, Freeman KH & Yamaguchi KE (**2010**) Iron and carbon isotope evidence for ecosystem and environmental diversity in the 2.7 to 2.5 Ga Hamersley Province, Western Australia. Earth and Planetary Science Letters **292**: 170-180.

D

Dahl TW, Anbar AD, Gordon GW, Rosing MT, Frei R & Canfield DE (**2010**) The behavior of molybdenum and its isotopes across the chemocline and in the sediments of sulfidic Lake Cadagno, Switzerland. Geochimica Cosmochimica Acta **74**: 144-163.

Dasí MJ & Miracle MR (**1991**) Distribución vertical y variación estacional del fitoplancton de una laguna cárstica meromíctica, La Laguna de la Cruz (Cuenca, España). Limnetica **7**: 37-59.

David LA & Alm EJ (**2011**) Rapid evolutionary innovation during an Archaean genetic expansion. Nature **469**: 93-96.

Davis CC, Chen HW & Edwards M (**2002**) Modeling silica sorption to iron hydroxide. Environmental Science & Technology **36**: 582-587.

De Gusseme B, De Schryver P, De Cooman M, Verbeken K, Boeckx P, Verstraete W & Boon N (**2009**) Nitrate-reducing, sulfide-oxidizing bacteria as microbial oxidants for rapid biological sulfide removal. Fems Microbiology Ecology **67**: 151-161.

Des Marais JD, Strauss H, Summons RE & Hayes JM (**1992**) Carbon isotope evidence for the stepwise oxidation of the proterozoic environment. Nature **359**: 605-609.

Des Marais DJ (**2000**) Evolution. When did photosynthesis emerge on Earth? Science **289**: 1703-1705.

Donlon BA, Razoflores E, Field JA & Lettinga G (**1995**) Toxicity of N-substituted aromatics to acetoclastic methanogenic activity in granular sludge. Applied and Environmental Microbiology **61**: 3889-3893.

Dupraz C, Reid RP, Braissant O, Decho AW, Norman RS & Visscher PT (**2009**) Processes of carbonate precipitation in modern microbial mats. Earth-Science Reviews **96**: 141-162.

E

Edwards KJ, Bond PL, Gihring TM & Banfield JF (**2000**) An archaeal iron-oxidizing extreme acidophile important in acid mine drainage. Science **287**: 1796-1799.

Edwards KJ, Rogers DR, Wirsen CO & McCollom TM (**2003**) Isolation and characterization of novel psychrophilic, neutrophilic, Fe-oxidizing, chemolithoautotrophic *alpha-* and, *gamma-Proteobacteria* from the deep sea. Applied and Environmental Microbiology **69**: 2906-2913.

Ehrenreich A & Widdel F (**1994**) Anaerobic Oxidation of Ferrous Iron by Purple Bacteria, a New-Type of Phototrophic Metabolism. Applied and Environmental Microbiology **60**: 4517-4526.

Ehrlich HL & Newman DK (**2009**) Geomicrobiology. CRC Press, NW.

Eigenbrode JL, Freeman KH & Summons RE (**2008**) Methylohopane biomarker hydrocarbons in Hamersley Province sediments provide evidence for Neoarchean aerobiosis. Earth and Planetary Science Letters **273**: 323-331.

El Albani A, Bengtson S, Canfield DE, et al. (**2010**) Large colonial organisms with coordinated growth in oxygenated environments 2.1 Gyr ago. Nature **466**: 100-104.

Emerson D & Moyer C (**1997**) Isolation and characterization of novel iron-oxidizing bacteria that grow at circumneutral pH. Applied and Environmental Microbiology **63**: 4784-4792.

Emerson D (**2000**) Microbial oxidation of Fe(II) and Mn(II) at circumneutral pH. Environmental metal-microbe interactions,(Lovley, ed.), p. 32-52. ASM press, Washington DC.

Erickson BE & Helz GR (**2000**) Molybdenum (IV) speciation in sulfidic waters: stability and lability of thiomolybdates. Geochimica Cosmochimica Acta **64**: 1149-1158.

Ettwig KF, Butler MK, Le Paslier D, et al. (**2010**) Nitrite-driven anaerobic methane oxidation by oxygenic bacteria. Nature **464**: 543-548.

F

Farquhar J, Wu N, Canfield DE & Oduro H (**2010**) Connections between sulfur cycle evolution, sulfur isotopes, sediments, and base metal sulfide deposits. Economic Geology **105**: 509-533.

Fedo CM, Whitehouse MJ & Kamber BS (**2006**) Geological constraints on detecting the earliest life on Earth: a perspective from the Early Archaean (older than 3.7 Gyr) of southwest Greenland. Philosophical Transactions of the Royal Society B-Biological Sciences **361**: 851-867.

Ferree MA & Shannon RD (**2001**) Evaluation of a second derivative UV/visible spectroscopy technique for nitrate and total nitrogen analysis of wastewater samples. Water Research **35**: 327-332.

Finneran KT, Forbush HM, VanPraagh CVG & Lovley DR (**2002**) Desulfitobacterium metallireducens sp nov., an anaerobic bacterium that couples growth to the reduction of metals and humic acids as well as chlorinated compounds. International Journal of Systematic and Evolutionary Microbiology **52**: 1929-1935.

Francois LM (**1986**) Extensive deposition of banded iron formation was possible without photosynthesis. Nature **320**: 352-354.

G

Garcia-Gil LJ, Borrego C, Hugas L, Casamitjana X & Abella CA (**1988**) Horizontal distribution of phototrophic bacterial population in an irregularly-shapped meromictic basin of Banyoles Lake (Banyoles, Spain). Scientia Gerundensis **14**: 71-79.

Garvin J, Buick R, Anbar AD, Arnold GL & Kaufman AJ (**2009**) Isotopic Evidence for an Aerobic Nitrogen Cycle in the Latest Archean. Science **323**: 1045-1048.

Godfrey LV & Falkowski PG (**2009**) The cycling and redox state of nitrogen in the Archaean ocean. Nature Geoscience **2**: 725-729.

Gold T (**1992**) The deep, hot biosphere. Proceedings of the National Academy of Sciences of the United States of America **89**: 6045-6049.

Grote J, Jost G, Labrenz M, Herndl GJ & Juergens K (**2008**) Epsilonproteobacteria Represent the Major Portion of Chemoautotrophic Bacteria in Sulfidic Waters of Pelagic Redoxclines of the Baltic and Black Seas. Applied and Environmental Microbiology **74**: 7546-7551.

H

Habicht KS, Gade M, Thamdrup B, Berg P & Canfield DE (**2002**) Calibration of sulfate levels in the Archean Ocean. Science **298**: 2372-2374.

Hadas O, Pinkas R & Erez J (**2001**) High chemoautotrophic primary production in Lake Kinneret, Israel: A neglected link in the carbon cycle of the lake. Limnology and Oceanography **46**: 1968-1976.

Hafenbradl D, Keller M, Dirmeier R, et al. (**1996**) Ferroglobus placidus gen nov, sp nov, a novel hyperthermophilic archaeum that oxidizes Fe2+ at neutral pH under anoxic conditions. Archives of Microbiology **166**: 308-314.

Haller L, Tonolla M, Zopfi J, Peduzzi R, Wild W & Pote J (**2011**) Composition of bacterial and archaeal communities in freshwater sediments with different contamination levels (Lake Geneva, Switzerland). water research **45**: 1213-1228.

Hamade T, Konhauser KO, Raiswell R, Goldsmith S & Morris RC (**2003**) Using Ge/Si ratios to decouple iron and silica fluxes in Precambrian banded iron formations. Geology **31**: 35-38.

Hanselmann K & Hutter R (**1998**) Geomicrobiological coupling of sulfur and iron cycling in anoxic sediments of a meromictic lake: sulfate reduction and sulfide sources and sinks in Lake Cadagno. Documenta Ist. ital. Idrobiol., Vol. **63** (Peduzzi R, Bachofen R & Tonolla M, eds.), p.85-98

Harrison TM, Schmitt AK, McCulloch MT & Lovera OM (**2008**) Early (>= 4.5 Ga) formation of terrestrial crust: Lu-Hf, delta O-18, and Ti thermometry results for Hadean zircons. Earth and Planetary Science Letters **268**: 476-486.

Hauck S, Benz M, Brune A & Schink B (**2001**) Ferrous iron oxidation by denitrifying bacteria in profundal sediments of a deep lake (Lake Constance). Fems Microbiology Ecology **37**: 127-134.

Hegler F, Posth NR, Jiang J & Kappler A (**2008**) Physiology of phototrophic iron(II)-oxidizing bacteria: implications for modern and ancient environments. FEMS Microbiology Ecology **66**: 250-260.

Heising S & Schink B (**1998**) Phototrophic oxidation of ferrous iron by a *Rhodomicrobium vannielii strain*. Microbiology-Uk **144**: 2263-2269.

Heising S, Richter L, Ludwig W & Schink B (**1999**) *Chlorobium ferrooxidans* sp. nov., a phototrophic green sulfur bacterium that oxidizes ferrous iron in coculture with a "*Geospirillum*" sp. strain. Arch Microbiol **172**: 116-124.

Holland HD (**1973**) Oceans - Possible Source of Iron in Iron-Formations. Economic Geology **68**: 1169-1172.

Holland HD (**1984**) The chemical evolution of the atmosphere and oceans Princeton University Press, Princeton, N.J.

Holland HD (**2006**) The oxygenation of the atmosphere and oceans. Philosophical Transactions of the Royal Society B-Biological Sciences **361**: 903-915.

Hongve D (**1999**) Long-term variation in the stability of the meromictic lake Nordbytjernet caused by groundwater fluctuations. Nordic Hydrology **30**: 21-38.

Hongve D (**2003**) Chemical stratigraphy of recent sediments from a depth gradient in a meromictic lake, Nordbytjernet, SE Norway, in relation to variable external loading and sedimentary fluxes. Journal of Paleolimnology **30**: 75-93.

Hren MT, Tice MM & Chamberlain CP (**2009**) Oxygen and hydrogen isotope evidence for a temperate climate 3.42 billion years ago. Nature **462**: 205-208.

J

Jiao Y, Kappler A, Croal LR & Newman DK (**2005**) Isolation and characterization of a genetically tractable photoautotrophic Fe(II)-oxidizing bacterium, *Rhodopseudomonas palustris* strain TIE-1. Applied and Environmental Microbiology **71**: 4487-4496.

Jiao Y & Newman DK (**2007**) The pio operon is essential for phototrophic Fe(II) oxidation in *Rhodopseudomonas palustris* TIE-1. Journal of Bacteriology **189**: 1765-1773.

Jobb G, Haeseler A & Strimmer K (**2004**) TREEFINDER: A powerful graphical analysis environment for molecular phylogenetics. *BMC Evol. Biol.* **4**, 18.

Johnson DB (**1998**) Biodiversity and ecology of acidophilic microorganisms. Fems Microbiology Ecology **27**: 307-317.

Johnson KJ, Ams DA, Wedel AN, Szymanowski JES, Weber DL, Schneegurt MA & Fein JB (**2007**) The impact of metabolic state on Cd adsorption onto bacterial cells. Geobiology **5**: 211-218.

Johnston DT, Wolfe-Simon F, Pearson A & Knoll AH (**2009**) Anoxygenic photosynthesis modulated Proterozoic oxygen and sustained Earth's middle age. Proceedings of the National Academy of Sciences of the United States of America **106**: 16925-16929.

Jones JG (**1983**) A note on the isolation and enumeration of bacteria which deposit and reduce ferric iron. Journal of Applied Bacteriology **54**: 305-310.

Julia R, Burjachs F, Dasi MJ, et al. (**1998**) Meromixis origin and recent trophic evolution in the Spanish mountain lake La Cruz. Aquatic Sciences **60**: 279-299.

K

Kappler A & Newman DK (**2004**) Formation of Fe(III)-minerals by Fe(II)-oxidizing photoautotrophic bacteria. Geochimica et Cosmochimica Acta **68**: 1217-1226.

Kappler A, Pasquero C, Konhauser KO & Newman DK (**2005**[1]) Deposition of banded iron formations by anoxygenic phototrophic Fe(II)-oxidizing bacteria. Geology **33**: 865-868.

Kappler A, Schink B & Newman DK (**2005**[2]) Fe(III) mineral formation and cell encrustation by the nitrate-dependent Fe(II)-oxidizer strain BoFeN1. Geobiology **3**: 235-245.

Kappler A, Posth NR, Hegler F & Koehler I (**2008**) Constraining the role of anoxygenic phototrophic Fe(II)-oxidizing bacteria in the deposition of Banded Iron Formations. Geochimica et Cosmochimica Acta **72**: A450.

Kashefi K & Lovley DR (**2000**) Reduction of Fe(III), Mn(IV), and toxic metals at 100 degrees C by *Pyrobaculum islandicum*. Applied and Environmental Microbiology **66**: 1050-1056.

Kasting JF (**2001**) Earth history - The rise of atmospheric oxygen. Science **293**: 819-820.

Kaufman AJ, Johnston DT, Farquhar J, et al. (**2007**) Late Archean biospheric oxygenation and atmospheric evolution. Science **317**: 1900-1903.

Kendall B, Reinhard CT, Lyons TW, Kaufman AJ, Poulton SW & Anbar AD (**2010**) Pervasive oxygenation along late Archean margins. Nature Geoscience **3**: 647-652.

Kjensmo J (**1967**) The development and some main features of "iron-meromictic" soft water lakes. Archiv für Hydrobiologie Supplement XXXII **2**: 137-313.

Klein C (**2005**) Some Precambrian banded iron-formations (BIFs) from around the world: Their age, geologic setting, mineralogy, metamorphism, geochemistry, and origin. American Mineralogist **90**: 1473-1499.

Kluber HD & Conrad R (**1998**) Effects of nitrate, nitrite, NO and N2O on methanogenesis and other redox processes in anoxic rice field soil. Fems Microbiology Ecology **25**: 301-318.

Knoll AH (**2003**) The geological consequences of evolution. Geobiology **1**: 3-14.

Knowles R (**1982**) Denitrification. Microbiological Reviews **46**: 43-70.

Konhauser KO, Hamade T, Raiswell R, Morris RC, Ferris FG, Southam G & Canfield DE (**2002**) Could bacteria have formed the Precambrian banded iron formations? Geology; **30**: 1079-1082.

Konhauser KO, Newman DK & Kappler A (**2005**) The potential significance of microbial Fe(III) reduction during deposition of Precambrian banded iron formations. Geobiology **3**: 167-177.

Konhauser KO, Amskold L, Lalonde SV, Posth NR, Kappler A & Anbar A (**2007**[1]) Decoupling photochemical Fe(II) oxidation from shallow-water BIF deposition. Earth and Planetary Science Letters **258**: 87-100.

Konhauser KO, Lalonde SV, Amskold L & Holland HD (**2007**[2]) Was there really an Archean phosphate crisis? Science **315**: 1234-1234.

Konhauser KO, Pecoits E, Lalonde SV, et al. (**2009**) Oceanic nickel depletion and a methanogen famine before the Great Oxidation Event. Nature **458**: 750-U785.

Kostka JE, Stucki JW, Nealson KH & Wu J (**1996**) Reduction of structural Fe(III) in smectite by a pure culture of *Shewanella putrefaciens* strain MR-1. Clays and Clay Minerals **44**: 522-529.

Kucera S & Wolfe RS (**1957**) A selective enrichement method for *Gallionelle ferruginea*. Journal of Bacteriology **74**: 344-349.

Kump LR & Seyfried WE (**2005**) Hydrothermal Fe fluxes during the Precambrian: Effect of low oceanic sulfate concentrations and low hydrostatic pressure on the composition of black smokers. Earth and Planetary Science Letters **235**: 654-662.

Kump LR (**2008**) The rise of atmospheric oxygen. Nature **451**: 277-278.

Küsel K, Dorsch T, Acker G & Stackebrandt E (**1999**) Microbial reduction of Fe(III) in acidic sediments: Isolation of *Acidiphilium cryptum* JF-5 capable of coupling the reduction of Fe(III) to the oxidation of glucose. Applied and Environmental Microbiology **65**: 3633-3640.

L

Lack JG, Chaudhuri SK, Chakraborty R, Achenbach LA & Coates JD (**2002**) Anaerobic biooxidation of Fe(II) by *Dechlorosoma suillum*. Microbial Ecology **43**: 424-431.

Lehours AC, Bardot C, Thenot A, Debroas D & Fonty G (**2005**) Anaerobic microbial communities in Lake Pavin, a unique meromictic lake in France. Applied and Environmental Microbiology **71**: 7389-7400.

Lehours AC, Evans P, Bardot C, Joblin K & Gerard F (**2007**) Phylogenetic diversity of archaea and bacteria in the anoxic zone of a meromictic lake (Lake Pavin, France). Applied and Environmental Microbiology **73**: 2016-2019.

Logan GA, Hayes JM, Hieshima GB & Summons RE (**1995**) Terminal Proterozoic reorganization of biogeochemical cycles. Nature **376**: 53-56.

Lovley DR & Phillips EJP (**1987**) Competitive mechanisms for inhibition of sulfate reduction and methane production in the zone of ferric iron reduction in sediments. Applied and Environmental Microbiology **53**: 2636-2641.

Lovley DR & Phillips EJP (**1994**) Novel processes for anaerobic sulfate production from elemental sulfur by sulfate-reducing bacteria. Applied and Environmental Microbiology **60**: 2394-2399.

Lovley DR (**2000**) Fe(III) and Mn(IV) reduction. Environmental metal-microbe interactions,(Lovley, ed.), p. 3-30. ASM press, Washington DC.

Lovley DR (**2004**) Potential role of dissimilatory iron reduction in the early evolution of microbial respiration. Origins, evolution, and biodiversity of microbial life,(Seckbach, ed.), pp. 301-313. Kluwer, Amsterdam.

Lovley DR, Holmes DE & Nevin KP (**2004**) Dissimilatory Fe(III) and Mn(IV) reduction. Advances in Microbial Physiology, Vol. **49** (Poole RK, ed.), p. 219-286. Academic Press Ltd.

Lunine JI (**1999**) Earth: Evolution of a habitable world. Cambridge University Press, New York.

Lyons TW, Anbar AD, Severmann S, Scott C & Gill BC (**2009**[1]) Tracking Euxinia in the Ancient Ocean: A Multiproxy Perspective and Proterozoic Case Study. Annual Review of Earth and Planetary Sciences **37**: 507-534.

Lyons TW, Reinhard CT & Scott C (**2009**[2]) Redox Redux. Geobiology **7**: 489-494.

M

Ma SF, Noble A, Butcher D, Trouwborst RE & Luther GW (**2006**) Removal of H2S via an iron catalytic cycle and iron sulfide precipitation in the water column of dead end tributaries. Estuarine Coastal and Shelf Science **70**: 461-472.

McCarty GW (1999) Modes of action of nitrification inhibitors. Biology and Fertility of Soils 29: 1-9.

MacCullagh P & Nelder JA (**1989**) Generalized linear models. Chapman & Hall, London.

"MacGrady Table" (1918) http://www2.ac-lyon.fr/enseigne/biotech/macgrady.htm

Mancinelli RL & McKay CP (**1988**) The evolution of nitrogen cycling. Origins of Life and Evolution of the Biosphere **18**: 311-325.

Manske AK, Glaeser J, Kuypers MM & Overmann J (**2005**) Physiology and phylogeny of green sulfur bacteria forming a monospecific phototrophic assemblage at a depth of 100 meters in the Black Sea. Appl Environ Microbiol **71**: 8049-8060.

Marshall D & Anglin CD (**2004**) CO2-clathrate destabilization: a new model of formation for molar tooth structures. Precambrian Research **129**: 325-341.

Martin JM (**1985**) The Pavin crater lake. Chemical processes in lakes,(Stumm W, ed.), p. 169-188. Wiley, New York, N.Y.

Meyer KM & Kump LR (**2008**) Oceanic euxinia in Earth history: Causes and consequences. Annual Review of Earth and Planetary Sciences **36**: 251-288.

Miot J, Benzerara K, Morin G, et al. (**2009**) Iron biomineralization by anaerobic neutrophilic iron-oxidizing bacteria. Geochimica et Cosmochimica Acta **73**: 696-711.

Miracle MR, Vicente E, et al. (**1992**) Biological studies in Spanish meromictic and karstic lakes. Limnetica **8**: 59-77.

Miracle MR, Camacho A, Julia R & Vicente E (**2001**) Sinking processes and their effect on the sedimentary record in the meromictic Lake La Cruz (Spain). International Association of Theoretical and Applied Limnology, Vol 27, Pt 3, Proceedings **27**: 1209-1213.

Mojzsis SJ, Arrhenius G, McKeegan KD, Harrison TM, Nutman AP & Friend CRL (**1996**) Evidence for life on Earth before 3,800 million years ago. Nature **384**: 55-59.

Mojzsis SJ, Harrison TM & Pidgeon RT (**2001**) Oxygen-isotope evidence from ancient zircons for liquid water at the Earth's surface 4,300 Myr ago. Nature **409**: 178-181.

Moorbath S, Taylor PN & Jones NW (**1986**) Dating the oldest terrestrial rocks - Fact and fiction. Chemical Geology **57**: 63-86.

Morford JL & Emerson SR (1999) The geochemistry of redox sensitive trace metals in sediments. Geochimica Cosmochimica Acta 63: 1735-1750.

Morford JL, Emerson SR, Breckel EJ & Kim SH (**2005**) Diagenesis of oxyanions (V, U, Re and Mo) in pore waters and sediments from a continental margin. Geochimica Cosmochimica Acta **69**: 5021-5032.

Muehe EM, Gerhardt S, Schink B & Kappler A (**2009**) Ecophysiology and the energetic benefit of mixotrophicFe(II) oxidation by various strains of nitrate-reducing bacteria. Fems Microbiology Ecology **70**: 335-343.

Muyzer G, Teske A, Wirsen CO & Jannasch HW (**1995**) Phylogenetic relationships of Thiomicrospira species and their identification in deep-sea hydrothermal vent samples by denaturing gradient gel-electrophoresis of 16S rDNA. Archives of Microbiology **164**: 165-172.

N

Navarro-Gonzalez R, McKay CP & Mvondo DN (**2001**) A possible nitrogen crisis for Archaean life due to reduced nitrogen fixation by lightning. Nature **412**: 61-64.

Nelson NB, Carlson CA & Steinberg DK (**2004**) Production of chromophoric dissolved organic matter by Sargasso Sea microbes. Marine Chemistry **89**: 273-287.

Neubauer SC, Emerson D & Megonigal JP (**2002**) Life at the energetic edge: Kinetics of circumneutral iron oxidation by lithotrophic iron-oxidizing bacteria isolated from the wetland-plant rhizosphere. Applied and Environmental Microbiology **68**: 3988-3995.

Nevin KP & Lovley DR (**2000**) Lack of production of electron-shuttling compounds or solubilization of Fe(III) during reduction of insoluble Fe(III) oxide by *Geobacter metallireducens*. Applied and Environmental Microbiology **66**: 2248-2251.

Nevin KP & Lovley DR (**2000**[2]) Potential for nonenzymatic reduction of Fe(III) via electron shuttling in subsurface sediments. Environmental Science & Technology **34**: 2472-2478.

Nielsen JL & Nielsen PH (**1998**) Microbial nitrate-dependent oxidation of ferrous iron in activated sludge. Environmental Science & Technology **32**: 3556-3561.

Nisbet EG & Sleep NH (**2001**) The habitat and nature of early life. Nature **409**: 1083-1091.

Nisbet E, Zahnle K, Gerasimov MV, et al. (**2007**[1]) Creating habitable zones, at all scales, from planets to mud micro-habitats, on earth and on mars. Space Science Reviews **129**: 79-121.

Nisbet EG, Grassineau NV, Howe CJ, Abell PI, Regelous M & Nisbet RER (**2007**) The age of Rubisco: the evolution of oxygenic photosynthesis. Geobiology **5**: 311-335.

Nutman AP & Friend CRL (**2006**) Petrography and geochemistry of apatites in banded iron formation, Akilia, W. Greenland: Consequences for oldest life evidence. Precambrian Research **147**: 100-106.

O

Olson JM (**2006**) Photosynthesis in the Archean Era. Photosynthesis Research **88**: 109-117.

Ohmoto H, Runnegar B, Kump LR, et al. (**2008**) Biosignatures in ancient rocks: a summary of discussions at a field workshop on biosignatures in ancient rocks. Astrobiology **8**: 883-895.

Orem WH, Burnett WC, Landing WM, Lyons WB & Showers W (**1991**) Jellyfish Lake, Palau - early diagenesis of organic-matter in sediments of an anoxic marine lake. Limnology and Oceanography **36**: 526-543.

Overmann J, Beatty JT, Krouse HR & Hall KJ (**1996**) The sulfur cycle in the chemocline of a meromictic salt lake. Limnology and Oceanography **41**: 147-156.

P

Paul C (**2011**) Cycle biogéochimique du fer et suivi saisonnier des communautés bactériennes dans le lac du Loclat. Thesis, Neuchâtel, Neuchâtel.

Park W, Nam YK, Lee MJ & Kim TH (**2009**) Anaerobic ammonia-oxidation coupled with Fe^{3+} reduction by an anaerobic culture from a piggery wastewater acclimated to NH_4^+/Fe^{3+} medium. Biotechnology and Bioprocess Engineering **14**: 680-685.

Peine A, Tritschler A, Kusel K & Peiffer S (**2000**) Electron flow in an iron-rich acidic sediment - evidence for an acidity-driven iron cycle. Limnology and Oceanography **45**: 1077-1087.

Picazo-Mozo A, Miracle RM, Vicente E & Camacho A (**2011**, *in prep.*) *Title not yet fixed*.

Pickard AL, Barley ME & Krapez B (**2004**) Deep-marine depositional setting of banded iron formation: sedimentological evidence from interbedded clastic sedimentary rocks in the early Palaeoproterozoic Dales Gorge Member of Western Australia. Sedimentary Geology **170**: 37-62.

Pierson BK (**1994**) The emergence, diversification, and role of photosynthetic eubacteria. Early Life on Earth,(Bengtson S, ed.), p.161-180. Columbia University Press, New York

Pierson BK, Parenteau MN & Griffin BM (**1999**) Phototrophs in high-iron-concentration microbial mats: physiological ecology of phototrophs in an iron-depositing hot spring. Appl Environ Microbiol **65**: 5474-5483.

Posth NR, Hegler F, Konhauser KO & Kappler A (**2008**) Alternating Si and Fe deposition caused by temperature fluctuations in Precambrian oceans. Nature Geoscience **1**: 703-708.

Poulton SW, Fralick PW & Canfield DE (**2004**) The transition to a sulphidic ocean similar to 1.84 billion years ago. Nature **431**: 173-177.

Pringault O & Garcia-Pichel F (2000) Monitoring of oxygenic and anoxygenic photosynthesis in a unicyanobacterial biofilm, grown in benthic gradient chamber. Fems Microbiology Ecology 33: 251-258.

Pronk JT & Johnson DB (**1992**) Oxidation and reduction of iron by acidophilic bacteria. Geomicrobiology Journal **10**: 153-171.

Pronk M, Goldscheider N & Zopfi J (**2009**) Microbial communities in karst groundwater and their potential use for biomonitoring. Hydrogeology Journal **17**: 37-48.

R

Raymond J, Zhaxybayeva O, Gogarten JP & Blankenship RE (**2003**) Evolution of photosynthetic prokaryotes: a maximum-likelihood mapping approach. Philosophical Transactions of the Royal Society of London Series B-Biological Sciences **358**: 223-230.

R Development Core Team (**2009**) R: a language and environment for statistical computing. R Foundation for Statistical Computing.

Ratering S & Schnell S (**2001**) Nitrate-dependent iron(II) oxidation in paddy soil. Environmental Microbiology **3**: 100-109.

Raghoebarsing AA, Pol A, van de Pas-Schoonen KT, et al. (**2006**) A microbial consortium couples anaerobic methane oxidation to denitrification. Nature **440**: 918-921.

Reinhard C, Raiswell R, Scott C, Anbar AD & Lyons TW (**2009**) A Late Archean sulfidic sea stimulated by early oxidative weathering of the continents. Science **326**: 713-716.

Repeta DJ, Simpson DJ, Jorgensen BB & Jannasch HW (**1989**) Evidence for anoxygenic photosynthesis from the distribution of bacteriochlorophylls in the Black Sea. Nature **342**: 69-72.

Roden EE & Urrutia MM (**2002**) Influence of Biogenic Fe(II) on Bacterial Crystalline Fe(III) Oxide Reduction. Geomicrobiology Journal **19**: 209-251.

Roden EE, Sobolev D, Glazer B & Luther GW (**2004**[1]) Potential for microscale bacterial Fe redox cycling at the aerobic-anaerobic interface. Geomicrobiology Journal **21**: 379-391.

Roden EE, Sobolev D, Glazer B & Luther GW (**2004**[2]) New insights into the biogeochemical cycling of iron in circumneutral sedimentary environments: potential for a rapid microscale bacterial Fe redox cycle at the aerobic-anaerobic interface. Iron in the Natural Environment: Biogeochemistry, Microbial Diversity, and Bioremediation (Coates JD & Zhang C, eds.) kluwer

Roden EE (**2006**) Geochemical and microbiological controls on dissimilatory iron reduction. Comptes Rendus Geoscience **338**: 456-467.

Rodrigo MA, Vicente A & Miracle MR (**1993**) Short-term calcite precipitation in the meromictic Lake La Cruz (Cuenca, Spain). Verh. Internat. Verain. Limnol. **25**: 711-719.

Rodrigo MA, Camacho A, Vicente E & Miracle MR (**1999**) Microstratified vertical distribution and migration of phototrophic microorganisms during a diel cycle in Lake Arcas-2 (Spain). Archiv Fur Hydrobiologie **145**: 497-512.

Rodrigo MA, Vicente E & Miracle MR (**2000**) The role of light and concentration gradients in the vertical stratification and seasonal development of phototrophic bacteria in a meromictic lake. Archiv Fur Hydrobiologie **148**: 533-548.

Rodrigo MA, Miracle MR & Vicente E (**2001**) The meromictic Lake La Cruz (Central Spain). Patterns of stratification. Aquatic Sciences **63**: 406-416.

Romero L, Camacho A, Vicente E & Miracle MR (**2006**) Sedimentation patterns of photosynthetic bacteria based on pigment markers in meromictic Lake La Cruz (Spain): paleolimnological implications. Journal of Paleolimnology **35**: 167-177.

Romero-Viana L, Keely BJ, Camacho A, Vicente E & Miracle MR (**2010**) Primary production in Lake La Cruz (Spain) over the last four centuries: reconstruction based on sedimentary signal of photosynthetic pigments. Journal of Paleolimnology **43**: 771-786.

Rothschild LJ (**2009**) Earth science - Life battered but unbowed. Nature **459**: 335-336.

Rozan TF, Taillefert M, Trouwborst RE, et al. (**2002**) Iron-sulfur-phosphorus cycling in the sediments of a shallow coastal bay: Implications for sediment nutrient release and benthic macroalgal blooms. Limnology and Oceanography **47**: 1346-1354.

Russell MJ & Hall AJ (**1997**) The emergence of life from iron monosulphide bubbles at a submarine hydrothermal redox and pH front. Journal of the Geological Society **154**: 377-402.

S

Sahrawat KL (**2004**) Nitrification inhibitors for controlling methane emission from submerged rice soils. Current Science **87**: 1084-1087.

Schadler S, Burkhardt C, Hegler F, Straub KL, Miot J, Benzerara K & Kappler A (**2009**) Formation of Cell-Iron-Mineral Aggregates by Phototrophic and Nitrate-Reducing Anaerobic Fe(II)-Oxidizing Bacteria. Geomicrobiology Journal **26**: 93-103.

Schanz F, Fischer-Romero C & Bachofen R (**1998**) Photosynthetic production and photoadaptation of phototrophic sulfur bacteria in Lake Cadagno (Switzerland). Limnology and Oceanography **43**: 1262-1269.

Schidlowski M, Hayes JM & Kaplan IR (**1983**) Isotopic inferences of ancient biochemistry: carbon, sulfur, hydrogen, and nitrogen. Earth's early biosphere, its origin and evolution,(Schopf JW, ed.), pp. 149-186. Priceton University Press, Princeton.

Schippers A & Jorgensen BB (**2002**) Biogeochemistry of pyrite and iron sulfide oxidation in marine sediments. Geochimica et Cosmochimica Acta **66**: 85-92.

Schwartzman D, Caldeira K & Pavlov A (**2008**) Cyanobacterial emergence at 2.8 gya and greenhouse feedbacks. Astrobiology **8**: 187-203.

Schweizer C & Aragno M (**1975**) Etudes des hydrogénobactéries dans un petit lac (le Loclat, ou Lac de Saint-Blaise). Bulletin de la Société des sciences naturelles de Neuchâtel **98**: 79-87.

Severmann S, Lyons TW, Anbar A, McManus J & Gordon G (**2008**) Modern iron isotope perspective on the benthic iron shuttle and the redox evolution of ancient ocean. Geology **36**: 487-490.

Severmann S & Anbar AD (**2009**) Reconstructing Paleoredox Conditions through a Multitracer Approach: The Key to the Past Is the Present. Elements **5**: 359-364.

Shelobolina ES, Vanpraagh CG & Lovley DR (**2003**) Use of ferric and ferrous iron containing minerals for respiration by *Desulfitobacterium frappieri*. Geomicrobiology Journal **20**: 143-156.

Shen Y, Bulck R & Canfield DE (**2001**) Isotopic evidence for microbial sulphate reduction in the early Archaean era. Nature **410**: 77-81.

Shen Y, Knoll AH & Walter MR (**2003**) Evidence for low sulphate and anoxia in a mid-Proterozoic marine basin. Nature **423**: 632-635.

Shrestha J, Rich JJ, Ehrenfeld JG & Jaffe PR (**2009**) Oxidation of Ammonium to Nitrite Under Iron-Reducing Conditions in Wetland Soils Laboratory, Field Demonstrations, and Push-Pull Rate Determination. Soil Science **174**: 156-164.

Sleep NH & Bird DK (**2008**) Evolutionary ecology during the rise of dioxygen in the Earth's atmosphere. philosophical Transactions of the Royal Society B **363**: 2651-2664.

Sobolev D & Roden EE (**2002**) Evidence for rapid microscale bacterial redox cycling of iron in circumneutral environments. Antonie Van Leeuwenhoek International Journal of General and Molecular Microbiology **81**: 587-597.

Steenmann Nielsen E (**1952**) The use of radioactive carbon (C^{14}) for measuring organic production in the sea. J. du Cons. Internat. Explor. Mer **18**: 117-140.

Stolz JF, Lovley DR & Haggerty SE (**1990**) Biogenic magnetite and the magnetization of sediments. Journal of Geophysical Research-Solid Earth and Planets **95**: 4355-4361.

Straub KL, Benz M, Schink B & Widdel F (**1996**) Anaerobic, nitrate-dependent microbial oxidation of ferrous iron. Applied and Environmental Microbiology **62**: 1458-1460.

Straub KL & Buchholz-Cleven BEE (**1998**) Enumeration and detection of anaerobic ferrous iron-oxidizing, nitrate-reducing bacteria from diverse European sediments. Applied and Environmental Microbiology **64**: 4846-4856.

Straub KL, Benz M & Schink B (**2001**) Iron metabolism in anoxic environments at near neutral pH. Fems Microbiology Ecology **34**: 181-186.

Straub KL, Schonhuber WA, Buchholz-Cleven BEE & Schink B (**2004**) Diversity of ferrous iron-oxidizing, nitrate-reducing bacteria and their involvement in oxygen-independent iron cycling. Geomicrobiology Journal **21**: 371-378.

Strous M & Jetten MSM (**2004**) Anaerobic oxidation of methane and ammonium. Annual Review of Microbiology **58**: 99-117.

Sundby B, Martinez P & Gobeil C (**2004**) Comparative geochemistry of cadmium, rhenium, uranium and molybdenum in continental margin sediments. Geochimica Cosmochimica Acta **68**: 2485-2493.

T

Taillefert M & Gaillard JF (**2002**) Reactive transport modeling of trace elements in the water column of a stratified lake: iron cycling and metal scavenging. Journal of Hydrology **256**: 16-34.

Tangalos GE, Beard BL, Johnson CM, et al. (**2010**) Microbial production of isotopically light iron(II) in a modern chemically precipitated sediment and implications for isotopic variations in ancient rocks. Geobiology **8**: 197-208.

Tera F, Papanast DA & Wasserbu GJ (**1974**) Isotopic evidence for a terminal lunar cataclysm. Earth and Planetary Science Letters **22**: 1-21.

Thamdrup B, Finster K, Hansen JW & Bak F (**1993**) Bacterial disproportionation of elemental sulfur coupled to chemical reduction of iron or manganese. Applied and Environmental Microbiology **59**: 101-108.

Thamdrup B (**2000**[1]) Bacterial manganese and iron reduction in aquatic sediments. Advances in Microbial Ecology, (Schink & Bernhard, Ed.), Vol **16** p. 41-84, Kluwer Academic & Plenum Publication, New York.

Thamdrup B, Rossello-Mora R & Amann R (**2000**[2]) Microbial manganese and sulfate reduction in Black Sea shelf sediments.

Applied and Environmental Microbiology **66**: 2888-2897.

Tice MM & Lowe DR (**2004**) Photosynthetic microbial mats in the 3,416-Myr-old ocean. Nature **431**: 549-552.

Tonolla M, Demarta A & Peduzzi R (**1998**) The chemistry of Lake Cadagno. Documenta dell'Istituto Italiano di Idrobiologia **63**: 11-17.

Tonolla M, Demarta A, Peduzzi R & Hahn D (**1999**) In situ analysis of phototrophic sulfur bacteria in the chemocline of meromictic Lake Cadagno (Switzerland). Applied and Environmental Microbiology **65**: 1325-1330.

Trendall AF & Blockley JG (**2002**) The significance of iron-formation in the Precambrian stratigraphic record. Int. Assoc. Sedimentol. Spec. Publ. **44**: 33-66.

V

Vargas M, Kashefi K, Blunt-Harris EL & Lovley DR (**1998**) Microbiological evidence for Fe(III) reduction on early Earth. Nature **395**: 65-67.

Vicente E & MR Miracle (**1988**) Physicochemical and microbial stratification in a meromictic karstic lake. Verh. Internat. Verein. Limnol. **23**: 522-529.

Viollier E, Inglett PW, Hunter K, Roychoudhury AN & Van Cappellen P (**2000**) The ferrozine method revisited: Fe(II)/Fe(III) determination in natural waters. Applied Geochemistry **15**: 785-790.

Visscher PT, Vandenende FP, Schaub BEM & Vangemerden H (**1992**) Competition between anoxygenic phototrophic bacteria and colorless sulfur bacteria in a microbial mat. Fems Microbiology Ecology **101**: 51-58.

Visscher PT, Dupraz C, Braissant O, Gallagher KL, Glunk C, Casillas L & Reed RES (**2010**) Biogeochemistry of carbon cycling in hypersaline mats: Linking the present to the past through biosignatures. Microbial mats: modern and ancient microorganisms in stratified systems,(Skeckbach J & Oren A, eds.), p. 445-468. Springer Verlag, Berlin.

Voegelin AR, Nagler TF, Beukes NJ & Lacassie JP (**2010**) Molybdenum isotopes in late Archean carbonate rocks: Implications for early Earth oxygenation. Precambrian Research **182**: 70-82.

W

Waldbauer JR, Sherman LS, Summner DY & Summons RE (**2009**) Late Archean molecular fossils from the Transvaal Supergroup records antiquity of microbial diversity and aerobiosis. Precambrian Research **169**: 28-47.

Weber KA, Picardal FW & Roden EE (**2001**) Microbially catalyzed nitrate-dependent oxidation of biogenic solid-phase Fe(II) compounds. Environmental Science & Technology **35**: 1644-1650.

Weber KA, Achenbach LA & Coates JD (**2006**[1]) Microorganisms pumping iron: anaerobic microbial iron oxidation and reduction. Nature Reviews Microbiology **4**: 752-764.

Weber KA, Pollock J, Cole KA, O'Connor SM, Achenbach LA & Coates JD (**2006**[2]) Anaerobic nitrate-dependent iron(II) bio-oxidation by a novel lithoautotrophic *betaproteobacterium*, strain 2002. Applied and Environmental Microbiology **72**: 686-694.

Weber KA, Urrutia MM, Churchill PF, Kukkadapu RK & Roden EE (**2006**[3]) Anaerobic redox cycling of iron by freshwater sediment microorganisms. Environmental Microbiology **8**: 100-113.

Wetzel RG (**2001**) Limnology: Lake and River Ecosystems, pp. 609-651, Academic Press, San Diego.

Whitehouse MJ, Myers JS & Fedo CM (**2009**) The Akilia Controversy: field, structural and geochronological evidence questions interpretations of > 3.8 Ga life in SW Greenland. Journal of the Geological Society **166**: 335-348.

Widdel F & Bak F (1992) Gram-negative mesophilic sulfate-reducing bacteria. The prokaryotes, Vol. vol. IV. (Balows A, Trüper HG, Dworkin M, Harder W & Schleifer K-H, eds.) Springer-Verlag, New York.

Widdel F, Schnell S, Heising S, Ehrenreich A, Assmus B & Schink B (**1993**) Ferrous iron oxidation by anoxygenic phototrophic bacteria. Nature 362: 834-836.

Wilde SA, Valley JW, Peck WH & Graham CM (**2001**) Evidence from detrital zircons for the existence of continental crust and oceans on the Earth 4.4 Gyr ago. Nature **409**: 175-178.

X

Xiong J, Fischer WM, Inoue K, Nakahara M & Bauer CE (**2000**) Molecular evidence for the early evolution of photosynthesis. Science **289**: 1724-1730.

Y

Yamashita Y, Takahashi Y, Haba H, Enomoto S & Shimizu H (**2007**) Comparison of reductive accumulation of Re and Os in seawater - sediment systems. Geochimica et Cosmochimica Acta **71**: 3458-3475.

Yung YL & Mcelroy MB (**1979**) Fixation of Nitrogen in the Prebiotic Atmosphere. Science **203**: 1002-1004.

Z

Zahnle K, Claire M & Catling D (**2006**) The loss of mass-independent fractionation in sulfur due to a Palaeoproterozoic collapse of atmospheric methane. Geobiology **4**: 271-283.

Zopfi J, Ferdelman TG, Jorgensen BB, Teske A & Thamdrup B (**2001**) Influence of water column dynamics on sulfide oxidation and other major biogeochemical processes in the chemocline of Mariager Fjord (Denmark). Marine Chemistry **74**: 29-51.

ANNEX I: Methods

I.1. Culture media for photoferrotrophs

	Stock solution			
Basal medium	$CaCl_2$ x 2 H_2O	1.25	g	**970.0 ml**
	KH_2PO_4	1.7	g	
	NH_4Cl	1.7	g	
	KCl	1.7	g	
	NaCl	1	g	
	$MgCl_2.6H_2O$	3.5	g	
	H2O: adjust to	4000	ml	

Trace elements	HCL (25% = 7.7 M)	12.5 ml	(100 mM)	**1.0 ml**
	$FeSO_4.7H_2O$	2100 mg	(7.5 mM)	
	H_3BO_3	30 mg	(0.5 mM)	
	$MnCl_2.4H_2O$	100 mg	(0.5 mM)	
	$CoCl_2.6H_2O$	190 mg	(0.8 mM)	
	$NiCl_2.6H_2O$	24 mg	(0.1 mM)	
	$CuCl_2.2H_2O$	2 mg	(0.01 mM)	
	$ZnSO_4.7H_2O$	144 mg	(0.5 mM)	
	$Na_2MoO_4.2H_2O$	36 mg	(0.15 mM)	
	H_2O: adjust to	1000 ml		

Tungstate / Selenite	NaOH	400 mg	(10 mM)	**1.0 ml**
	Na_2SeO_3	3.5 mg	(0.02 mM)	
	$Na_2WO_4.2H_2O$	8 mg	(0.02 mM)	
	H_2O: adjust to	1000 ml		

FILTER STERILIZE 0.2 µm ⬇

Vitamine B12	Vitamin B12 0.002%	2 mg		**5.0 ml**
	Water distilled	100 ml		

Bicarbonate	$NaHCO_3$	42 g	(1 M)	**30.0 ml**
	Water distilled	500 ml		

Fe(II) carbonate	Na_2CO_3	10.6 g		**10.0 ml**
	$FeSO_4$ x 7 H_2O	28 g		
	Water distilled	100 ml		

Acetate	$CH_3COONa.3H_2O$	13.6 g	(1 M)	**1.0 ml**
	Water distilled	100 ml		

I.2. Culture media for nitrate-dependant chemoferrotrophs

	Stock solution			
Basal medium	$CaCl_2$ x 2 H_2O	1.25	g	**970.0 ml**
	KH_2PO_4	1.7	g	
	NH_4Cl	1.7	g	
	KCl	1.7	g	
	NaCl	1	g	
	$MgCl_2.6H_2O$	3.5	g	
	H2O: adjust to	4000	ml	
Trace elements	HCL (25% = 7.7 M)	12.5 ml	(100 mM)	**1.0 ml**
	$FeSO_4.7H_2O$	2100 mg	(7.5 mM)	
	H_3BO_3	30 mg	(0.5 mM)	
	$MnCl_2.4H_2O$	100 mg	(0.5 mM)	
	$CoCl_2.6H_2O$	190 mg	(0.8 mM)	
	$NiCl_2.6H_2O$	24 mg	(0.1 mM)	
	$CuCl_2.2H_2O$	2 mg	(0.01 mM)	
	$ZnSO_4.7H_2O$	144 mg	(0.5 mM)	
	$Na_2MoO_4.2H_2O$	36 mg	(0.15 mM)	
	H_2O: adjust to	1000 ml		
Tungstate / Selenite	NaOH	400 mg	(10 mM)	**1.0 ml**
	$Na_2SeO_3.5H_2O$	6 mg	(0.02 mM)	
	$Na_2WO_4.2H_2O$	8 mg	(0.02 mM)	
	H_2O: adjust to	1000 ml		
Vitamine mix	4-aminobenzoïc acid	4 mg		**1.0 ml**
	D(+)-biotin	1 mg		
	Nicotinic acid	10 mg		
	Calcium D(+)-pentothenate	5 mg		
	Pyridoxine dihydrochloride	15 mg		
	Cyanocobalamine (B12)	5 mg		
	sodium phosphate buffer	100 ml	(pH7.1; 10mM)	
	FILTER STERILIZE 0.2 µm			
Thiamine solution	Thiamine chloride dihydrochloride	10 mg		**1.0 ml**
	sodium phosphate buffer	100 ml	(pH3.4 ; 25mM)	
Bicarbonate	$NaHCO_3$	42 g	(1 M)	**30.0 ml**
	Water distilled	500 ml		
Fe(II) carbonate	Na_2CO_3	10.6 g		**30.0 ml**
	$FeSO_4$ x 7 H_2O	28 g		
	Water distilled .	100 ml		
Acetate	$CH_3COONa.3H_2O$	13.60 g	(1 M)	**1.0 ml**
	Water distilled	100 ml		
Nitrate	$NaNO_3$	17.00 g	(1 M)	**4.0 ml**
	Water distilled	200 ml		

I.3. Culture media for Fe(III)-reducing bacteria

Defined Multipurpose Medium (Widdel and Bak, 1992)

	Stock solution			
Basal medium	$CaCl_2$ x 2 H_2O	0.4	g	**870.0 ml**
	KH_2PO_4	0.4	g	
	NH_4Cl	0.4	g	
	KCl	0.4	g	
	NaCl	1.0	g	
	$MgCl_2.6H_2O$	0.8	g	
	H2O: adjust to	4000	ml	
Trace elements	HCL (25% = 7.7 M)	12.5 ml	(100 mM)	**1.0 ml**
	$FeSO_4.7H_2O$	2100 mg	(7.5 mM)	
	H_3BO_3	30 mg	(0.5 mM)	
	$MnCl_2.4H_2O$	100 mg	(0.5 mM)	
	$CoCl_2.6H_2O$	190 mg	(0.8 mM)	
	$NiCl_2.6H_2O$	24 mg	(0.1 mM)	
	$CuCl_2.2H_2O$	2 mg	(0.01 mM)	
	$ZnSO_4.7H_2O$	144 mg	(0.5 mM)	
	$Na_2MoO_4.2H_2O$	36 mg	(0.15 mM)	
	H_2O: adjust to	1000 ml		
Tungstate / Selenite	NaOH	400 mg	(10 mM)	**1.0 ml**
	$Na_2SeO_3.5H_2O$	6 mg	(0.02 mM)	
	$Na_2WO_4.2H_2O$	8 mg	(0.02 mM)	
	H_2O: adjust to	1000 ml		
Vitamine mix	4-aminobenzoïc acid	4 mg		**1.0 ml**
	D(+)-biotin	1 mg		
	Nicotinic acid	10 mg		
	Calcium D(+)-pentothenate	5 mg		
	Pyridoxine dihydrochloride	15 mg		
	Cyanocobalamine (B12)	5 mg		
	sodium phosphate buffer	100 ml	(pH7.1; 10mM)	
	FILTER STERILIZE 0.2 µm			
Thiamine solution	Thiamine chloride dihydrochloride	10 mg		**1.0 ml**
	sodium phosphate buffer	100 ml	(pH3.4 ; 25mM)	
Bicarbonate	NaHCO3	42 g	(1 M)	**30.0 ml**
	Water distilled	500 ml		
Fe(III) oxides poorly crystalline	NaOH	10 g	(1 M)	**100.0 ml**
	$FeCl_3$	16.2 g	(0.5 M)	
	Water distilled .	100 ml		
Acetate	$CH_3COONa.3H_2O$	13.60 g	(2 M)	**5.0 ml**
	Water distilled	100 ml		

I.4. Fe analysis in freshwater and sediment samples

REACTIVE :

-Ferrozine solution with **100 mM** HEPES
-HCl **0.5 M**
-Hydroxylamine solution **1.5 M**
-Fe(II) stock solution **1 mM**
-Fe(III) stock solution **1 mM**

REACTIVE PREPARATION:

Ferrozine solution :

-Clean a **1 l** volumetric flask with HCl (**6 M**)
-Rinse with milliQ water
-Add 500 ml milliQ water
-Add **23.830 g** of HEPES (Mr = 238.31 g mol^{-1})
-Rinse glass walls with milliQ water
-Add **1 g** of ferrozine (Fluka, 82950)
-Adjust at **1l**
-Adjust at **pH 7** with a solution of NaOH

5 M HCl:

-Clean a **100 mL** volumetric flask with HCl (**6 M**)
-Rinse with milliQ water
-Add 500 ml milliQ water
-Add **41.55 ml** of HCL 37%
-Adjust at **100 ml**

1.5 M hydroxylamine:

-Clean a **250 ml** volumetric flask with HCl (**6 M**)
-Rinse with milliQ water
-Add 100 ml **0.25M** HCl
-Add **26.1 g** of hydroxylamine (Mr = 69.49 g mol^{-1})
-Rinse glass walls with **0.25M** HCl
-Adjust at **250 mL**

1 mM Fe(II) stock solution:

-Clean a **1 l** volumetric flask with HCl (**6 M**)
-Rinse with milliQ water
-Add 500 ml milliQ water
-Add **41.55 ml** of HCL 37%
-Add **392.14 mg** $FeH_8N_2S_2O_8.6H_2O$ (Mr=392.14 g mol^{-1})
-Adjust at **1l** with milliQ water

1 mM Fe(III) stock solution:

-Clean a **1 l** volumetric flask with HCl (**6 M**)
-Rinse with milliQ water
-Add 500 ml milliQ water
-Add **41.55 ml** of HCL 37%
-Add **526,80 mg** $FeH_4N_4S_2O_8.12H_2O$ (Mr = 526,80 g mol^{-1})
-Adjust at **1l** with milliQ water

SAMPLE PREPARATION:

Freshwater sample:

-Add **1 ml** 5 M HCl in a 12 ml tube
-Add 9 mL of sample
-Conserve away from light

Sediment sample:

-Weigh "approximately precisely" 0.3 g of sediment as fast as possible to avoid any Fe(II)-oxidation
-Add 5 mL 0.5 M HCl
-Agitate for a complete ionization of Fe(II)/Fe(III) during 30 min
-Centrifuge at 2800 rpm during 5 min
-Transfer supernatant in a new tube
-Conservation in the dark

SAMPLE ANALYSIS:

Fe(II) measurment :

-Take 100 µL sample
-Add 900 µL Ferrozine reactive
-Immediately (within 2 min) read absorbance at **562 nm**
-Attention prepare a blank:
Fe(II) = 100 µL 0.5 M HCl + 900 µL Ferrozine

Fe(III) measurment :

-Add 150 µL Hydroxylamine
-Take 100 µL sample
-Add 900 µL Ferrozine reactive
-Immediately (within 2 min) read absorbance at **562 nm**
-Attention prepare a blank:
Fe(III) = 100 µL 0.5 M HCl + 900 µL Ferrozine

-Stookey L.L. (1970). Ferrozine- A new spectrophotometric reagent for iron. Analytical Chemisrty, vol 42, 7 : 779-781
-Thamdrup B., Fossing H. and Jørgensen B.B. (1994). Manganèse, iron, and sulfur cycling in a coastal marine sediment, Aarhus Bay, Denmark. Geochimica et Cosmochimica Acta, vol 58, 23 : 5115-5129
-Viollier E, Inglett PW, Hunter K, Roychoudhury AN & Van Cappellen P (2000) The ferrozine method revisited: Fe(II)/Fe(III) determination in natural waters. *Applied Geochemistry* **15**: 785-790.

I.5. ^{14}C-bicarbonate incubations

Introduction

^{14}C-bicarbonate incubation is a common method used for primary production estimation (Steenmann Nielsen, 1952). It is based on the fact that ^{14}C-bicarbonate uptake by autotrophic organisms is proportional to the total dissolved inorganic carbon (DIC). Knowing the initial DIC, the ^{14}C-DIC added, the ^{14}C uptake and the metabolic discriminatory factor between ^{12}C-DIC and ^{14}C-DIC, we can calculate the total DIC uptaken by autotrophy:

C consumed = (DIC * ^{14}C-POC * 1.06)/(^{14}C-DIC added)

C consumed = total DIC fixed
DIC = dissolved inorganic carbon
^{14}C-POC (particulate organic carbon) = ^{14}C-DIC fixed in the biomass
^{14}C-DIC = ^{14}C-DIC added to the sample
1.06 = discriminatory factor between ^{12}C-DIC and ^{14}C-DIC

Here, the method was used, not for primary production measurement, but for anaerobic ferroautotrophy detection in the chemocline of a stratified water column. Two types of organisms were under investigation: (i) photoferrotrophic bacteria (IOP), anoxigenic phototrophs which oxidize Fe(II) and (ii) Fe(II)-oxidizing nitrate-dependent bacteria (NDIO), chemoautotrophic organisms which oxidize Fe(II) using nitrate as electrons acceptor.

The principle of the method is to take water samples from a precise layer of water column, where the target organisms are thought to be present. After the addition of different solutions containing Fe(II), NO_3^-, H_2S, DCMU and/or nitrapyrine (N-serve) (Tab. 9), the comparison of primary production rates in the different samples will enable to determine the impact of these elements on autotrophy. Thus, the presence or absence of ferroautotrophic organisms can be assessed. Simultaneous incubations of the different treatments at light and in the dark enable to differentiate between photoautotrophy and chemoautotrophy.

Table 9: The different solutions added, and their expected effects.

Added product	Purpose
Fe(II)	Electrons donor for ferrotrophs. Stimulation of ferroautotrophy.
NO_3^-	Electrons acceptor for NDIOs Stimulation of chemoautotrophy.
H_2S	Alternative electron donor. Stimulation of anaerobic photosynthesis.
DCMU	Photosystem II inhibitor. Inhibition of oxygenic photosynthesis.
N-Serve	Nitrification inhibitor. Inhibition of nitrate production in-vitro.

DCMU water saturated:

- Add 100 mg of DCMU to 50 ml anoxic MilliQ H_2O
- Let 24 h under agitation
- Filter-sterilize (0.2 µm)
- Flush the solution with N_2 for anoxia

Preparation of the stock solutions

Fe(II) 27.5 mM:

- Wash a 1 liter bottle with HCl ~6 M
- Rinse with H_2O MilliQ
- Add 5.4673 g of $FeCl_2$ to ~500 ml anoxic MilliQ H_2O
- Complete to 1 liter with anoxic MilliQ H_2O
- Filter-sterilize (0.2 µm)
- Keep anoxia by working under a N_2 atmosphere

H_2S 9.8 mM:

- Add 0.7648 g of Na_2S to 1 liter anoxic MilliQ H_2O
- Filter-sterilization while keeping anoxia (0.2 µm)

NO_3^- 2.2 mM:

- Add 0.1868 g of $NaNO_3$ to ~800 ml MilliQ H_2O
- Complete to 1 liter with MilliQ H_2O
- Filter-sterilize (0.2 µm)
- Flush the solution with N2 for anoxia

N-Serve 1.2 mM:

- Add 27.45 mg of N-Serve to 300 µl EthOOH 100%
- Complete to 100 ml with MilliQ H_2O
- Filter-sterilize (0.2 µm)
- Flush the solution with N_2 for anoxia

^{14}C-bicarbonate 20 µCi/ml:

- Order $NaH^{14}CO_3$ solution of 1 mCi ml^{-1} (DHI, 2970 Hørsholm)
- Dilute this solution (1/50) in Tris-buffer 10 mM pH 9
- Flush the solution with N_2 for anoxia

Sampling and treatments

Once the sampling depth were determined, on the basis of the physico-chemical profiling of the water column, water samples were collected in plastic bottles (1.5 l) using a battery-driven peristaltic pump. Anoxia is guaranteed by filling the bottle from the bottom and avoiding the presence of an air bubble at the liquid surface. Incubations are done in 13 ml N_2-preflushed vacutainer tubes. Samples (10 ml) were injected using syringes to keep anoxia during samples handling, and then the stock solutions were added (Tab. 10).

Table 10: Added volumes of the different stock solutions and the corresponding concentrations.

	Fe(II)	NO_3^-	H_2S	DCMU	N-Serve	^{14}C
Initial concentration	27.5 mM	2.2 mM	9.8 mM	Water saturated	1.2 mM	20 µCi/ml
Volume added	200 µl	200 µl	200 µl	200 µl	200 µl	250 µl
Final concentration	500 µM	40 µM	178 µM	1/50 [vol/vol])	0.02 mM	5 µCi/tube

Tubes were spiked with anoxic ^{14}C-bicarbonate just prior the *in situ* incubation and incubated for 3-4 hours in the lake. This duration is the longer possible to avoid organic matter turnover: incorporation into heterotrophic biomass of radiolabeled organic matter excreted by autotrophic organisms. For greater signal, incubations were performed during mid-day when temperature and light was at their maximum.

Each treatment was incubated both in light and dark conditions for the estimation of photoautotrophy and chemoautotrophy, respectively. Dark condition was guaranteed by wrapping aluminium sheets around tubes and by putting them in black plastic bags. Each treatment was incubated at two different depths: sampling depth for the real C fixation, and above cyanobacterial plate with higher light intensity for the potential C fixation. After incubations the samples were immediately killed (fixed) with formalin (2% final concentration). Each incubation treatment was done in duplicate.

Samples were filtered (polycarbonate (PC), 0.2 µm) as soon as possible. Filters were rinsed twice with 0.5 M HCl and finally twice with milliQ water. High HCl concentration could lyse the cells, but if it's not enough concentrated, carbonates bounded to organic matter will not be dissolved. After a drying period of 36 h under a fume-hood, filters were filed in 10 ml of scintillation liquid (Sigma-Fluor LSC cocktail, for non-aqueous samples). Scintillations were measured with Wallac 1409 liquid scintillation counter (using non-aqueous samples program) for the determination of fixed ^{14}C.

Primary production rates were calculated according to: $\text{Uptake rate} = {}^{14}\text{C-fixed} \times [\Sigma CO_2] \times (1.06 / \Sigma^{14}CO_2) \times t$, where ^{14}C-fixed was the radioactivity counts per filter (minus control), $[\Sigma CO_2]$ is the total DIC concentration in the water at the sampling depth, 1.06 is the correction factor for isotopic fractionation between ^{12}C-DIC and ^{14}C-DIC, $\Sigma^{14}CO_2$ was the total DIC radioactivity per vial, and *t* was the incubation time. Uptake rates were used to build a generalized linear model (-C- uptake ~ Fe + NO_3- + H_2S) with a binomial distribution (MacCullagh & Nelder, 1989). The influences of the treatments on carbon uptake were tested using ANOVA. All analyses were performed using the statistical software "R" (R Development Core Team, 2009).

Test performed for the use of bigger volumes

For improving the accuracy and the representativity of the primary production measurements we proposed to use bigger volume of water samples (50 ml). This may cause problems with the filters which can be blocked by to the large amount of particles present in samples. Therefore, ^{14}C incubations were carried on in the laboratory in order to test two different types of filters: one single polycarbonate (PC) filter (0.2 µm), two PC filters, one single GF/F filter (0.7 µm) and one GF/F filter above a PC filter.

For the experiment we used a *Synenococcus sp.* culture (108 cells/ml). Tubes containing 100 ml of this culture were spiked with 5 µCi of ^{14}C-bicarbonate and incubated for 2 hours at 15°C with a light intensity of 61 µE/m2. Filtration (60 ml) and filters analyses followed the same protocol as previously presented. Triplicates were realized for each type of filter (Tab. 11).

Table 11: Results of the filters tests. The filter type "GF/F + PC"shows the highest mean value of decomposition per minute (dpm), indicating a better efficiency of the method. Indeed, C fixation rate should be the same from one treatment to another, as the culture and the incubation conditions are the same for every samples. Lowest values can be attributed to cells loss.

	PC	PC + PC	GF/F	GF/F + PC
Tripl. 1 (dpm)	919988	510421	1122841	1149342
Tripl. 2 (dpm)	357052	478068	1144863	1124575
Tripl. 3 (dpm)	256436	796801	1140574	1152507
Mean	508592	595097	1136093	1142141

Treatment (filter type) presenting the highest values can be considerate as the best result. The lower values observed with PC filters can be attributed to organic matter loss: after the filter obstruction, the pressure exerted by the vacuum lyse the cells, thus losing their radiolabelled organic matter in the filtrate. Results showed that the use of one GF/F filter above a PC filter is the most appropriate (Tab. 11). The use of one single GF/F filter could allow particles to pass, due to the too large pores, thus losing part of the radiolabelled material. However, results showed that this loss is little. Therefore, the use of one GF/F filter above a PC filter is a solution to avoid the obstruction problem of the PC filter when a small amount of samples are treated. But for huge series, the use of only one GF/F filter would be a good compromise.

I.6. DGGE analysis

I Stock denaturing solutions

I.1 Material

- 2 graduated cylinders with magnetic stirrers
- Gloves, lab coat
- Pipette 50 µl.
- Pipette 5000 µl.
- 2 x 100 ml flasks covered with aluminium foil.

I.2 Preparation of the stock solutions

- Mix the following components in the graduated cylinders, the magnetic stirrers dissolve urea.

	Denaturant concentration							
	0%	**25%**	**30%**	**40%**	**45%**	**55%**	**60%**	**100%**
Acrylamide 40 %	20 ml	20 ml	20 ml	20 ml	20 ml	20 ml	20 ml	20 ml
TAE Bu• er 50x	2 ml	2 ml	2 ml	2ml	2 ml	2 ml	2 ml	2 ml
Formamide	0ml	10 ml	12 ml	16 ml	18 ml	22 ml	24 ml	40 ml
Urea (O-398)	0 g	10.5 g	12.6 g	16.8 g	18.9 g	23.1 g	25.2 g	42 g
H20 nanopure qsq	100 ml	100 ml	100 ml	100 ml	100 ml	100 ml	100 ml	100 ml

- Filter the solutions with a filter paper (Schleicher & Schuell LS 17 ½ 150 ø mm).
- Store the solutions at 4 °C away from light (aluminium foil).

II Casting the gel

II.1 Apparatus preparation

The most important source of "error" comes from glass plate not well cleaned. The residual acrylamide or dust interferes in the gel cast (gradient) and the DNA migration

- To assemble the gel sandwich, take one short plate (inner plate) and one large plate (outer plate): Clean both glass plates with milliQ water and then with alcohol. Do not take a sponge!! Just paper.
- Clean also the two plastic spacers and the rubber joint that closes the lower part of the plates during gel polymerisation.
- Put the spacers on the borders of the large plate and then place the short one on it (Fig. 1).
- Fix the plates with the sandwich clamps, do not screw to much (Fig. 1).

Figure 1:

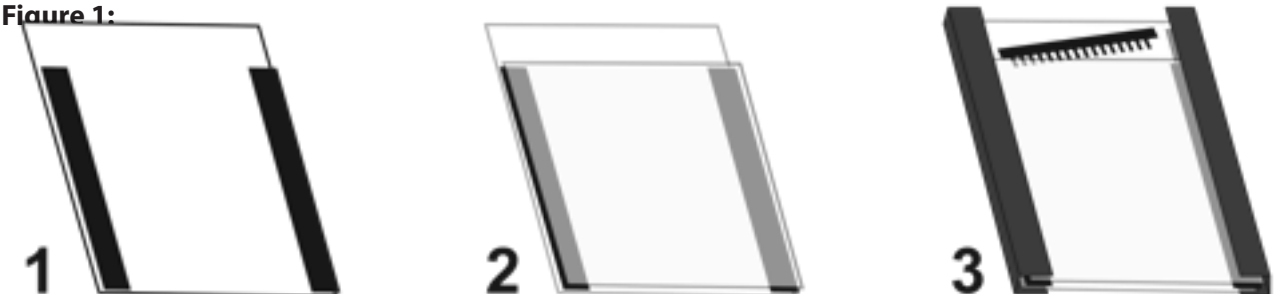

- Place the sandwich assembly in the alignment slot of the casting stand. Be careful that the plates don't slip!
- Insert the alignment card, previously washed with alcohol, to keep the spacers parallel to the clamps. Optimize the construction so that both plates are as straight as possible, with the spacers arriving at the bottom of the construction (leak source).
- Screw without forcing the clamps.
- Remove the alignment card
- Place a clean gray gasket in each casting slot of the casting stand
- Place the aligned sandwich into the casting slot with the large plate (outer plate) facing you
- Add the 16-well comb, previously washed with alcohol, in diagonal (to avoid formation of air bubble; Fig. 2)

II. 2 Gel cast

- Connect the mixing gradient chambers with the peristaltic pump.
- Pour deionised water only in the right chamber (high), in order to see if the channel between the two chambers is not clogged by polymerised acrylamide.
- Switch on the pump and rinse the tube and needle (catch the water in a flask).
- Close the connection between chambers (switch horizontal ==> switch vertical)
- Prepare 10 % w/w solution of APS (ammonium persulphate) in an Eppendorf tube (0,1 g APS + 1 ml H2O).
- Put the needle in the middle of the glass plates, between the large plate and the16-well comb.
- Place a magnetic stirrer in the High chamber (=mixing chamber) and start stirring.

	Beaker Low	Beaker High
Denaturant. **Low**	16 ml	
Denaturant. **Hight**		16 ml
Xylencyanol FF 1% (w/v)		40 µl
Temed (tetramethylethylendiamide)	60 µl	60 µl
APS	60 µl	60 µl

- Prepare two Beakers and mix rapidly:

- Fill the chambers with the high solution (H) in the right and the low solution (L) in the left. The connection between the low and high chamber is closed
- Switch-on the pump and immediately open the channel between chambers (switch vertical ==> switch horizontal)
- Verify visually that the "low solution" is mixing in the high solution. (Coloration dilution; "low" level in the weel diminish)

During casting, watch carefully that the needle tip is always kept 2-5 cm above the liquid level to avoid disturbance of the denaturant gradient (Fig. 2).

- Wait until the solution arrives at the top of the short glass plate and put the needle into a Beaker to collect the remaining volume of acrylamide solution Then push the comb, in the middle, from one side to the other, in order to avoid having tinny air bubbles at the comb tip (Fig. 2).

The bubbles will interfere in the DNA migration and you won't be able to use the results of your gel.

- When the gel is cast, rinse immediately the with deionised water by filling the chambers. Rinse the Beaker. Wait 1-2 hour for polymerisation and if the gradient seems undisturbed (gradient coloration),

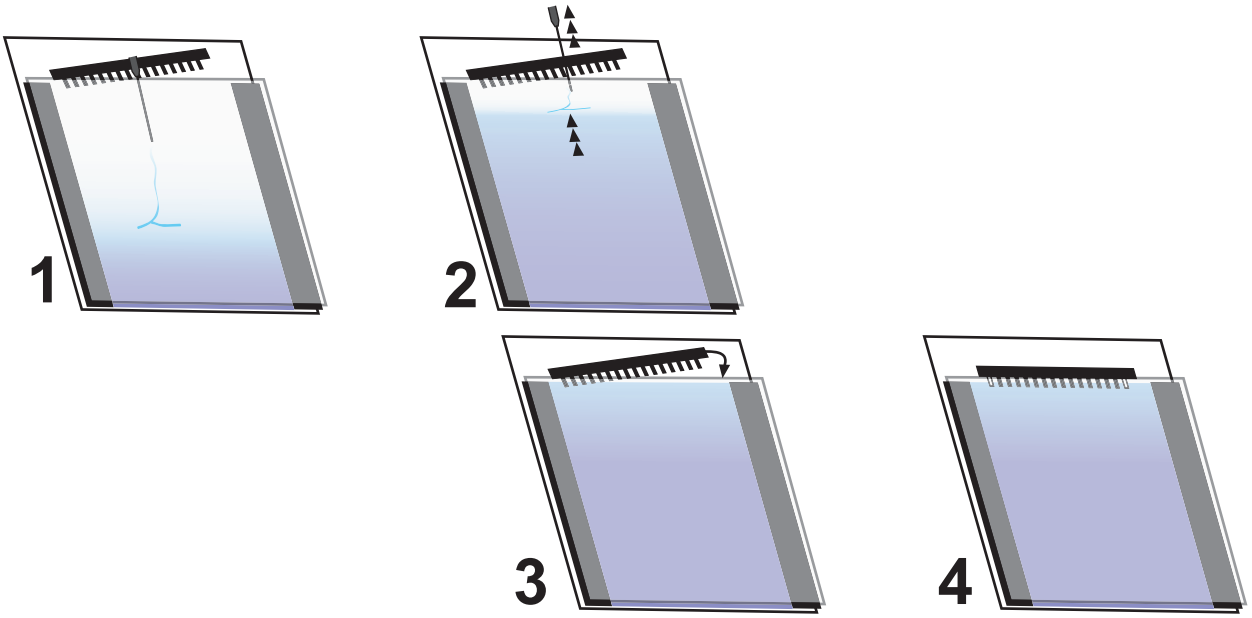

run the gel.

Figure 2:

III Loading the gel

III.1 Preparing the loading buffer: 10x-LB (GelRed=8x)

The LB is composed of 60% sucrose, 0.25% of Bromophenol blue and 0.25% of Xylencyanol FF.

- Add 6 g of sucrose in a 10 ml graduated flask
- Add 2.5 ml of Bromophenol blue 1% (w/v)
- Add 2.5 ml of Xylencyanol FF 1% (w/v)
- Heat until dissolved
- Take out the magnetic stirrer, and adjust to 10 ml with deionised water.
- Then filtrate the solution at 0.45 µm pore size.

III.2 Loading the gel and run

- You must load the same quantity of GC-clamp DNA in each well:
- Pure strains: 50 to 100 ng
- Complex DNA: 600 to 1000 ng
- Add the loading buffer

	Volume
Buffer	5 µl
Sol. ADN	≈ µl
Total	15-20 µl

- Put inside the electrophoresis tank 120 ml of TAE 50x.
- Add 6 litres of preheated deionised water (Oven 60°C).

Note: It is recommended that the running buffer not be reused. Reusing the running buffer may affect the migration rate and band resolution

- Prepare 1 litre of TAE 1x (20 ml TAE 50x + 980 ml H20 deionised).
- Remove delicately the comb and put the gel on the core (slide the sandwichclamps on the white marks and push until it blocks.
- Place the core in the electrophoresis tank
- Pour the 1 liter of TAE in the space between the glass plates until the level is between "Run" and "Maximum"mark.
- Place the electrophoresis control module on top of the electrophoresis tank. Turn power, pump and heater on. Set the temperature at 5°C more than the run temperature. Set the temperature ramp rate to 200°C/hr to allow the buffer to reach the desired temperature the quickest.

Never switch on the pump if the pump is not immersed in water.

- When the temperature is reached, remove electrophoresis control module.

Don't forget to shut down heating device when taking the upper apparatus out of the tank.

- Clean the wells with a TAE-1x 30 ml syringe (+needle).
- Let the first and last wells empty
- Load the reference (composite) of both sides of the gel and the samples between (15 µl sample + 5µl loading) with 20 µl Hamilton syringe (note from which side you start loading each gel: not to mix sample when reading the gel).
- Place the electrophoresis control module on top of the electrophoresis tank and Turn power, pump and heater on. Switch on the power supply and set voltage at 40V during 10 min in order to pack the sample in the beginning of the gel.

ATTENTION: the migration time depend on the denaturing gradient and on the DNA-strand length.

- After that switch to 150V during 4h40 min (200 base pair DNA strand).

It is important to stop the electrophoresis when the blue dye (loading buffer) reach the bottom end of the gel. (note the corresponding total migration time).

IV Reading the gel

- Remove the gel from the DGGE tank.
- Remove the gel within the glass plates by pressing on the black holders.
- Place the glass plates on the square box (small plate under).
- Remove the sandwich clamps and remove delicately the spacers.

Clean your nitril glove by rubbing-it 3 times under deionised water. If not, small white stain will be left on the gel.

- Gently dissociate the 2 glass plates using water: the gel always sticks to one of the plate.
- Takeout the large plate.
- Cut-out the acrylamide between well spaces.
- Cut the upper corner on the side from which you start loading your samples (to recognize the sample order if the gel shift).
- Fill-up a tank with 250 ml of TAE 1x containing 75 µl of Gel-red (3x final concentration).

- Put the gel in a plastic tank (with a cover).
- Keep-it in the dark during 25-30 min for staining.
- Take the gel out and drain-it (not dry).
- Clean the photo chamber with deionised water.
- Smoothly slide the gel inside. If it sticks on your glass plate, add water.
- Add water with a wash water bottle to remove the air bubbles between the gel and the trans-illuminator.
- Adjust intensity of most intense band in the gel at the limit of saturation.
- Take photos of the gel and save your gel image. (Tiff format is recommended if you want to analyse gel with Gelcompar software)

V Cleaning the material

- Throw the acrylamide gel in the dedicated plastic bin.
- Take back the 250 ml TAE+Gel-red and store-it in an aluminium-covered bottle at 4-10°C.
- Rinse the DCode System (Bio-Rad) by letting the pump run with deionised water (8 litres).
- Rinse Hamilton syringe with deionised water.
- Rinse the plate with deionised water and rub with paper.
- Re-rinse and re-rub with ethanol.
- Re-re-rinse and re-re-rub with deionised water and let-it dry.
- Re-fill the tank of deionised water and store-it at 60°C.
- Stop and unplugged the DCode System.

VI Problems

Current problems	Solutions
The gel leaks when it's casted	- Stop immediately the pump, put deionised water in both chambers of the mixing gradient, remove the needle and put it in a flask, switch back on the pump so to clean the tube. Clean the workplace and the contaminated material so there is no trace left of the gel (carcinogenic!). -The set of glass plates must be assembled as precisely as possible. Verify that the plates are not broken in some parts and that the mounting is correct; i.e. the spacers and the plates should be aligned on both sides and on the bottom, leaving no space between them.
The gel polymerises before it is totally poured	Before adding it, put APS in the fridge a few minutes. Go faster! Have all your products ready and know exactly what you are doing at each step.
The mixing gradient apparatus is clogged	Pass it under warm water and shake vigorously. Once the cork of polymerised acrylamide has gone off, rinse the mixing gradient with deionised water
An air bubble appears when you cast the gel.	Tap with your finger on the plate so that the bubble ascends.
The gel still doesn't polymerise after one hour	Verify if the products are not too old. APS can sometimes hydrate itself.

ANNEX II: Results

Fe II	Soluble (µM)						
Depth (m)	06/09/2007	Depth (m)	07/02/2008	Depth (m)	13/10/2008	Depth (m)	29/09/2009
0.10	0.00	0.10	0.00	0.50	0.00	0.50	0.15
4.00	0.36	4.00	1.07	8.00	0.91	5.00	0.15
7.00	0.00	8.00	0.00	9.00	0.00	8.25	0.15
8.50	0.00	11.00	0.00	9.50	0.00	10.00	0.00
9.00	0.00	13.00	0.71	9.75	0.45	10.20	0.75
9.50	0.00	13.50	0.00	10.00	0.00	10.40	0.15
10.00	0.36	14.00	0.00	10.50	0.00	10.60	0.30
10.25	0.71	14.30	0.00	10.75	0.91	10.80	0.30
10.50	0.00	14.60	0.00	11.00	0.00	11.00	0.30
10.75	0.36	14.90	1.43	11.25	0.00	11.20	0.60
11.00	0.00	15.20	5.00	11.50	0.45	11.40	0.90
11.25	0.36	15.50	15.00	11.75	1.36	11.60	0.90
11.50	0.71	15.80	30.00	12.00	3.64	11.80	2.41
11.75	1.79	16.10	41.07	12.25	3.18	12.00	4.06
12.00	2.14	16.40	63.93	12.50	3.64	12.30	4.06
12.25	2.14	16.70	83.57	12.75	5.00	12.60	4.66
12.50	2.50	17.00	115.00	13.00	5.91	12.90	4.96
12.75	2.14	17.30	144.64	14.00	11.36	13.20	5.41
13.00	4.64	17.60	166.07	15.00	24.55	13.50	7.22
13.25	5.00	17.90	196.07	16.00	56.82	13.80	8.12
13.50	4.29	18.20	215.71	17.00	142.27	14.10	10.38
14.00	6.07	18.50	212.86	18.00	236.36	14.40	11.13
14.50	9.29	18.80	227.14	19.00	243.64	14.70	12.33
15.00	12.14	19.10	236.07			15.00	15.79
15.50	18.21	19.40	252.86			16.00	43.17
15.75	23.93	19.70	249.64			17.00	131.00
16.00	28.57					18.00	220.20
16.25	41.07					19.00	236.74
16.25	42.50						
16.50	58.21						
17.00	105.71						
17.50	154.64						
18.00	191.07						
18.50	210.71						
19.00	220.36						
19.50	222.86						
20.00	220.71						

Fe II	Total (µM)		
Depth (m)	13/10/2008	Depth (m)	29/09/2009
0.50	0.00	0.50	0.25
9.00	0.00	5.00	0.00
10.00	0.00	8.25	0.50
11.00	0.00	10.00	0.00
11.50	0.45	10.20	0.75
11.75	1.36	10.40	0.50
12.00	2.73	10.60	1.75
12.25	3.64	10.80	1.50
12.50	4.09	11.00	1.25
12.75	5.00	11.20	1.25
13.00	6.82	11.40	1.25
14.00	11.36	11.60	1.00
15.00	25.00	11.80	1.25
16.00	58.18	12.00	3.51
17.00	148.18	12.30	4.01
18.00	239.09	12.60	5.51
19.00	255.45	12.90	5.51
		13.20	6.26
		13.50	8.51
		13.80	9.77
		14.10	10.77
		14.40	12.52
		14.70	15.03
		15.00	17.53
		16.00	54.34
		17.00	156.02
		18.00	248.67
		19.00	269.21

Fe II	Filter (µM)				
Depth (m)	06/09/2007	Depth (m)	07/02/2008	Depth (m)	13/10/2008
0.10	0.18	0.10	2.57	10.00	0.27
4.00	0.14	4.00	0.64	11.50	0.82
7.00	0.14	8.00	0.36	11.75	0.55
8.50	0.32	11.00	0.36	12.00	0.59
9.00	0.96	13.00	0.86	12.25	0.41
9.50	2.64	13.50	0.82	12.50	0.55
10.00	0.50	14.00	0.32	12.75	0.32
10.25	2.93	14.30	4.64	13.00	0.68
10.50	0.75	14.60	0.29	14.00	0.64
10.75	1.25	14.90	0.96	15.00	0.55
11.00	11.79	15.20	2.14	16.00	1.05
11.25	0.46	15.50	1.14	17.00	1.91
11.50	0.86	15.80	0.96	18.00	2.73
11.75	0.61	16.10	2.36		
12.00	0.32	16.40	1.86		
12.25	0.75	16.70	3.21		
12.50	0.54	17.00	2.14		
12.75	0.25	17.30	2.25		
13.00	0.36	17.60	5.64		
13.25	0.79	17.90	3.36		
13.50	0.43	18.20	3.93		
14.00	0.71	18.50	7.50		
14.50	0.61	18.80	3.79		
15.00	0.64	19.10	6.54		
15.50	0.71	19.40	7.86		
15.75	0.89	19.70	2.64		
16.00	0.89				
16.25	0.89				
16.50	0.89				
17.00	0.89				
17.50	0.89				
18.00	0.86				
18.50	0.64				
19.00	1.11				
19.00	1.00				
19.50	1.04				
20.00	0.79				

Fe III	Colloidal (µM)						
Depth (m)	06/09/2007	Depth (m)	07/02/2008	Depth (m)	13/10/2008	Depth (m)	29/09/2009
0.10	0.46	0.10	0.00	0.50	-0.04	0.50	-0.15
4.00	0.38	4.00	0.00	8.00	0.00	5.00	0.02
7.00	0.34	8.00	0.00	9.00	0.51	8.25	-0.15
8.50	0.36	11.00	0.00	9.50	-0.04	10.00	0.00
9.00	0.80	13.00	0.09	9.75	0.00	10.20	0.30
9.50	1.24	13.50	3.60	10.00	0.51	10.40	-0.15
10.00	0.86	14.00	3.20	10.50	-0.04	10.60	0.22
10.25	1.83	14.30	0.40	10.75	0.00	10.80	0.05
10.50	0.85	14.60	0.80	11.00	-0.04	11.00	0.05
10.75	1.55	14.90	1.77	11.25	1.07	11.20	0.62
11.00	1.93	15.20	1.80	11.50	0.06	11.40	0.84
11.25	0.62	15.50	0.00	11.75	0.26	11.60	0.84
11.50	1.39	15.80	0.00	12.00	0.21	11.80	1.08
11.75	0.55	16.10	0.00	12.25	1.77	12.00	0.48
12.00	0.70	16.40	0.00	12.50	0.21	12.30	0.65
12.25	0.99	16.70	0.00	12.75	3.29	12.60	0.40
12.50	0.42	17.00	0.00	13.00	0.16	12.90	0.80
12.75	3.21	17.30	0.00	14.00	0.26	13.20	0.52
13.00	0.16	17.60	0.00	15.00	0.41	13.50	0.46
13.25	0.13	17.90	0.00	16.00	1.57	13.80	0.26
13.50	1.45	18.20	0.00	17.00	5.01	14.10	-0.08
14.00	1.01	18.50	0.00	18.00	11.42	14.40	0.04
14.50	0.39	18.80	0.00	19.00	13.64	14.70	-0.29
15.00	0.32	19.10	11.10			15.00	0.61
15.50	0.21	19.40	0.00			16.00	0.47
15.75	0.35	19.70	0.00			17.00	1.99
16.00	0.47					18.00	3.72
16.25	0.31					19.00	3.24
16.25	0.15						
16.50	0.31						
17.00	0.43						
17.50	0.38						
18.00	0.52						
18.50	0.69						
19.00	0.40						
19.50	0.44						
20.00	0.41						

Fe III	Total (µM)		
Depth (m)	13/10/2008	Depth (m)	29/09/2009
0.50	0.10	0.50	0.00
9.00	0.10	5.00	0.58
10.00	0.10	8.25	0.37
11.00	1.80	10.00	0.58
11.50	1.30	10.20	0.12
11.75	1.50	10.40	0.66
12.00	0.70	10.60	-0.01
12.25	0.40	10.80	1.11
12.50	1.00	11.00	0.78
12.75	1.80	11.20	1.07
13.00	0.00	11.40	0.78
14.00	0.00	11.60	2.49
15.00	0.10	11.80	2.82
16.00	2.50	12.00	1.72
17.00	7.50	12.30	1.80
18.00	12.10	12.60	0.59
19.00	14.60	12.90	1.17
		13.20	1.29
		13.50	0.49
		13.80	0.11
		14.10	0.27
		14.40	1.43
		14.70	0.00
		15.00	1.36
		16.00	2.61
		17.00	2.65
		18.00	3.91
		19.00	3.65

Fe III	Filter (µM)				
Depth (m)	06/09/2007	Depth (m)	07/02/2008	Depth (m)	13/10/2008
0.10	0.28	0.10	1.15	10.00	1.62
4.00	0.23	4.00	0.60	11.50	1.29
7.00	0.19	8.00	0.28	11.75	1.62
8.50	0.04	11.00	0.40	12.00	1.13
9.00	0.00	13.00	0.38	12.25	1.15
9.50	0.00	13.50	0.58	12.50	0.79
10.00	0.36	14.00	0.84	12.75	0.96
10.25	0.00	14.30	0.44	13.00	0.98
10.50	0.10	14.60	0.51	14.00	0.92
10.75	0.00	14.90	0.60	15.00	0.68
11.00	0.00	15.20	0.86	16.00	0.93
11.25	0.11	15.50	-0.02	17.00	1.04
11.50	0.45	15.80	0.20	18.00	1.22
11.75	0.00	16.10	0.28		
12.00	0.12	16.40	0.06		
12.25	0.00	16.70	0.00		
12.50	0.00	17.00	0.00		
12.75	0.00	17.30	0.03		
13.00	0.00	17.60	0.32		
13.25	0.00	17.90	0.00		
13.50	0.10	18.20	0.19		
14.00	0.00	18.50	0.00		
14.50	0.00	18.80	0.00		
15.00	0.00	19.10	0.00		
15.50	0.00	19.40	0.00		
15.75	0.00	19.70	0.00		
16.00	0.00				
16.25	0.00				
16.50	0.00				
17.00	0.00				
17.50	0.00				
18.00	0.00				
18.50	0.00				
19.00	0.00				
19.00	0.00				
19.50	0.00				
20.00	0.00				

II.2. Sulfide and sulfate concentrations measured in Lake La Cruz

H_2S	Soluble (μM)						
Depth (m)	06/09/2007	Depth (m)	07/02/2008	Depth (m)	13/10/2008	Depth (m)	29/09/2009
0.10	0.16	0.10	0.20	0.50	0.00	0.50	0.00
4.00	0.24	4.00	0.08	8.00	0.00	5.00	0.00
7.00	0.20	8.00	0.08	9.00	0.00	8.25	0.00
9.00	0.24	11.00	0.08	9.50	0.00	10.00	0.10
10.00	0.52	13.00	0.20	9.75	0.00	10.20	0.10
10.50	0.52	13.50	0.04	10.00	0.00	10.40	0.40
10.75	0.56	14.00	0.56	10.50	0.00	10.60	0.95
11.00	0.52	14.30	0.00	10.75	0.00	10.80	1.10
11.25	0.64	14.60	0.00	11.00	0.00	11.00	0.60
11.50	1.56	14.90	0.00	11.25	0.00	11.20	0.70
11.75	1.60	15.20	1.44	11.50	0.00	11.40	0.65
12.00	4.28	15.50	5.16	11.75	0.00	11.60	2.75
12.25	5.76	15.80	6.44	12.00	0.00	11.80	3.45
12.50	6.36	16.10	4.04	12.25	1.04	12.00	4.70
12.75	6.08	16.40	3.88	12.50	2.37	12.30	7.30
13.00	1.64	16.70	1.84	12.75	7.25	12.60	10.15
13.25	12.68	17.00	3.04	13.00	9.05	12.90	11.75
13.50	13.88	17.30	2.56	14.00	12.51	13.20	14.10
14.00	13.72	17.60	2.28	15.00	10.76	13.50	20.40
14.50	12.68	17.90	2.60	16.00	11.90	13.80	21.15
15.00	8.08	18.20	1.44	17.00	15.83	14.10	21.40
15.50	4.92	18.50	0.32	18.00	18.15	14.40	21.55
15.75	12.04	18.80	0.80	19.00	16.26	14.70	20.90
16.00	11.76	19.10	2.52			15.00	20.90
16.25	10.28	19.40	0.36			16.00	18.10
16.50	12.56	19.70	2.40			18.00	19.30
17.00	17.76					19.00	19.35
17.50	16.64						
18.00	19.04						
18.50	19.12						
19.00	16.56						
19.50	16.04						
20.00	13.88						

SO_4^{2-}	Soluble (μM)				
Depth (m)	07/02/2008	Depth (m)	13/10/2008	Depth (m)	29/09/2009
0.10	31.21	0.50	32.27	0.50	30.83
4.00	31.00	8.00	27.16	5.00	28.94
8.00	24.18	9.00	25.22	8.25	25.84
11.00	21.39	9.50	25.97	10.00	25.49
13.00	32.62	9.75	25.92	10.20	24.49
13.50	36.25	10.00	25.56	10.40	23.93
14.00	38.22	10.28	26.71	10.60	24.94
14.90	46.29	10.50	24.93	10.80	25.65
15.20	35.82	10.75	25.46	11.00	26.44
15.80	33.30	11.00	26.37	11.20	24.93
16.40	29.67	11.25	24.92	11.40	24.48
17.00	22.05	11.50	26.80	11.60	23.40
17.90	21.26	12.00	25.69	11.80	22.66
19.10	15.15	12.50	25.12	12.00	21.94
		13.00	21.74	12.60	23.36
		14.00	23.97	13.20	22.36
		15.00	20.63	13.80	22.46
		16.00	15.94	14.40	21.24
		17.00	12.72	15.00	19.84
		18.00	12.18	16.00	17.66
		19.00	8.93	17.00	15.64
				18.00	11.88
				19.00	9.93

06/09/2007							
Depth (m)	Total Phosphorus (µM)	Soluble Phosphorous (µM)	Organic Phosphorous (µM)	Total Nitrogen (µM)	N-org uM	NH_4^+ (µM)	NO_3^- (µM)
0.10	1.48	0.11	1.36	38.50	32.29	-	4.36
4.00	2.11	0.07	2.04	77.00	70.83	-	4.51
7.00	0.72	0.04	0.67	58.30	50.47	-	5.73
8.50	1.52	0.04	1.48	48.40	40.96	-	5.24
9.00	1.70	0.05	1.65	58.30	49.96	-	5.34
9.50	2.17	0.07	2.09	100.10	90.46	-	4.04
9.75	1.45	0.06	1.39	122.10	112.49	-	3.71
10.00	1.85	0.04	1.81	106.70	98.95	6.50	1.25
10.50	3.03	0.04	2.99	103.40	94.75	7.80	0.85
11.00	0.73	0.07	0.65	91.30	82.00	9.30	-
11.50	0.39	0.03	0.36	115.50	105.00	10.50	-
11.80	0.28	0.16	0.12	93.50	9.14	84.36	-
12.50	1.97	0.06	1.91	96.80	73.30	23.50	-
13.00	1.44	0.04	1.41	125.40	56.90	68.50	-
13.50	0.59	0.04	0.55	133.10	32.60	100.50	-
14.00	3.00	0.06	2.94	214.50	41.90	172.60	-
15.00	3.48	0.03	3.45	322.30	92.20	230.10	-
15.50	2.47	0.03	2.44	366.30	26.00	340.30	-
16.00	2.77	0.03	2.74	542.30	40.00	502.30	-
16.50	2.22	0.03	2.19	899.80	57.50	842.30	-
17.00	3.33	0.06	3.26	1686.30	108.10	1578.20	-
17.50	2.98	0.06	2.92	2214.30	79.00	2135.30	-
18.00	4.36	0.84	3.52	2610.30	86.70	2523.60	-
18.50	8.34	4.35	3.99	2819.30	165.50	2653.80	-
19.00	9.68	6.91	2.77	2997.30	240.70	2756.60	-
19.50	11.79	8.06	3.73	3096.30	197.00	2899.30	-
20.00	12.46	8.30	4.16	3152.30	100.00	3052.30	-

06/09/2007								
Depth (m)	Temperature (°C)	Electroconductivity (µS cm^{-1})	Chloropyll a (µg l^{-1})	Oxygen (µM)	Depth (m)	Turbidity (NTU)	Redox potential (mV)	c-DOM (AU)
0.99	23.46	580.10	8.10	239.44	0.54	1.50	112.21	6.76
0.79	23.17	578.92	8.01	242.77	0.76	1.53	111.60	6.68
1.15	22.60	578.90	8.36	249.81	0.99	1.47	106.77	6.68
1.15	22.59	581.38	8.53	249.83	1.09	1.50	106.77	6.59
1.24	22.53	579.20	8.45	250.14	1.26	1.53	106.16	6.68
1.39	22.57	579.51	8.79	249.79	1.49	1.50	104.95	6.84
1.39	22.57	579.58	8.83	249.82	1.54	1.53	104.95	6.76
1.51	22.48	579.00	8.83	249.50	1.74	1.59	104.35	6.84
1.51	22.48	578.81	8.92	249.35	1.76	1.59	104.35	6.93
1.68	22.35	578.79	9.09	251.44	1.98	1.53	102.54	6.84
1.68	22.34	578.96	9.05	251.79	2.03	1.56	101.93	6.93
1.82	22.34	578.81	9.05	252.25	2.24	1.59	101.33	6.84
1.83	22.33	578.77	9.05	252.30	2.27	1.53	101.93	6.93
2.08	22.18	578.43	9.65	254.18	2.49	1.59	100.72	6.93
2.08	22.18	578.67	9.61	254.35	2.52	1.56	100.72	7.01
2.27	22.16	578.50	9.74	255.02	2.75	1.59	100.12	7.09
2.29	22.17	578.69	10.04	254.81	2.79	1.59	100.12	7.01
2.71	22.02	578.26	9.78	254.57	2.99	1.62	98.91	7.09
2.71	22.02	577.88	9.65	254.41	3.00	1.59	98.91	7.09
2.99	22.01	578.25	9.82	254.80	3.24	1.59	98.91	7.17
3.00	22.00	578.79	9.91	254.66	3.27	1.62	98.91	7.01
3.32	21.97	578.44	9.91	254.69	3.50	1.65	98.30	7.17
3.34	21.97	578.46	9.95	254.55	3.51	1.62	98.30	7.17
3.77	21.94	578.28	10.30	254.88	3.74	1.59	98.30	7.26
3.80	21.93	578.18	10.25	254.91	3.75	1.65	98.30	7.17
4.08	21.92	578.52	10.51	254.12	3.99	1.62	98.30	7.26
4.08	21.91	578.56	10.34	254.43	4.02	1.59	98.30	7.26
4.30	21.92	578.27	10.51	254.41	4.28	1.59	98.30	7.17
4.53	21.90	578.32	10.42	254.38	4.49	1.56	98.30	7.34
4.58	21.90	578.32	10.60	254.38	4.50	1.56	97.70	7.26
4.95	21.85	578.48	10.55	253.58	4.76	1.59	97.70	7.34
4.96	21.85	578.48	10.47	253.87	4.76	1.59	98.30	7.34
5.05	21.85	578.65	10.55	253.30	4.96	1.59	98.30	7.26
5.08	21.85	578.51	10.60	253.31	5.00	1.59	98.30	7.42
5.09	21.85	578.52	10.68	253.32	5.02	1.56	98.30	7.26
5.15	21.85	578.57	10.34	252.75	5.23	1.62	98.30	7.34
5.16	21.85	578.05	10.60	252.90	5.28	1.62	98.30	7.26
5.29	21.84	578.57	10.68	252.77	5.49	1.59	98.30	7.34
5.30	21.85	578.74	10.81	252.91	5.50	1.62	97.70	7.34
5.62	21.82	578.30	10.90	252.30	5.76	1.59	97.70	7.26
5.64	21.82	578.39	11.07	252.19	5.78	1.59	97.70	7.34
5.91	21.76	578.93	11.11	251.47	6.00	1.59	98.30	7.51
5.94	21.76	578.71	11.20	251.46	6.02	1.59	98.30	7.59
5.95	21.76	578.87	10.85	251.01	6.03	1.62	97.70	7.59
6.15	21.51	578.93	11.46	250.92	6.26	1.62	98.30	8.25
6.16	21.49	579.77	11.89	250.31	6.26	1.56	98.91	8.50
6.31	21.22	583.54	12.40	252.08	6.51	1.56	101.93	14.32
6.34	21.21	583.98	12.58	253.32	6.53	1.56	101.33	15.06
6.52	20.13	599.16	14.77	289.88	6.74	1.43	101.93	17.72
6.52	19.99	601.26	14.77	293.29	6.77	1.43	101.93	17.72
6.69	19.35	604.58	16.23	327.13	6.99	1.40	106.16	18.96
6.71	19.30	600.99	16.36	327.17	7.00	1.37	106.77	19.21
6.80	18.61	605.93	16.62	335.81	7.26	1.31	109.19	19.46
6.79	18.64	606.10	16.71	335.61	7.27	1.31	109.79	19.55
6.97	18.01	602.37	17.22	339.61	7.49	1.25	110.39	19.55
6.97	17.74	605.84	17.05	341.38	7.50	1.25	110.39	19.46
7.14	17.20	606.75	17.65	331.66	7.76	1.25	111.00	19.38
7.32	16.16	609.28	19.37	317.02	8.00	1.25	111.60	19.38

06/09/2007								
Depth (m)	Temperature (°C)	Electroconductivity (µS cm^{-1})	Chloropyll a (µg l^{-1})	Oxygen (µM)	Depth (m)	Turbidity (NTU)	Redox potential (mV)	c-DOM (AU)
7.35	16.19	607.13	19.33	313.19	8.05	1.25	111.60	19.38
7.50	15.52	608.57	20.41	317.05	8.25	1.25	112.21	19.46
7.52	15.58	604.72	20.28	316.70	8.26	1.25	112.21	19.38
7.68	14.95	609.93	21.74	308.50	8.49	1.25	112.21	19.21
7.71	14.94	608.93	21.78	307.19	8.51	1.25	112.21	19.21
7.99	13.63	609.29	26.56	285.78	8.75	1.25	112.21	19.21
8.03	13.67	610.64	26.69	284.17	8.78	1.28	111.60	19.21
8.36	12.66	608.82	30.21	253.87	8.96	1.28	111.60	19.30
8.41	12.46	610.40	30.13	253.76	9.00	1.28	111.60	19.30
8.60	11.69	614.54	32.71	217.30	9.24	1.31	111.60	19.30
8.61	11.65	615.40	33.01	214.80	9.27	1.31	112.21	19.38
8.95	10.72	620.49	38.82	161.32	9.49	1.56	110.39	19.55
8.96	10.74	620.56	39.51	156.84	9.50	1.53	110.39	19.63
9.25	9.79	622.52	45.92	109.86	9.74	1.50	107.37	19.63
9.26	9.68	623.22	46.22	105.70	9.76	1.47	107.37	19.63
9.48	9.25	626.41	42.52	40.95	9.99	1.47	104.35	19.55
9.48	9.23	626.41	46.95	39.26	10.01	1.47	104.35	19.63
9.70	8.51	626.86	58.74	28.42	10.25	1.53	101.33	19.30
9.72	8.48	626.99	64.25	27.30	10.28	1.56	101.33	19.30
9.79	8.76	627.34	67.21	27.79	10.52	1.62	99.51	18.63
9.82	8.83	623.95	66.66	28.30	10.53	1.62	98.91	18.55
9.87	8.68	625.86	66.83	17.70	10.75	1.65	91.65	18.13
9.86	8.64	624.26	65.36	17.15	10.76	1.65	90.45	18.22
9.87	8.41	626.68	61.62	13.46	11.00	1.68	77.75	17.55
9.87	8.43	627.30	60.68	13.25	11.01	1.71	75.94	17.64
9.88	8.42	624.46	56.98	10.17	11.25	1.83	47.52	17.47
9.88	8.40	626.41	56.33	10.18	11.26	1.80	46.92	17.55
9.95	8.12	625.93	61.06	8.60	11.51	1.74	8.84	17.30
9.94	8.07	627.61	61.28	8.43	11.52	1.77	5.81	17.22
9.99	7.72	626.82	53.36	6.66	11.75	1.71	-64.92	17.14
9.99	7.72	627.83	54.91	6.66	11.77	1.68	-66.73	17.14
9.98	7.70	626.89	46.82	5.88	11.97	1.65	-84.26	17.14
9.98	7.71	627.01	47.47	5.88	12.00	1.65	-86.07	17.06
10.27	7.48	626.71	47.94	4.81	12.24	1.62	-103.60	16.89
10.26	7.46	624.98	48.11	4.62	12.25	1.56	-104.81	17.06
10.57	7.12	626.00	41.23	3.79	12.50	1.50	-127.79	16.89
10.58	7.07	628.09	41.27	3.81	12.51	1.50	-128.39	16.89
10.62	7.04	628.36	41.01	3.82	12.52	1.47	-129.60	16.89
10.88	7.01	630.52	29.57	3.04	12.74	1.43	-147.13	16.72
10.89	7.03	630.67	29.40	3.03	12.75	1.40	-147.73	16.72
11.20	6.53	630.89	25.96	2.84	13.00	1.34	-165.27	16.64
11.22	6.43	633.27	25.18	2.89	13.04	1.37	-167.08	16.64
11.40	6.37	631.87	23.76	2.31	13.24	1.37	-178.56	16.64
11.41	6.38	633.25	23.80	2.10	13.28	1.37	-179.17	16.72
11.58	6.08	637.16	23.68	2.22	13.52	1.34	-187.03	16.72
11.61	6.06	636.97	23.59	2.03	13.56	1.34	-187.63	16.72
11.76	5.90	640.12	21.83	2.09	13.74	1.31	-193.07	16.81
11.78	5.88	641.21	21.70	1.90	13.76	1.31	-193.68	16.81
11.92	5.79	643.75	20.53	1.73	13.97	1.28	-199.12	17.06
11.97	5.78	643.83	20.58	1.73	14.00	1.31	-199.72	16.97
12.13	5.70	645.86	19.89	1.56	14.25	1.28	-206.37	17.30
12.17	5.70	645.38	19.85	1.35	14.26	1.31	-206.98	17.39
12.36	5.55	647.38	19.46	1.21	14.49	1.31	-211.21	17.89
12.40	5.55	646.84	19.20	1.00	14.51	1.34	-211.81	17.97
12.59	5.49	649.51	18.64	1.02	14.75	1.28	-214.23	18.55
12.68	5.45	650.96	18.56	0.83	14.77	1.31	-214.23	18.72
12.91	5.37	652.46	17.09	0.66	14.99	1.31	-216.65	19.38
12.93	5.41	653.88	17.35	0.64	15.01	1.31	-216.65	19.30
13.13	5.32	658.52	16.10	0.26	15.24	1.31	-219.67	19.88
13.16	5.32	661.79	16.02	0.47	15.27	1.34	-219.67	20.04
13.28	5.33	662.21	15.41	0.25	15.51	1.31	-219.67	21.37
13.28	5.37	659.07	15.33	0.04	15.53	1.34	-219.67	21.46
13.46	5.33	662.66	16.75	0.00	15.74	1.34	-219.67	23.78
13.47	5.32	664.89	16.66	0.00	15.77	1.34	-220.28	24.20
13.77	5.25	674.61	14.51	0.00	16.01	1.37	-217.25	28.35
13.78	5.25	674.79	14.21	0.00	16.01	1.37	-217.25	28.51
14.02	5.24	683.56	13.26	0.00	16.25	1.43	-218.46	30.59
14.03	5.24	685.23	13.31	0.00	16.27	1.43	-217.86	30.84
14.28	5.26	693.57	12.70	0.00	16.51	1.40	-217.86	32.17
14.31	5.26	693.74	12.70	0.00	16.52	1.43	-218.46	32.17
14.63	5.28	702.32	12.66	0.00	16.75	1.47	-219.07	34.82
14.65	5.28	695.12	12.70	0.00	16.77	1.47	-219.07	35.40
14.91	5.33	717.10	12.66	0.00	16.98	1.56	-215.44	53.26
14.93	5.33	718.72	12.88	0.00	17.00	1.56	-216.04	54.25
15.15	5.37	732.50	12.83	0.00	17.25	1.56	-214.23	57.90
15.17	5.37	732.90	13.18	0.00	17.29	1.56	-214.84	58.24
15.41	5.42	756.95	13.61	0.00	17.49	1.59	-216.04	61.48
15.44	5.43	754.97	13.74	0.00	17.51	1.59	-216.04	61.72
15.60	5.43	760.36	13.78	0.00	17.74	1.59	-216.65	63.88
15.61	5.44	759.93	13.78	0.00	17.76	1.59	-217.25	64.88
15.93	5.55	850.59	13.91	0.00	17.98	1.65	-217.86	71.85
15.94	5.56	870.93	13.78	0.00	18.00	1.68	-217.86	72.43
16.21	5.64	953.27	13.18	0.00	18.25	1.65	-217.25	75.51
16.23	5.65	957.35	13.09	0.00	18.26	1.65	-217.25	75.76
16.45	5.66	980.27	12.70	0.00	18.51	1.68	-217.86	77.25
16.47	5.67	982.87	13.13	0.00	18.52	1.65	-217.86	77.50
17.68	6.09	1501.98	14.08	0.00	18.70	1.71	-217.86	80.07
17.69	6.11	1500.45	14.25	0.00	18.72	1.71	-217.86	79.24
17.75	6.13	1513.99	15.07	0.00	18.74	1.68	-218.46	79.74
17.76	6.13	1521.27	15.03	0.00	18.73	1.68	-218.46	79.91

3.2 Winter stratification: 07/02/08

07/02/2008												
Depth (m)	Oxygen (µM)	Depth (m)	Electroconductivity (µS cm⁻¹)	c-DOM (AU)	Turbidity (NTU)	Redox potential (mV)	Temperature (°C)	Depth (m)	pH	Depth (m)	Chloropyll a (µg l⁻¹; HPLC)
0.7	172.125	0.51	364.30	10.74	1.04	130.34	4.35	0.76	7.03	0.10	5.85
1.1	167.0625	0.75	364.45	10.66	1.07	126.11	4.35	1.05	7.03	4.00	4.25
1.6	164.5313	1.05	363.45	10.66	1.10	130.95	4.31	1.25	7.03	8.00	7.20
2.1	167.0625	1.25	363.63	10.66	1.07	131.55	4.31	1.54	7.03	11.00	6.85
2.6	164.5313	1.54	363.82	10.66	1.07	131.55	4.31	1.73	7.02	13.00	14.66
3.1	164.5313	1.78	363.51	10.66	1.07	132.16	4.31	2.01	7.02	13.50	12.97
3.6	164.5313	2.00	363.72	10.74	1.10	132.16	4.32	2.24	7.02	14.00	12.49
4.1	162	2.26	363.43	10.83	1.07	132.76	4.31	2.50	7.02	14.90	12.04
4.6	162	2.51	363.46	10.74	1.07	133.37	4.31	2.75	7.02	15.20	11.61
5.1	162	2.79	363.16	10.83	1.07	133.97	4.31	3.03	7.02	15.80	3.60
5.6	162	3.02	363.01	10.83	1.07	133.97	4.32	3.24	7.02	16.40	3.80
6.1	162	3.24	363.38	10.83	1.07	134.38	4.30	3.51	7.02	17.00	4.05
6.6	159.4688	3.50	362.9081	10.9109	1.0989	134.5755	4.2867	3.74	7.02	17.90	5.70
7.1	159.4688	4.018	363.1087	10.8279	1.0989	135.18	4.2606	4.00	7.02	19.10	5.99
7.6	159.4688	4.253	363.1087	10.9939	1.0684	136.389	4.2651	4.26	7.02		
8.1	156.9375	4.552	362.9553	10.9109	1.0684	136.389	4.2691	4.50	7.02		
8.6	154.4063	4.742	362.9671	10.9109	1.0684	136.389	4.258	4.75	7.02		
9.1	149.3438	5.013	362.979	10.9109	1.0684	136.389	4.2545	5.00	7.02		
9.6	149.3438	5.275	362.8255	10.9109	1.0684	136.9936	4.25	5.25	7.02		
10.1	144.2813	5.502	362.6603	10.9109	1.0684	137.5981	4.2229	5.52	7.02		
10.6	141.75	5.746	362.5069	10.9939	1.0989	137.5981	4.2198	5.76	7.02		
11.1	134.1563	6.017	362.684	10.9939	1.0989	137.5981	4.2244	6.00	7.02		
11.6	131.625	6.253	362.5306	10.9939	1.0684	138.2026	4.2137	6.25	7.02		
12.1	118.9688	6.506	362.3772	11.0769	1.0684	138.8071	4.1943	6.51	7.02		
12.6	113.9063	6.75	362.4126	11.0769	1.0684	138.8071	4.1888	6.75	7.01		
13.1	81	7.013	362.2828	10.9939	1.0684	138.8071	4.1898	7.01	7.02		
13.2	73.4063	7.257	362.4952	11.0769	1.0684	138.8071	4.1897	7.258	7.018		
13.3	45.5625	7.511	362.6958	11.0769	1.0989	138.8071	4.1896	7.503	7.013		
13.4	53.1563	8.027	362.7313	11.16	1.0989	139.4116	4.1819	7.747	7.018		
13.5	30.375	8.244	362.4008	11.243	1.0989	140.0162	4.183	8.001	7.018		
13.6	12.6563	8.507	362.9083	11.243	1.0989	139.4116	4.1797	8.254	7.013		
13.7	5.0625	8.751	362.7549	11.243	1.0989	139.4116	4.1841	8.508	7.013		
13.8	2.5313	9.005	362.1058	11.243	1.0989	139.4116	4.1938	8.761	7.013		
13.9	0	9.503	362.6606	11.4091	1.0989	139.4116	4.1855	9.006	7.013		
14	0	9.757	362.5189	11.4091	1.0989	139.4116	4.1487	9.26	7.013		
14.1	0	10.002	362.7196	11.4091	1.0989	140.0162	4.1544	9.504	7.013		
		10.255	362.9202	11.4921	1.0684	139.4116	4.16	9.74	7.013		
		10.5	363.4041	11.5751	1.0989	139.4116	4.1558	10.003	7.013		
		10.754	363.7346	11.5751	1.0989	139.4116	4.17	10.247	7.013		
		11.008	363.5694	11.6581	1.0684	139.4116	4.1895	10.501	7.013		
		11.243	363.7346	11.6581	1.0989	138.8071	4.1961	10.746	7.013		
		11.524	364.2422	11.6581	1.0989	138.8071	4.2016	11.008	7.013		
		11.751	364.4192	11.7412	1.0989	138.8071	4.2016	11.253	7.008		
		12.014	365.4344	11.8242	1.1295	138.2026	4.2276	11.507	7.013		
		12.25	365.9657	11.9072	1.1295	138.2026	4.2167	11.743	7.008		
		12.504	367.6423	12.2393	1.16	138.2026	4.2156	12.024	7.013		
		12.758	371.1383	12.9036	1.282	137.5981	4.2319	12.241	7.013		
		13.021	372.9695	13.1526	1.282	136.9936	4.2481	12.504	7.013		
		13.502	373.3121	13.3187	1.282	129.7394	4.2762	12.749	7.008		
		13.756	373.4894	13.3187	1.282	122.4851	4.2794	13.003	7.008		
		14.019	373.3476	13.2357	1.3126	107.3722	4.4017	13.257	7.008		
		14.5	375.002	13.3187	1.3431	95.2818	4.4038	13.511	7.008		
		15.008	390.3784	14.232	1.4347	36.6436	4.4208	13.756	7.008		
		15.254	408.236	15.5605	1.4042	-28.6443	4.4229	14.019	7.008		
		15.508	443.9612	19.3798	1.3737	-110.8587	4.4368	14.265	7.008		
		15.753	492.4104	27.1844	1.4042	-167.0788	4.5738	14.519	7.008		
		16.016	535.3756	31.5019	1.4042	-214.8357	4.6482	14.764	7.008		
		16.262	570.7377	34.906	1.4652	-247.4797	4.6773	15	7.003		
		16.516	636.2075	41.7973	1.4652	-264.4062	5.099	15.263	6.998		
		16.752	697.8706	47.3602	1.5263	-272.8694	5.3169	15.517	6.988		
		17.016	760.7041	55.4139	1.5568	-278.9146	5.6082	15.744	6.988		
		17.261	808.6889	63.8828	1.6179	-281.3327	5.747	16.008	6.978		
		17.552	883.6463	73.6801	1.6179	-282.5417	5.9246	16.253	6.978		
		17.752	932.7906	79.9072	1.7094	-284.3553	5.9815	16.507	6.983		
		18.006	962.407	85.7192	1.6789	-284.3553	6.0321	16.752	6.983		
		18.288	989.5522	89.5385	1.7094	-284.9598	6.0721	17.007	6.983		
								17.252	6.983		
								17.506	6.988		
								18.006	6.988		

3.4 Summer stratification: 29/09/09

13/10/2008

Depth (m)	Temperature (°C)	Electroconductivity (µS cm⁻¹)	Chloropyll a (µg l⁻¹)	Oxygen (µM)	c-DOM (AU)	pH	Turbidity (NTU)
0.1	18.61	605.10	7.18	254.29	9.75	8.62	2.15
0.2	18.61	605.50	7.38	258.52	9.67	8.63	2.18
0.5	18.6	605.70	7.25	261.13	9.67	8.62	2.06
0.7	18.6	602.20	7.24	261.42	9.54	8.61	2.11
1	18.6	605.30	7.59	261.88	9.50	8.61	2.05
1.2	18.6	604.80	7.65	261.92	9.42	8.61	2.05
1.5	18.61	607.3	7.42	261.84	9.49	8.61	2.07
1.7	18.6	605.7	7.43	261.7	9.41	8.61	2.05
2	18.6	611.8	7.22	261.94	9.5	8.61	2.06
2.2	18.61	605.8	7.29	262.14	9.41	8.61	2.05
2.5	18.6	606	7.41	261.51	9.4	8.61	2.05
2.7	18.6	605.6	7.43	262.07	9.38	8.61	2.04
3	18.6	604.6	7.33	262.07	9.43	8.61	2.05
3.2	18.6	605.3	7.19	261.77	9.52	8.61	2.06
3.5	18.6	605.2	7.2	262.35	9.51	8.61	2.04
3.7	18.6	606.5	7.2	262.11	9.36	8.61	2.05
4	18.6	605.1	7.2	261.86	9.42	8.61	2.05
4.2	18.6	605.1	7.25	261.69	9.42	8.62	2.04
4.5	18.6	604.9	7.3	261.95	9.47	8.62	2.05
4.7	18.6	605.1	7.15	261.98	9.42	8.62	2.05
5	18.6	605	6.94	261.92	9.37	8.62	2.06
5.2	18.6	605.3	7.12	261.95	9.33	8.62	2.05
5.5	18.6	605.4	7.14	262.46	9.5	8.62	2.05
5.7	18.6	605.2	7.05	262.24	9.42	8.62	2.05
6	18.6	605.3	7.09	262.19	9.33	8.62	2.05
6.2	18.6	605.2	7.01	262.33	9.34	8.62	2.05
6.5	18.6	605.6	7.17	261.73	9.37	8.62	2.05
6.7	18.59	604.8	7.09	262.08	9.42	8.62	2.05
7	18.59	605.6	7.18	261.79	9.34	8.62	2.05
7.2	18.59	605.7	7.24	261.55	9.33	8.62	2.05
7.5	18.4	603.9	7.69	265.97	9.49	8.62	2.06
7.7	18.16	607	9.04	305.98	15.83	8.58	2.05
8	15.4	606.2	12.69	366.11	23.17	8.47	2.1
8.2	14.6	606.5	15.73	369.51	24.06	8.42	2.12
8.5	13.01	608.4	19.2	359.6	24.95	8.39	2.16
8.7	12.24	609.1	19.85	349.88	25.28	8.4	2.16
9	11.28	611	21.46	329.91	25.52	8.39	2.17
9.2	10.93	611.6	26.64	297.47	25.77	8.38	2.23
9.5	9.85	618.5	35.91	223.78	26.27	8.33	2.29
9.7	9.65	619.5	36.42	189.76	26.36	8.3	2.35
10	8.89	626.7	38.62	90.23	26.35	8.21	2.4
10.2	8.51	629.2	39.49	20.04	25.64	8.15	3.03
10.5	8.1	632.5	37.41	5.85	24.82	8.06	5.76
10.7	7.72	634.1	38.16	4.05	24.2	8.01	7.87
11	7.12	638	35.11	3.1	23.45	7.89	12
11.2	6.89	640.7	27.26	2.38	23.52	7.81	12.11
11.5	6.56	644.2	20.53	1.49	22.57	7.76	9.91
11.7	6.44	650.5	16.78	0.93	22.45	7.69	8.84
12	6.22	655.4	15.44	0.59	22.24	7.63	6.28
12.2	6.05	657.3	13.8	0.44	22.12	7.61	4.97
12.5	5.9	660.8	12.73	-0.14	21.97	7.58	4.24
12.7	5.9	660.8	11.63	-0.33	22.19	7.57	3.65
13	5.72	667.9	10.67	-0.47	22.18	7.52	2.57
13.2	5.68	672.8	9.97	-0.72	22.44	7.5	2.41
13.5	5.64	681.1	9.77	-0.89	22.65	7.47	2.37
13.7	5.64	682	9.03	-0.87	23.15	7.44	2.33
14	5.58	697.6	8.38	-1	23.88	7.38	2.29
14.2	5.6	710.6	7.73	-1.19	24.44	7.32	2.27
14.5	5.61	719.2	7.7	-1.28	25.01	7.25	2.32
14.7	5.62	730.8	7.75	-1.33	25.77	7.17	2.29
15	5.68	759.2	7.53	-1.5	26.53	7.1	2.28
15.2	5.7	777.3	7.94	-1.51	29.37	6.99	2.28
15.5	5.77	845	7.99	-1.63	32.04	6.9	2.31
15.7	5.79	896.7	8.03	-1.32	31.83	6.85	2.36
16	5.85	1009.1	7.96	-1.6	45.96	6.7	2.39
16.2	5.87	1070.9	8.03	-1.78	42.15	6.64	2.47
16.5	5.95	1207.9	8	-1.82	52.13	6.49	2.49
16.7	6.01	1276.1	8.08	-1.48	61.86	6.39	2.49
17	6.05	1327	8.33	-0.23	69.72	6.31	2.49
17.2	6.13	1426.4	8.58	1.15	73.38	6.28	2.49
17.5	6.19	1483.1	8.81	2.25	82.58	6.22	2.49
17.7	6.23	1523.5	8.86	2.81	86.32	6.19	2.49
18	6.29	1539.2	9.14	2.36	89.7	6.17	2.49

3.3 Summer stratification: 13/010/08

13/10/2008

Depth (m)	Temperature (°C)	Electroconductivity (µS cm⁻¹)	c-DOM (AU)	Turbidity (NTU)	pH	Redox potential (mV)
0.17	17.05	583.70	7.84	2.90	8.90	150.29
0.2	17.1	584.22	7.84	2.93	8.90	147.87
0.58	16.79	584.75	7.84	2.90	8.92	147.27
1.26	16.52	583.60	7.92	2.99	8.94	146.06
1.59	16.47	584.12	8.00	3.11	8.94	145.46
1.77	16.48	584.48	8.09	3.11	8.94	144.85
2.02	16.36	584.45	8.00	3.08	8.94	144.85
2.49	16.3	584.15	8.25	3.17	8.95	143.64
2.77	16.32	584.49	8.25	3.30	8.95	143.04
3	16.33	584.31	8.25	3.05	8.95	141.83
3.25	16.34	584.60	8.25	3.14	8.95	141.83
3.51	16.35	584.28	8.17	3.11	8.95	141.23
3.76	16.29	584.35	8.25	3.17	8.95	140.62
4	16.27	584.86	8.34	3.17	8.95	140.02
4.24	16.26	584.79	8.34	3.11	8.95	139.41
4.55	16.25	584.18	8.34	3.11	8.95	139.41
4.75	16.24	584.47	8.42	3.11	8.95	138.81
4.97	16.24	584.42	8.5	3.14	8.95	138.2
5.27	16.23	584.22	8.5	3.45	8.95	137.6
5.51	16.23	584.02	8.42	3.3	8.95	138.2
5.74	16.22	583.72	8.5	3.14	8.95	137.6
6.01	16.23	584.31	8.42	3.39	8.95	137.6
6.26	16.21	584.1	8.5	3.27	8.95	136.99
6.49	16.21	583.42	8.5	3.33	8.95	136.99
6.75	16.2	583.3	8.5	3.11	8.95	136.39
7	16.2	583.15	8.5	3.11	8.95	135.78
7.25	16.2	583.21	8.67	3.24	8.95	135.78
7.51	16.2	583.77	8.59	3.24	8.95	135.78
7.75	16.2	584.85	8.5	3.3	8.95	135.18
8	16.19	584.76	8.59	3.33	8.95	135.18
8.24	16.19	585.95	8.59	3.45	8.95	135.18
8.5	16.18	585.04	8.59	3.42	8.94	135.18
8.74	16.15	585.23	8.75	3.36	8.94	133.97
9	15.91	587.73	9.25	3.33	8.94	134.58
9.2	15.66	591.61	12.74	4.15	8.91	134.58
9.4	14.91	603.73	17.22	4.52	8.85	135.78
9.59	14.24	615.34	19.88	7.36	8.77	136.99
9.8	13.38	621.54	22.87	7.23	8.64	138.2
10	12.58	625.04	24.36	6.75	8.57	139.41
10.2	11.99	624.84	24.86	5.77	8.54	140.02
10.4	11.43	627.34	24.94	5.53	8.52	140.02
10.59	11.32	619.29	24.78	5.59	8.54	138.81
10.8	10.65	622.15	23.95	5.49	8.57	137.6
11	10.08	626.3	23.53	6.93	8.58	135.78
11.2	9.37	632.99	22.37	10.29	8.56	133.97
11.4	8.99	639.56	21.37	16.06	8.42	129.13
11.6	8.12	646.68	20.46	21.7	8.24	104.95
11.81	7.8	648.03	19.79	20.09	8.18	61.43
12.01	7.4	653.13	19.21	19.11	8.17	-0.23
12.2	7.27	658.65	19.13	14.56	8.14	-36.5
12.39	7.21	659.48	19.05	14.22	8.12	-77.01
12.6	6.86	660.74	18.72	12.18	8.09	-113.88
12.8	6.62	664.57	18.38	10.71	8.08	-136.25
13	6.47	669.37	18.38	9.28	8.04	-154.38
13.2	6.39	672.83	18.38	8.82	8.01	-168.29
13.4	6.28	677.56	18.38	8.09	7.96	-177.96
13.61	6.18	684.63	18.47	7.54	7.92	-187.03
13.8	6.02	696.24	18.8	7.08	7.84	-193.68
14.01	5.99	704.65	19.05	6.75	7.8	-197.91
14.19	5.91	720.05	19.55	7.08	7.73	-200.33
14.41	5.87	739.08	20.46	6.23	7.68	-202.14
14.6	5.85	763.08	21.37	6.11	7.62	-203.95
14.8	5.86	792.42	23.03	6.47	7.53	-204.56
15.01	5.86	829.83	24.36	6.53	7.47	-203.95
15.24	5.87	863.3	27.43	7.11	7.35	-202.75
15.4	5.88	910.15	29.34	7.36	7.26	-203.35
15.6	5.9	950.69	32.66	7.39	7.17	-203.35
15.8	5.91	1009.06	34.82	7.97	7.09	-202.14
16.01	5.93	1029.19	39.14	8.18	7.01	-201.54
16.27	5.96	1120.85	42.79	8.52	6.95	-201.54
16.4	5.98	1157.35	45.78	8.64	6.91	-200.93
16.61	6.02	1238.13	51.26	8.52	6.85	-200.93
16.82	6.07	1314.83	56.41	9.49	6.79	-200.93
17	6.13	1391.73	67.04	10.41	6.73	-200.93
17.1	6.13	1411.69	67.54	11.05	6.7	-200.93
17.19	6.16	1444.24	68.37	11.17	6.69	-200.93
17.35	6.2	1471.59	73.93	10.53	6.67	-201.54

Depth (m)	Oxygen (µM)	Chloropyll a (µg l⁻¹)
0.19	236.14	7.07
0.20	237.16	7.41
0.43	237.07	7.41
1.26	238.55	8.01
1.59	239.42	8.66
1.78	239.82	8.92
2.02	240.71	8.70
2.49	241.61	8.57
2.77	241.68	8.88
2.99	241.71	9.09
3.25	241.97	9.52
3.51	241.99	9.52
3.76	242.18	9.99
4.00	242.07	9.91
4.24	241.65	10.04
4.55	241.36	10.08
4.75	241.71	10.04
4.97	241.87	10.21
5.27	241.56	10.30
5.51	241.43	10.42
5.73	240.96	10.42
6.01	240.50	10.47
6.27	240.68	10.30
6.49	240.69	10.21
6.75	240.23	10.38
6.98	239.90	10.08
7.25	240.42	10.17
7.51	240.27	10.21
7.75	240.29	10.85
7.99	240.32	10.42
8.24	240.51	10.64
8.5	239.72	10.34
8.76	239.56	10.77
9.01	239.31	10.77
9.22	225.93	12.23
9.41	175.99	20.19
9.58	161.06	22.08
9.81	110.58	27.20
10.01	82.18	28.88
10.19	70.83	28.75
10.41	71.56	26.69
10.6	62.68	25.05
10.81	49.85	25.78
11	20.06	53.58
11.22	10.47	97.03
11.4	7.28	93.16
11.62	5.17	35.21
11.8	3.93	26.69
12	3.69	29.35
12.2	2.46	19.63
12.39	1.54	19.24
12.6	1.04	19.24
12.8	0.88	18.30
13	0.04	18.51
13.21	0.00	18.64
13.4	0.00	17.44
13.6	0.00	16.06
13.79	0.00	14.98
14.01	0.00	14.64
14.22	0.00	14.94

II.4. Closest relatives of the clones retrieved from winter stratification

4.1 16S rRNA gene sequences retrieved from 15.5 m depth

Clone number	similarity %	Closest affiliation	Hit length
15.5-1	100	Uncultured bacterium clone FGL3_B32 16S ribosomal RNA gene, partial sequence (FJ437749)	1463
15.5-2 (x6)	99	Uncultured bacterium clone 5T3-19 16S ribosomal RNA gene, partial sequence (GQ472452)	1492
15.5-3 (x3)	99	Uncultured bacterium clone YU-ARD-G11 16S ribosomal RNA gene, partial sequence (DQ656577)	1455
15.1-4	99	Uncultured delta proteobacterium partial 16S rRNA gene, clone C16-18S78 (FR729085)	1493
15.5-5	100	Uncultured bacterium clone nbw218d09c1 16S ribosomal RNA gene, partial sequence (GQ074964)	1232
15.5-6	100	Uncultured bacterium clone MD2904-B7 16S ribosomal RNA gene, partial sequence (EU386104)	1469
15.5-7	100	Uncultured bacterium clone FFCH11021 16S ribosomal RNA gene, partial sequence-(EU132678)	1477
15.5-8	98	Uncultured bacterium clone NBLE311B 16S ribosomal RNA gene, partial sequence (GU389854)	1491
15.5-9	100	Uncultured Desulfomonile sp. partial 16S rRNA gene, clone C14S36 (FR729663)	1487
15.5-10 (x4)	100	Uncultured bacterium clone HH277 16S ribosomal RNA gene, partial sequence (FJ502272)	1470
15.5-11	100	Uncultured bacterium clone aab00c05 16S ribosomal RNA gene, partial sequence (DQ816838)	1474
15.5-12 (x2)	100	Lamprocystis sp. D21 partial 16S rRNA gene, strain D21 (AM086643)	1463
15.5-13	100	Uncultured bacterium clone HDB_SIPP405 16S ribosomal RNA gene, partial sequence (HM187215)	1448
15.5-14	100	Uncultured bacterium clone SUL_779_C06 16S ribosomal RNA gene, partial sequence (EU644294)	1465
15.5-15	98	Uncultured bacterium clone MIGF04324 16S ribosomal RNA gene, partial sequence (HM565426)	1446
15.5-16 (x3)	100	Uncultured bacterium clone ncd938g05c1 16S ribosomal RNA gene, partial sequence (HM329852)	1178
15.5-17	100	Uncultured bacterium clone Zplanct26 16S ribosomal RNA gene, partial sequence (EF602487)	1478
15.5-18	100	Uncultured bacterium clone Z243 16S ribosomal RNA gene, partial sequence (GQ388865)	1471
15.5-20 (x4)	100	Lamprocystis purpurea partial 16S rRNA gene, strain A12.3 (AM086644)	1480
15.5-21 (x2)	100	Uncultured bacterium partial 16S rRNA gene, clone E64 (AM085483)	1480
15.5-22	100	Iron-reducing bacterium enrichment culture clone HN29 16S ribosomal RNA gene, partial sequence (FJ269056)	1450
15.5-23	100	Uncultured bacterium clone Z22 16S ribosomal RNA gene, partial sequence (GQ388841)	1459
15.5-24	100	Uncultured Synechococcus sp. clone XZZLH49 16S ribosomal RNA gene, partial sequence (EU703487)	1412
15.5-25 (x2)	100	Uncultured bacterium clone WM13 16S ribosomal RNA gene, partial sequence (DQ415754)	1453
15.5-26 (x3)	95	Uncultured bacterium clone EtOH_2_112 16S ribosomal RNA gene, partial sequence (HM460949)	1465
15.5-27	100	Bacillus horikoshii strain A2 16S ribosomal RNA gene, partial sequence (GQ304778)	1481
15.5-28	100	Uncultured candidate division OP11 bacterium clone Alk1-1E 16S ribosomal RNA gene, partial sequence(HM992553)	891
15.5-29 (x4)	100	Uncultured bacterium clone PE1 MKM3 16S ribosomal RNA gene, partial sequence (HM047815)	1459
15.5-30	100	Uncultured bacterium clone KD2-88 16S ribosomal RNA gene, partial sequence (AY218597)	1449
15.5-31	100	Uncultured bacterium clone 007A9 16S ribosomal RNA gene, partial sequence (EU734916)	1441
15.5-32	95	Uncultured Mollicutes bacterium clone KS-112 16S ribosomal RNA gene, partial sequence (EU809832)	1465
15.5-34	100	Uncultured bacterium clone HH286 16S ribosomal RNA gene, partial sequence (FJ502275)	1434
15.5-35	100	Uncultured bacterium clone Z22 16S ribosomal RNA gene, partial sequence (GQ388841)	1459
15.5-36	100	Uncultured deep-sea bacterium 16S rRNA gene, clone Ucd1524 (AM997561)	1381
15.5-37	100	Uncultured deep-sea bacterium 16S rRNA gene, clone Ucd1524 (AM997561)	1381
15.5-38	98	Uncultured bacterium clone M0111_43 16S ribosomal RNA gene, partial sequence (EU104042)	1466
15.5-39	100	Uncultured bacterium clone LA10Ba21 16S ribosomal RNA gene, partial sequence (GU133269)	908
15.5-40	97	Uncultured bacterium partial 16S rRNA gene, clone B114 (AM162485)	1455
15.5-41	100	Uncultured bacterium clone CK_2C2_7 16S ribosomal RNA gene, partial sequence (EU488119)	1476
15.5-42	98	Uncultured bacterium clone F9P26500_S_M09 16S ribosomal RNA gene, partial sequence (HQ672998)	1420
15.5-43	100	Uncultured bacterium clone B1F 16S ribosomal RNA gene, partial sequence (FJ205231)	1424
15.5-44	100	Uncultured bacterium partial 16S rRNA gene, clone BuhD-218 (FM877560)	1461
15.5-45	99	Uncultured bacterium clone YU-ARD-G11 16S ribosomal RNA gene, partial sequence (DQ656577)	1455
15.5-46	99	Uncultured bacterium clone D24 16S ribosomal RNA gene, partial sequence (EU234315)	1466
15.5-47	100	Uncultured Bacteroidetes bacterium clone AS136 16S ribosomal RNA gene, complete sequence (EU283405)	1441
15.5-48	98	uncultured bacterium partial 16S rRNA gene, clone PeH17 (AJ576334)	1443
15.5-49	100	Uncultured bacterium partial 16S rRNA gene, clone CsOx41 (FN377790)	1458
15.5-50	100	Uncultured bacterium clone 2B4-8 16S ribosomal RNA gene, partial sequence (GQ472313)	1512
15.5-51	98	Uncultured bacterium clone ORS10C_h09 16S ribosomal RNA gene, partial sequence (EF392974)	1487
15.5-52	98	Uncultured bacterium clone ORS10C_h09 16S ribosomal RNA gene, partial sequence (EF392974)	1487
15.5-53	100	Uncultured marine bacterium clone RS.Water.252 16S ribosomal RNA gene, partial sequence (DQ417908)	1236
15.5-55 (x2)	100	Uncultured bacterium clone Z22 16S ribosomal RNA gene, partial sequence (GQ388841)	1459
15.5-58	98	Uncultured bacterium clone ORS10C_h09 16S ribosomal RNA gene, partial sequence (EF392974)	1487
15.5-59	100	Uncultured bacterium clone MSB-1E4 16S ribosomal RNA gene, partial sequence (EF125406)	1463
15.5-60	100	Uncultured Lentisphaerae bacterium clone SGSH1109 16S ribosomal RNA gene, partial sequence (GQ347406)	1433
15.5-61	100	Uncultured bacterium clone HH277 16S ribosomal RNA gene, partial sequence (FJ502272)	1470
15.5-62	98	Uncultured bacterium clone 148 16S ribosomal RNA gene, partial sequence (HQ538638)	1466
15.5-63 (x2)	99	Uncultured Bacteroidetes bacterium clone JB1A12 16S ribosomal RNA gene, partial sequence (HQ532596)	1455
15.5-64	98	Uncultured bacterium clone zEL41 16S ribosomal RNA gene, partial sequence (DQ415834)	1502
15.5-65	100	Uncultured bacterium clone BS7_65 16S ribosomal RNA gene, partial sequence (GQ458219)	1456
15.5-66	100	Uncultured bacterium clone SAW1_B81 16S ribosomal RNA gene, partial sequence (FJ716326)	1243
15.5-67	99	Uncultured bacterium clone Foos8B_57 16S ribosomal RNA gene, partial sequence (EU431801)	1431
15.5-68	98	uncultured bacterium partial 16S rRNA gene, clone PeH17 (AJ576334)	1443
15.5-69	100	Uncultured bacterium clone HH277 16S ribosomal RNA gene, partial sequence (FJ502272)	1470
15.5-70	100	Uncultured bacterium clone SS1_B_08_35 16S ribosomal RNA gene, partial sequence (EU050937)	1272
15.5-71	100	Uncultured Saprospiraceae bacterium partial 16S rRNA gene, clone MS-Mond1-H (AJ786321)	1447
15.5-73	100	Uncultured bacterium clone YU-ARD-G11 16S ribosomal RNA gene, partial sequence (DQ656577)	1455
15.5-74	100	Uncultured Synechococcus sp. clone XZXXH51 16S ribosomal RNA gene, partial sequence (EU703437)	1414
15.5-75	100	Uncultured bacterium clone FGL3_B32 16S ribosomal RNA gene, partial sequence (FJ437749)	1464

Numbers in bracket indicate the number of sequences having the same restriction profiles.

4.2 16S rRNA gene sequences retrieved from 17.0 m depth

Clone number	similarity %	Closest affiliation	Hit length
17.0-2	99	Uncultured bacterium clone ncd2423f02c1 16S ribosomal RNA gene, partial sequence (JF210504)	1465
17.0-3 (x2)	99	Uncultured bacterium clone SUL_805_E09 16S ribosomal RNA gene, partial sequence (EU644300)	1491
17.0-4	99	Uncultured Bacteroidetes bacterium clone JB1A12 16S ribosomal RNA gene, partial sequence (HQ532596)	1455
17.0-5	100	Uncultured bacterium clone B1F 16S ribosomal RNA gene, partial sequence (FJ205231)	1424
17.0-7	100	Uncultured bacterium clone B1F 16S ribosomal RNA gene, partial sequence (FJ205231)	1424
17.0-8	98	Uncultured bacterium clone YU-ARD-G11 16S ribosomal RNA gene, partial sequence (DQ656577)	1455
17.0-9	100	Uncultured bacterium clone BlkFLOCS_E01 16S ribosomal RNA gene, partial sequence (GQ433941)	1424
17.0-10	100	Uncultured candidate division OP11 bacterium clone Pav-OP14 16S ribosomal RNA gene, partial sequence (FJ482195)	1386
17.0-11	95	Uncultured bacterium clone 654961 16S ribosomal RNA gene, partial sequence (DQ404889)	1474
17.0-12 (x3)	100	Uncultured bacterium clone Z243 16S ribosomal RNA gene, partial sequence (GQ388865)	1471
17.0-13	99	Uncultured bacterium clone FGL3_B32 16S ribosomal RNA gene, partial sequence (FJ437749)	1464
17.0-14	99	Uncultured bacterium partial 16S rRNA gene, clone SHA-95 (AJ306788)	1362
17.0-15	100	Uncultured Rhodocyclaceae bacterium partial 16S rRNA gene, clone 117 (FM207947)	1149
17.0-16	100	Uncultured bacterium clone FFCH4225 16S ribosomal RNA gene, partial sequence (EU134919)	654
17.0-17 (x2)	98	Uncultured bacterium clone anSH01 16S ribosomal RNA gene, partial sequence (EF034811)	1381
17.0-18	100	Uncultured bacterium clone F1Q32TO06G636S 16S ribosomal RNA gene, partial sequence (GU547505)	1381
17.0-19	100	Uncultured bacterium clone EPR3965-I2-Bc40 16S ribosomal RNA gene, partial sequence (EU491859)	1401
17.0-21 (x2)	99	Uncultured bacterium clone YU-ARD-G11 16S ribosomal RNA gene, partial sequence (DQ656577)	1455
17.0-22	100	Uncultured bacterium clone LA10Ba21 16S ribosomal RNA gene, partial sequence (GU133269)	908
17.0-24	100	Uncultured bacterium 16S rRNA gene, clone SS_LKC22_UB175 (AM490694)	892
17.0-25 (x2)	100	Uncultured bacterium clone EPR3970-MO1A-Bc86 16S ribosomal RNA gene, partial sequence (EU491673)	1507
17.0-26	100	Uncultured bacterium clone Pav-050 16S ribosomal RNA gene, partial sequence (DQ642362)	994
17.0-27 (x2)	100	Uncultured bacterium clone SINH613 16S ribosomal RNA gene, partial sequence (HM128140)	1449
17.0-28	100	Uncultured anaerobic bacterium clone B-1AV 16S ribosomal RNA gene, partial sequence (AY953162)	1454
17.0-29	100	Uncultured Deltaproteobacteria bacterium 16S rRNA gene from clone QEDR3DD08 (CU922581)	1492
17.0-31	99	Uncultured bacterium clone YU-ARD-G11 16S ribosomal RNA gene, partial sequence (DQ656577)	1455
17.0-32	98	Uncultured bacterium clone RB_Par_1113 16S ribosomal RNA gene, partial sequence (EU644139)	1448
17.0-33	99	Uncultured bacterium clone SUL_805_E09 16S ribosomal RNA gene, partial sequence (EU644300)	1491
17.0-34 (x2)	100	Bacillus simplex strain CG3 16S ribosomal RNA gene, partial sequence (JF271855)	616
17.0-35	100	Bacterium str. 47083 16S ribosomal RNA gene, partial sequence (AF227837)	1484
17.0-36	99	Uncultured bacterium clone FGL3_B176 16S ribosomal RNA gene, partial sequence (FJ437801)	1492
17.0-37	100	Uncultured bacterium partial 16S rRNA gene, clone T4_198 (FM206206)	1496
17.0-39	98	Uncultured bacterium clone YU-ARD-G11 16S ribosomal RNA gene, partial sequence (DQ656577)	1455
17.0-40	100	Uncultured Carboxydocella sp. clone L6B-416 16S ribosomal RNA gene, partial sequence (GU000287)	1473
17.0-41 (x2)	100	Uncultured bacterium clone SUL_779_C06 16S ribosomal RNA gene, partial sequence (EU644294)	1456
17.0-42	98	Uncultured bacterium clone ncd2429c04c1 16S ribosomal RNA gene, partial sequence (JF201282)	1403
17.0-43	98	Uncultured bacterium clone LD D09 small subunit ribosomal RNA gene, partial sequence (HQ290438)	1453
17.0-45	100	Uncultured bacterium clone 1103200831280 16S ribosomal RNA gene, partial sequence (EU843590)	1448
17.0-46	100	Uncultured bacterium clone 655964 16S ribosomal RNA gene, partial sequence (DQ404835)	1447
17.0-47	100	Unidentified eubacterium clone vadinBE97 16S ribosomal RNA gene, partial sequence (UEU81707)	1290
17.0-48	100	Uncultured bacterium clone 656061 16S ribosomal RNA gene, partial sequence (DQ404616)	1447
17.0-49	100	Uncultured bacterium clone Z22 16S ribosomal RNA gene, partial sequence (GQ388841)	1459

Numbers in bracket indicate the number of sequences having the same restriction profiles.